

**DEVELOPMENT OF ACCELERATED  
ONE-DIMENSIONAL CONSOLIDATION TESTING  
METHODS**

*A THESIS*

*submitted by*

**RAHEENA M.**

*for the award of the degree*

*of*

**DOCTOR OF PHILOSOPHY**



**GEOTECHNICAL ENGINEERING DIVISION  
DEPARTMENT OF CIVIL ENGINEERING  
INDIAN INSTITUTE OF TECHNOLOGY MADRAS**

**MAY 2018**



*Dedicated to  
my best friend - my husband*



## **THESIS CERTIFICATE**

This is to certify that the thesis entitled **DEVELOPMENT OF ACCELERATED ONE-DIMENSIONAL CONSOLIDATION TESTING METHODS**, submitted **RAHEENA M**, to the Indian Institute of Technology Madras, for the award of the degree of **Doctor of Philosophy** is a bonafide record of research work carried out by her under my supervision. The contents of this thesis, in full or in parts, have not been submitted to any other Institute or University for the award of any degree or diploma.

Chennai 600036

Date: 16<sup>th</sup> May, 2018

**Dr. R. G. Robinson**

Research Guide

Professor

Geotechnical Engineering Division

Department of Civil Engineering

IIT Madras



## ACKNOWLEDGMENTS

I would like to express the deep sense of gratitude to my research guide **Prof. R. G. Robinson** for his valuable guidance, invaluable suggestions and constant encouragement and support during my research. I would like to thank him for being the best teacher and guide during my course of study at IIT Madras.

I express my sincere thanks to **Prof. K. Ramamurthy**, Head, Department of Civil Engineering and to my Doctoral Committee members **Prof. R. Velmurugan**, **Prof. J. Murali Krishnan**, and **Dr. Subhadeep Banerjee** for their time and effort in reviewing my progress and for their valuable suggestions.

I would like to thank **Prof. S. R. Gandhi**, **Prof. K. Rajagopal**, **Prof. A. Boominathan**, **Prof. G. R. Dodagoudar**, **Dr. V. B. Maji**, **Dr. T. Thyagaraj** and **Dr. Dali Naidu Arnepalli** faculty members of Geotechnical Engineering Division, for their critical comments and invaluable suggestions at various stages of the research work.

I express my sincere thanks to **Mr. Murali**, **Mr. David**, **Mr. Balasubrahmaniam** and **Mr. Prince** Civil Engineering workshop, for their immense help to fabricate experimental set-up with great care. I would like to thank **Mr. K. Om Prakash**, **Mr. P. Suresh**, **Mr. Dhasthageer** and **Mr. Aravind Raj**, for their help while doing experiments in the Geotechnical Engineering Laboratory. I would like to thank the staff of Head of Department office for their help in academic related matters.

I would like to thank my husband **Mr. B. Shareef** and parents for being the best supporters in my life. Thank you so much for being with me at all times.

I thank you my dear friends **Prashanthi**, **Soumyaranjan Mishra**, **Soni**, **Krishna Prasad**, **Sai Geethesh**, **Praveen Jha**, **Yuvraj**, **Kalyan**, **Nagaraj**, **Sherrin**, **Lini**, **Joytshna**, **Azneb**, **Amal**, **Anu**, **Sridhar**, **Ashok**, **Suganya**, **Aparna**, **Swagathika**, **Madhusudhan** for helping me and making me smile during my tough times.

**RAHEENA M.**





## ABSTRACT

**KEYWORDS:** Consolidation, incremental loading consolidation test, constant rate of strain consolidation test, permeability, pore pressure measurement, degree of consolidation.

Accurate determination of consolidation properties of the soils is required for the design of geotechnical engineering structures. Consolidation properties are commonly determined by performing laboratory one-dimensional consolidation test. Conventionally, consolidation parameters are determined from one-dimensional incremental loading (IL) consolidation tests which generally requires about 10-14 days, if the duration between successive load increments is kept as 24 hours. In addition, the number of data points obtained is discrete, which often fails to depict the complete void ratio ( $e$ ) -consolidation pressure ( $\sigma_v'$ ) curve. In order to overcome the limitations of IL consolidation test, several other types of tests like the constant rate of strain (CRS) consolidation test and controlled gradient (CG) consolidation tests etc. are also proposed in the literature. Though CRS test is widely used, reliable guidelines are not available to fix the strain rate. Guidelines are also not available to control the rate in the controlled- strain loading (CSL) consolidation test.

In the present study, a rational method of fixing the strain rate of strain-controlled consolidation test is proposed. Initially, the strain rate of constant rate of strain (CRS) test is fixed based on permeability measurement using a falling head permeability set-up using 3 mm diameter pipe. The CRS consolidation tests are conducted so as to study the development of pore pressure. As it was found that pore pressure development depends on the strain rate and coefficient of consolidation, an observational approach to control the strain rate during CSL test is also proposed, so as to obtain the maximum allowable pore pressure ratio of 0.15 as per ASTM D4186-12 (2012). Detailed experimental works are carried out on several fine grained soils, so as to validate the proposed methodology. The results obtained show a very good comparison with IL consolidation test. However, the duration required to complete the CSL consolidation test is quite high for low permeable soils with  $c_v < 3 \times 10^{-8}$  m<sup>2</sup>/s, because the pore pressure ratio is inversely proportional to the coefficient of consolidation.

In order to perform CRS test special cell with provision to measure pore pressure at the base is required. The standard apparatus as per ASTM D4186-06 (2006) are quite expensive. Hence, a simplified CRS apparatus was developed. In addition, the modifications to conventional consolidometer are suggested to determine the consolidation parameters from CRS test. Tests were conducted based on the proposed methodology. The results obtained using the proposed cells are compared with the apparatus as per ASTM D4186-12 (2012) and IL consolidation test.

Though CSL test has several advantages, the time required for completing consolidation test is quite high. Hence, a stress controlled (SC) consolidation test procedure with pore pressure measurement is proposed. The test is like an IL consolidation test with one-way drainage condition through the top. The pore pressure developed at the base of the sample was continuously monitored and when the base pore pressure reached 15% of the total stress applied, the next increment was applied. The validity of the proposed method is verified on soils with varying plasticity characteristics. The SC test with pore pressure measurement is about 2 times faster than the CSL consolidation test.

The CSL test and SC tests require controlling devices for pressure application when compared with the conventional IL test. The IL consolidation test is always simple and easy to run. As the test is conducted under two-way drainage conditions, it is expected to be faster. Therefore, in the present investigation attempts were also made to accelerate the IL consolidation test using the standard curve fitting procedure, such as Taylor's  $\sqrt{t}$  method and Inflection point method. The testing procedure is similar to IL consolidation test, with the difference that the subsequent loading is applied once the degree of consolidation is identified using the standard curve fitting procedure. The validity of the proposed procedure was verified by performing tests on several fine grained soils. By adopting the inflection point method, consolidation tests could be completed on a working day, within 2.5 to 9 hours depending on the coefficient of consolidation of the soils.

From the research, it is concluded that the strain controlled consolidation test cannot be made faster for low permeable soils, as the strain rate depends on the coefficient of consolidation. But the stress-controlled consolidation test can be made faster without allowing 100% degree of consolidation with appropriate interpretation.

# TABLE OF CONTENTS

<b>ACKNOWLEDGMENTS</b>	i
<b>ABSTRACT</b>	iii
<b>TABLE OF CONTENTS</b>	v
<b>LIST OF TABLES</b>	ix
<b>LIST OF FIGURES</b>	xi
<b>ABBREVIATIONS</b>	xix
<b>NOTATIONS</b>	xxi
<b>1 INTRODUCTION</b>	1
1.1 BACKGROUND	1
1.2 INCREMENTAL LOADING (IL) CONSOLIDATION TEST	1
1.2.1 Conventional IL (Oedometer) Consolidation Test	2
1.2.2 Rapid Consolidation Test	2
1.2.2 End-Of-Primary (EOP) Consolidation Test	3
1.3 CONSTANT RATE OF STRAIN (CRS) CONSOLIDATION TEST	3
1.3.1 Apparatus for CRS Test	3
1.3.2 Theories of CRS Test	4
1.3.3 Strain Rate Selection Criteria	5
1.4 NEED FOR THE STUDY	6
1.5 OBJECTIVES	7
1.6 ORGANISATION OF THE THESIS	7
<b>2 LITERATURE REVIEW</b>	9
2.1 INTRODUCTION	9
2.2 TYPES OF ONE-DIMENSIONAL CONSOLIDATION TESTS	9
2.2.1 Incremental Loading (IL) Consolidation Test	11
2.2.2 Constant Rate of Strain (CRS) Consolidation Test	11
2.2.3 Controlled Gradient (CG) Test	11
2.2.4 Constant Rate of Loading (CRL) Test	12
2.2.5 Restricted Flow Consolidation (RFC) Test	12
2.2.6 Constant Pressure Ratio (CPR) Test	12
2.2.7 Back Pressure Consolidation (BPC) Test	13
2.3 REVIEW OF IL CONSOLIDATION TEST	13
2.3.1 Theory of One-Dimensional Consolidation	13

2.3.2 Apparatus for IL Test	15
2.3.3 Determination of Coefficient of Consolidation ( $c_v$ )	21
2.3.4 Total Settlement Parameters	26
2.3.5 Rapid IL Consolidation Test	28
2.3.6 End-Of-Primary (EOP) Consolidation Test	30
2.4 CONSTANT RATE OF STRAIN (CRS) CONSOLIDATION TEST	31
2.4.1 Theories of CRS Test	31
2.4.2 Apparatus for CRS Test	41
2.4.3 Strain Rate Selection Criteria and Effect on the Soil Behaviour	46
2.4.4 Interpretation of CRS Test Data	50
2.4.5 Time Taken to Complete the CRS Test	52
2.5 SUMMARY OF LITERATURE REVIEW	52
<b>3 MATERIALS AND CONTROL TESTS</b>	57
3.1 INTRODUCTION	57
3.2 SELECTION OF SOILS	57
3.3 INDEX PROPERTIES OF THE SOILS	58
3.4 CONTROL CONSOLIDATION TESTS	63
3.4.1 Sample Preparation	63
3.4.2 Testing Procedure	65
3.4.3 Results and Discussions	67
3.5 SUMMARY	88
<b>4 METHOD TO FIX STRAIN RATE FOR CONTROLLED-STRAIN LOADING CONSOLIDATION TEST</b>	91
4.1 INTRODUCTION	91
4.2 EXPERIMENTAL PROGRAMME	91
4.3 PROPOSED METHOD TO FIX INITIAL STRAIN RATE OF CSL TEST	94
4.3.1 Theoretical Considerations	94
4.3.2 Experimental Methodology	95
4.3.3 Interpretation of CRS Consolidation Test Data	98
4.3.4 Results and Discussions	99
4.4 OBSERVATIONAL APPROACH TO CONTROL THE STRAIN RATE	106
4.4.1 Theoretical Considerations	106
4.4.2 Results and Discussions	108
4.5 SUMMARY	119

<b>5 DESIGN AND DEVELOPMENT OF SIMPLIFIED CRS APPARATUS</b>	121
5.1 INTRODUCTION	121
5.2 SIMPLIFIED CRS APPARATUS	121
5.2.1 Details of the Apparatus	121
5.2.2 Experimental Programme	125
5.2.3 Results and Discussions	127
5.3 MODIFIED FIXED RING CONSOLIDOMETER TO PERFORM CRS TEST	135
5.3.1 Details of the Modified Consolidation Cell	135
5.3.2 Experimental Programme	139
5.3.3 Results and Discussions	142
5.5 SUMMARY	150
<b>6 STRESS CONTROLLED TEST WITH PORE PRESSURE MEASUREMENT</b>	151
6.1 INTRODUCTION	151
6.2 THEORETICAL CONSIDERATIONS	151
6.3 EXPERIMENTAL PROGRAMME	154
6.4 RESULTS AND DISCUSSIONS	157
6.4.1 Normally Consolidated Soils	158
6.4.2 Overconsolidated Soils	168
6.4.3 Time Required for Complete the Test	178
6.5 SUMMARY	178
<b>7 ACCELERATED INCREMENTAL LOAD (AIL) CONSOLIDATION TEST USING CURVE FITTING METHODS</b>	181
7.1 INTRODUCTION	181
7.2 ACCELERATED IL TEST USING THE $\sqrt{t}$ METHOD	182
7.2.1 Theoretical Considerations	182
7.2.2 Experimental Programme	185
7.2.3 Results and Discussions	187
7.3 ACCELERATED IL TEST USING INFLECTION POINT METHOD	195
7.3.1 Theoretical Considerations	195
7.3.2 Experimental Programme	196
7.3.3 Results and Discussions	198
7.4 SUMMARY	214

<b>8 SUMMARY AND CONCLUSIONS</b>	217
8.1 SUMMARY	217
8.2 CONCLUSIONS	219
8.3 SCOPE FOR FUTURE STUDY	221
<b>APPENDICES</b>	223
<b>REFERENCES</b>	247
<b>LIST OF PUBLICATIONS</b>	253

## LIST OF TABLES

<b>Table</b>	<b>Title</b>	<b>Page</b>
2.1	Variation of $c_v$ in the consolidation (Leonards and Ramiah, 1959)	26
2.2	Maximum allowable pore pressure ratio recommended in the literature	49
2.3	Rate of strain as per ASTM D4186	50
2.4	Evaluation of consolidation parameters based on various theories	51
2.5	Duration of CRS Tests from the literature	53
3.1	Properties of the soils used for the study	60
3.2	Minerals present in the reconstituted soils	62
3.3	Classification of soils based on secondary compressibility (Mesri, 1973)	74
3.4	Coefficient of secondary compression from the IL consolidation test	75
3.5	Compression index and Recompression index of the soils	85
3.6	Preconsolidation pressure and OCR	87
3.7	Time taken for complete the EOP test	88
4.1	Strain rates as per ASTM D4186-12 (2012) and the proposed method	100
4.2	Time required for the CSL test as per the proposed method	112
4.3	Compression indices and Recompression indices from IL test and CSL test	119
4.4	Values of preconsolidation pressure from IL test and CSL test	119
5.1	Comparison of Compression index and Recompression Index values of reconstituted soils	130
5.2	Compression index, recompression Index and preconsolidation pressure values of undisturbed Cochin marine clay (19.5 m)	133
5.3	Comparison of compression index and recompression index values	144
5.4	Compression index, recompression Index and preconsolidation values of undisturbed Cochin marine clay (19.5 m)	148
6.1	Typical calculation of effective stress and average degree of consolidation	154

<b>Table</b>	<b>Title</b>	<b>Page</b>
6.2	Values of preconsolidation pressure	173
6.3	Time required for the CSL test and the SC Test	179
7.1	Typical calculation of mid plane pore pressure and effective stress at $U = 90\%$	185
7.2	Values of compression index, recompression index and pre-consolidation pressure from the EOP test and proposed test	193
7.3	Time required for the consolidation test as the proposed $\sqrt{t}$ method	194
7.4	Details of Pore water pressure measurements and estimate	204
7.5	Compression index and recompression index values for Kaolinite	204
7.6	Values of preconsolidation pressure, $c_c$ and $c_r$ from the EOP consolidation test and the proposed test (Inflection point method) for the undisturbed soils	210
7.7	Time required for the conventional EOP consolidation test and the proposed inflection point method	213
7.8	Values of coefficient of secondary compression index	214



## LIST OF FIGURES

Figure	Caption	Page
2.1	(a-g) Types of one-dimensional consolidation tests (Head, 1983)	10
2.2	Components of consolidation cell (a) Model 1 (b) Model 2 (c) Assembled cell of model 1 and (d) Assembled cell of model 2	16
2.3	Schematic of (a) fixed ring consolidometer and (b) floating ring consolidometer	17
2.4	(a) Schematic of typical Rowe cell and (b) Photograph of Rowe cell	19
2.5	(a) Conventional loading Frame (b) Pneumatic consolidation frame (www.globalgilson.com) and (c) Automated consolidation frame	20
2.6	Determination of $c_v$ using the $\log t$ method (Casagrande and Fadum, 1940)	21
2.7	Determination of $c_v$ using $\sqrt{t}$ method (Taylor, 1942)	23
2.8	Determination of $c_v$ using the inflection point method (Robinson, 1997)	23
2.9	Variation of $c_v$ with consolidation pressure (Leonards and Ramiah, 1959)	24
2.10	Typical $e$ - $\log \sigma_v'$ plot for overconsolidated clayey soils	26
2.11	Determination of preconsolidation pressure using (a) Casagrande's method and (b) $\log(1+e)$ versus $\log \sigma_v'$ method	27
2.12	Typical $e$ - $\log \sigma_v'$ plot of structured clay (Ladd and DeGroot, 2003)	27
2.13	Variation of the slope of different modes of representation of $U$ - $T_v$ relationship with $U$ (Sridharan and Prakash, 1997)	29
2.14	Secondary compression effect on (a) $e$ - $\log \sigma_v'$ (Bjerrum, 1967) and (b) Time effect on overconsolidation (Mesri and Castro, 1987)	31
2.15	Strain distribution within specimen for various average strain (a) $c_v/RH_0=0.10$ (b) $c_v/RH_0=1.0$ (c) $c_v/RH_0=10.0$ (Umehara and Zen, 1980)	36

<b>Figure</b>	<b>Caption</b>	<b>Page</b>
2.16	Variation of the consolidation ratio of bottom strain to top strain $F$ for average strain (Umehara and Zen, 1980)	37
2.17	Pore pressure diffusion process during CRS consolidation (a) at immediately after the tests (b) at any intermediate time and (c) when the whole depth participates	39
2.18	CRS test apparatus used by Smith and Wahls (1969)	42
2.19	CRS test apparatus developed by Wissa <i>et al.</i> (1971)	42
2.20	CRS test apparatus suggested by Gorman <i>et al.</i> (1978)	44
2.21	CRS test apparatus suggested by Armour and Drnevich (1986)	44
2.22	CRS test apparatus suggested by Prashant and Vikash (2014)	45
2.23	CRS cell suggested in ASTM D4186-12 (2012)	45
2.24	(a) The plot of $\Delta e$ versus $\log \sigma_v'$ and (b) plot of $c_v$ versus $\Delta e$ for Massena clay (Smith and Wahls, 1969)	47
3.1	Soils selected in the Plasticity chart	61
3.2	Grain size distribution curve	61
3.3	Typical XRD pattern of Red soil 1	62
3.4	Various stages of sample preparation (a) Components of consolidation cell (b) Assembling consolidation ring and collar (c) Pouring the slurry into the ring with collar (d) Preloading stage and (e) Trimming off the extra sample	64
3.5	Typical time-settlement response in IL consolidation test with 24 hours duration for (a) Reconstituted specimen of Gummudipoondi clay and (b) Undisturbed specimen of Cochin marine clay sampled at 21 m depth	66
3.6	EOP consolidation using $\sqrt{t}$ method	68
3.7	Time-settlement plot from the EOP test for Gummudipoondi clay	68
3.8	$c_v$ - $\sigma_v'$ plots from the IL test with 24 hours duration using (a) $\sqrt{t}$ method and	70
3.9	$c_v$ - $\sigma_v'$ plot from the EOP test (a) $\sqrt{t}$ method and (b) Inflection point method	71
3.10	Comparison of $c_v$ values from $\sqrt{t}$ method and Inflection point method from the (a) IL Test with 24 hours and (b) EOP Test	72

<b>Figure</b>	<b>Caption</b>	<b>Page</b>
3.11	Comparison of $c_v$ values from the IL Test with 24 hours and the EOP Test using (a) $\sqrt{t}$ method and (b) Inflection point method	73
3.12	Typical $e$ - $\log t$ curve for Bombay marine clay for the pressure range of 50-100 kPa	74
3.13	Coefficient of permeability from the IL test with 24 hours duration(a) calculated and (b) measured	77
3.14	Coefficient of permeability calculated from the EOP test	78
3.15	Comparison of the coefficient of permeability calculated and measured from the conventional IL test with 24 hours duration	78
3.16	Comparison of coefficient of permeability calculated from the conventional IL test with 24 hours duration and the EOP test	79
3.17	$e$ - $\log \sigma_v'$ curves for (a) Red soil 1 (b) Red soil 2 (c) Gummudipoondi clay (d) Kaolinite (e) Taramani clay (f) Siruseri clay and (g) Bombay marine clay	81
3.18	$e$ - $\log \sigma_v'$ curves for Undisturbed clays from the IL test with 24 hours (a) Madhavaram clay (6 m) (b) Bombay marine clay (12 m) (c) Cochin marine clay (21 m) (d) Cochin marine clay (5 m) (e) Cochin marine clay (19.5 m) and (f) Cochin marine clay (16 m)	83
3.19	$e$ - $\log \sigma_v'$ curves for Undisturbed clays from the EOP test (a) Madhavaram clay (6 m) (b) Cochin marine clay (21 m) and (c) Cochin marine clay (16 m)	84
3.20	Comparison of compression indices and recompression indices from the IL test 24 hours and the EOP test	86
3.21	$\log(1+e)$ - $\log \sigma_v'$ plot for Cochin marine clay 19.5 m	87
4.1	(a) Schematic diagram of the CRS cell (b) Components of the cell and (c) Assembled cell	93
4.2	(a) Schematic diagram of the permeability set-up (b) Photograph of the permeability set-up and (c) Capillarity rise observed in the 3mm diameter burette	96
4.3	(a) Schematic diagram and (b) Photograph of CRS set-up used for the study	97
4.4	Validation of the 3 mm diameter burette used for measuring $k$ , typically for Bombay marine clay 12 m (UDS)	98

<b>Figure</b>	<b>Caption</b>	<b>Page</b>
4.5	Pore pressure ratio variation with effective stress of reconstituted soils based on the (a) ASTM D4186-12 (2012) standard and (b) Proposed procedure	101
4.6	Variation of $m_v \times \sigma_v'$ with effective stress	104
4.7	Coefficient of consolidation variation with effective stress from the IL test	104
4.8	Pore pressure ratio variation with the effective stress of the overconsolidated soils	105
4.9	Comparison of CSL Test with IL Test results for Kaolinite	109
4.10	Comparison of CSL Test with IL Test results for Gummudipoondi clay	111
4.11	Comparison of $c_c$ and $c_r$ from CSL Test and IL test for the reconstituted normally consolidated soils	112
4.12	Comparison of CSL Test and IL Test results for the overconsolidated Kaolinite specimen with $\sigma_c' = 200$ kPa	114
4.13	Comparison of CSL Test and IL Test results for the overconsolidated Gummudipoondi clay specimen with $\sigma_c' = 50$ kPa	115
4.14	Comparison of CSL Test and IL Test results for CMC (16 m)	116
4.15	Comparison of CSL Test and IL Test results for CMC (5 m)	117
4.16	Comparison of CSL Test and IL Test results for CMC (19.5 m)	118
5.1	Schematic diagram of the standard CRS cell	122
5.2	Schematic diagram of the simplified CRS Cell	123
5.3	Photographic view of the proposed CRS apparatus (a) Components of the cell and (b) Assembled cell	124
5.4	Photograph of CRS set-up used for the study	126
5.5	Total stress and Pore pressure –Axial strain plot for (a) Red Soil 1 (b) Kaolinite (c) Taramani clay and (d) Bombay marine clay	128
5.6	$e$ - $\log \sigma_v'$ plot for (a) Red Soil 1 (b) Kaolinite (c) Taramani clay and (d) Bombay marine clay	129
5.7	$c_v$ - $\log \sigma_v'$ plot for (a) Red Soil 1 (b) Kaolinite (c) Taramani clay and (d) Bombay marine clay	131

<b>Figure</b>	<b>Caption</b>	<b>Page</b>
5.8	<i>e</i> -log <i>k</i> plot for (a) Red Soil 1(b) Kaolinite (c) Taramani clay and (d) Bombay marine clay	132
5.9	(a) Total stress and pore pressure–axial strain plot (b) <i>e</i> -log $\sigma_v'$ plot (c) <i>c<sub>v</sub></i> -log $\sigma_v'$ plot and (d) <i>e</i> -log <i>k</i> plot for the undisturbed Cochin marine clay (19.5 m)	134
5.10	Photographs of (a) Type-1 and (b) Type-2 consolidation cells	136
5.11	Schematic diagram of type-1 consolidation cell after modification	137
5.12	Photographic view of (a) components of the proposed CRS apparatus and (b) assembled apparatus	138
5.13	Schematic diagram of type-2 consolidation cell after modification	139
5.14	Modified consolidation cell for CRS test assembled in the triaxial loading frame	141
5.15	Total stress and pore pressure –axial strain plot for reconstituted specimens of (a) Red Soil 1(b) Kaolinite (c) Taramani clay and (d) Bombay marine clay	143
5.16	Pore pressure ratio versus effective stress	144
5.17	<i>e</i> -log $\sigma_v'$ plot for (a) Red Soil 1 (b) Kaolinite (c) Taramani clay and (d) Bombay marine clay	145
5.18	<i>c<sub>v</sub></i> -log $\sigma_v'$ plot for (a) Red Soil 1 (b) Kaolinite (c) Taramani clay and (d) Bombay marine clay	146
5.19	<i>e</i> -log <i>k</i> plot for (a) Red Soil 1 (b) Kaolinite (c) Taramani clay and (d) Bombay marine clay	147
6.1	Variation of degree of dissipation with degree of consolidation	153
6.2	Schematic diagram of the cell	156
6.3	(a) Components of the cell (b) Assembled cell and (c) Complete set-up	156
6.4	Pore pressure versus time of Gummudipoondi clay (100-200 kPa)	157
6.5	(a) Time-excess pore pressure and (b) Time-settlement/swell data for Red soil 2	159

<b>Figure</b>	<b>Caption</b>	<b>Page</b>
6.6	Comparison of $e$ - $\log \sigma_v'$ plot from SC test, IL test and CSL test of reconstituted soils in NC state for (a) Red soil 1 (b) Red soil 2 (c) Gummudipoondi clay (d) Kaolinite (e) Taramani clay (f) Siruseri clay and (g) Bombay marine clay	161
6.7	Comparison of Compression index and Recompression index from the proposed test with IL test	162
6.8	Comparison of $c_v$ - $\sigma_v'$ variation from SC test, IL test and CSL test of reconstituted soils in NC state for (a) Red soil 1 (b) Red soil 2 (c) Gummudipoondi clay (d) Kaolinite (e) Taramani clay (f) Siruseri clay and (g) Bombay marine clay	164
6.9	Comparison of coefficient of consolidation from the proposed test with IL test	165
6.10	Comparison of $e$ - $\log k$ curve from SC test, IL test and CSL test of reconstituted soils for (a) Red soil 1 (b) Red soil 2 (c) Gummudipoondi clay (d) Kaolinite (e) Taramani clay (f) Siruseri clay and (g) Bombay marine clay	167
6.11	(a) Time-excess pore pressure and (b) Time-settlement data from the proposed test of undisturbed soil (CMC 19.5 m)	169
6.12	Comparison of $e$ - $\log \sigma_v'$ plot from SC test, IL test and CSL test of reconstituted soils in OC state (a) Gummudipoondi clay (b) Kaolinite and (c) Taramani clay	170
6.13	Comparison of $e$ - $\log \sigma_v'$ plot from SC test, IL test and CSL test of undisturbed soils (a) Cochin marine clay (5 m) (b) Cochin marine clay (19.5 m) and (c) Bombay marine clay (12 m)	171
6.14	Comparison of Compression index and Recompression index from the proposed test with IL test	172
6.15	Typical $\log(1+e)$ versus $\log \sigma_v'$ plot for Cochin marine clay (19.5 m)	172
6.16	Comparison of $c_v$ - $\sigma_v'$ variation from SC test, IL test and CSL test of reconstituted soils in OC state (a) Gummudipoondi clay (b) Kaolinite and (c) Taramani clay	174
6.17	Comparison of $c_v$ - $\sigma_v'$ variation from SC test, IL test and CSL test of undisturbed soils (a) Cochin marine clay (5 m) (b) Cochin marine clay (19.5 m) and (c) Bombay marine clay (12 m)	175

<b>Figure</b>	<b>Caption</b>	<b>Page</b>
6.18	Comparison of $e$ -log $k$ curve from SC test, IL test and CSL test of reconstituted soils (a) Gummudipoondi clay (b) Kaolinite and (c) Taramani clay	176
6.19	Comparison of $e$ -log $k$ curve from SC test, IL test and CSL test of undisturbed soils (a) Cochin marine clay (5 m) (b) Cochin marine clay (19.5 m) and (c) Bombay marine clay (12 m)	177
7.1	Variation of pore pressure ratio ( $u/u_0$ ) with ( $z/d$ )	183
7.2	Evaluation of degree of consolidation- $\sqrt{t}$ method	186
7.3	$\sqrt{t}$ –settlement plot for Gummudipoondi clay	187
7.4	Comparison of $e$ -log $\sigma_v'$ curves of reconstituted soils obtained from the EOP test and the proposed methods for (a) Red soil 1 (b) Red soil 2 (c) Gummudipoondi clay (d) Taramani clay and (e) Bombay marine clay	189
7.5	Comparison of values of compression index and recompression index obtained from the EOP and the $\sqrt{t}$ methods	190
7.6	Comparison of $c_v$ values from the EOP and the $\sqrt{t}$ tests of reconstituted soils	190
7.7	Comparison of $e$ -log $\sigma_v'$ curves of undisturbed soils obtained from the conventional IL consolidation test and the $\sqrt{t}$ method for (a) Cochin marine clay (5 m) (b) Bombay marine clay (12 m) and (c) Madhavaram clay (6 m)	192
7.8	Comparison of $c_v$ values from the EOP and $\sqrt{t}$ methods for undisturbed soils	193
7.9	Variation of pore pressure ratio ( $u/u_0$ ) with ( $z/d$ )	196
7.10	Identification of inflection point	197
7.11	Comparison of coefficient of consolidation from the EOP and the proposed methods	198
7.12	Comparison of $e$ -log $\sigma_v'$ curves of reconstituted soils from the EOP and proposed tests for (a) Red soil 1 (b) Red soil 2 (c) Gummudipoondi clay (d) Taramani clay and (e) Bombay marine clay	200

<b>Figure</b>	<b>Caption</b>	<b>Page</b>
7.13	Comparison of Compression index and Recompression index obtained from the EOP and the proposed methods of reconstituted soils	201
7.14	(a) Time-settlement curve (b) Time-pore pressure curve and (c) $e$ - $\log \sigma_v'$ for Kaolinite during loading stages	203
7.15	(a) Time-swelling curve (b) Time-negative pore pressure curve and (c) $e$ - $\log \sigma_v'$ for Kaolinite during unloading stages	205
7.16	Swelling curve based on the ultimate swelling estimate for kaolinite	207
7.17	Swelling curves from the EOP method and the proposed method using inflection point method based on the ultimate swelling	208
7.18	Recompression index obtained from the EOP method and the proposed method (Inflection point method) based on the ultimate swelling estimation of reconstituted soils	209
7.19	Swelling curves from the EOP method and the proposed method using $\sqrt{t}$ method based on the ultimate swelling	209
7.20	Comparison of $e$ - $\log \sigma_v'$ curves of undisturbed soils obtained from the EOP and the proposed method for (a) Cochin marine clay (21 m) (b) Cochin marine clay (16 m) and (c) Madhavaram clay (6 m)	211
7.21	Coefficient of consolidation from the EOP and the proposed method (Inflection point method) for the undisturbed soils	212
7.22	Coefficient of secondary compression from $e$ - $\log t$ curve for Bombay marine clay	214



## ABBREVIATIONS

ADU	Autonomous Data Unit
ASTM	American Society of Testing Materials
BMC	Bombay marine clay
BPC	Back Pressure Control
BS	British Standard
CG	Controlled Gradient
CH	Clayey soil with High plasticity
CI	Clayey soil with Intermediate plasticity
CL	Clayey soil with Low plasticity
CMC	Cochin marine clay
COV	Coefficient Of Variance
CPR	Constant Pore pressure Ratio
CRL	Constant Rate of Loading
CRS	Constant Rate of Strain
CSL	Controlled-Strain Loading
EOP	End-Of-Primary
ICDD	International Centre for Diffraction Data
IL	Incremental Loading
IPM	Inflection Point Method
IS	Indian Standard
LI	Liquidity Index
LIR	Load Increment Ratio
LVDT	Linear Variable Displacement Transducer
MC	Madhavaram clay
MH	Silty soil with High plasticity

MI	Silty soil with Intermediate plasticity
NC	Normally Consolidated
OC	Overconsolidated
OCR	Overconsolidation Ratio
OH	Organic soil with High plasticity
OI	Organic soil with Intermediate plasticity
PPT	Pore Pressure Transducer
PwP	Pore water Pressure
RFC	Restricted Flow Consolidation
SC	Stress Controlled
UDS	Undisturbed Soil
USCS	Unified Soil Classification System
XRD	X- Ray Diffraction

# NOTATIONS

## English Symbols

$A^0$	Angstrom
$a_v$	Coefficient of compressibility
$b$	Constant (Smith and Wahls, 1969)
$c_c$	Compression Index
$c_r$	Recompression Index
$c_v$	Coefficient of vertical consolidation
$c_\alpha$	Coefficient of secondary compression
$d$	Drainage path
$e$	Void ratio
$e_p$	End-Of-Primary void ratio
$\bar{e}$	Average void ratio
$e_0$	Initial void ratio
$F_3$	Transient term
$H$	Thickness of clay layer
$H_i, H_0$	Initial height of the specimen
$H_d, H_{ud}$	Depth of drained, undrained phase
$I_p$	Plasticity index
$K_0$	Coefficient of earth pressure at rest
$k$	Coefficient of permeability

$k_i$	Initial permeability
$m$	Proportionality constant
$m_v$	Coefficient of volume compressibility
$P_a$	Atmospheric pressure
$p'$	Mean normal effective stress
$q$	Deviator stress
$R, r$	Rate of strain
$r_u$	Pore pressure ratio
$r_{ua}$	Allowable pore pressure ratio
$(r_{ua})_{max}$	Maximum allowable pore pressure ratio
$S$	Settlement
$S_{90}$	Settlement @ 90% degree of consolidation
$S_0$	Initial settlement
$S_{100}$	Primary settlement
$T_v$	Time factor
$t$	Time
$t_i$	Time for inflection
$t_{50}, t_{70.15}, t_{90}, t_{100}$	Time for 50, 70.15, 90 and 100% consolidation
$t_f$	Time of failure
$t_p$	Time for primary consolidation
$U$	Average degree of consolidation
$U_b$	Degree of dissipation

$U_z$	Degree of consolidation
$u$	Pore water pressure
$u_b$	Base pore water pressure
$u_r$	Residual pore pressure
$u_t$	Pore water pressure at any time
$u_0$	Initial pore water pressure
$w_l$	Liquid limit
$w_n$	Natural water content
$X$	Dimensionless depth factor
$z$	Depth
$z_p$	Depth of interface

## Greek Symbols

$\alpha$	Constant (Smith and Wahls, 1969)
$\beta$	Dimensionless strain parameter
$\Delta p'$	Change in mean effective stress
$\Delta \sigma_t$	Total stress increment
$\Delta u$	Excess pore pressure
$\delta t$	Time interval
$\delta z$	Change in thickness
$\delta_{70.15}, \delta_{100}$	Settlements corresponding to $U = 70.15\%$ , $100\%$
$\varepsilon$	Strain
$\varepsilon_E$	Eulerian Strain
$\bar{\varepsilon}$	Average strain
$\phi'$	Angle internal friction
$\gamma_b$	Bulk unit weight
$\gamma_w$	Unit weight of water
$\gamma_d$	Dry unit weight
$\mu$	Micron
$\rho$	Settlement
$\rho_p$	Ultimate settlement
$\sigma_{hu}$	Total horizontal stress
$\sigma, \sigma_v$	Total stress

$(\sigma_v)_{max}$	Maximum total stress
$\sigma_c'$	Preconsolidation pressure
$\sigma_v', \sigma_i', \sigma_{i-1}'$	Effective stress
$\sigma_{v0}'$	In-situ overburden pressure
$\theta$	Scattering angle





# CHAPTER 1

## INTRODUCTION

### 1.1 BACKGROUND

Consolidation properties are essential for the design of a variety of geotechnical engineering structures. These properties are derived by performing one-dimensional consolidation tests. The important consolidation properties derived from one-dimensional consolidation test are compression index ( $c_c$ ), recompression index ( $c_r$ ), preconsolidation pressure ( $\sigma_c'$ ), coefficient of volume compressibility ( $m_v$ ), coefficient of consolidation ( $c_v$ ) and the coefficient of secondary compression ( $c_\alpha$ ). Coefficient of permeability ( $k$ ) is often derived from the one-dimensional consolidation test. Various types of one-dimensional consolidation tests are available in the literature to determine the consolidation properties. Conventionally available one-dimensional consolidation test is an incremental loading (IL) consolidation test and the test takes about 10-14 days to complete if the duration between successive increment is 24 hours (Sridharan *et al.* 1999). In addition, the number of data points obtained is also limited, which often fails to depict the complete void ratio ( $e$ )-consolidation pressure ( $\sigma_v'$ ) curve.

In order to overcome the limitations of conventional IL consolidation test, attempts were made in the literature to reduce the duration of the load increment of IL test. Several other types of tests like constant rate of strain (CRS) consolidation test and controlled gradient (CG) consolidation tests etc. are also reported in the literature. Though CRS test is widely used, reliable guidelines are not available to fix the strain rate. It is attempted in the present study to develop both stress controlled and strain controlled consolidation testing procedures, so as to develop faster testing procedures.

### 1.2 INCREMENTAL LOADING (IL) CONSOLIDATION TEST

Incremental loading one-dimensional consolidation test is a stress controlled test, in which the load is incrementally applied to a laterally confined soil specimen and the

resulting vertical deformations are continuously recorded. These tests are advanced slowly, as sufficient time is allowed between increments. Terzaghi (1925) developed the one-dimensional consolidation theory for the case of sustained loading. Various types of IL consolidation test are available in the literature to determine consolidation parameters, which are oedometer test, rapid consolidation test and End-Of-Primary consolidation test.

### **1.2.1 Conventional IL (Oedometer) Consolidation Test**

Incremental Loading (IL) consolidation test is the most commonly used consolidation test in which the load is incrementally applied and the resulting vertical deformations are continuously recorded for 24 hours. The procedure for conventional one-dimensional IL consolidation test is well established and is widely used in practice. Several protocols are also available (for example ASTM D2435-11 (2011); BS 1377-5 (1990); IS 2720-15 (1986)). One of the main limitations of the IL consolidation test is that it takes about 10-14 days to complete one test, as sufficient time is allowed between increments.

### **1.2.2 Rapid Consolidation Test**

Newland and Allely (1960) recommended reducing the duration of load increment of conventional IL consolidation by applying the subsequent load increment as soon as 100% primary consolidation is over. The procedure suggested may save considerable consolidation time compared to 24 hour duration test. However, high plastic clays may take longer time to reach 100% primary consolidation. Effect of short duration of load on consolidation test was studied by Sridharan *et al.* (1994). They observed that load duration of 30 minutes is sufficient for kaolinite and 4 hours is required for a black cotton soil. As the load duration required depends on the type of soil, judging the duration required for different types of soils is difficult.

Subsequently, Sridharan *et al.* (1999) suggested a rapid consolidation testing procedure. The time-settlement data is monitored during the consolidation and the degree of consolidation is evaluated continuously using the rectangular hyperbola method. Once the straight line part is obtained in the transformed plot of time/settlement versus time plot, which occurs in the range of degree of consolidation ( $U$ ) of about 60%-90%, the next increment is applied. The effective stress is derived based on degree of consolidation

which is not appropriate. The other limitation is that the progress of consolidation process is not directly evident as the rectangular hyperbolic plot is a transformed plot in which the settlement is divided by time. In addition, the unloading part of the consolidation test was not analyzed in their study which is essential for evaluating the recompression index.

### **1.2.2 End-Of-Primary (EOP) Consolidation Test**

End-Of-Primary consolidation is taken as the condition at which the excess pore pressure developed for each increment of load dissipates to zero or to a very small value such as 1 kPa (Terzaghi *et al.* 1996). Generally, the excess pore pressure is not measured during conventional IL consolidation test. Therefore, each increment of load is applied and allowed to act long enough to define the EOP void ratio ( $e_p$ ). The EOP consolidation can be identified by the standard graphical procedures such as  $\log t$  and  $\sqrt{t}$  methods. In the conventional IL consolidation test with 24 hours duration, some secondary compression occurs. Therefore, the  $e$ - $\log \sigma_v'$  curve obtained based on 24 hours duration includes some secondary compression. The  $e$ - $\log \sigma_v'$  curve without secondary compression is called as the End-of-Primary (EOP) consolidation curve.

## **1.3 CONSTANT RATE OF STRAIN (CRS) CONSOLIDATION TEST**

Constant rate of strain consolidation test is a strain controlled test in which the soil specimen is subjected to uniform deformations in a strain controlled loading frame. Hamilton and Crawford (1959) were the first to introduce the constant rate of strain (CRS) consolidation test. During the CRS test, the load carried by the specimen and the pore water pressure developed at the base are continuously measured. Several theories are reported to model the pore pressure variations within the specimen. As the CRS test is strain rate dependent, the selection of strain rate is critical and was studied by many researchers.

### **1.3.1 Apparatus for CRS Test**

Conventional fixed ring consolidation cell with triaxial compression machine, to apply the deformation, was used by Hamilton and Crawford (1959). Subsequently, Smith and Wahls (1969) also used fixed ring consolidometer, but the base was sealed to measure the

base pore pressure with a pore pressure transducer. After several modifications, Wissa *et al.* (1971) proposed a general purpose consolidometer for conducting CRS test in which the specimen can be saturated at constant volume under a back pressure with no lateral strain. Gorman *et al.* (1978) modified the triaxial cell to perform the CRS test. The triaxial chamber with consolidation ring and a loading press were used to deform the specimen at constant rate. Similarly, Armour and Drnevich (1986) modified the CRS equipment to measure the permeability in addition to the base pore pressure. Recently, Vikash (2013) modified the triaxial cell for CRS test. The consolidation ring was placed inside the regular triaxial cell. Suitable connections were made from the base of the consolidation cell to the outlet port of the triaxial cell. ASTM D4186-12 (2012) standardized the apparatus which is similar to the one developed by Wissa *et al.* (1971). A simple CRS apparatus like oedometer cell is lacking in the literature.

### **1.3.2 Theories of CRS Test**

Smith and Wahls (1969) were the first to develop a theory for CRS consolidation and derived an approximate solution. They expressed the void ratio variation with respect to depth and time. This theory has two major issues. First, the assumption that the void ratio is a linear function of the time and depth variables is difficult to be evaluated. The second problem is that they assumed a parameter  $b$  which is not known, and there is no procedure for its determination. Since the results depend on the chosen value of  $b$ , it requires a reference test to be performed on similar specimens. Thereafter, Wissa *et al.* (1971) ignored some of the assumptions of the theory by Smith and Wahls (1969) and developed more comprehensive theory for analysing the CRS consolidation test. They formulated the governing equation based on strain distribution across the depth of the specimen and derived a solution which consist of transient and steady state components. Since then, the theory of Wissa *et al.* (1971) is widely used to interpret the CRS consolidation data, and also was incorporated in ASTM D4186-82 (1982). Yoshikuni *et al.* (1995) developed a much simpler theory, with the assumption that once steady state is reached the strain rate at every location is equal to the average strain. Among these theories, the theory of Smith and Wahls (1969) does not consider the transient condition, whereas other theories considered it. As the existence of transient state is likely to happen, the theories of Wissa *et al.* (1971) and Yoshikuni *et al.* (1995) are better for the interpretation of CRS test data.

Few more theories are available for the interpretation of large strain consolidation test. Umehara and Zen (1980) and Lee (1981) developed theories and the governing differential equations were solved numerically with appropriate boundary conditions and assuming non-dimensional parameters. They came up with a series of charts to determine the consolidation parameters. No rational procedure was reported to which of the curves better approximate to the true material behaviour. Recently, Vikash (2013) developed a theory based on the moving boundary concept.

### **1.3.3 Strain Rate Selection Criteria**

Fixing proper strain rate is the most crucial part of the CRS test in order to obtain compressibility characteristics which are consistent with the Oedometer test. Smith and Wahls (1969) provided the results of constant rate of strain consolidation tests on two clays such as Massena clay and Calcium montmorillonite. The comparison showed that for higher rates of strain, the  $e$ - $\log \sigma_v'$  curve obtained from the CRS tests deviate considerably from those obtained from the conventional tests. High strain rate will result in rapid increase in excess pore pressure leading to overestimation of preconsolidation pressure and steady state condition will not be achieved when the increase in pore pressure is too rapid. When the rate is too low there will be no significant increase in pore water pressure which will result in unreasonably high values of  $c_v$  (Smith and Wahls, 1969). Therefore, correct rate of strain shall be fixed so as to obtain reliable parameters.

Several guidelines were suggested by researchers so as to select the right strain rate to perform CRS test. Smith and Wahls (1969) suggested a method based on the theoretical model. However, the equation of strain includes consolidation parameters. Therefore, some parameter needs to be assumed before starting the CRS test. Lee (1981) proposed a dimensionless strain parameter ( $\beta$ ), which depends on coefficient of consolidation. Armour and Drnevich (1986) developed an equation to fix strain rate based on the liquidity index and permeability. Similarly, ASTM standards originally recommended the use of liquid limit as the basis (ASTM D4186-82 (1982)). However, later in (2012) it was revised based on soil classification. The available methods either require the assumption of critical parameters or rely on empirical relations. One of the problems associated with fixing the rate based on liquid limit is that the coefficient of consolidation need not be the same for two soils having the same liquid limit. Similarly, soil in a particular group can

exhibit different value of  $c_v$ . Crawford (1988) reported that the strain rate does not depend on the liquid limit.

In addition to the strain rate selection, there is related problem of the maximum allowable pore pressure ratio ( $r_u$ , defined as the ratio of pore pressure developed at the base of the specimen to the applied total stress) and different researchers suggested range of maximum allowable pore pressure ratio ( $r_{ua}$ ), which varies from 3%-50%. ASTM D4186-12 (2012) recommended the range of allowable pore pressure ratio of 3%-15%, which is generally used in practice.

#### **1.4 NEED FOR THE STUDY**

The need for study are summarized below

- a) Several guidelines are suggested in the literature to select proper strain rate to conduct CRS Test. These methods either require the assumption of critical parameters or rely on empirical relations or an advance test. No rational procedure to fix the strain rate for conducting CRS Test is available.
- b) Various apparatus are suggested in the literature to perform constant rate of strain consolidation test. However, the apparatus design is not simple. Development of a simplified CRS cell is scarce in literature.
- c) While CRS test with pore pressure measurement at the base of the specimen is popular in the literature, studies on stress controlled consolidation test with pore pressure measurements so as to reduce the test duration is not attempted in the literature.
- d) Reduced duration of conventional IL consolidation test based on standard curve fitting procedure is not properly addressed in the literature. Development of procedure and interpretation techniques for faster consolidation testing based on conventional IL test needs to be studied.

## 1.5 OBJECTIVES

The overall objective of the present study is to develop procedures for carrying out one-dimensional consolidation tests in short duration. The specific objectives are

- (a) To develop a rational procedure to fix the strain rate of CRS test and guidelines to control the strain rate during CRS test, so as to limit the pore pressure ratio within the permissible limits.
- (b) To develop a simplified CRS apparatus and to modify the conventional fixed ring consolidometer to perform CRS test.
- (c) To study the stress controlled (SC) consolidation test with pore pressure measurements, so as to develop a faster consolidation testing procedure and
- (d) To develop testing procedures for accelerated incremental load consolidation test using standard curve fitting procedures.

## 1.6 ORGANISATION OF THE THESIS

The thesis is organized into eight chapters. The methodologies adopted to meet the objectives are described in the respective chapters. This chapter (**Chapter 1**) gives a brief introduction to the present work and the objectives.

State of the art related to various types of one-dimensional consolidation testing methods to determine the consolidation parameters are reviewed in **Chapter 2**. Studies related to one-dimensional consolidation test under incremental loading and strain controlled consolidation test are discussed in detail.

Detailed experimental works were performed to validate the proposed methodologies. Soils with varying plasticity characteristics and few undisturbed soils were collected. The basic characterization of the selected soils and the control test results are discussed in **Chapter 3**. The conventional one-dimensional IL consolidation test with 24 hours duration and EOP consolidation tests are performed as control tests.

Constant rate of strain (CRS) consolidation test is one of the widely used one-dimensional consolidation tests. However, guidelines to fix proper strain rate are not well established. In **Chapter 4**, a rational method is proposed to fix the initial strain rate of CRS consolidation test, which is based on the initial permeability measurements. An observational approach to control the strain rate during the CRS consolidation test, so as to maintain the pore pressure ratio within the permissible limits, is also described. Detailed experimental works were carried out to validate the proposed methods.

**Chapter 5** deals with the design and fabrication of CRS apparatus to perform one-dimensional consolidation test. A simplified CRS apparatus is proposed, where the loading piston is the main component. In addition, the modification required in the conventional fixed ring consolidometer to perform the CRS test is also presented.

**Chapter 6** deals with a new stress controlled (SC) consolidation testing procedure with pore pressure measurements, where the increment of load was applied based on pore pressure dissipation. To accelerate the stress controlled consolidation test with pore pressure measurement, the pore pressure was allowed to dissipate to 15% of the total stress applied, before applying the next increment. The results obtained are compared with CRS test and IL test, so as to validate the proposed method.

**Chapter 7** deals with accelerated incremental load tests to determine the End-of-Primary (EOP) parameters, where the duration of load increments is reduced based on standard curve fitting procedures. Taylor's  $\sqrt{t}$  method and Inflection point method are used to evaluate the degree of consolidation. The results obtained are compared with EOP consolidation test.

Finally, the summary of the study and the major conclusions drawn are given in **Chapter 8**.



# **CHAPTER 2**

## **LITERATURE REVIEW**

### **2.1 INTRODUCTION**

Accurate determination of consolidation parameters of soils is required for the design of many geotechnical engineering structures. The consolidation settlement estimation has two parts such as the total settlement and rate of settlement. The consolidation parameters related to the total settlement are compression index ( $c_c$ ), recompression index ( $c_r$ ), and preconsolidation pressure ( $\sigma'_c$ ). The parameters related to the rate of settlement are coefficient of consolidation ( $c_v$ ) and coefficient of secondary compression ( $c_\alpha$ ). Instead of  $c_c$ , the coefficient of volume change ( $m_v$ ) is often used. Coefficient of permeability ( $k$ ) can be derived from  $c_v$  and  $m_v$ . These parameters are conventionally determined by performing one-dimensional consolidation test. A comprehensive review of the literature related to one-dimensional consolidation tests is done in this chapter.

### **2.2 TYPES OF ONE-DIMENSIONAL CONSOLIDATION TESTS**

Consolidation properties are usually determined from laboratory one-dimensional consolidation tests in which a laterally confined soil specimen is subjected to consolidation. Various types of one-dimensional consolidation testing methods are reported in the literature (Head, 1983). The one-dimensional consolidation testing methods are classified based on the controlling factors as shown in Figure 2.1. Incremental Loading (IL) consolidation test, Constant Rate of Strain (CRS) consolidation test, Controlled Gradient (CG) consolidation tests, Constant Rate of Loading (CRL) test, Restricted Flow Consolidation (RFC) test, Constant Pore pressure Ratio (CPR) test and Back Pressure Control (BPC) consolidation tests are the consolidation testing methods reported in the literature which are briefly explained in the next sections.

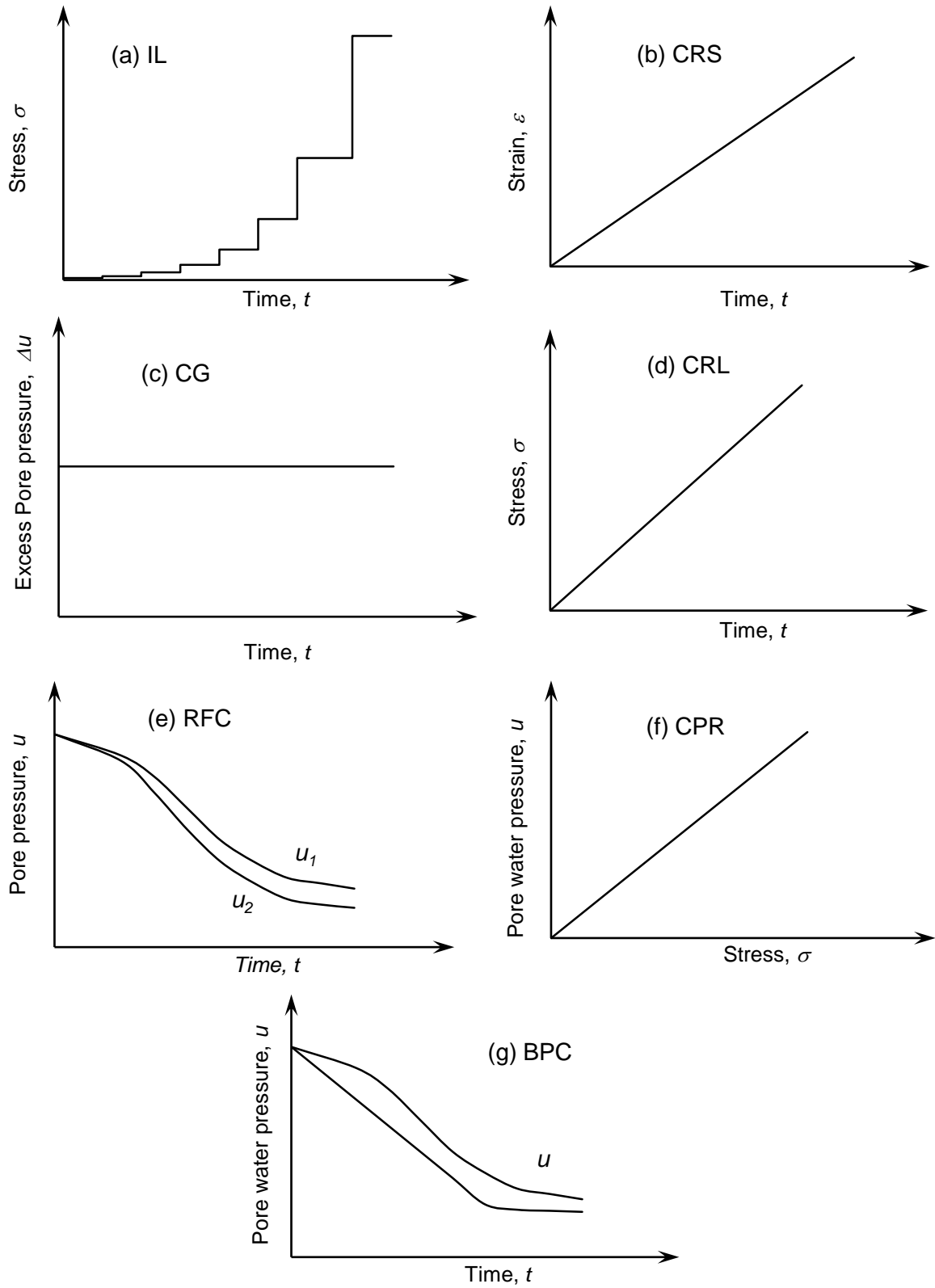


Figure 2.1: (a-g) Types of one-dimensional consolidation tests (Head, 1983)

### **2.2.1 Incremental Loading (IL) Consolidation Test**

The most commonly used one-dimensional consolidation test is the incrementally loading (IL) consolidation test which is also called as oedometer test. It is a stress controlled test in which a laterally confined soil specimen is subjected to a sustained load (Figure 2.1(a)) with load increment ratio (LIR) of 1.0 and the resulting vertical deformations are continuously recorded for 24 hours. The testing procedure of IL consolidation test is well established, interpretation is straight forward and many protocols are also available (ASTM 2435-11 (2011); BS 1377-5 (1990); IS 2720-15 (1986)). The test is advanced slowly and takes about two weeks to complete (Sridharan *et al.* 1999).

### **2.2.2 Constant Rate of Strain (CRS) Consolidation Test**

Hamilton and Crawford (1959) developed the constant rate of strain consolidation test and is a strain controlled test (Figure 2.1(b)). In the CRS test, a laterally confined specimen is subjected to uniform deformation in a strain controlled loading frame under one-way drainage through the top. During the CRS test, the load carried by the specimen and the pore water pressure developed at the base of the specimen are continuously recorded. Smith and Wahls (1969) developed the theory to analyse CRS test data. Subsequently, many developments took place both in the theory and experimental procedure. However, fixing the proper strain rate is critical for the CRS test.

### **2.2.3 Controlled Gradient (CG) Test**

The CG test was proposed by Lowe *et al.* (1969) which is similar to the CRS test except that the specimen is loaded at a rate such that the excess pore pressure generated at the base of the specimen remained constant (Figure 2.1(c)). A constant hydraulic gradient is, therefore, established across the consolidating specimen. Controlled gradient equipment was developed to load the specimen at a rate that will maintain a constant pore water pressure at the base of the specimen. The CG test requires continuous monitoring and automation.

#### **2.2.4 Constant Rate of Loading (CRL) Test**

Aboshi *et al.* (1970) proposed a constant rate of loading (CRL) test (Figure 2.1(d)). The procedure was developed based on the theoretical work of Schiffman (1958). The CRL test can simulate the construction loading conditions like those imposed by embankments, dams etc. One of the advantages of CRL test is that the test is faster compared to standard IL test. The CRL test requires two to five days to complete the test. However, the test has few limitations such as (i) a pacer control is required for the CRL test and (ii) the rate of loading has to be selected before the commencement of test which is critical. The rate of loading depends on the permeability and compressibility of the soils.

#### **2.2.5 Restricted Flow Consolidation (RFC) Test**

Hoare (1980) developed a restricted flow consolidation (RFC) test (Figure 2.1(e)). The principle of RFC test is that the pore pressure distribution across the specimen is controlled nearly uniform. Drainage is not allowed in the early stage of test till the pore pressure is equal to total stress. If the drainage is allowed at one face, the pressure drops at the drained face. Therefore, the pressure drop is controlled by using a flow restrictor. The permeability of flow restrictor should be less than the soil permeability. Therefore, it is possible to obtain continuous void ratio- effective stress curve by applying one total stress increment. The advantages of RFC test are: (i) the permeability of soil can be measured during test and (ii) the pore pressure distribution is linear and does not require any theoretical assumptions. The limitation of the test are: (i) it requires a differential pore pressure transducer to measure the difference in pore pressure between the undrained and drained faces and (ii) in case any leakage at the undrained face, the differential pore pressure transducer may get damaged.

#### **2.2.6 Constant Pressure Ratio (CPR) Test**

Janbu *et al.* (1981) proposed a Constant Pressure Ratio (CPR) test (Figure 2.1(f)). It is a continuous loading test, in which the pore pressure ratio ( $r_u$ , defined as the ratio of the pore pressure developed at the base ( $u$ ) to the total stress ( $\sigma_v$ )) is maintained constant. A computer control is essential for maintaining a constant pore pressure ratio.

### **2.2.7 Back Pressure Consolidation (BPC) Test**

Head (1983) developed a Back pressure control consolidation (BPC) test (Figure 2.1(g)). The test is similar to the restricted flow consolidation test. One load application and controlling the back pressure is required. Rate of change in back pressure needs to be decided before the test. The set up requires a feed-back control and motorized pressure application system.

*Out of the testing methods reviewed above, the IL test and CRS test are the popular consolidations testing methods widely used in practice. Other one-dimensional consolidation tests require special controlling equipment or continuous automation so as to maintain the excess pore water pressure. Hence, the focus of the present study is on IL and CRS tests. Therefore, the literature related to IL test and CRS tests are reviewed in detail in the subsequent sections.*

## **2.3 REVIEW OF IL CONSOLIDATION TEST**

Incremental Loading (IL) consolidation test is the most commonly used consolidation test in which the load is incrementally applied and the resulting vertical deformations are continuously recorded for 24 hours. The basic theory of one-dimensional consolidation, apparatus details, testing procedure are reviewed in this chapter. In addition, attempts made in the literature to shorten the testing time of IL tests are also reviewed.

### **2.3.1 Theory of One-Dimensional Consolidation**

Terzaghi (1925) developed the theory of one-dimensional consolidation for the case of sustained loading. The theory was developed based on the following simplifying assumptions.

- Soil is homogeneous and completely saturated
- Compression and flow are one-dimensional (vertical)
- Compression of soil layer is due to squeezing out of water from the voids
- Darcy's law is valid
- Both soil grain and water are incompressible
- Coefficient of consolidation ( $c_v$ ) is constant during the consolidation

Based on the above assumptions, the governing differential equation for consolidation theory was derived as

$$\frac{\partial u}{\partial t} = c_v \frac{\partial^2 u}{\partial z^2} \quad (2.1)$$

where,  $c_v$  is the coefficient of consolidation,  $u$  is the excess pore water pressure developed,  $t$  is the time,  $z$  is the depth and  $\gamma_w$  is the unit weight of water. The differential Eq. (2.1) is solved for mid plane pore water pressure for double drainage as

$$u_m = \sum_{m=0}^{m=\infty} \frac{2u_0}{M} \sin M \exp(-M^2 T_v) \quad (2.2)$$

where,  $M = \frac{(2m+1)\pi}{2}$  and  $T_v = \frac{c_v t}{d^2}$

$u_0$  is the initial pore water pressure,  $d$  is the length of the drainage path and,  $T_v$  is the time factor. The degree of consolidation ( $U_z$ ) based on pore pressure at depth  $z$  and time  $t$  for the layer thickness  $2d=H$ , is given by

$$U_z = \frac{u_0 - u_t}{u_0} = 1 - \sum_{m=0}^{m=\infty} \frac{2}{M} \sin\left(\frac{Mz}{d}\right) \exp(-M^2 T_v) \quad (2.3)$$

where  $u_t$  is the pore pressure at any time  $t$ . The average degree of consolidation ( $U$ ) can be expressed as a function of  $T_v$  by integrating the excess pore pressure (Eq. 2.2) with respect to  $z$  as follows:

$$U = 1 - \sum_{m=0}^{m=\infty} \frac{2}{M^2} \exp(-M^2 T_v) \quad (2.4)$$

For all practical purpose, the average degree of consolidation ( $U$ ) is of interest. Therefore, the average degree of consolidation is given in terms the of the consolidation settlement which is the ratio of consolidation settlement ( $\rho$ ) at any time to the ultimate consolidation settlement ( $\rho_p$ ) given by:

$$U = \frac{\rho}{\rho_p} \times 100\% \quad (2.5)$$

By knowing the average degree of consolidation and time settlement data for each increment of load, the value of coefficient of consolidation can be determined.

### 2.3.2 Apparatus for IL Test

Consolidation apparatus is required to perform the consolidation test in the laboratory. The apparatus for one-dimensional consolidation test is called as oedometer, which consists of a consolidation cell and a loading unit.

#### *Consolidation cell*

The two commonly used models of consolidation cells are shown in Figure 2.2. Both models are commercially available in the market. One of the important components of the consolidation cell is the consolidation ring as shown in Figure 2.2, in which the soil specimen is placed. The ring is made up of non-corrosive material like stainless steel or brass. The inner surface of the ring is highly polished to reduce the friction. The ring shall have sufficient thickness so that the lateral deformation due to loading shall be negligible. The other important requirement of consolidation ring is that the friction between the soil and the ring shall be minimum. This is achieved by keeping the diameter sufficiently larger than the thickness of the specimen. As per IS 2720-15 (1986), the minimum inner diameter of the ring shall be 60 mm with a diameter to thickness ratio of 3. ASTM D2435-11 (2011), recommends a diameter to thickness ratio of 2.5. The minimum diameter recommended is 50 mm. However, the thickness of the specimen shall not be less than 10 times the maximum particle size.

The soil specimen in the ring is sandwiched between two porous stones. The permeability of the porous stones shall be at least 100 times higher than the soil so that the condition of free drainage prevails at the boundaries. The other components are the loading cap which has perforation to permit the water to flow. The entire assembly is placed in the outer chamber where water is filled to saturate the specimen throughout the test. Photographs of components of two models (Model 1 and Model 2) are shown in Figure 2.2 (a) and (b) and the assembled cell is shown in Figure 2.2 (c) and (d).

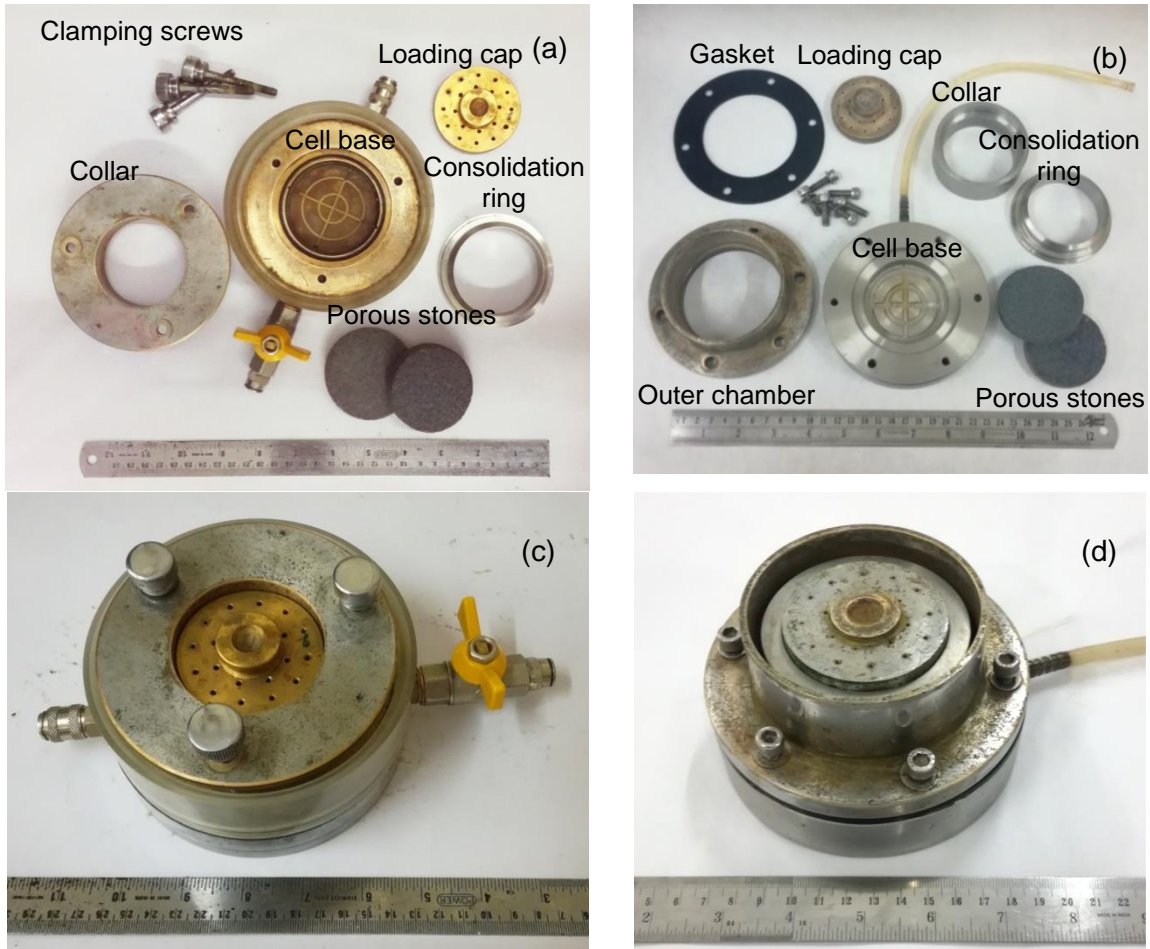


Figure 2.2: Components of consolidation cell (a) Model 1 (b) Model 2 (c) Assembled cell of model 1 and (d) Assembled cell of model 2

Depending on the assembly of top and bottom porous stones (Figure 2.3 (a, b)), the consolidometer can be classified as floating ring type and fixed ring type. In the floating ring type, as the name indicates, the soil specimen gets compressed on both top and bottom so that the friction between soil and the ring is less. In the fixed ring consolidometer, the ring is fixed at the base of cell so that compression of the specimen occurs only from the top. The main advantage of fixed ring consolidation cell is that permeability measurements can be made with suitable modifications by connecting a burette to the base of the specimen. Saturation of specimens in the conventional cell is done by pouring water in the outer chamber and allowing for saturation for 24 hours.



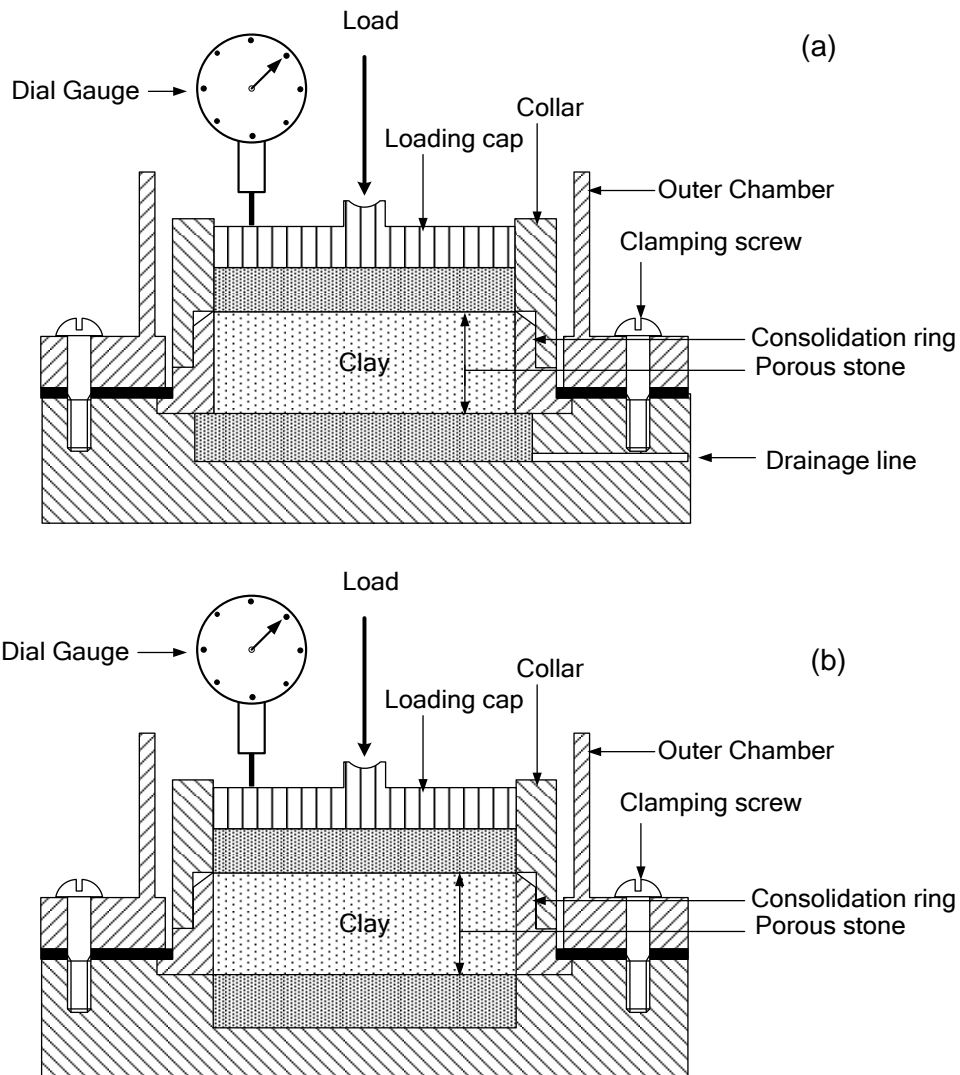


Figure 2.3: Schematic of (a) fixed ring consolidometer and (b) floating ring consolidometer

Rowe and Barden (1966) developed a consolidation cell called as Row cell or hydraulic consolidation cell, in which the soil specimen can be saturated by the application of back pressure. Schematic diagram of Rowe cell is shown in Figure 2.4(a). A photograph of Rowe cell is shown in Figure 2.4(b). The test specimen is loaded by hydraulic pressure through a flexible diaphragm. Drainage can be controlled from both top and bottom of the specimen. Therefore, the specimen can be saturated by back pressure saturation technique. If required, pore pressure can be also measured at the bottom of the specimen. Rowe cell is widely used for the determination of coefficient of consolidation in the radial direction.

Detailed description of the apparatus and the test procedure can be found in Head (1986). As the consolidation pressure is applied hydraulically, larger size specimens can be used. Specimen size of 250 mm was reported in the literature. The load applied is less susceptible to vibrations, when compared to the conventional oedometer. One of the limitations of Rowe cell is that the diaphragm resists the applied load and needs calibration. Rowe cell is expensive when compared to the conventional cell.

### ***Loading unit***

The loading unit enables the application of vertical stress to the specimen in suitable increments. The device shall be capable of maintaining specified loads for longer period of time with variation of less than 1% of the applied load (IS 2720-15 (1986)). There shall be suitable arrangements to mount the dial gauge and displacement transducer to monitor vertical deformation of the specimen.

The conventional lever loading unit (Figure 2.5(a)) consists of a mechanical loading arrangement with a lever arm of 10. The main advantage of this type of loading unit is that the unit is very simple and inexpensive. System compliance is one of the issues associated with these arrangements. Therefore, the system is generally calibrated before use. The other limitations are that even a slight vibration leads to disturbance. The load is applied manually and the load capacity is also limited. Therefore, higher stress levels are difficult to achieve, where specimen of larger diameter are used.

In order to overcome the above limitations, pneumatic consolidometer (Figure 2.5(b)) and automatic consolidation apparatus (Figure 2.5(c)) were subsequently developed (Pratoom and Tangwiboonpanich, 2014). These set-ups occupy less foot print area compared to the conventional lever loading system. In the pneumatic consolidometer, the load is applied using air pressure through a pneumatic cylinder. Servo-controlled mechanism is adopted in the automated consolidation apparatus. Both pneumatic consolidometer and automated consolidation apparatus can be completely automated with the use of computers without user intervention between successive loadings.

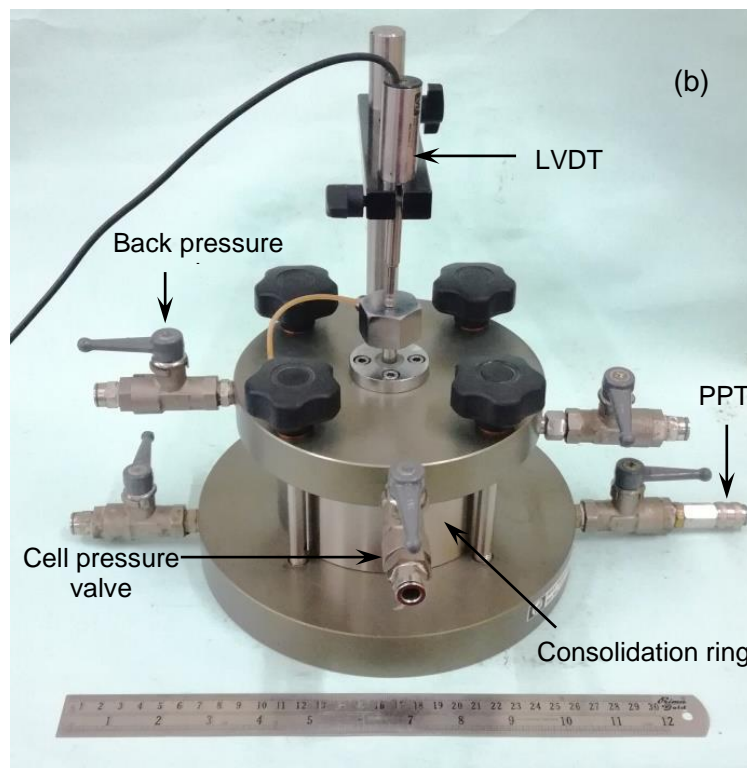
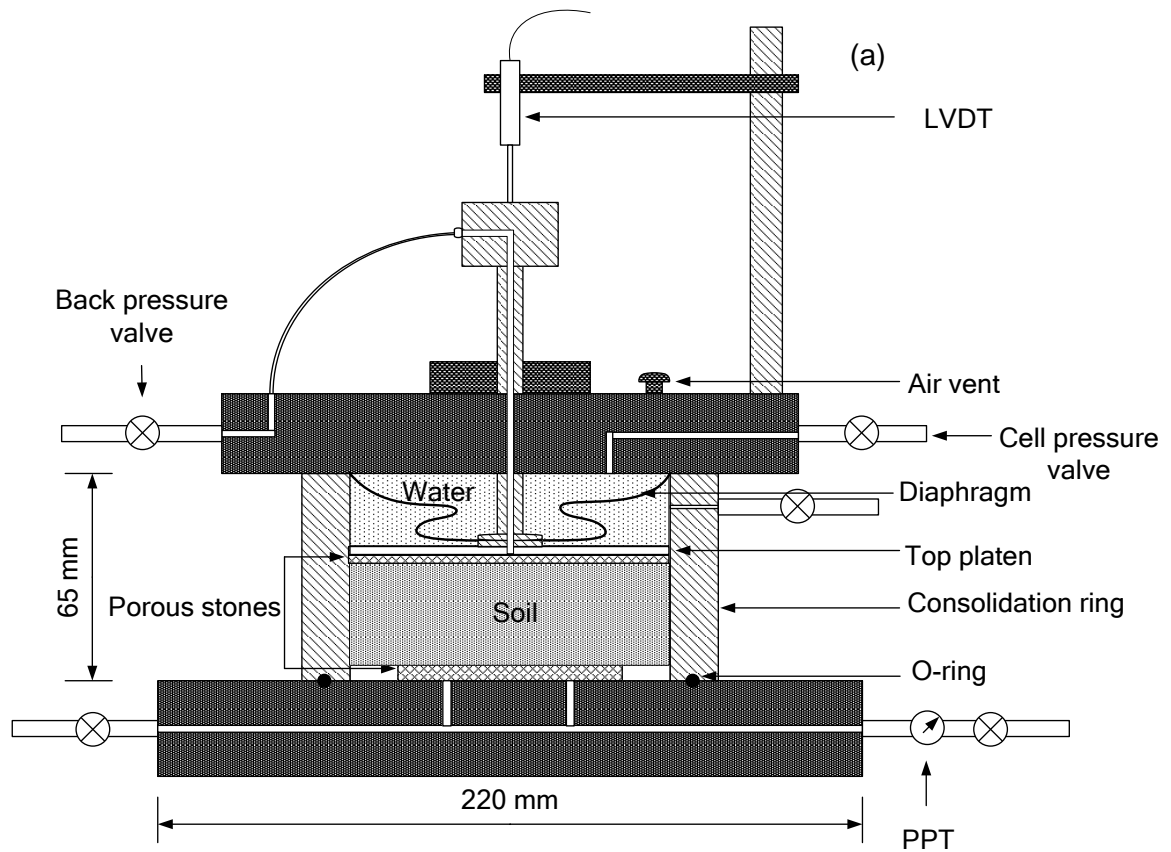


Figure 2.4: (a) Schematic of typical Rowe cell and (b) Photograph of Rowe cell



Figure 2.5: (a) Conventional loading Frame (b) Pneumatic consolidation frame ([www.globalgilson.com](http://www.globalgilson.com)) and (c) Automated consolidation frame

### 2.3.3 Determination of Coefficient of Consolidation ( $c_v$ )

During IL consolidation test, the time-settlement data are continuously recorded. From the time-settlement data, the values of coefficient of consolidation ( $c_v$ ) and the coefficient of secondary compression ( $c_{\alpha}$ ) are determined. Several methods are available in the literature for the determination of  $c_v$ . Review of the methods can be found in Olson (1986), Sridharan *et al.* (1995) and Shukla *et al.* (2009). Casagrande's log  $t$  method (Casagrande and Fadum, 1940) and Taylor's  $\sqrt{t}$  method (Taylor, 1942) are considered as standard methods and are reviewed in this chapter. In addition, the Inflection point method (Cour, 1971; Robinson, 1997; Mesri *et el.* 1999) is also discussed.

In the log  $t$  method, a plot of log  $t$  versus settlement ( $S$ ) is plotted. Coefficient of consolidation is evaluated from the time for 50% degree of consolidation ( $t_{50}$ ) which is determined from the  $S$ -log  $t$  plot as shown in Figure 2.6. Knowing  $t_{50}$ ,  $c_v$  is determined as

$$c_v = \frac{0.196d^2}{t_{50}} \quad (2.6)$$

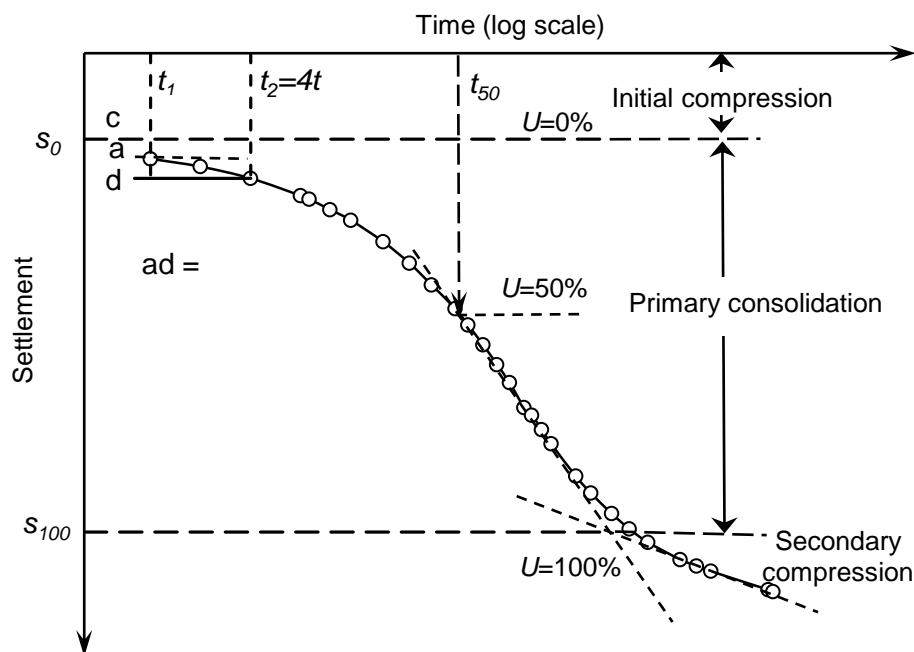


Figure 2.6: Determination of  $c_v$  using the log  $t$  method (Casagrande and Fadum, 1940)

Coefficient of secondary compression can be also calculated using the  $\log t$  plot. Mesri (1973) suggested that the slope of void ratio (instead of  $S$ ) versus  $\log$  of time as the coefficient of secondary compression (Eq. 2.7):

$$c_{\alpha} = \frac{\Delta e}{\Delta \log t} \quad (2.7)$$

In the Taylor's  $\sqrt{t}$  method (Taylor, 1942),  $c_v$  is determined from the time for 90% degree of consolidation ( $t_{90}$ ). A plot of root of time ( $\sqrt{t}$ ) versus settlement ( $S$ ) is plotted as shown in Figure 2.7. The time ( $t_{90}$ ) corresponding to 90% degree of consolidation is identified by fitting a straight line for the initial part of the curve up to a degree of consolidation of about 60% and a straight line whose slope is (1/1.15) times of the initial tangent. The point when the latter straight line cuts the  $S$ - $\sqrt{t}$  curve is the square root of time of  $t_{90}$  (Figure 2.7). Knowing  $t_{90}$ ,  $c_v$  is determined as

$$c_v = \frac{0.848d^2}{t_{90}} \quad (2.8)$$

Time settlement data for a short duration is sufficient to obtain  $t_{90}$  whereas in the  $\log t$  method data upto about 24 hours is required. However, coefficient of secondary compression cannot be obtained in the  $\sqrt{t}$  method.

In the inflection point method, the point corresponding to the maximum slope of  $S$  versus  $\log t$  plot is identified. The time ( $t_i$ ) corresponding to the inflection point can be easily identified by plotting  $\Delta S/\log t$  (Slope of  $S$ - $\log t$  curve) versus  $\log t$ . It occurs at a time factor of 0.405, which corresponds to degree of consolidation 70.15% (Robinson, 1997). Typical plot of experimental data is shown in Figure 2.8. The coefficient of consolidation can be determined from

$$c_v = \frac{0.405d^2}{t_i} \quad (2.9)$$

where,  $d$  is the length of the maximum drainage path.

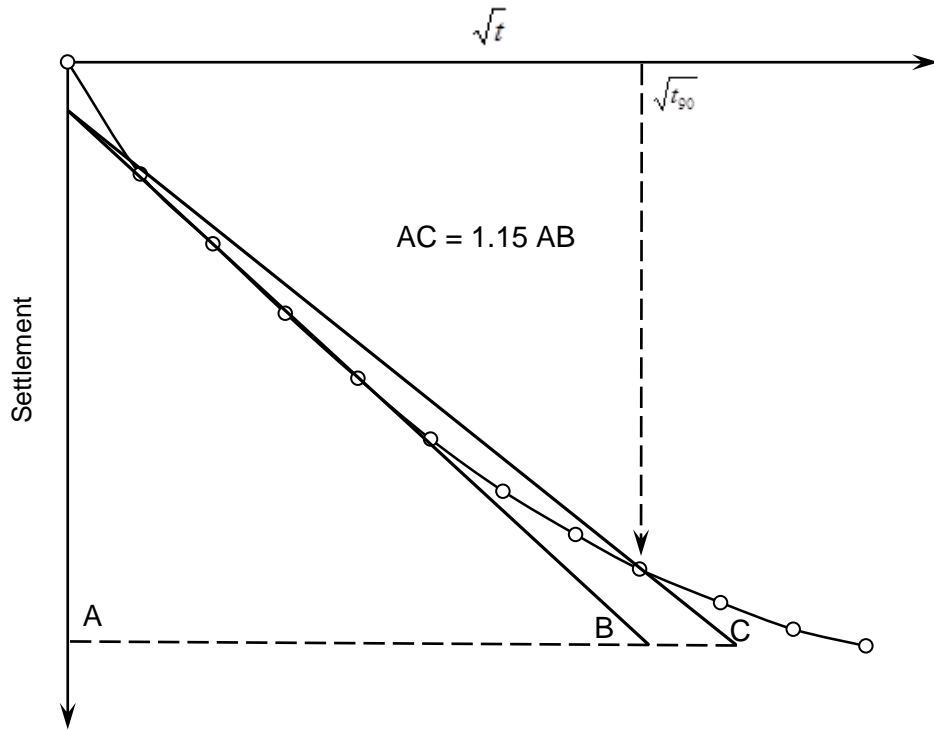


Figure 2.7: Determination of  $c_v$  using  $\sqrt{t}$  method (Taylor, 1942)

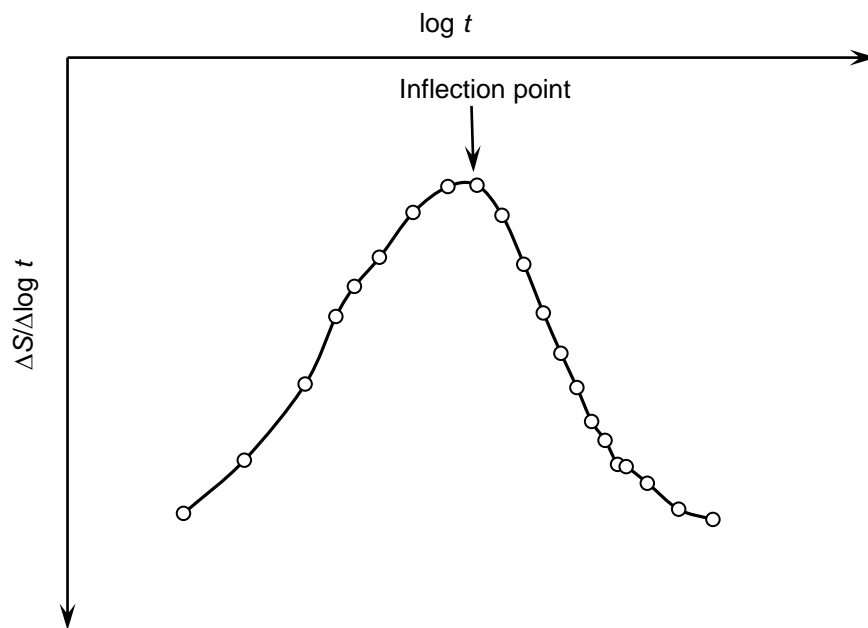


Figure 2.8: Determination of  $c_v$  using the inflection point method (Robinson, 1997)

Coefficient of permeability,  $k$  is often derived from the consolidation test. By knowing the coefficient of consolidation ( $c_v$ ) and the coefficient of volume change ( $m_v$ ), the coefficient of permeability can be determined from the following equation.

$$k = c_v m_v \gamma_w \quad (2.10)$$

Terzaghi and Peck (1967) reported that  $k$  and  $m_v$  decreases rapidly with decrease in void ratio (increase in consolidation pressure), hence  $c_v$  is expected to be constant over a wide range of consolidation pressures as per Eq. (2.10). However, the trend of variation of  $c_v$  with consolidation pressure is not unique but depends on the physicochemical factors and mechanical factors (Olson and Mesri, 1970; Sridharan and Rao, 1976). Robinson and Allam (1998) reported that soils with kaolinite or illite as the dominant clay minerals will have a trend that  $c_v$  increases with increasing consolidation pressure as the compressibility of such clays are influenced by mechanical factors. On the other hand, for montmorillonitic soils  $c_v$  decreases with consolidation pressure for which physicochemical factors influence the compressibility. Review of the available data of  $c_v$  variation with consolidation pressure in the literature also shows that  $c_v$  variation with consolidation pressure is not unique. Typical plot showing the variation of  $c_v$  with consolidation pressure is shown in Figure 2.9.

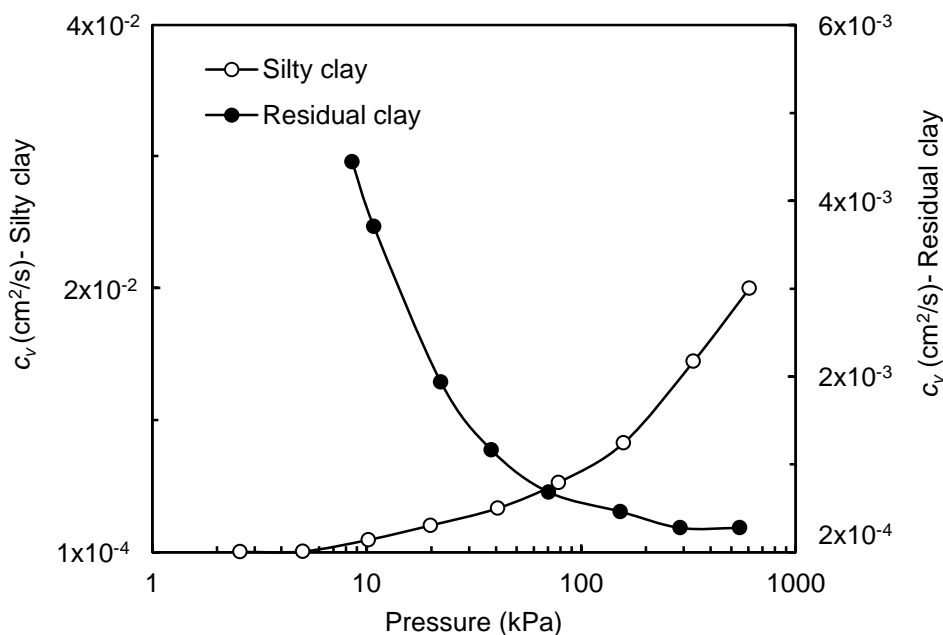


Figure 2.9: Variation of  $c_v$  with consolidation pressure (Leonards and Ramiah, 1959)



The trend observed in the literature is summarized in Table 2.1. Clearly, the trend is not unique. This trend of  $c_v$  variation will have an influence on the strain rate selection of CRS test, which will be discussed subsequently.

Table 2.1: Variation of  $c_v$  in the consolidation (Leonards and Ramiah, 1959)

Source	Soil Type	$w_l$ (%)	$I_p$ (%)	Variation in $c_v$ with pressure
Leonards and Ramiah (1959)	Residual clay	59	31	Decreases
	Glacial clay	28	8	Increases
Samarasinghe <i>et al.</i> (1982)	Sandy clay	27	14	Increases
	Don Valley Clay	41	22	Increases
	New Liskeard clay	67	40	Increases
	Bentonite	118	72	Decreases
	Kaolinite	-	-	Increases
Nakase <i>et al.</i> (1984)	Kawasaki clay	53.6	26.9	Increases
	Kaolinite	49	11.8	Increases
Robinson and Allam (1998)	Kaolinite	53	21	Increases
	Illite	131	53	Increases
	Montmorillonite	321	263	Decreases
Sridharan <i>et al.</i> (1999)	Brown soil	58.5	26.4	Decreases
	Bentonite	320	263.4	Decreases
	Kaolinite	55	23.5	Increases
Sridharan and Nagaraj (2004)	Red Earth	37	19	Decreases
	Silty soil	39	9.5	≈constant
	Illitic soil	73.4	21.5	Increases
	Black cotton soil	73.5	37.9	Decreases
	Cochin clay	35.4	18.3	Increases

Note:  $w_l$ - liquid limit;  $I_p$ - plastic limit

### 2.3.4 Total Settlement Parameters

The total settlement parameters such as compression index ( $c_c$ ), coefficient of volume change ( $m_v$ ) and recompression index ( $c_r$ ) are determined from the  $e$ - $\log \sigma_v'$  curve. From the ultimate consolidation settlement (taken as the settlement corresponding to 24 hour) the void ratio ( $e$ ) - consolidation pressure ( $\sigma_v'$ ) relationship is obtained. As each load is sustained for 24 hours, the test takes about 10-14 days to complete (Sridharan *et al.* 1999). For normally consolidated soils, the loading curve plots into a straight line with a slope of  $c_c$ . The slope of the unloading part is the recompression index ( $c_r$ ). For the over-consolidated soils, it is essential to determine the preconsolidation pressure ( $\sigma_c'$ ). A typical  $e$ - $\log \sigma_v'$  plot of over consolidated soil is shown in Figure 2.10.

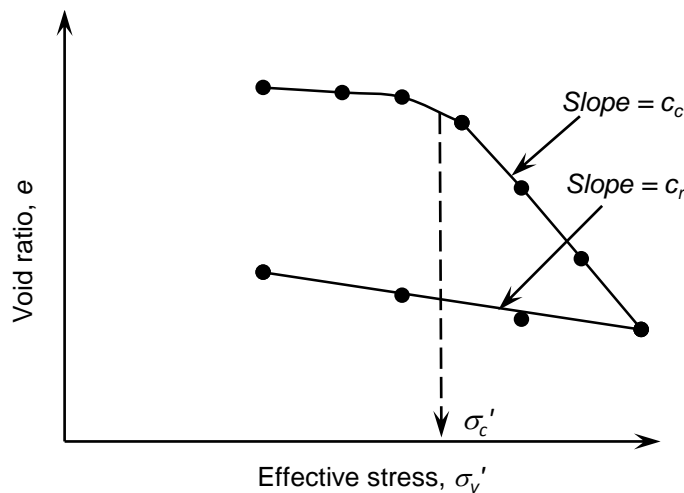


Figure 2.10: Typical  $e$ - $\log \sigma_v'$  plot for overconsolidated clayey soils

Casagrande's method (Casagrande, 1936) is one of the popular methods for the determination of  $\sigma_c'$ . The graphical construction procedure is shown in Figure 2.11(a). The values obtained by this method depend on the judgment of the user. The other method often used is  $\log(1+e)$  versus  $\log \sigma_v'$  plot (Sridharan *et al.* 1991) in which the data falls in to a bi-linear plot as shown in Figure 2.11(b). The intersection of the bi-linear plot is the preconsolidation pressure. As the method is based on the intersection of two straight lines, personal error is minimum.

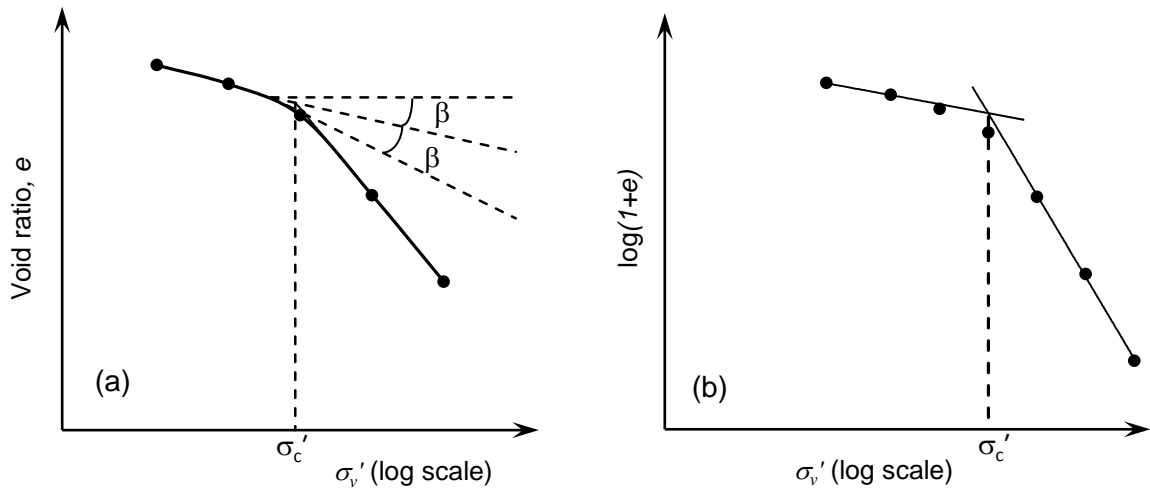


Figure 2.11: Determination of preconsolidation pressure using (a) Casagrande's method and (b)  $\log(1+e)$  versus  $\log \sigma'_v$  method

Unlike Figure 2.10, the structured clays exhibit a sharp transition between normally consolidated and overconsolidated phases (Olson, 1986). Typical plot is shown in Figure 2.12. Therefore, estimation of accurate value of preconsolidation pressure is often difficult if IL consolidation test with discrete data points are obtained.

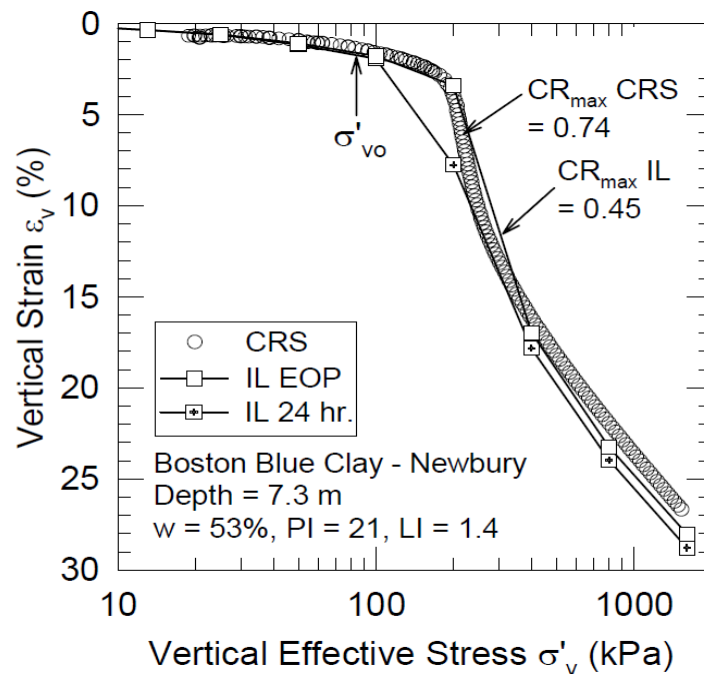


Figure 2.12: Typical  $e$ - $\log \sigma'_v$  plot of structured clay (Ladd and DeGroot, 2003)

The main advantage of IL consolidation test is that the testing procedure is well established and the interpretation of data is straight forward as Terzaghi's theory was developed for stress controlled consolidation test. Some of the limitations of IL consolidation test are:

- i. Time required for completion of test is high, often exceeding 10 days
- ii. Several load increments are required to establish the void ratio ( $e$ ) - consolidation pressure ( $\sigma_v'$ ) relationship.
- iii. The  $e$ - $\log \sigma_v'$  curve is often not well established for soils like structured clays which exhibit a sharp transition to normally consolidation state, as the data points from IL tests are discrete but not continuous. Therefore, the estimation of yield stress is often difficult for such soils.

### **2.3.5 Rapid IL Consolidation Test**

Rapid consolidation test is an incremental loading test in which the load under each load increment is kept for less than 24 hours. The theory and apparatus used are the same as that of conventional IL consolidation test. Newland and Allely (1960) recommended applying the subsequent load increment as soon as 100% primary consolidation is over. The procedure suggested by Newland and Allely (1960) saves considerable consolidation time compared to 24 hours duration test. However, high plastic clays may take long time to reach 100% primary consolidation. Sandbaekken *et al.* (1986), at the Norwegian Geotechnical Institute, used three increments on a working day to complete the consolidation tests faster.

Sridharan *et al.* (1994) studied the effect of load duration on consolidation test. One-dimensional consolidation tests were carried out on two types of soils such as kaolinite and black cotton soil (which contains montmorillonite as the dominant clay mineral) for varying durations of 30 minutes to 24 hours under each load increment. They observed that load duration of 30 minutes is sufficient for kaolinite and 4 hours is required for a black cotton soil. As the load duration required depends on the type of soil, judging the duration required for different types of soils is difficult.

Sridharan *et al.* (1999) also suggested a method using rectangular hyperbola method (Sridharan *et al.* 1987). The time-settlement data is monitored during the consolidation and the degree of consolidation is evaluated continuously using the rectangular hyperbola method. Once a straight line part is obtained in the transformed plot of time/settlement versus time plot, which is expected to occur in the range of degree of consolidation ( $U$ ) of about 60%-90%, the next increment is applied. The effective stress in the sample ( $\sigma_i'$ ) due to the pressure increment ( $\Delta\sigma_i$ ) is evaluated as

$$\sigma_i' = \sigma_{i-1}' + U(\Delta\sigma_i) \quad (2.11)$$

where,  $\sigma_{i-1}'$  is the initial effective stress before the application of the pressure increment  $\Delta\sigma_i$ . It may be noted that  $U$  used in Eq. (2.11) is derived based on degree of consolidation and is not appropriate. The other limitation is that the progress of consolidation process is not directly evident as the rectangular hyperbolic plot is a transformed plot in which the settlement is divided by time, the unloading part of the consolidation test was not analyzed in their study which is essential for evaluating the recompression index. In the rectangular hyperbola method, the relation between  $U$  and  $T_v$  was fitted as a rectangular hyperbola in the range  $60\% < U < 90\%$  based on the assumption that the plot of  $T_v/U$  versus  $T_v$  plot linear in this range. However, Sridharan and Prakash (1997) compared the slopes obtained for various methods as shown in Figure 2.13.

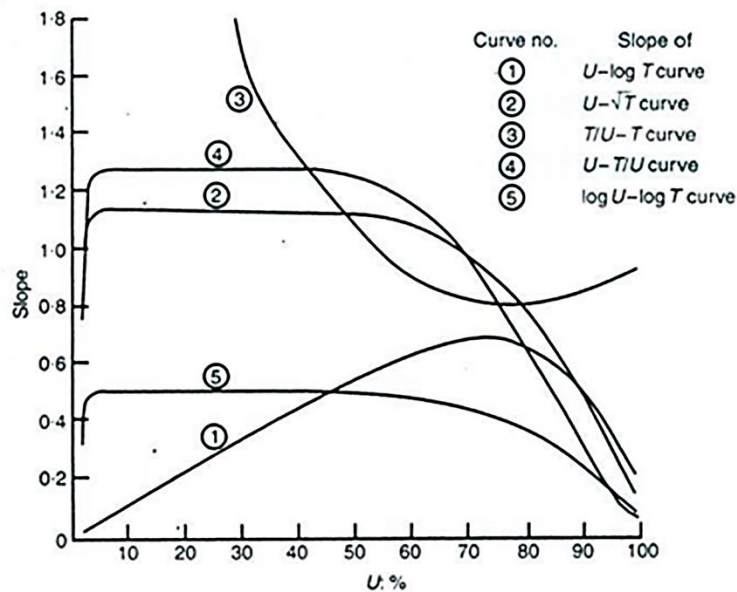


Figure 2.13: Variation of slope of different modes of representation of  $U-T_v$  relationship with  $U$  (Sridharan and Prakash, 1997)

It can be clearly seen from the plot that the slope of the modified plot of the rectangular hyperbola ( $T_v/U$  versus  $T_v$  plot) is not constant. The slope decreases as the degree of consolidation increases, reaches a minimum at a degree of consolidation of about 77% and then increases. Therefore, theoretically  $T_v$  versus  $U$  relationship is not a rectangular hyperbola but is an approximation.

### 2.3.6 End-Of-Primary (EOP) Consolidation Test

In the conventional IL consolidation test with 24 hours duration, some secondary compression occurs. Therefore, the  $e$ - $\log \sigma_v'$  curve obtained based on 24 hours duration includes some secondary compression. The  $e$ - $\log \sigma_v'$  curve without secondary compression is called as End-of-Primary (EOP) consolidation curve. Ideally, EOP consolidation curve can be obtained by performing an IL consolidation test such a way that the subsequent consolidation pressure is applied when the excess pore pressure measured at the bottom of the specimen dissipates to zero or to a very small value such as 1 kPa (Terzaghi *et al.* 1996). Generally, the excess pore pressure is not measured during conventional IL consolidation test. Therefore, each increment of load is applied and allowed to act long enough to define the EOP void ratio ( $e_p$ ). The EOP consolidation can be identified by the standard graphical procedures such as the  $\log t$  and the  $\sqrt{t}$  methods. If Casagrande's  $\log t$  procedure is used, some secondary compression must be allowed beyond the time required to complete primary consolidation ( $t_p$ ) so as to identify the linear secondary compression portion. Taylor's procedure may underestimate  $e_p$  of soils that experience significant destruction during pressure increment (Terzaghi *et al.* 1996)

The effect of duration of load was studied by Bjerrum (1967) and observed that the plots of  $e$ - $\log \sigma_v'$  is parallel to each other with increased duration of sustained loading as shown in Figure 2.14(a). Similar observations were reported by Sridharan *et al.* (1994) and Mesri (2003). This is because the value of  $c_\alpha$  is directly related to  $c_c$  (Mesri and Godlewski, 1977) and they developed a ( $c_\alpha/c_c$ ) concept. Soils with appreciable secondary compression show an induced overconsolidation as shown in Figure 2.14(b) (Mesri and Castro, 1987).

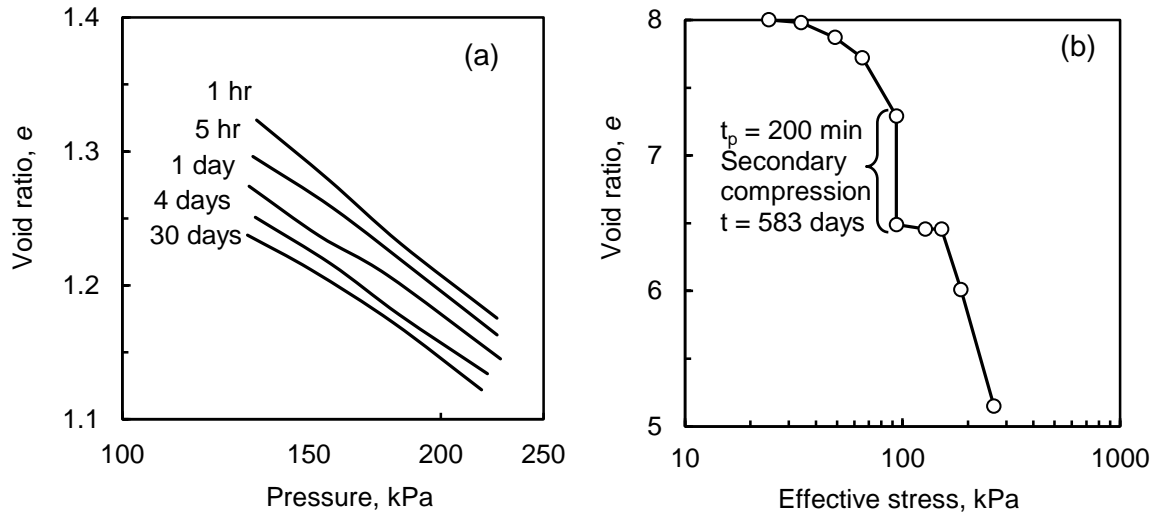


Figure 2.14: Secondary compression effect on (a)  $e$ - $\log \sigma'_v$  (Bjerrum, 1967) and (b) Time effect on overconsolidation (Mesri and Castro, 1987)

## 2.4 CONSTANT RATE OF STRAIN (CRS) CONSOLIDATION TEST

Constant rate of strain consolidation test is a strain controlled test. Hamilton and Crawford (1959) were the first to develop a constant rate of strain consolidation test. In the CRS test, the specimen is subjected to uniform deformation using a strain controlled loading frame. During the process, the load carried by the specimen and the pore water pressure developed at the base of the specimen are continuously recorded. Subsequently, many developments took place both in the theory and experimental procedure. These aspects are discussed in this section.

### 2.4.1 Theories of CRS Test

Several theories were developed to model the pore pressure variation within the specimen when subjected to constant rate of strain. The theories are grouped in to small strain theory and large strain theory. The small strain theory is based on the assumption that the strains are infinitesimally small so that the thickness variation during the test is insignificant. In the large strain theory, the change in thickness of the specimen during the test is considered.

### ***Small strain theories***

Smith and Wahls (1969) were the first to develop a theory for strain controlled tests which is similar to Terzaghi's one-dimensional consolidation theory. They expressed the void ratio variation with respect to depth and time. The basic equation derived based on the assumptions as that of Terzaghi's theory is:

$$\frac{k}{\gamma_w} \left( \frac{\partial^2 u}{\partial z^2} \right) = \frac{1}{1+e_0} \frac{\partial e}{\partial t} \quad (2.12)$$

where,  $e$  is the void ratio,  $e_0$  is initial void ratio and  $z$  is the co-ordinate of the soil element. In Eq. (2.12),  $e$  was assumed as a linear function of  $z$  and  $t$ , which is given by

$$e(z,t) = e_0 - r_e t \left[ 1 - \frac{b}{r} \left( \frac{z - 0.5H}{H} \right) \right] \quad (2.13)$$

where,  $b$  is a constant,  $b/r$  is a dimensionless ratio which indicates the variation of void ratio with depth. Eq. (2.12) was solved by substituting  $e(z, t)$  from Eq. (2.13),  $(1+e)$  was replaced by  $1+\bar{e}$  ( $\bar{e}$  is not a function of  $z$ ) and applied the boundary conditions  $u(0,t) = 0$  and  $\frac{\partial u(H,t)}{\partial z} = 0$ . A simplified approximate solution was obtained for the pore pressure at any depth as

$$u = \left[ \frac{\gamma_w r}{k(1+\bar{e})} \right] \left[ \left( Hz - \frac{z^2}{2} \right) - \frac{b}{r} \left( \frac{z^2}{4} - \frac{z^3}{6H} \right) \right] \quad (2.14)$$

The pore pressure measured at the base of the specimen during CRS test was evaluated from Eq. (2.14) by substituting  $z=H$  as

$$u_{z=H} = u_b = \left[ \frac{\gamma_w r H^2}{k(1+\bar{e})} \right] \left( \frac{1}{2} - \frac{1}{12} \frac{b}{r} \right) \quad (2.15)$$



This theory has two major issues. First, the assumption that the void ratio is a linear function of the time and depth variables is difficult to be evaluated. The second issue is that they assumed a parameter  $b$  which is not known, and there is no procedure for its determination. Since the results depend on the chosen value of  $b$ , it requires a reference test to be performed on similar specimens.

Wissa *et al.* (1971) proposed a more comprehensive theory for CRS consolidation. They assumed that the strain increments remain infinitesimally small in the subsequent time increments, and the coefficient of consolidation is constant along the depth at any time during the test. They formulated the governing equation based on strain distribution across the depth of the specimen. The developed equation of CRS consolidation in terms of strain was given as

$$c_v \frac{\partial^2 \varepsilon}{\partial z^2} = \frac{\partial \varepsilon}{\partial t} \quad (2.16)$$

where,  $\varepsilon$  is the vertical strain,  $t$  is the time and  $z$  is the vertical coordinate of a point. The solution for Eq. (2.16) is as follows:

$$\varepsilon(X, T_v) = rt[1 + F(X, T_v)] \quad (2.17)$$

where,  $X = \frac{z}{H}$ ,  $T_v = \frac{c_v t}{H^2}$  and

$$F(X, T_v) = \frac{1}{6T_v} (2 - 6X + 3X^2) - \frac{2}{\pi^2 T_v} \sum_{n=1}^{\infty} \frac{\cos n\pi X}{n^2} \exp(-n^2 \pi^2 T_v) \quad (2.18)$$

In the above equations  $X$  and  $T_v$  are the dimensional factors. Eq. (2.17) has two parts: the first part represents the average strain within the sample. The second part of the Eq. (2.17) is given in Eq. (2.18), which has two terms (Eq. 2.18). The first term shows the steady state case, which represents the deviation from the average strain and the term with exponent shows the transient state, which represents the decay of the initial discontinuities set-up when the test is started. The transient component will be insignificant for  $T_v > 0.5$ , which is called as ‘steady state’ by Wissa *et al.* (1971). The steady state equation is given as:

$$\varepsilon(z,t) = rt + \frac{rH^2}{c_v} \left\{ \frac{1}{6} \left[ 3 \left( \frac{z^2}{H} \right) - 6 \frac{z}{H} + 2 \right] \right\} \quad (2.19)$$

The transient conditions can be interpreted based on strain relationship from Eq. (2.17) at any time,  $t$

$$\frac{\varepsilon(H,t)}{\varepsilon(0,t)} = \frac{1 + F(1, T_v)}{1 + F(0, T_v)} = F_3(T_v) \quad (2.20)$$

The value of term  $F_3$  defines the transient condition and depends only on  $T_v$ . If  $T_v$  is 0.5,  $F_3$  nearly equal to 0.4.

The transient conditions can be interpreted based on stress relations. For a linear (constant  $m_v$ ) material the strain will be proportional to the change in effective stress.

$$F_3 = \frac{(\sigma_v - \sigma_{v@t=0}) - u_b}{(\sigma_v - \sigma_{v@t=0})} \quad (2.21)$$

For a non-linear (constant  $c_c$ ) material, the strain will be proportional to logarithm of effective stress.

$$F_3 = \frac{\log(\sigma_v - u_h) - \log(\sigma_{v@t=0})}{\log(\sigma_v) - \log(\sigma_{v@t=0})} \quad (2.22)$$

Theory of Wissa *et al.* (1971) is widely used to interpret the CRS consolidation data. The theory was also incorporated in ASTM D4186-06 (2006).

Yoshikuni *et al.* (1995) proposed a much simpler theory to find the solution for CRS consolidation test compared to the other two theories discussed above. They assumed that the strain rate at every location in the specimen is equal to the average strain rate once the steady state is reached. Based on this assumption, they expressed the rate of strain at any location  $z$  at any time  $t$  as:

$$\frac{\partial \varepsilon(z,t)}{\partial t} = \frac{\partial \bar{\varepsilon}(t)}{\partial t} = r \quad (2.23)$$

in which  $\varepsilon(z,t)$  is the strain at any location  $z$  at any time  $t$ .  $\bar{\varepsilon}(t)$  is the average strain of the specimen at time  $t$ . The governing equation for CRS consolidation test is given as

$$\frac{k}{\gamma_w} \frac{\partial^2 u}{\partial z^2} = \frac{\partial \varepsilon(z,t)}{\partial t} = \frac{\partial \bar{\varepsilon}(t)}{\partial t} = r \quad (2.24)$$

By applying the boundary conditions  $u = 0$  at  $z = 0$  and  $\frac{\partial u}{\partial z} = 0$  at  $z = H$ , the following solution for excess pore water pressure is obtained

$$u = \frac{\gamma_w r}{k} \left( \frac{1}{2} z^2 - zH \right) \quad (2.25)$$

Among these theories, the theory of Smith and Wahls (1969) does not consider the transient condition, whereas other theories considered it. As the existence of transient state is likely to happen, the theories of Wissa *et al.* (1971) and Yoshikuni *et al.* (1995) are better for the interpretation of CRS test data.

### ***Large strain theories***

In the literature, a few theories were developed by considering the change in thickness during the test. One of the theories was developed by Umehara and Zen (1980). The theory proposed by Umehara and Zen (1980) is based on the large strain consolidation theory of Mikasa (1963). The governing equation is

$$\frac{\partial \zeta}{\partial t} = c_v \zeta^2 \frac{\partial^2 \zeta}{\partial z^2} \quad (2.26)$$

where,  $\zeta = \frac{1+e_0}{1+e} = \frac{1}{1-\varepsilon}$

They assumed a non-dimensional parameter  $c_v R / H_0$  (where  $R$  is the rate of deformation, and  $H_0$  is the initial thickness of the specimen). Eq. (2.26) was solved numerically with the appropriate boundary conditions and for various values of  $c_v R / H_0$ . A series of charts were constructed, relating the consolidation ratio to the strains and the non-dimensional parameter, as shown in Figure 2.15.

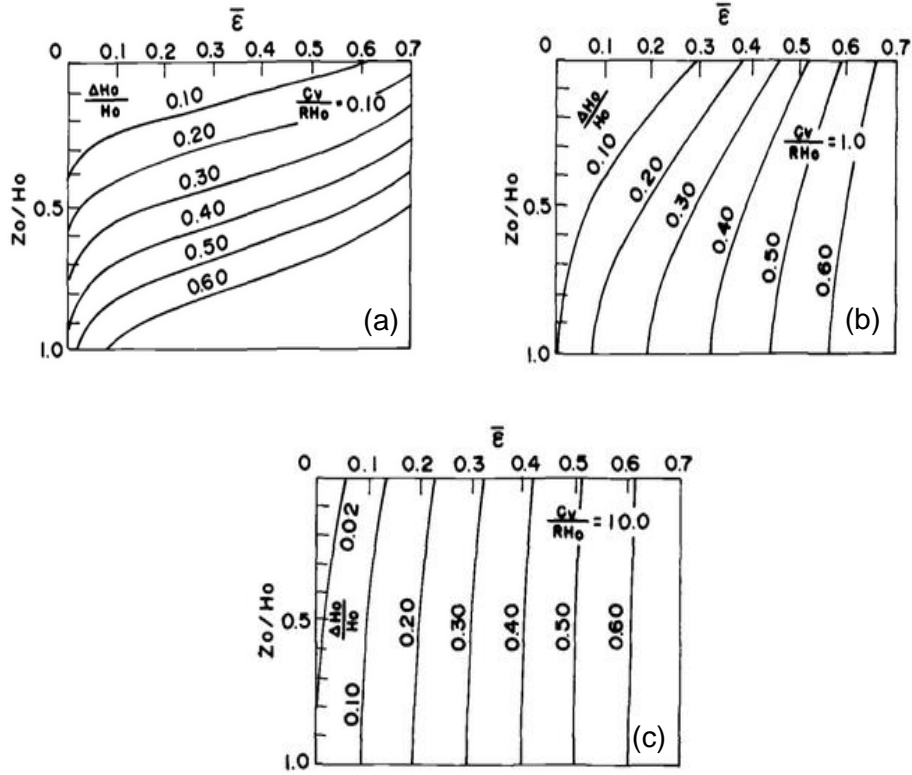


Figure 2.15: Strain distribution within specimen for various average strain (a)  $c_v/RH_0=0.10$  (b)  $c_v/RH_0=1.0$  (c)  $c_v/RH_0=10.0$  (Umehara and Zen, 1980)

The experimental data is interpreted using a parameter  $F$ , given by:

$$F = \frac{\log(\sigma_v - u_b) - \log(\sigma'_{v0})}{\log \sigma_v - \log \sigma'_{v0}} \quad (2.27)$$

where,  $\sigma'_{v0}$  is the initial effective vertical stress. Using the charts, the value for the parameter  $c_v R/H_0$  corresponding to the ratio  $F$  can be obtained. The consolidation ratio at both ends of the specimen can be obtained from other charts as shown in Figure 2.16, if the parameter is known. Thus, both the coefficient of consolidation and the effective vertical stress-void ratio relationship can be obtained.

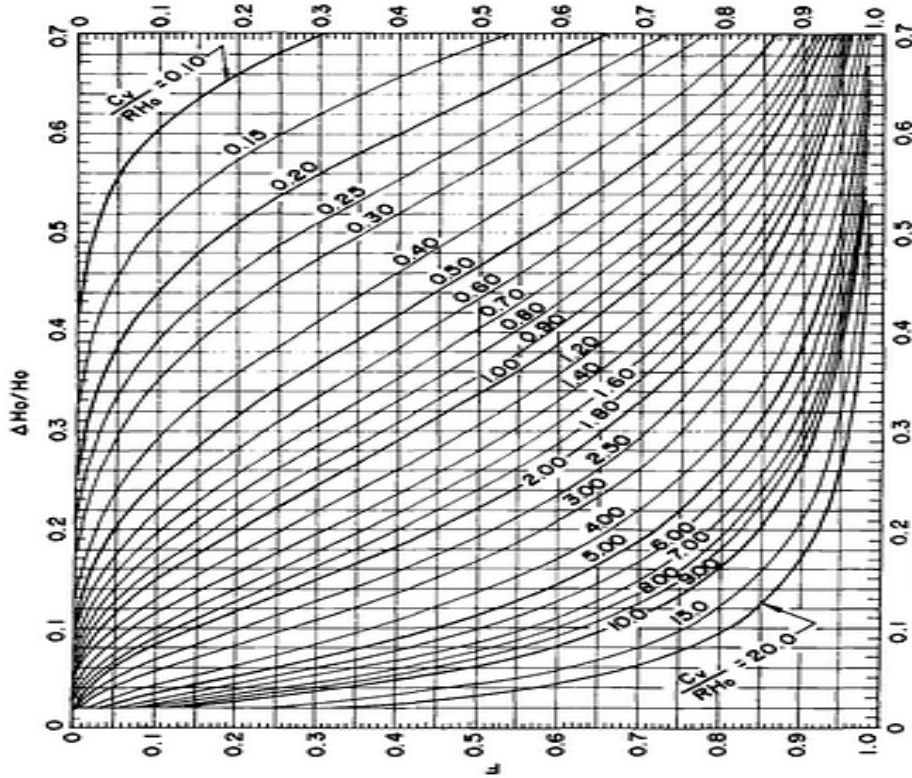


Figure 2.16: Variation of consolidation ratio of bottom strain to top strain  $F$  for average strain (Umehara and Zen, 1980)

Lee (1981) suggested a governing equation based on the moving boundary theory developed by Lee and Sills (1980) for the finite strain consolidation under step loading. In the theory, a constant  $c_v$  was assumed throughout the specimen. The governing equation, initial conditions and boundary conditions were obtained for constant rate of consolidation as follows:

$$\frac{\partial \varepsilon_E}{\partial T_v} = \frac{\partial^2 \varepsilon_E}{\partial X^2}, \quad 0 \leq X \leq \eta(T_v), \quad 0 \leq T_v \leq T_f \quad (2.28)$$

$$\varepsilon_E(X, 0) = 0$$

$$\frac{\partial \varepsilon_E}{\partial X}(0, T) = 0$$

$$\frac{\partial \varepsilon_E}{\partial X}(\eta, T_v) = \beta[1 + \varepsilon_E(\eta, T_v)]$$

$$\eta(T_v) = \frac{h}{h_0} = 1 - \beta T_v$$

where,  $X$  and  $T_v$  are normalized depth and time factor, respectively.  $\beta$  is a dimensionless parameter (normalized strain rate) defined as:

$$\beta = \frac{rH_0^2}{c_v} \quad (2.29)$$

Value of  $\beta$  estimated from published results varies over a range because of the variation in  $c_v$  during the test. It was observed that higher values of  $\beta$  do not have a good agreement with the standard conventional test. Therefore, an upper limit to  $\beta$  value was suggested as 0.2. The procedure was also divided into two parts: the steady state and transient state. In the transient state, exactly the same analysis as suggested by Wissa *et al.* (1971) was recommended. Some additional assumptions were required to get similar steady state analysis proposed by Wissa *et al.* (1971). The first assumption is that the strain distribution within the specimen can be approximated by a parabolic function. An approximated solution for steady state was given as:

$$\varepsilon_E = \frac{\beta T_v}{1 - \beta T_v} + \frac{\beta}{2 \left[ 1 - \frac{1}{3} \beta (1 - \beta T_v) \right]} \left[ \left( \frac{X}{\eta} \right)^2 - \frac{1}{3} \right] \quad (2.30)$$

The Eulerian strain,  $\varepsilon_E$  at the base  $X = 0$  was given as

$$\varepsilon_E = \frac{\beta T_v}{1 - \beta T_v} - \frac{\beta}{6 \left[ 1 - \frac{1}{3} \beta (1 - \beta T_v) \right]} \quad (2.31)$$

The theories and the governing differential equations developed by Umehara and Zen (1980) and Lee (1981), were solved numerically with appropriate boundary conditions and assuming non-dimensional parameters. They have presented a series of charts to determine the consolidation parameters. No rational procedure was reported to choose the correct curve in the chart which provides better parameters.

Vikash (2013) proposed a theory to explain the pore pressure distribution at the early stages of the CRS test based on the moving boundary concept. It was assumed that strain increments are infinitesimally small in the successive time intervals and an undrained

interface moves towards the base of the specimen as the test progress. Moving undrained interface divides the sample into two parts. Top part of the interface is pervious ( $H_d$ ) and the lower part will not take part in the diffusion ( $H_{ud}$ ), because the hydraulic gradient is zero. The schematic illustration of pore pressure diffusion process is shown in Figure 2.17. The water flowing out from the interface in the duration  $\delta t$  will be equal to the change in thickness of the interface ( $\delta z$ ) in the same duration. A non-homogenous parabolic partial differential equation for CRS consolidation test was derived based on the above assumption as follows

$$c_v(t) \frac{\partial^2 u}{\partial z^2} = \frac{\partial u}{\partial t} - \frac{\partial \sigma}{\partial t} \quad (2.32)$$

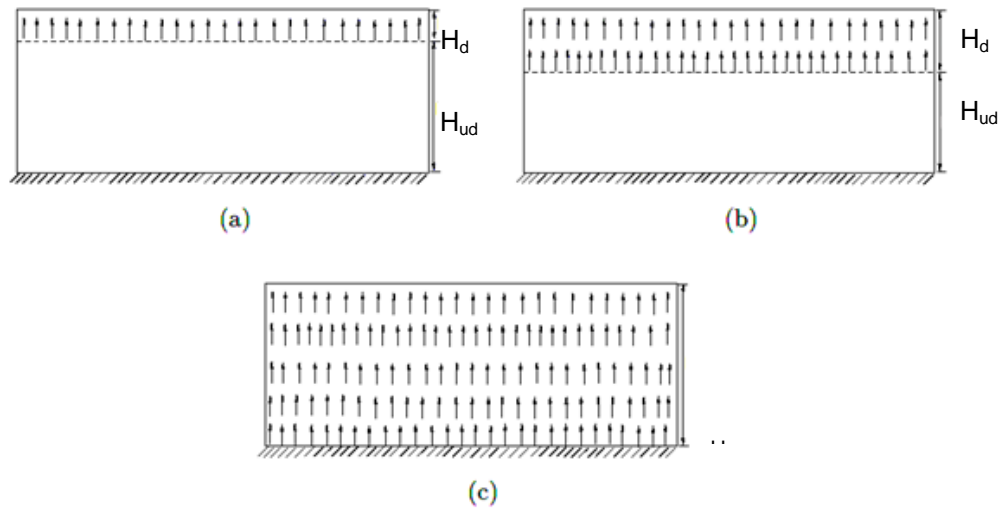


Figure 2.17: Pore pressure diffusion process during CRS consolidation (a) at immediately after the tests (b) at any intermediate time and (c) when the whole depth participates

Initial conditions, the moving boundary conditions and the boundary conditions used for solving the governing Eq. (2.32) are as follows:

$$0 \leq z \leq z_p(t), \quad z_p(t,0) = 0, \quad z_p(t = \tau) = H, \quad u(0,t) = 0, \quad u(z,0) = 0$$

$$u(z,t) = u(z_p,t), \quad z_p(t) \leq z \leq H$$

$$\frac{\partial u}{\partial z} \Big|_{z=z_p(t)} = 0, \quad \frac{dz_p}{dt} = \frac{k}{\gamma_w} \frac{\partial u}{\partial z} (z_p, t + \delta t)$$

where,  $z_p$  is the depth that participates in the diffusion. Based on the Neumann similarity transformation  $z_p$  is given as

$$z_p = \lambda \sqrt{c_v(t)} t^{1/2} \quad (2.33)$$

The solution of the Eq. (2.32) consists of transient state and steady state. Wissa *et al.* (1971) interpreted that transient state completely dissipates for  $T_v \geq 0.5$ . Therefore, end of the dissipation of transience can be defined as:

$$t = \frac{0.5H_d^2}{c_v} \quad (2.34)$$

where,  $H_d$  is the depth that participates in the diffusion process ( $H_d = z_p(t)$ ). Eq. (2.32) was simplified by neglecting the transient component and expressed as:

$$c_v \frac{\partial^2 u}{\partial z^2} = -\frac{\partial \sigma}{\partial t} = r \quad (2.35)$$

where,  $r$  is the strain rate. Eq. (2.35) can be rewritten by substituting of  $m_v = -\overline{d\varepsilon}/d\sigma'$

and  $c_v = \frac{k}{m_v \gamma_w}$  as:

$$\frac{k}{\gamma_w} \frac{\partial^2 u}{\partial z^2} = \frac{\partial \overline{\varepsilon}(t)}{\partial t} = r \quad (2.36)$$

The solution of Eq. (2.36) is obtained as

$$u = \frac{\gamma_w r}{k} \left( z \times z_p(t) - \frac{z^2}{2} \right) \quad (2.37)$$

The pore pressure at the base can be expressed as

$$u_b = \frac{r \gamma_w z_p^2(t)}{2k} \quad (2.38)$$



As the governing equation is a nonlinear partial differential equation, they could derive only an approximate solution. The governing equation (Eq. 2.32) is based on the small strain theory. However, the solution (Eq. 2.37) suggested for the early stages of the CRS test includes the variation of  $z_p$  with time, which is a time dependent variable up to time domain  $t=\tau$ , which is contradicting the assumptions of the theory.

*The main difference between the small strain theory and large strain theory is that the change in height of the specimen during the test is not considered in the small strain theory. Many numerical studies (Lee, 1981; Rui et al. 2013; Fox and Pu, 2012) showed that there is significant difference in results between small and large strain theories, because of the reduction of specimen height during consolidation test (Fox and Pu, 2012; Pu et al. 2013; Fox et al. 2014). However, the height of specimen is known at any time during CRS test and it can be considered for the determination of consolidation parameters.*

#### **2.4.2 Apparatus for CRS Test**

Hamilton and Crawford (1959) were the first to introduce the constant rate of strain consolidation test. They used the conventional fixed ring consolidation cell for the test and a triaxial loading machine was used to apply the required deformation rate. Smith and Wahls (1969) also used the fixed ring consolidometer but the base was sealed to measure the base pore pressure with a pore water pressure transducer. The consolidometer was placed in an axial load press in conjunction with load cell and an extensometer was used to measure the deformation of the specimen. Schematic diagram of the CRS test apparatus used by Smith and Wahls (1969) is shown in Figure 2.18.

After several modifications, Wissa *et al.* (1971) proposed a general purpose consolidometer for CRS test in which the specimen can be saturated at constant volume under a back pressure with no lateral strain. The apparatus can be loaded by increments, constant rate of stress or constant rate of strain. The schematic diagram of general purpose consolidometer by Wissa *et al.* (1971) is shown Figure 2.19.

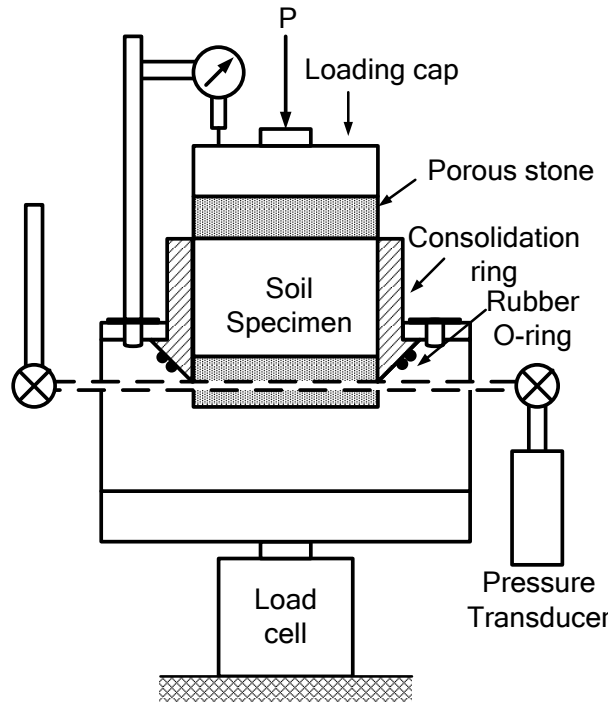


Figure 2.18: CRS test apparatus used by Smith and Wahls (1969)

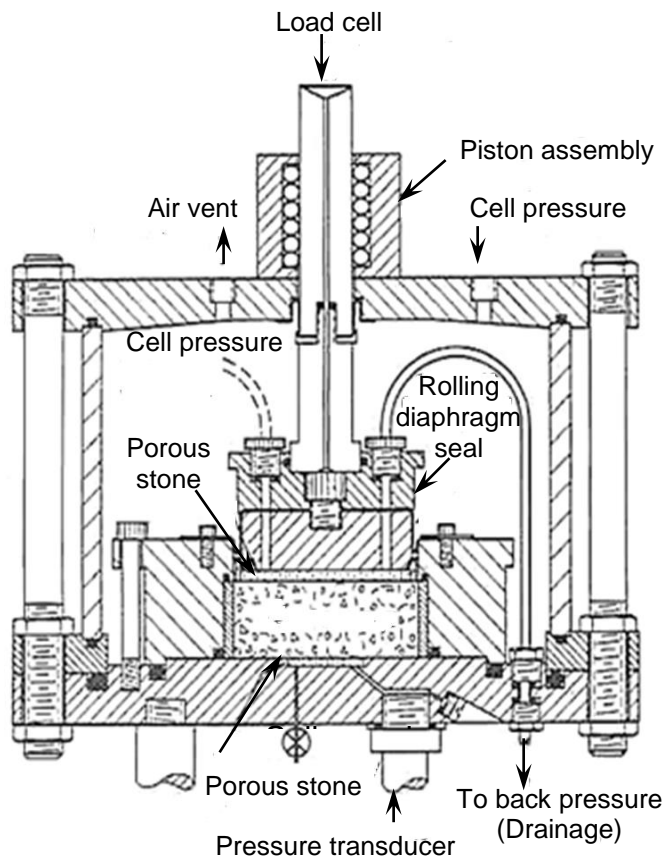
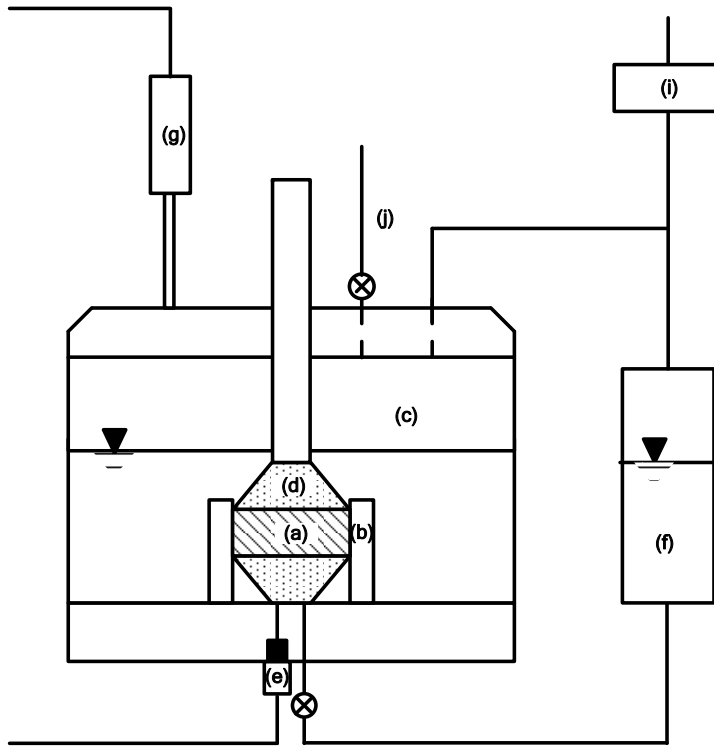


Figure 2.19: CRS test apparatus developed by Wissa *et al.* (1971)

Gorman *et al.* (1978) modified a triaxial equipment to perform the CRS test. The triaxial chamber with consolidation ring and a loading press were used to perform the CRS test on the specimen at constant rate as shown in Figure 2.20. Armour and Drnevich (1986) improved the CRS equipment to measure the permeability in addition to the base pore pressure. A schematic of the CRS testing apparatus is shown in Figure 2.21. The equipment is similar to that described by Gorman *et al.* (1978) with the only difference that an extra valve was added to the back pressure line to measure the permeability. Prashant and Vikash (2014) also modified the triaxial cell for the CRS test. The experimental set up is shown in Figure 2.22. The consolidation ring is placed inside the regular triaxial cell. Suitable connections are made from the base of the consolidation cell to the outlet port of the triaxial cell. The constant rate of deformation was applied using the triaxial frame.

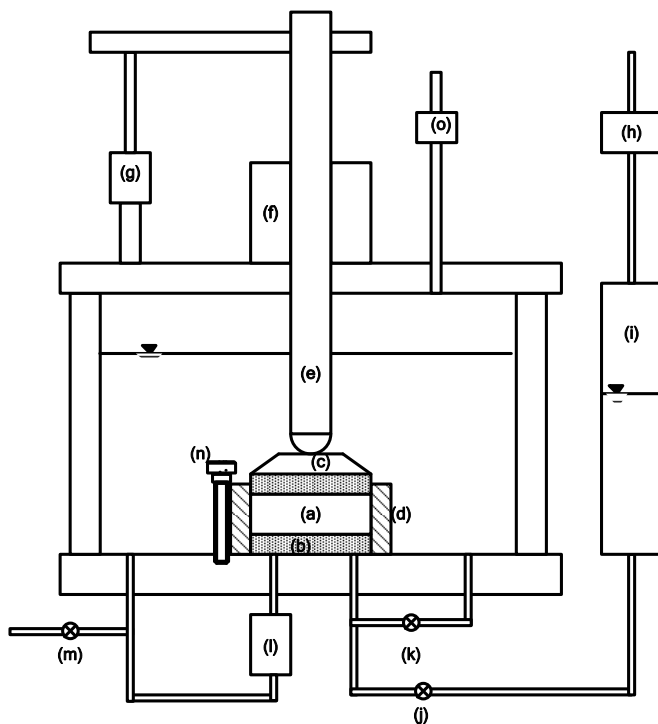
The CRS test apparatus as per ASTM D4186-12 (2012) is shown in Figure 2.23. The apparatus was designed such a way that the specimen in the confinement ring is sealed to a rigid base, with porous stones on each faces of the specimen and a cell pressure chamber. The pressure chamber contains the cell water and provides alignment and a pressure seal for the piston. The axial loading piston transfers the force to the specimen and passes through the pressure chamber. Transducers are required to measure the base pressure, the cell pressure, the axial deformation and the axial force. Any compression device which can apply a constant rate of deformation is an essential requirement.

*It can be concluded that various set-ups are used for performing CRS test. The apparatus developed by Wissa et al. (1971) is widely used; however, the design of the apparatus is not simple. Other set-ups are mainly modified triaxial cells to perform CRS test. Hence, it will be good to have a modified consolidometer for performing CRS test rather than triaxial cell, which will be discussed in subsequent sections.*



- (a) Specimen
- (b) Consolidation ring
- (c) Chamber
- (d) Porous stone
- (e) Pore pressure transducer
- (f) Reservoir
- (g) Displacement transducer
- (h) Loading ram
- (i) Back pressure regulator
- (j) Air vent

Figure 2.20: CRS test apparatus suggested by Gorman *et al.* (1978)



- (a) Soil specimen
- (b) Porous stones
- (c) Loading platen
- (d) Consolidation ring
- (e) Loading piston
- (f) Low friction seal
- (g) Displacement transducer
- (h) Regulator for permeability test
- (i) Burette
- (j) Valve for permeability test
- (k) Back pressure valve
- (l) Differential pressure transducer
- (m) Valve to water reservoir
- (n) Fastening post for consolidation ring
- (o) Cell pressure regulator

Figure 2.21: CRS test apparatus suggested by Armour and Drnevich (1986)

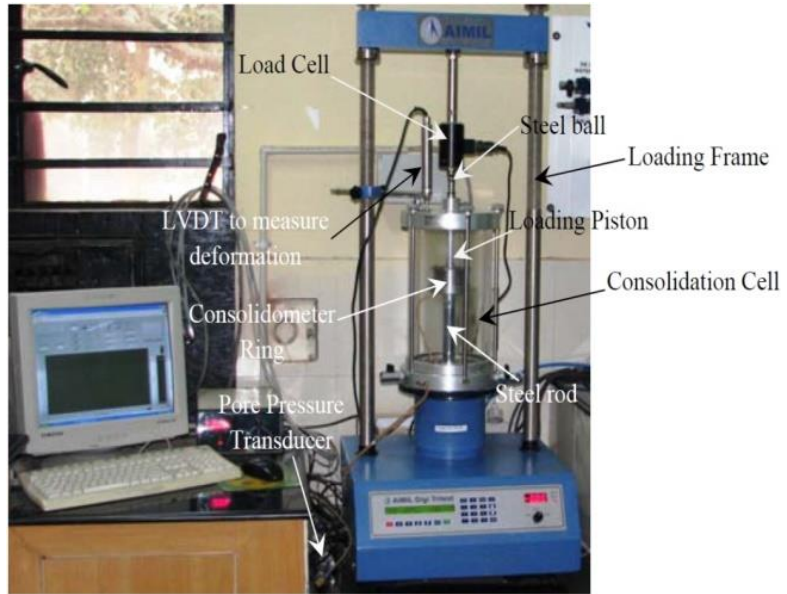


Figure 2.22: CRS test apparatus suggested by Prashant and Vikash (2014)

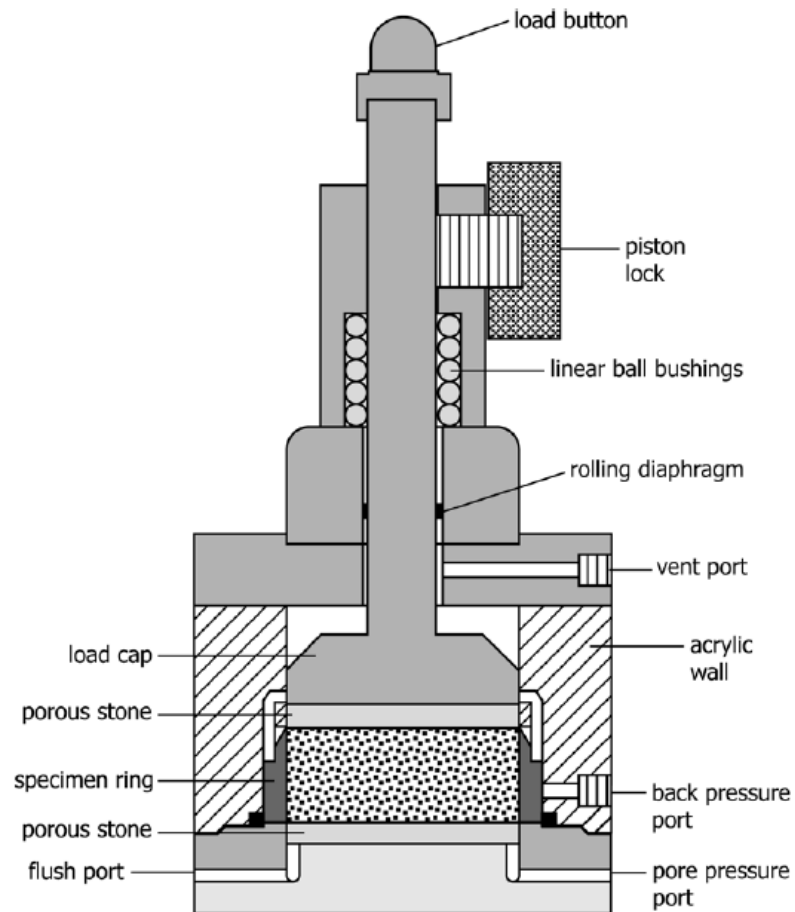


Figure 2.23: CRS cell suggested in ASTM D4186-12 (2012)

### 2.4.3 Strain Rate Selection Criteria and Effect on the Soil Behaviour

The consolidation parameters obtained from the CRS test is strain rate dependent (Olson, 1986). Therefore, fixing proper strain rate is one of the most crucial parts of the CRS test, in order to obtain consolidation parameters which are consistent with the IL consolidation test. Many studies were reported in the literature, which investigate the strain rate effect on consolidation parameters (Leroueil *et al.* 1985; Sheahan and Watters, 1997; Adams, 2011; Sample and Shackelford, 2012).

Smith and Wahls (1969) performed the constant rate of strain consolidation tests on two clays such as Massena clay and Calcium montmorillonite. The tests were conducted at various rates of strain ranging from 0.0024% per min to 0.06% per min. Figure 2.24 shows the results obtained from the tests conducted with Massena clay. For higher rates of strain, the  $e$ - $\log \sigma_v'$  curve obtained from the CRS test deviates considerably from those obtained from the conventional tests. High strain rate results in rapid increase in excess pore pressure thereby over estimating preconsolidation pressure, and steady state condition will not be achieved when the increase in pore pressure is too rapid (Leroueil *et al.* 1983; Larsson and Salfors, 1986; Silvestri *et al.* 1986). When the rate is too low, there will be no significant increase in pore water pressure which will result in unreasonably high values of  $c_v$  (Smith and Wahls, 1969). Therefore, correct rate of strain shall be fixed so as to obtain reliable parameters.

The effect of strain rate on the compressibility was studied by a few researchers. It was observed that the effect of strain rate is more noticeable in structured clays (Vaid *et al.* 1979; Leroueil *et al.* 1985) than in the reconstituted clays (Smith and Wahls, 1969; Sheahan and Watters, 1997). The strain rate effect on hydraulic conductivity is also studied in the literature (Moriwaki and Umehara, 2003; Ahmadi *et al.* 2011; Adam, 2011). Total settlement parameters (compression index and recompression index) are generally independent of selected strain rate (Jia *et al.* 2010). Similar conclusions were also made by Pu and Fox (2016) from the numerical investigation of strain rate effect on CRS test results.

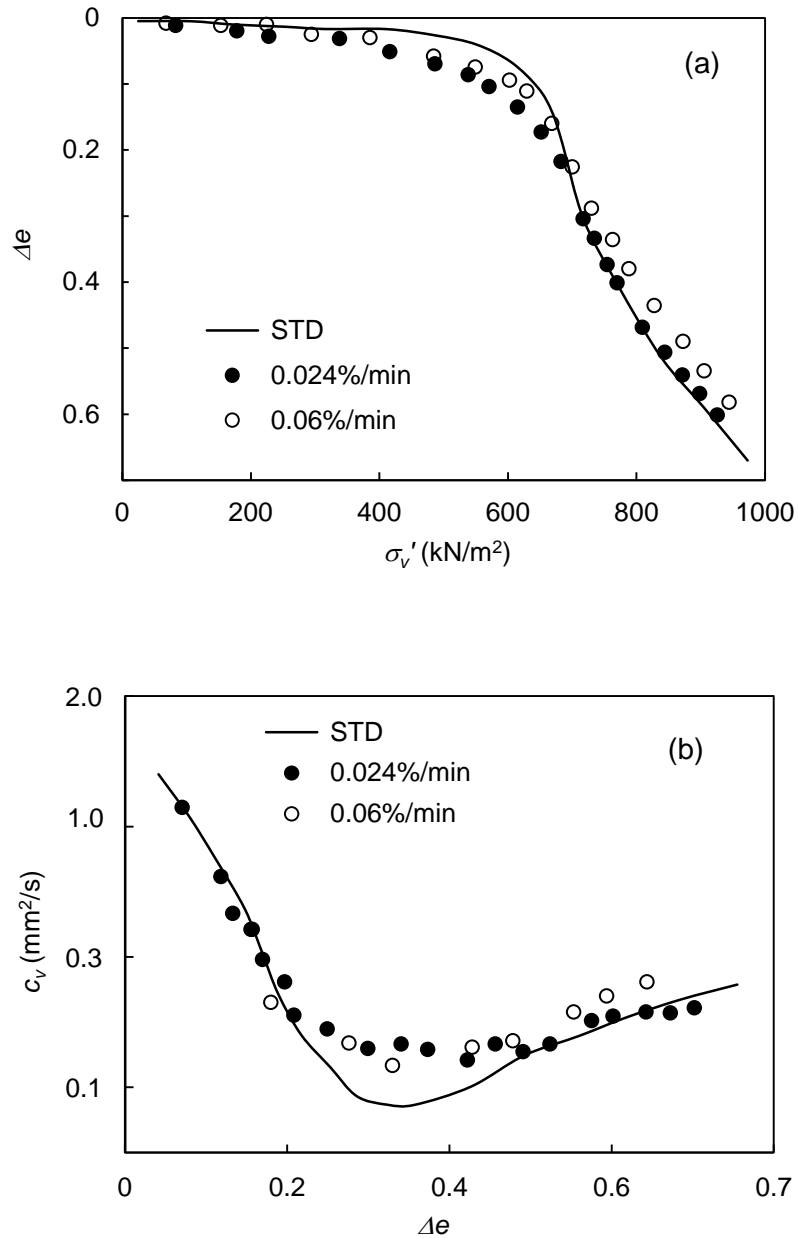


Figure 2.24: (a) Plot of  $\Delta e$  versus  $\log \sigma'_v$  and (b) plot of  $c_v$  versus  $\Delta e$  for Massena clay (Smith and Wahls, 1969)

Likewise, the development of the pore water pressure at the base of the specimen is also dependent on the strain rate. Some researchers suggested values of the maximum allowable pore pressure ratio ( $r_u$ , which is the ratio of pore water pressure at the base to the total stress). The reported values (Table 2.2) vary between 3%-50% in the literature.

Table 2.2: Maximum allowable pore pressure ratio recommended in the literature

Reference	Recommended, $r_u$	Remarks
Smith and Wahls (1969)	0.5	Kaolinite, Calcium montromonolite, Massana clay were used
Wissa <i>et al.</i> (1971)	0.05	Artificially sedimented boston blue clay was used
Sallfors (1975)	0.1-0.5	Bakebol clay was used
Gorman <i>et al.</i> (1978)	0.3-0.5	Kentucky soils were used
Lee <i>et al.</i> (1993)	0.15	Singapore marine clay was used, for $\beta \leq 0.1$
ASTM D4186-12(2012)	0.03-0.15	Restrict the transient condition in the CSL tests

ASTM standards (ASTM D4186-12 (2012)) recommends that the strain rate can be controlled during the test, such a way that the pore pressure ratio is limited to 0.03-0.15, so as to restrict the transient condition. Therefore, the rate is controlled during the test so as to maintain the pore pressure ratio. Subsequently, the CRS test is named as Controlled-Strain Loading (CSL) consolidation test. Henniche and Belkacemi (2018) conducted a numerical study, where Terzaghi's theory under constant loading is used to simulate the CRS consolidation test at small and large strains. They observed that the pore pressure ratio criterion recommended by ASTM standard leads to CRS test results comparable to those of IL consolidation test. Proper guideline for the selection of strain rate is not available in the literature. Few empirical approaches suggested in the literature are discussed in the next section.

Smith and Wahls (1969) suggested a strain rate equation based on the theoretical model as follows:

$$R = \frac{c_v c_c}{mH^2(1+e_0)} \left( \frac{\frac{u_b}{\sigma_1}}{1 - 0.7 \left( \frac{u_b}{\sigma_1} \right)} \right) \quad (2.39)$$



where,  $c_v$  is the coefficient of consolidation,  $c_c$  is the compression index,  $m$  is a proportionality constant corresponding to time of development of the maximum allowable pore pressure ( $u_b$ ) and  $H$  and  $e_0$  are the initial height and void ratio of the specimen, respectively. As  $c_v$  and  $c_c$  are not known apriori, the method requires an advance IL consolidation test before performing the CRS test.

Gorman *et al.* (1978) suggested an empirical correlation for the selection of strain rate criteria based on liquid limit of soils. If the liquid limit of soils  $> 60\%$ , CRS consolidation test can be conducted at a strain rate of 0.3% per hour and for lower liquid limit the strain rate can be doubled. Similarly, ASTM standard (ASTM D4186-82 (1982)) has recommended the use of liquid limit as the basis to choose the rate. Crawford (1988) reported that the strain rate does not depend on the liquid limit. Later in ASTM D4186-12 (2012) it was revised based on soil classification as shown in Table 2.3. Numerical study conducted by Pu *et al.* (2016) suggested that the strain rate recommended based on soil classification leads to erroneous results, depending on the variation in the values of coefficient of consolidation.

Table 2.3: Rate of strain as per ASTM D4186

ASTM D4186-82 (1982)		ASTM D4186-12 (2012)	
Liquid limit range	Rate of strain % per minute	Soil classification	Rate of strain % per minute
Upto 40	0.04	MH	0.1667
40-60	0.01	CL	0.0167
60-80	0.004	CH	0.0016
80-100	0.001		
100-120	0.0004		
120-140	0.0001		

Lee (1981) proposed a dimensionless strain rate parameter ( $\beta$ ) as given in Eq. (2.29). Lee *et al.* (1993) proposed that the upper limit of  $\beta$  as 0.1, the rate  $r$  can be determined by knowing the coefficient of consolidation  $c_v$ . Pu and Fox (2016) conducted a numerical study using  $\beta < 0.1$  and recommended that the CRS consolidation test yields very good accuracy for both linear and nonlinear soils.

Subsequently, Armour and Drnevich (1986) recommended Eq. (2.40) based on the theory of Wissa *et al.* (1971) which requires the liquidity index (LI) and the initial permeability of the soil ( $k_i$ ).

$$r = \frac{-8 \exp(8 - 3LI) P_a k_i}{\gamma_w H_i^2} \log(1 - r_{u,\max}) \quad (2.40)$$

where,  $P_a$  is the atmospheric pressure,  $r_{u,\max}$  is the maximum allowable base pore pressure ratio and  $H_i$  is the initial height of the sample.

Recently, Ozer *et al.* (2012) developed a semi empirical method to determine the appropriate strain rate for the CRS tests. The prime requirement of the method is that, an IL consolidation test need to be performed prior to CRS test. The above methods require critical parameters or rely on empirical relations or basic properties of soils or reference tests.

#### 2.4.4 Interpretation of CRS Test Data

The purpose of CRS test is to obtain the consolidation parameters comparable to the standard IL consolidation test. During CRS test the specimen is not fully drained and excess pore pressure gets developed within the specimen. Therefore, it is essential to obtain the average effective stress on the specimen. By knowing the effective stress, the total settlement parameters can be obtained from the  $e$ - $\log \sigma_v'$  curve. The other consolidation parameters such as coefficient of consolidation ( $c_v$ ) and the coefficient of permeability ( $k$ ) can be evaluated by selecting suitable theory. As brought out in the previous sections, many theories are available to model the CRS test. The method of evaluating the effective stress and the consolidation parameters based on the theory are summarized in Table 2.4.

Fox *et al.* (2014) conducted a numerical investigation of the accuracy of linear and nonlinear data analysis methods for the CRS test and concluded that the most appropriate method for soils with linear compressibility as per the linear theory in ASTM D4186-12 (2012) and the nonlinear theory is erroneous. They developed a modified nonlinear (MNL) theory for nonlinear compressibility soils.

Table 2.4: Evaluation of Consolidation parameters based on various theories

Sl. No.	Theory	Parameters		
		$\sigma_v'$	$c_v$	$k$
1	Smith and Wahls (1969)	$\sigma_v' = \sigma_v - \alpha \times u_b$ $\alpha = \frac{\bar{u}}{u_b} = \frac{\frac{1}{H} \int_0^H u dz}{u_b} = \frac{\frac{1}{3} - \frac{1}{24} \left(\frac{b}{r}\right)}{\frac{1}{2} - \frac{1}{12} \left(\frac{b}{r}\right)}$	$c_v = \frac{rH^2}{a_v u_b} \left[ \frac{1}{2} - \frac{b}{r} \left( \frac{1}{12} \right) \right]$	$k = \frac{\gamma_w r H^2}{(1+e) u_b} \left[ \frac{1}{2} - \frac{b}{r} \left( \frac{1}{12} \right) \right]$
2	Wissa <i>et al.</i> (1971)	<p>Linear stress-strain relation:</p> $\sigma_v' = \sigma_v - \frac{2}{3} u_b$ <p>Non-linear stress-strain relation:</p> $\sigma_v' = (\sigma^3 - 2\sigma^2 u_b + \sigma_v u_h^2)^{1/3}$	$c_v = \frac{rH^2}{2u_h m_v}$ $c_v = \frac{-0.434 r H^2}{2\sigma_v' m_v \log\left(1 - \frac{u_b}{\sigma}\right)}$	$k = \frac{\gamma_w r H^2}{2u_h}$ $k = \frac{-0.434 \gamma_w r H^2}{2\sigma_v' \log\left(1 - \frac{u_b}{\sigma}\right)}$
3	Yoshikuni <i>et al.</i> (1995)	$\sigma_v' = \sigma_v - \bar{u} = \sigma_v - \frac{2}{3} u_b$	$c_v = \frac{rH^2}{2u_b m_v}$	$k = \frac{r\gamma_w H^2}{2u_b}$
4	Umehara and Zen (1980)	Solved numerically. A series of charts with curves relating the consolidation ratio to the strains and the non-dimensional parameter has been constructed.		
5	Lee (1981)	Solved numerically	$c_v = \frac{H^2 \Delta \sigma_v}{2u_b \Delta t}$	Solved numerically
6	Vikash (2013)	$\sigma_v' = \sigma_v - \bar{u} = \sigma_v - \frac{2}{3} u_b$	$c_v = \frac{r v H^2}{2u_b m_v}$	$k = \frac{r\gamma_w v H^2}{2u_b}$

#### **2.4.5 Time Taken to Complete the CRS Test**

The duration required for the CRS test are reinterpreted from the data available in the literature, is summarized in Table 2.5. The reported time in Table 2.5 is to reach the maximum pressure during loading phase only, without the unloading phase. In addition, consolidation tests are generally conducted to consolidation pressure  $(\sigma_v)_{\max}$  of about 800 kPa or more. Except Smith and Wahls (1969), the maximum pressure used by other authors, in Table 2.5, is less than 800 kPa. The expected time to reach 800 kPa, is calculated by extrapolating the  $e$ - $\log \sigma_v'$  data available upto  $(\sigma_v')_{\max}$  is also given in Table 2.5. The time taken ranges from 18.3-140 hours. In addition, if the test is conducted to get the swelling line (unloading phase), the time required will be even more. Therefore, CRS test also takes long time though the time taken is less compared to IL test with 24 hours duration.

### **2.5 SUMMARY OF LITERATURE REVIEW**

A detailed review of the available testing methods for one-dimensional consolidation test was described in this chapter. The summary of the literature review and research gaps are given below:

Consolidation parameters are conventionally determined from the oedometer test. The procedure for performing the one-dimensional consolidation test is well developed and many protocols are available in the literature. In the IL test, a laterally confined soil specimen is subjected to increment loading (IL) with a load increment ratio of generally 1.0. The test is a stress controlled test and the time-settlement data is continuously recorded for 24 hours under each loading stage. Many load increments are required to establish the void ratio ( $e$ )-consolidation pressure ( $\sigma_v'$ ) relationship both during loading and unloading stages. Usually, the test takes about 10-14 days to complete. The advantage of IL consolidation test is that the testing procedure is well established and the interpretation of data is straight forward. However, the test takes very long time.

Table 2.5: Duration of CRS Tests from the literature

Sl. No.	Reference	Soil	$c_v$ (m <sup>2</sup> /s)	rate, %/min	$(r_u)_{\max}$ %	$(\sigma_v)_{\max}$ , kPa	Time, hours	
							$(\sigma_v)_{\max}$ ,	800 kPa
1	Smith and Wahls (1969)	Massena clay	$1 \times 10^{-6}$ - $1 \times 10^{-7}$	0.024	4	800	18.3	18.3
2	Salfors (1975)	Bakebol clay	$1 \times 10^{-7}$ - $1 \times 10^{-8}$	0.017	10	600	34	40
3	Armour and Drnedvich (1986)	Cumberland river silty clay	$4 \times 10^{-8}$ - $1 \times 10^{-8}$	0.003	13.3	160	6	23
4	Sheahan and Watters (1997)	Resedimented Boston blue clay	$9 \times 10^{-7}$ - $5 \times 10^{-8}$	0.002	3	340	75	140
5	Ahmadi <i>et al.</i> (2014)	Gotberg soil	$2 \times 10^{-8}$	0.006	15	400	80	120

Attempts were also made in the literature to reduce the test time of IL load test. The procedure suggested by Newland and Allely (1960) saves considerable consolidation time compared to 24 hour duration test. However, high plastic clays may take long time for 100% primary consolidation. Sridharan *et al.* (1999) suggested a method based on the rectangular hyperbola method, where effective stress correction was derived based on degree of consolidation. Interpretation based on pore pressure estimate or measurement is more appropriate.

Hamilton and Crawford (1959) developed constant rate of strain (CRS) consolidation test which is a strain controlled consolidation test. Several theories and test procedure were suggested by various researchers to get more accurate consolidation properties when compared with incremental loading test. After the development of theories to interpret CRS test, the test has gained popularity because of the following reasons:

- (i) The test is faster than the incremental loading test with 24 hours duration between successive pressure increments.
- (ii) Continuous data points are acquired, so that more accurate determination of preconsolidation pressure is possible.

Although the CRS test has the above advantages, the major limitation is that the procedure for fixing proper rate of strain for conducting CRS test is not yet fully established and the required rate for unloading phase is not clear. Therefore, it is essential to develop a rational way to fix proper strain rate of CRS test

The other consolidation methods such as CG, CRL, RFC, CPR and BPC test methods are not simple as they require continuous monitoring and automation.

Based on the literature review covered in this chapter, the need for the study are arrived as follows:

- a) Several guidelines are suggested in the literature to select proper strain rate of CRS test. These methods either require the assumption of critical parameters or

rely on empirical relations or an advance test. No rational procedure to fix the strain rate of CRS test is available.

- b) Various apparatus are suggested in the literature to perform constant rate of strain (CRS) consolidation test. However, the design of the apparatus are not simple. Development of a simplified CRS cell is scarce in literature.
- c) While CRS test with pore pressure measurement at the base of the sample is popular in the literature, studies on stress controlled (SC) consolidation with pore pressure measurements so as to reduce the test duration is not attempted in the literature.
- d) Reduced duration of conventional IL consolidation test based on standard curve fitting procedure is not properly addressed in the literature. Development of procedure and interpretation techniques for faster consolidation, based on conventional IL consolidation test needs to be studied.

The objectives of the present research work are as follows:

- (a) To develop a rational procedure to fix the strain rate of CRS test and guidelines to control the strain rate during the CRS test, so as to limit the pore pressure ratio within the permissible limits.
- (b) To develop a simplified CRS apparatus and to modify the conventional fixed ring consolidometer to perform CRS test.
- (c) To study stress controlled (SC) consolidation test with pore pressure measurements, so as to develop a faster consolidation testing procedure and
- (d) To develop testing procedures for accelerated incremental load consolidation test using standard curve fitting procedures.

The scope of the present work is limited to studies on reconstituted soils samples. Few undisturbed soil samples will also be used.





## **CHAPTER 3**

### **MATERIALS AND CONTROL TESTS**

#### **3.1 INTRODUCTION**

As discussed in the previous chapter, the main objective of the present research is the development of accelerated consolidation testing procedures. A detailed experimental work needs to be carried out on fine grained soils to validate the methods. The fine grained soil samples were collected from various parts of India, which comprise of both disturbed and undisturbed soils. This chapter presents the details of soils selected for the study and basic characterization. The one-dimensional incremental loading (IL) consolidation test forms the control test. Therefore, the sample preparation technique, testing procedure and the results obtained from the conventional incremental loading consolidation test are also included in this chapter.

#### **3.2 SELECTION OF SOILS**

The fine grained soils were selected such a way that it covers a wide range of plasticity characteristics. Seven disturbed soil samples namely, Red soil 1, Red soil 2, Gummudipoondi clay, Kaolinite, Taramani clay, Siruseri clay and Bombay marine clay were collected for carrying out tests on reconstituted soils. The Red soils, Gummudipoondi clay, Taramani clay and Siruseri clay were procured from different parts of Chennai, Tamil Nadu, India. Kaolinite is commercially available which was procured in powder form. The Bombay marine clay was collected from a site near the Bombay port, Maharashtra, India. The selected soil samples were processed and sieved through 425 $\mu$  sieve, so as to remove the shells and other foreign materials. The processed soil samples were stored in air-tight plastic containers in slurry form with water content of about 1.5 to 2 times the liquid limit for testing.

Few undisturbed soil (UDS) samples were also collected from various sites in India. Mainly marine clay samples were collected from different sites in Cochin and Bombay. The Cochin Marine Clay samples were collected from depths of 5 m, 16 m, 19.5 m and

21 m. The Bombay Marine Clay samples were collected from depths of 6 m and 12 m. In addition, an UDS sample was collected from a site at Madhavaram near Chennai at a depth of 6 m. The collected UDS samples were stored in sampling tubes with wax coating at the ends so as to eliminate loss of moisture due to evaporation.

The reconstituted soil samples were used to perform series of experiments to validate the proposed one-dimensional consolidation testing methods. In addition, the undisturbed samples were used based on their availability, as only limited number of samples were available. The basic characterizations of the selected soil samples were done as per the Indian standard specifications and the values are reported in the next section.

### **3.3 INDEX PROPERTIES OF THE SOILS**

The index properties of the fine grained soils were determined for identification and classification as per various parts of IS 2720. Specific gravity of the soils were determined using density bottle method as per the testing procedure in IS 2720-3 (1985).

Atterberg limit tests were conducted as per IS 2720-5 (1980). The liquid limit was determined using Casagrande apparatus. The plastic limit was determined by making 3 mm diameter thread. The marine clay samples were never allowed to dry before the test as the properties change on drying (Rao *et al.* 1989; Ayyar *et al.* 1990; Basma *et al.* 1994; Babu *et al.* 2008; Suganya and Sivapullaiah, 2016). The Atterberg limits of the soils are summarized in Table 3.1 along with the soil classification as per IS 1498 (1970). In Table 3.1 the soils are arranged in the order of increasing plasticity characteristics. The plasticity chart of the soils is shown in Figure 3.1. It can be observed that the soils cover a wide range of plasticity characteristics with liquid limit of the soils varying from 32%-165%. It can be also seen that most of the soils lie above A-line and are clayey soils, except Bombay marine clay, Bombay marine clay (12 m) and Cochin marine clay (21 m) were found to below A-line. These soils are either MH or OH. Therefore, they are further classified by conducting liquid limit test on oven dried state. As per IS 1489 (1970), on oven drying the liquid limit of OH types of soils will be reduced to less than 0.75 times the liquid limit of soil in the natural state. The liquid limit of oven dried Cochin marine clay (21 m) was reduced to 68% from 131% and hence, it was classified as OH type soils. The oven dried liquid limit of Bombay marine clays was 95%, which is 0.9 times the

liquid limit in its natural state. Hence, the Bombay marine clay was classified as MH type.

Grain size distribution of the soils were determined as per IS 2720-4 (1985). Wet sieve analysis using a 75 $\mu$  IS sieve was carried out on the oven dried samples. Dry sieve analysis was carried out on the fraction retained on the 75 $\mu$  IS sieve. Hydrometer analysis was carried out on the fractions passing through the 75 $\mu$  IS sieve and dispersion agents were added to avoid flocculation. Grain size distribution curve was established by combined results of dry sieve analysis and hydrometer analysis. The combined grain size distribution curve is shown in Figure 3.2. The marine clay samples were directly wet sieved without oven drying, as it was reported in the literature that oven drying will change the soil properties of marine clays (Rao *et al.* 1989; Ayyar *et al.* 1990; Basma *et al.* 1994; Babu *et al.* 2008; Suganya and Sivapullaiah, 2016). The percentages of sand, silt size and clay size are calculated from the grain size distribution curve and are also reported in Table 3.1. Except Red soil 1, Red soil 2 and Madhavaram clay, all other soils contain negligible amount of sand fraction.

In order to find out the mineralogy of the clay specimens, X-ray diffraction (XRD) analyses was carried out on the clay fraction. 50 g of fines (< 75 $\mu$ ) was mixed to form a slurry with solid to liquid ratio of 1:20. The slurry was allowed to settle for 24 hours so that the silt size gets settled. The suspension, which consists of predominantly clay sized particles were decanted. The decanted suspension was oven dried and made to powder. PANalytical X-Ray diffractometer was used to perform the test. The XRD analysis was performed on the powdered sample starting from  $2\theta$  angle of  $4.5^{\circ}$  with a scanning rate of  $1^{\circ}$  per min. The XRD patterns of all reconstituted soils are shown in Appendix A. A typical XRD plot for Red soil 1 is shown in Figure 3.3. The XRD data were analysed using ICDD standard. The clay and non-clay minerals were identified and semi quantitative analyses were carried out using the ICDD database. The XRD results obtained for all the reconstituted soils are summarized in the Table 3.2. It can be seen that the selected soils consists of predominantly the basic clay minerals such as kaolinite, illite and montmorillonite. Traces of iron oxides and parent rock minerals such as feldspar and muscovite and some amount of quartz were also present.

Table 3.1: Properties of the soils used for the study

Sl. No.	Soil Type	$G_s$	Atterberg limits (%)			Grain size limits (%)			Classification
			$w_l$	$w_p$	$I_p$	Sand	Silt size	Clay size	
<i>Reconstituted soils</i>									
1	Red soil 1	2.66	32	15	17	43	43	14	CL
2	Red soil 2	2.70	47	23	24	25	22	53	CI
3	Gummudipoondi clay	2.60	59	25	34	8	34	58	CH
4	Kaolinite	2.69	63	29	34	0	31	69	CH
5	Taramani clay	2.67	72	27	45	12	28	60	CH
6	Siruseri clay	2.68	80	32	52	7	22	71	CH
7	Bombay marine clay	2.71	104	47	59	1	40	59	MH
<i>Undisturbed soils</i>									
8	Madhavaram clay (6 m)*	2.64	39	16	23	70	8	22	CI
9	Bombay marine clay (12 m)	2.75	105	40	55	3	42	55	MH
10	Cochin marine clay (21 m)	2.56	131	53	78	3	39	58	OH
11	Cochin marine clay (5 m)	2.20	134	48	86	2	54	44	CH
12	Cochin marine clay (19.5 m)	2.60	162	56	106	0	44	56	CH
13	Cochin marine clay (16 m)	2.44	165	55	110	3	59	38	CH

Note:  $G_s$ - Specific gravity,  $w_l$ -Liquid limit,  $w_p$ - Plastic limit,  $I_p$ - Plasticity index, \* Values in parenthesis represent the depth at which the samples were collected

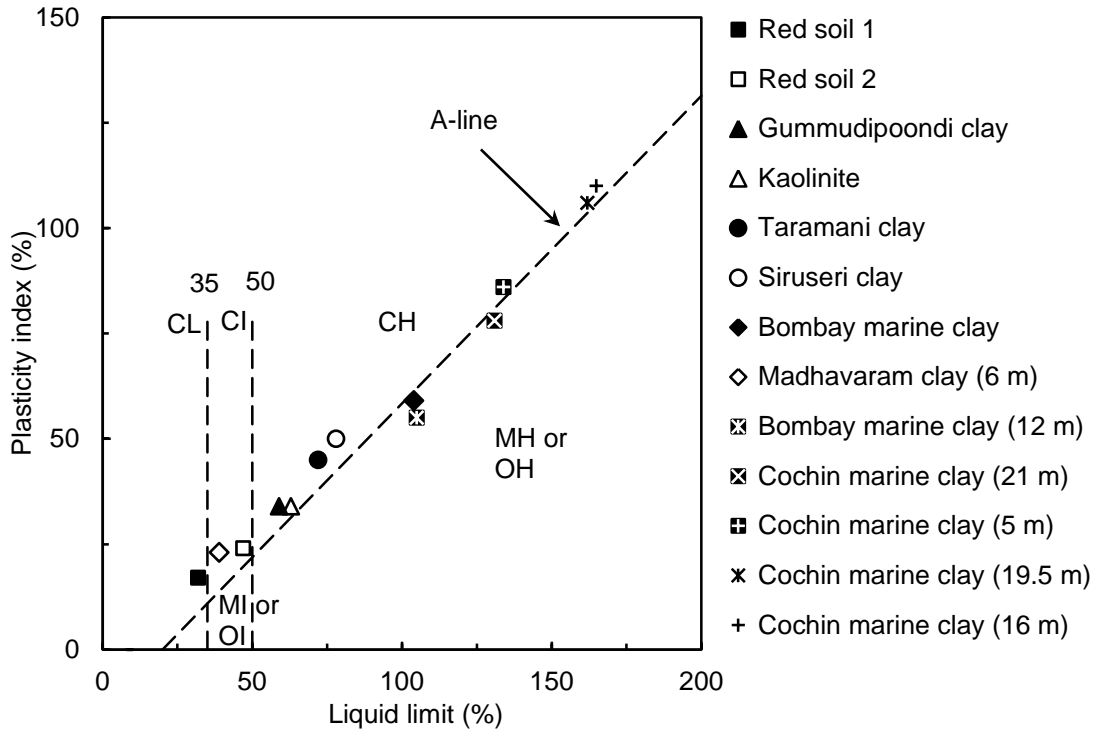


Figure 3.1: Soils selected in the Plasticity chart

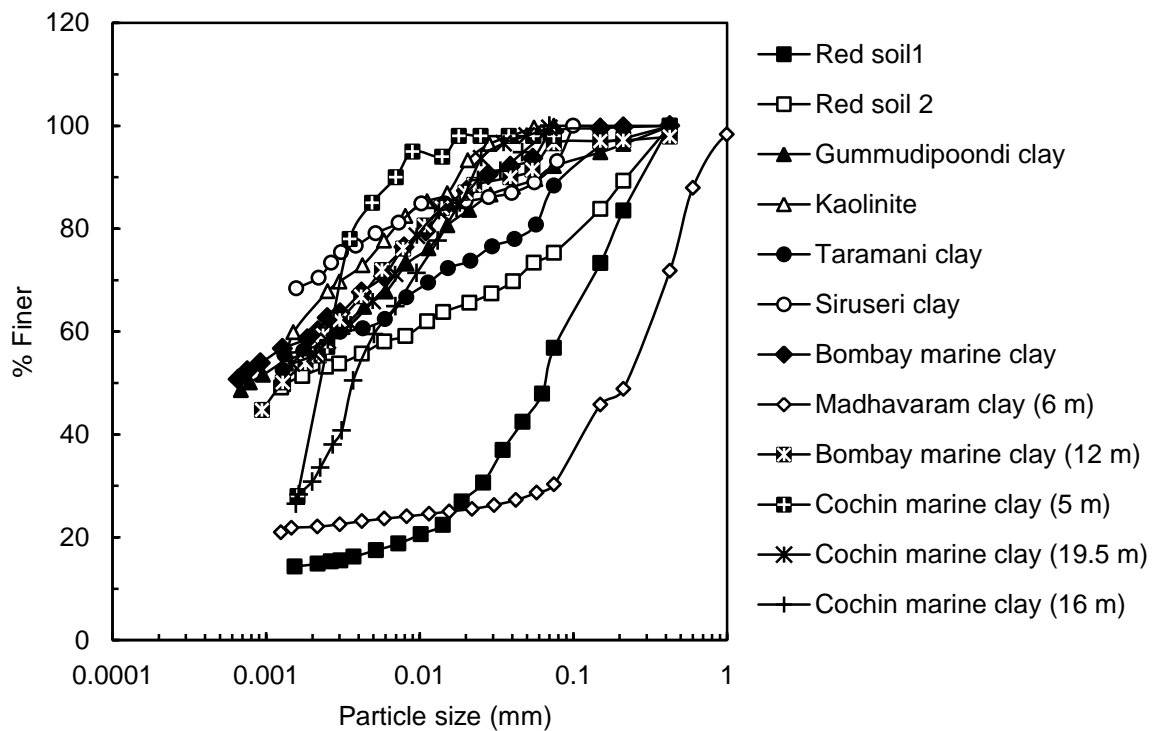


Figure 3.2: Grain size distribution curve

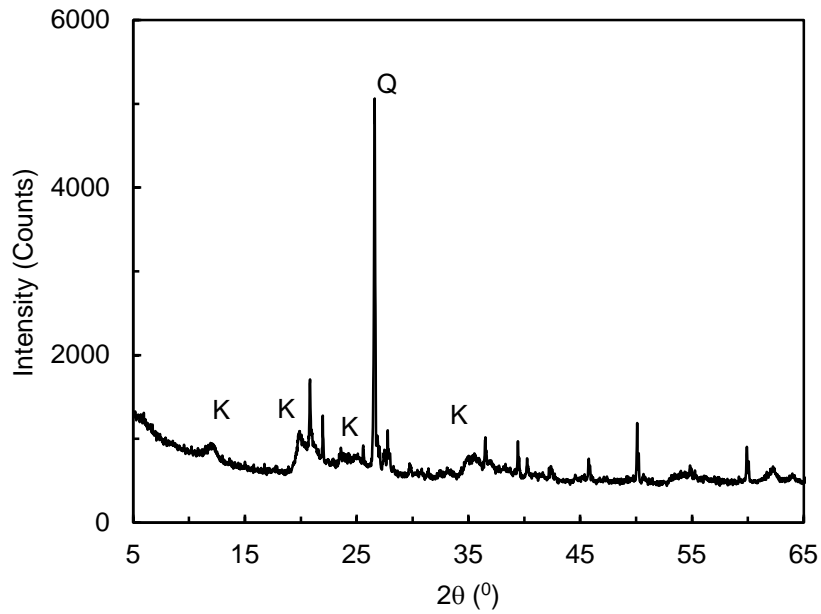


Figure 3.3: Typical XRD pattern of Red soil 1

Table 3.2: Minerals present in the reconstituted soils

Sl. No.	Soil	Minerals	
		Non clay	Clay
1	Red soil 1	Quartz, Feldspar, Magnetite	Kaolinite
2	Red soil 2	Quartz, Hematite	Kaolinite, Illite
3	Gummudipoondi clay	Quartz	Vermiculite, Montmorillonite
4	Kaolinite	Muscovite	Kaolinite
5	Taramani clay	Quartz, Feldspar, Magnetite	Montmorillonite, Illite
6	Siruseri clay	Quartz	Montmorillonite, Vermiculite
7	Bombay marine clay	Quartz, Magnetite, Calcite	Illite, Kaolinite

The selected soils were subjected to series of one-dimensional consolidation testing, where conventional one-dimensional incremental loading (IL) consolidation test with 24 hours duration and End-Of-Primary (EOP) consolidation test were taken as the control test. The sample preparation technique, testing procedure and results obtained are discussed in the next section.

### **3.4 CONTROL CONSOLIDATION TESTS**

Control tests were performed for comparing and validating the results of the proposed one-dimensional consolidation testing methods under stress controlled and strain controlled conditions. Two types of one-dimensional incremental loading consolidation tests were performed as control tests, one was the conventional IL consolidation test with load duration of 24 hours under each increment and the other type was the EOP consolidation test in which the load was maintained only upto the EOP consolidation based on the  $\sqrt{t}$  method (Section 2.3.6). The stages of sample preparation, testing procedure and the results obtained from the control tests are discussed in the subsequent sections.

#### **3.4.1 Sample Preparation**

In the present study, consolidation ring of 60 mm diameter and 20 mm thickness was used (Figure 3.4(a)). The consolidation rings are made of stainless steel of grade 316. The inner surface of the rings was highly polished. In addition, Silicone grease was smeared on the inner surface so as to reduce the friction between the soil and the ring. Two porous stones were used at the ends of the specimen to allow for two-way drainage. The porous stones were saturated by boiling in water. Filter papers were used as separators between the specimen and the porous stones to prevent clogging of porous stones. An O-ring was placed at the base of the cell to avoid the leakage from the bottom of the specimen, so that falling head permeability tests could be performed during one-dimensional consolidation testing, between successive load increments. The reconstituted soil specimens were prepared by consolidating the soil slurry with water content of 1.5 to 2 times the liquid limit water content. The slurry was directly reconstituted in the consolidation ring itself so as to reduce disturbance. After assembling the apparatus in the consolidation apparatus, a collar of 15 mm thickness having the same inner diameter as that of the consolidation ring was placed above the consolidation ring so that the total thickness available for preparing the specimen is 35 mm (Figure 3.4(b)). The clay slurry was carefully poured in to the consolidation ring with the collar to a thickness of 30 mm (Figure 3.4(c)). A small loading frame was used for preloading the specimen as shown in Figure 3.4(d) and a dial gauge was used to monitor the time-settlement data there by ensuring the end of primary consolidation.

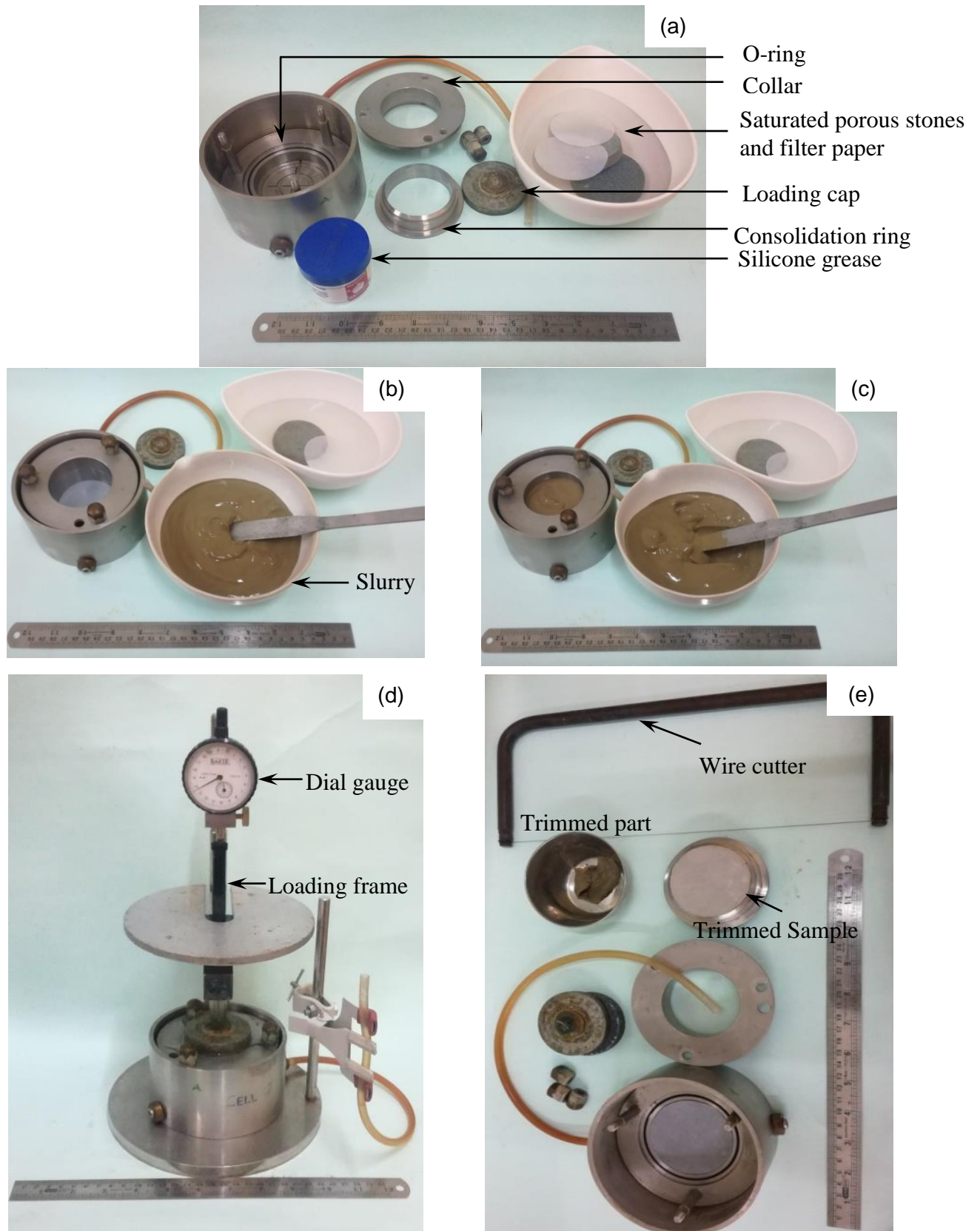


Figure 3.4: Various stages of sample preparation (a) Components of consolidation cell (b) Assembling consolidation ring and collar (c) Pouring the slurry into the ring with collar (d) Preloading stage and (e) Trimming off the extra sample



To study the normally consolidated (NC) behaviour, the slurry was consolidated to a consolidation pressure of 12.5 kPa (Figure 3.4(d)) in steps. Once the consolidation was over, the ring with the specimen was carefully taken out and the excess soil above the consolidation ring was trimmed-off using a thin wire cutter so that the initial thickness of the specimen is 20 mm (Figure 3.4(e)). The trimmed part was used to determine the initial water content of the specimen.

Similarly, overconsolidated specimens with known preconsolidation pressure were prepared by preconsolidating to a higher pressure instead of 12.5 kPa using the conventional loading frame. The undisturbed soil specimens were directly trimmed in to the consolidation ring using a cutting ring and a wire cutter. The prepared specimens were subjected to one-dimensional consolidation test as per the procedure explained in the next section.

### **3.4.2 Testing Procedure**

The soil specimen was set up in the loading frame with a seating pressure of 12.5 kPa, which is equal to the initial preconsolidation pressure (Section 3.4.1) used for the preparation from the slurry. The specimen was loaded with a load increment ratio of 1.0, with loading sequence of 12.5-25, 25-50, 50-100, 100-200, 200-400 and 400-800 kPa and then unloaded to 800-200, 200-50, 50-12.5 kPa. Two one-dimensional IL consolidation tests were performed on each specimen such as conventional IL test with duration of 24 hours and end-of-primary (EOP) consolidation test.

In the conventional IL consolidation test, each increment of load was maintained for 24 hours and time-settlement data were continuously recorded throughout the loading period. Typical plot of time-settlement data from IL consolidation test with duration of 24 hours, for a reconstituted soil (Gummudipoondi clay) and for an undisturbed soil (Cochin marine clay 21 m), are shown in Figures 3.5(a) and 3.5(b), respectively. These data are used to determine the rate of consolidation parameters such as coefficient of consolidation ( $c_v$ ) and coefficient of secondary compression ( $c_\alpha$ ). The time-settlement plots for all other specimens are presented in Appendix B.

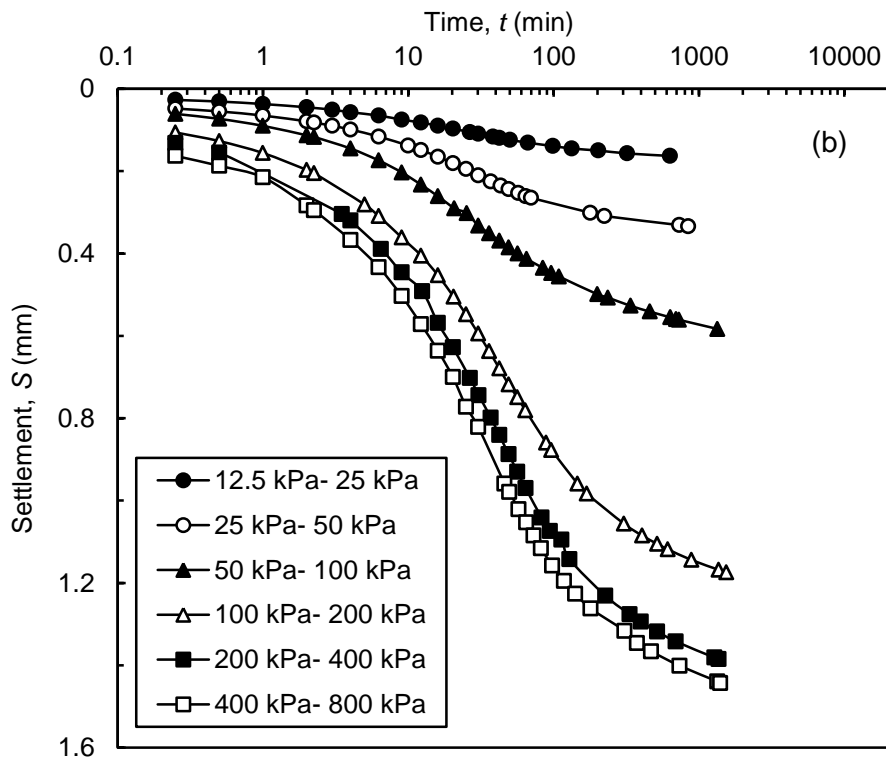
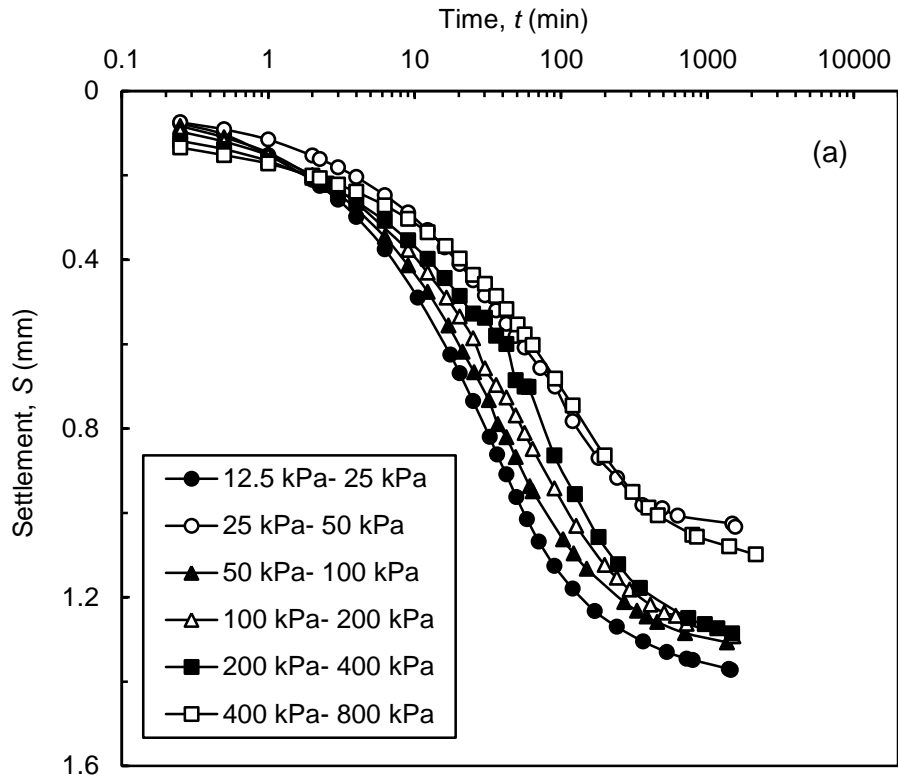


Figure 3.5: Typical time-settlement response in IL consolidation test with 24 hours duration for (a) Reconstituted specimen of Gummudipoondi clay and (b) Undisturbed specimen of Cochin marine clay sampled at 21 m depth

The end-of-primary (EOP) consolidation test was also performed as one of the control tests. It can be performed in two ways, one is based on curve fitting procedure and other is based on pore pressure measurements (Section 2.2.1). In the present study, Taylor's  $\sqrt{t}$  curve fitting procedure was selected to define EOP as given in Terzaghi *et al.* (1996). The progress of the consolidation was continuously monitored using the  $\sqrt{t}$  plot (Figure 3.6). Knowing the settlement corresponding to  $U = 90\%$  ( $S_{90}$ ), at D, and the initial compression  $S_0$ , the settlement required to reach  $U = 100\%$  is determined as:

$$S_{100} = \frac{100}{90} \times (S_{90} - S_0) + S_0 \quad (3.1)$$

where,  $S_0$  is the initial compression,  $S_{90}$  is the settlement corresponding to 90% degree of consolidation. Once the settlement corresponding to  $S_{100}$  is reached at E, the next increment of load was applied. Similar procedure was followed for unloading also. During the EOP test, time-settlement data during loading and time-swelling data during unloading were continuously recorded. A typical plot for a reconstituted specimen of Gummudipoondi clay is shown in Figure 3.7. Time-settlement graphs for other soils from the EOP test are presented in Appendix C. The time-settlement and time-swell data from one-dimensional IL consolidation test with duration of 24 hours and EOP test were analysed and the results are discussed in the next section.

### 3.4.3 Results and Discussions

One-dimensional consolidation parameters of the soils used were determined from the time-settlement data obtained for each pressure increment. Terzaghi's theory of one-dimensional consolidation was used to analyse the consolidation test data. The rate of settlement parameters such as coefficient of consolidation ( $c_v$ ) and coefficient of secondary compression ( $c_\alpha$ ) and the total settlement parameters such as compression index ( $c_c$ ), recompression index ( $c_r$ ) and preconsolidation pressure ( $\sigma_c'$ ) were determined from the test data. The results obtained from the IL test with duration of 24 hours and EOP test are discussed in the next section.

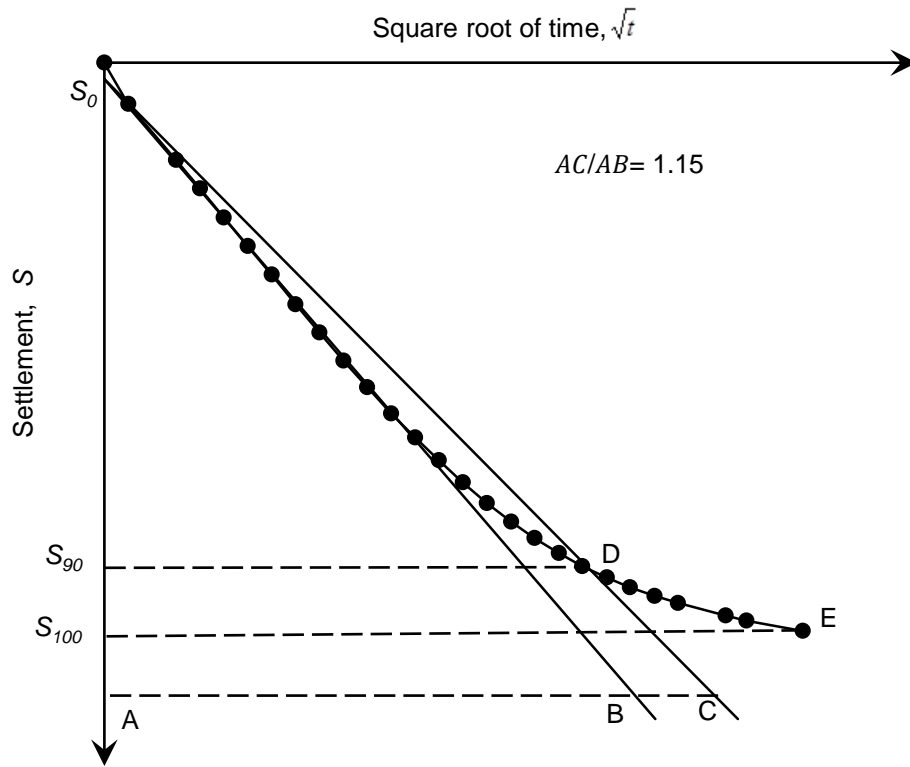


Figure 3.6: EOP consolidation using  $\sqrt{t}$  method

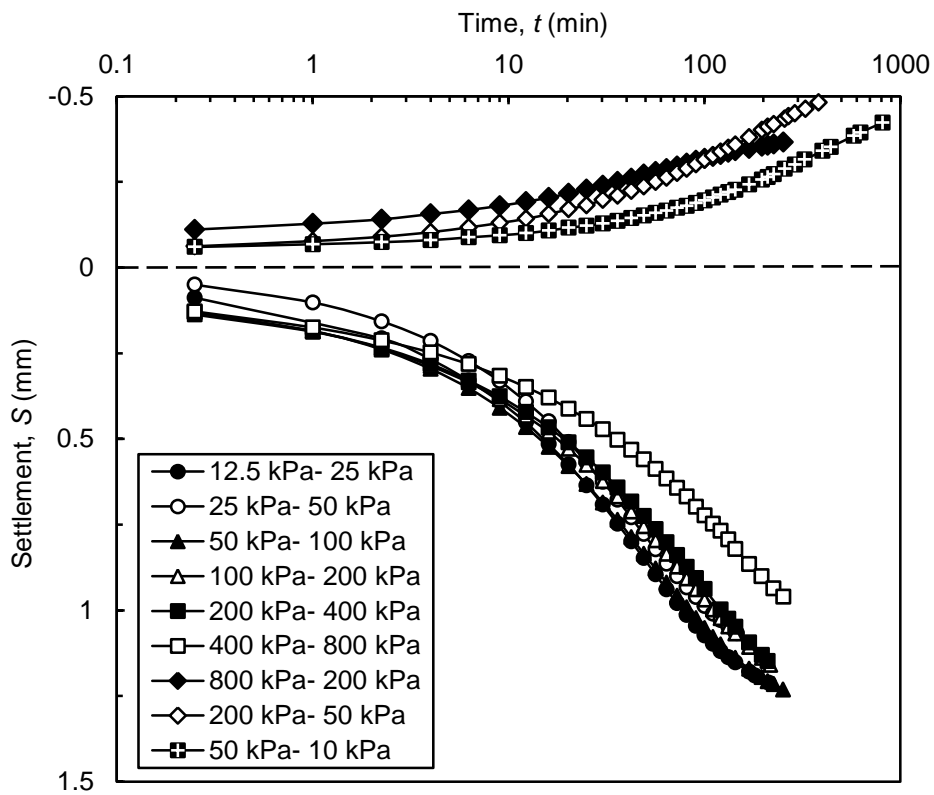


Figure 3.7: Time-settlement plot from the EOP test for Gummudipoondi clay

### ***Rate of settlement parameters***

Coefficient of consolidation ( $c_v$ ) from the conventional IL test with duration of 24 hours was calculated using Taylor's  $\sqrt{t}$  method (Taylor, 1942) and Inflection point method (Robinson, 1997) for each pressure ranges (Section 2.3.3). The  $c_v$  values obtained for both reconstituted and undisturbed soils for IL test with 24 hours duration are plotted with consolidation pressure as shown in Figure 3.8(a) and 3.8(b), respectively. The  $c_v$  values from the EOP test was calculated using the inflection point method and the  $\sqrt{t}$  method and plotted with consolidation pressure as shown in Figure 3.9(a) and Figure 3.9(b), respectively.

In Figures 3.8 and 3.9, it can be observed that the variation of coefficient of consolidation with effective stress is not unique but may increase or decrease with consolidation pressure. Similar observations were already reported in the literature (Section 2.3.3). Robinson and Allam (1998) reported that the variation of coefficient of consolidation with consolidation pressure can be attributed to the clay mineralogy of fine grained soils. For soils with Kaolinite and Illite as the dominant clay minerals the  $c_v$  values will increase with consolidation pressure and Montmorillonite clays the  $c_v$  values decrease with consolidation pressure. Red soils and Bombay marine clay shows an increasing trend of  $c_v$  with consolidation pressure. As it can be seen in Table 3.2, Kaolinite and Illite are the predominant clay minerals in these soils. Similarly, Gummudipoondi clay, Taramani clay and Siruseri clay where predominant clay minerals are Montmorillonite and Vermiculite show a decreasing trend of  $c_v$  with consolidation pressure.

The  $c_v$  values were calculated using  $\sqrt{t}$  method and inflection point method from the IL test with 24 hours duration and the EOP consolidation test and are presented in Figure 3.10(a) and 3.10(b), respectively. The average coefficient of variance (COV) is 23% and 19% for IL test and EOP test, respectively. Though COV is quite high, it is acceptable for the case of  $c_v$ , as  $c_v$  values are method dependent (Sridharan *et al.* 1994; Leonards and Ramiah, 1959). Similarly, the  $c_v$  values from the IL test and the EOP test are compared in Figure 3.11. It can be seen that the comparison is reasonable.

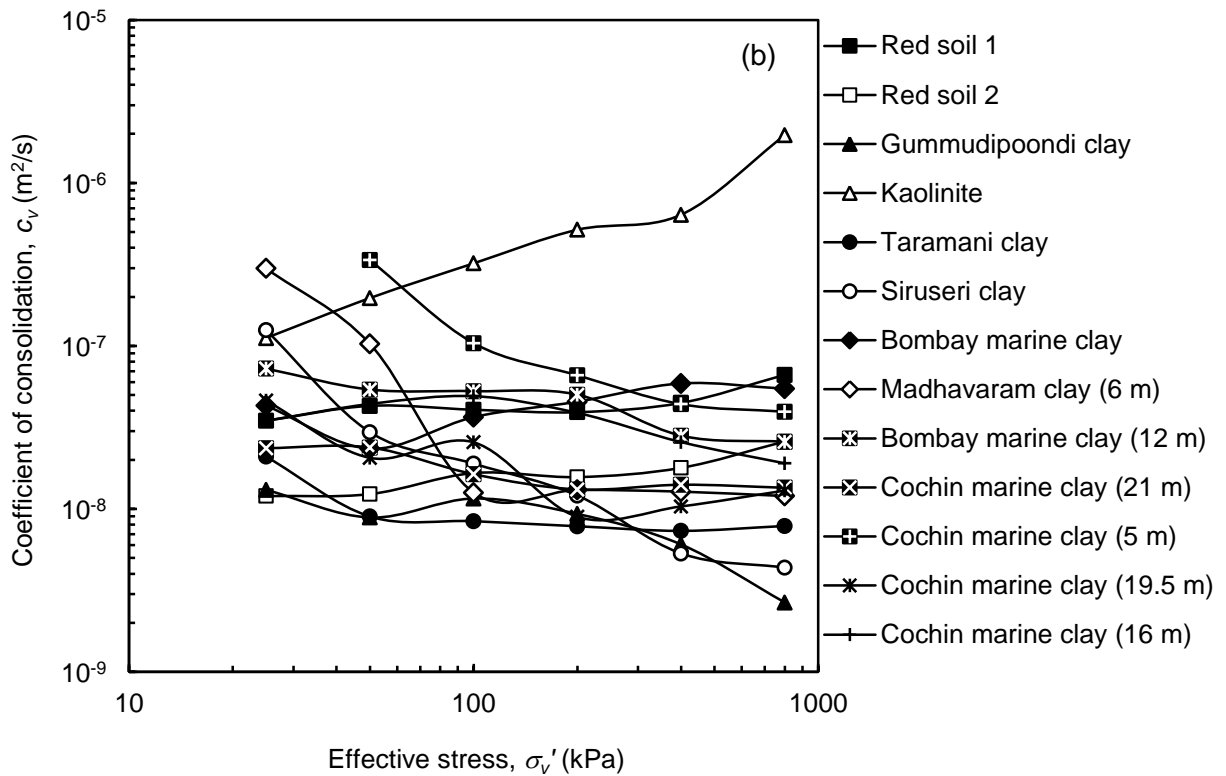
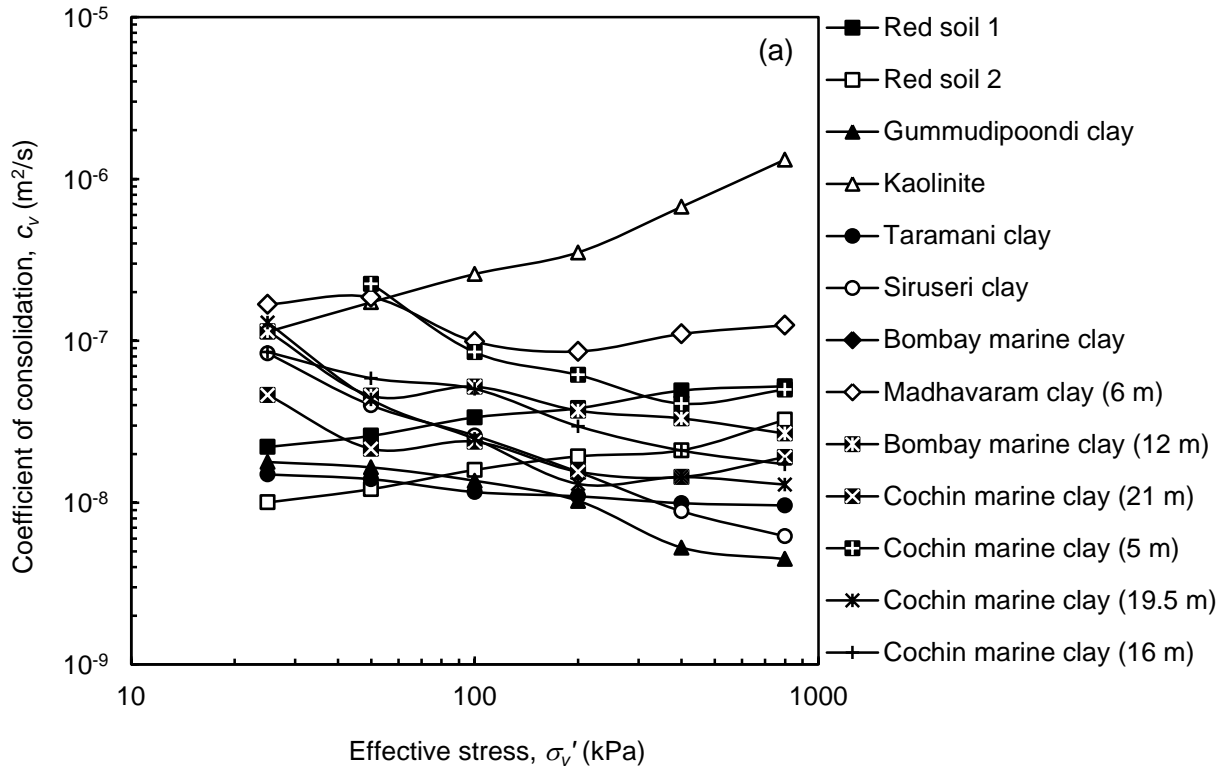


Figure 3.8:  $c_v$ - $\sigma'_v$  plots from the IL test with 24 hours duration using (a)  $\sqrt{t}$  method and (b) Inflection point method

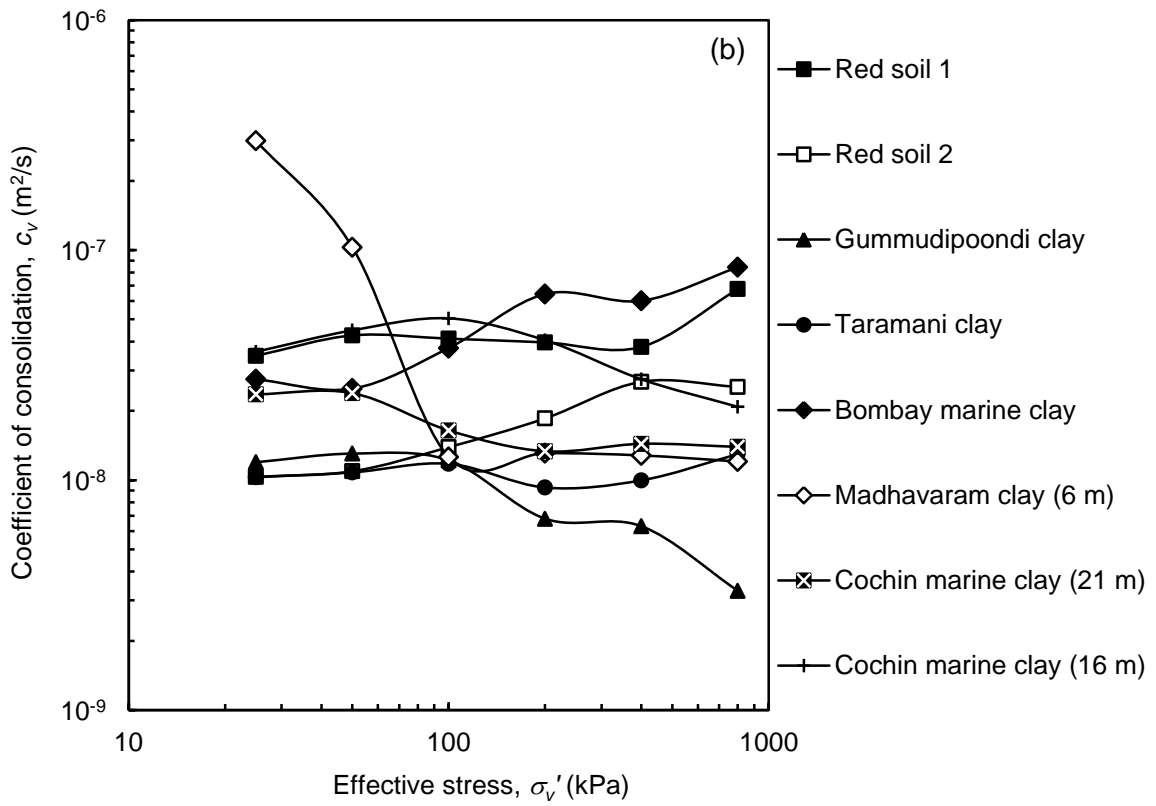
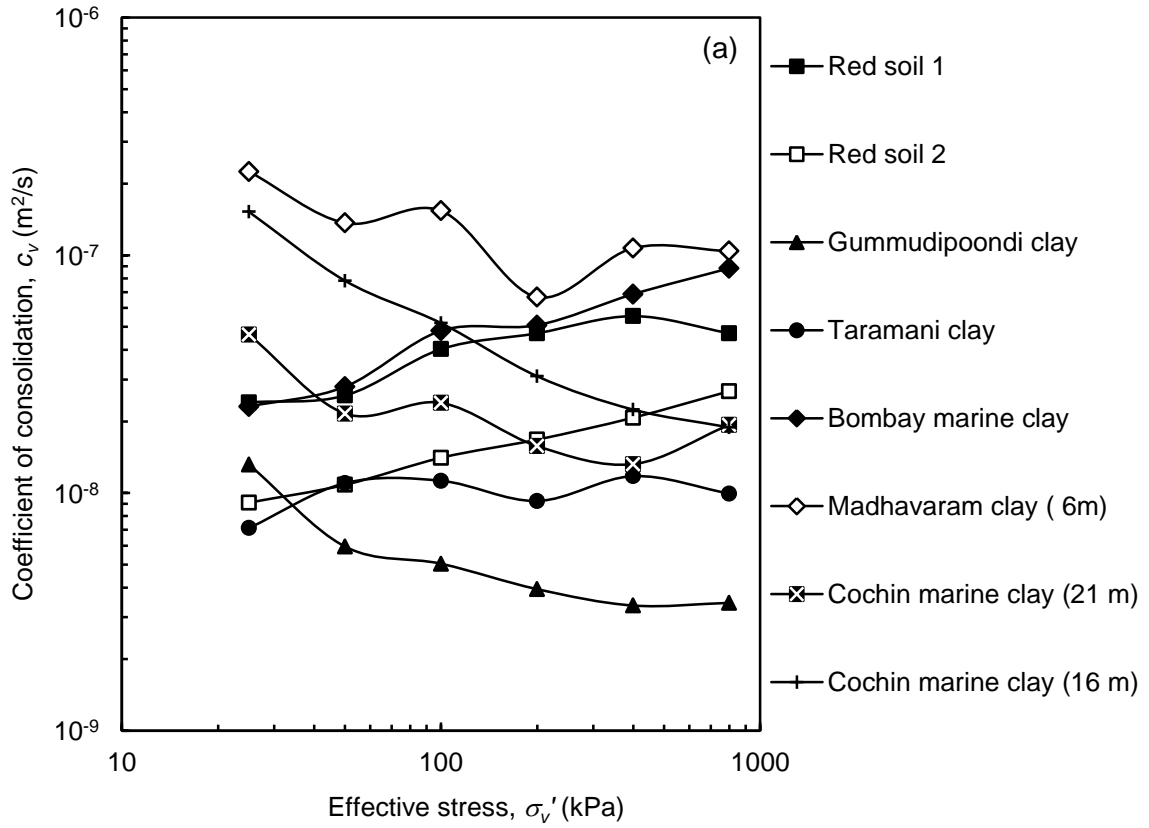


Figure 3.9:  $c_v$ - $\sigma'_v$  plot from the EOP test (a)  $\sqrt{t}$  method and (b) Inflection point method

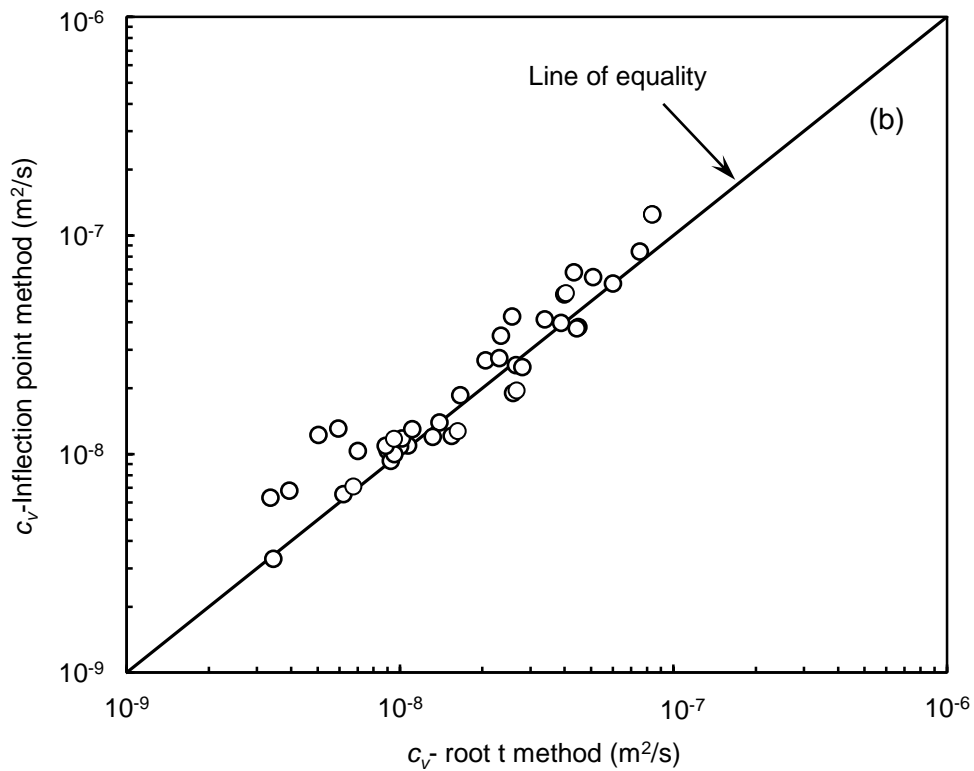
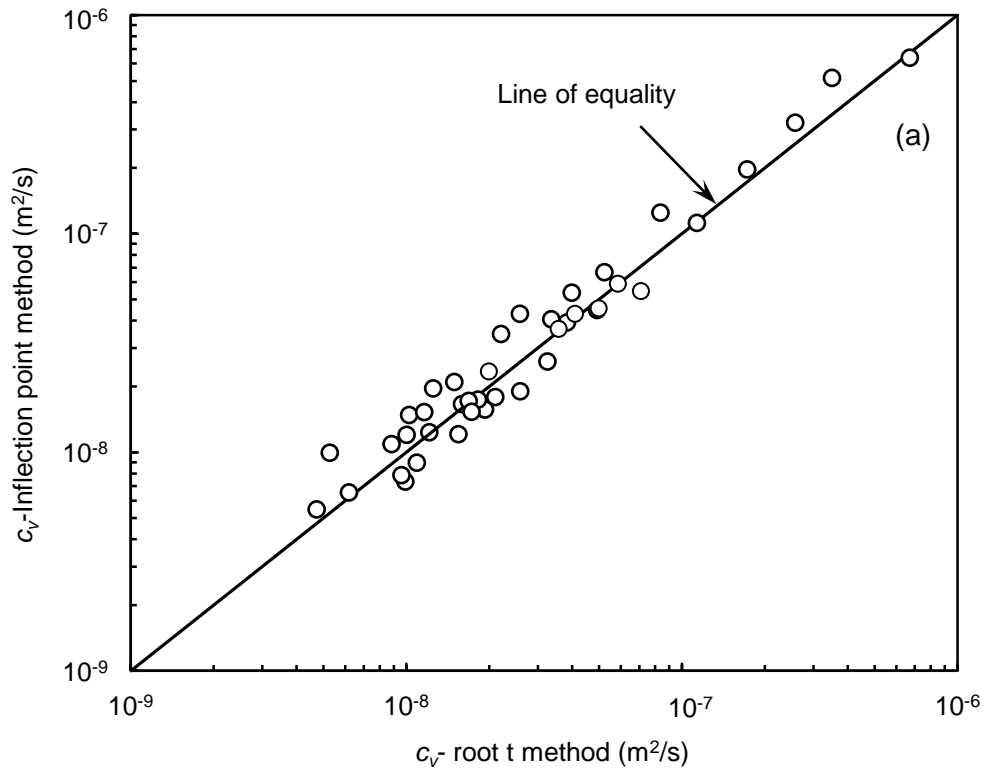


Figure 3.10: Comparison of  $c_v$  values from  $\sqrt{t}$  method and Inflection point method from the (a) IL Test with 24 hours and (b) EOP Test



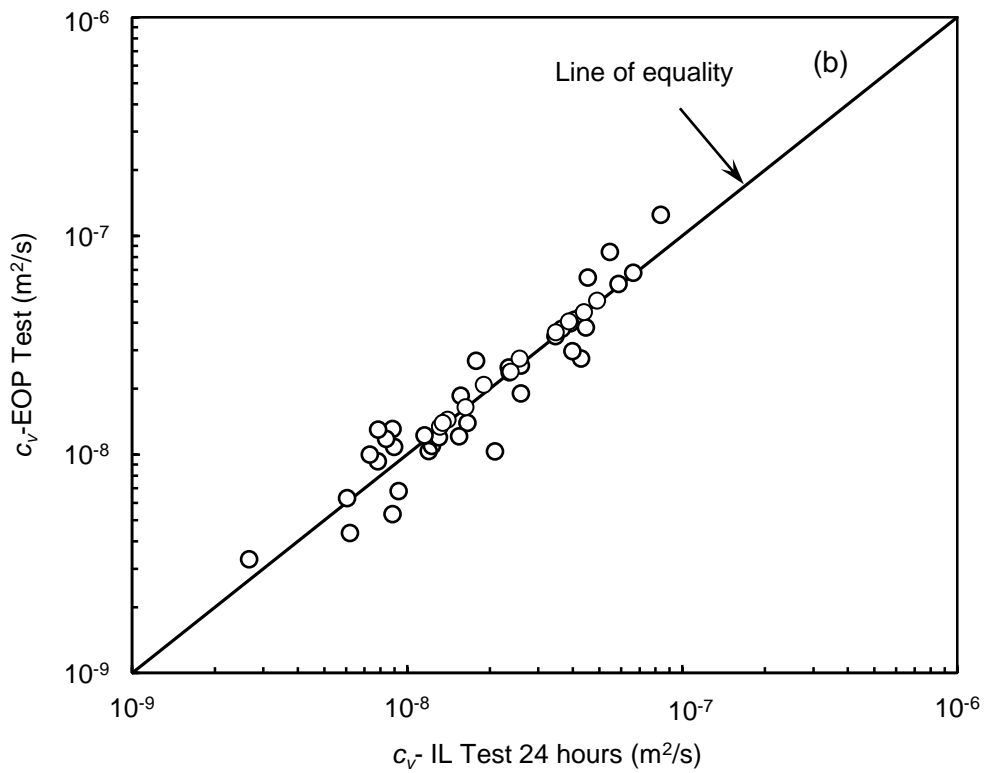
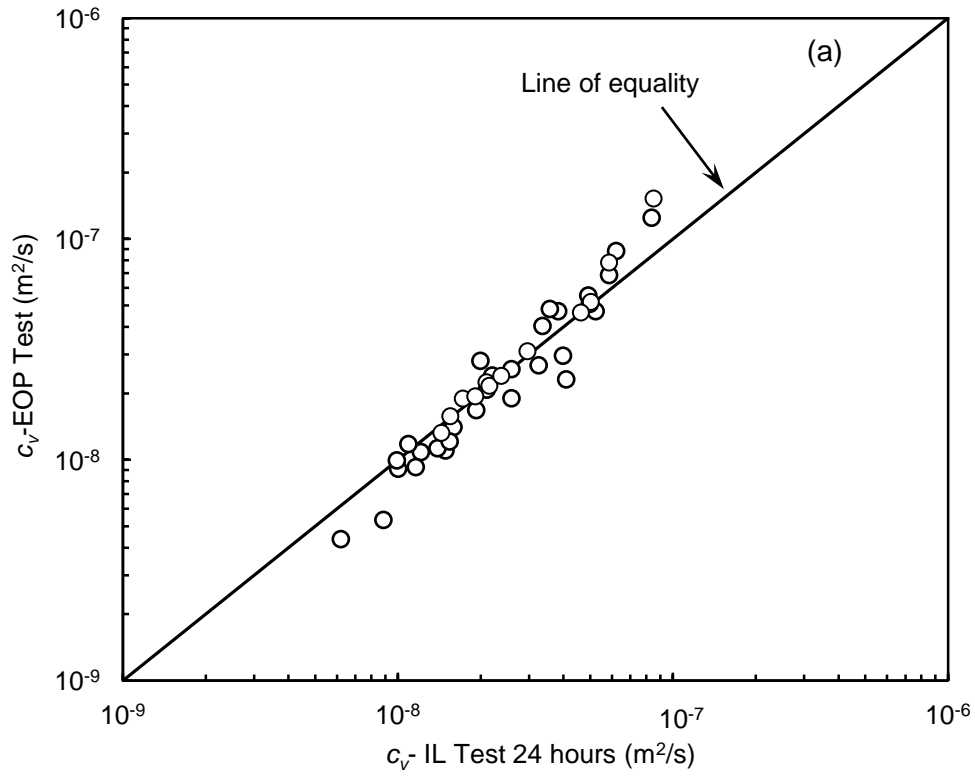


Figure 3.11: Comparison of  $c_v$  values from the IL Test with 24 hours and the EOP Test using (a)  $\sqrt{t}$  method and (b) Inflection point method

During IL test with duration of 24 hours of sustained loading, some amount of secondary compression occurs. The coefficient of secondary compression was determined using the log  $t$  method suggested by Mesri (1973). A typical  $e$ -log  $t$  plot for Bombay marine clay for the pressure range of 50-100 kPa is shown in Figure 3.12. The slope of secondary compression phase directly gives the coefficient of secondary compression ( $c_{\alpha}$ ). Mesri (1973) suggested a soil classification based on coefficient of secondary compression as shown in Table 3.3. The  $c_{\alpha}$  values obtained for all the soils are classified and summarised in Table 3.4. It can be observed that the selected soils exhibit secondary compressibility varying from very low secondary compressibility to extremely high secondary compressibility. Therefore, it is possible to obtain coefficient of secondary compression.

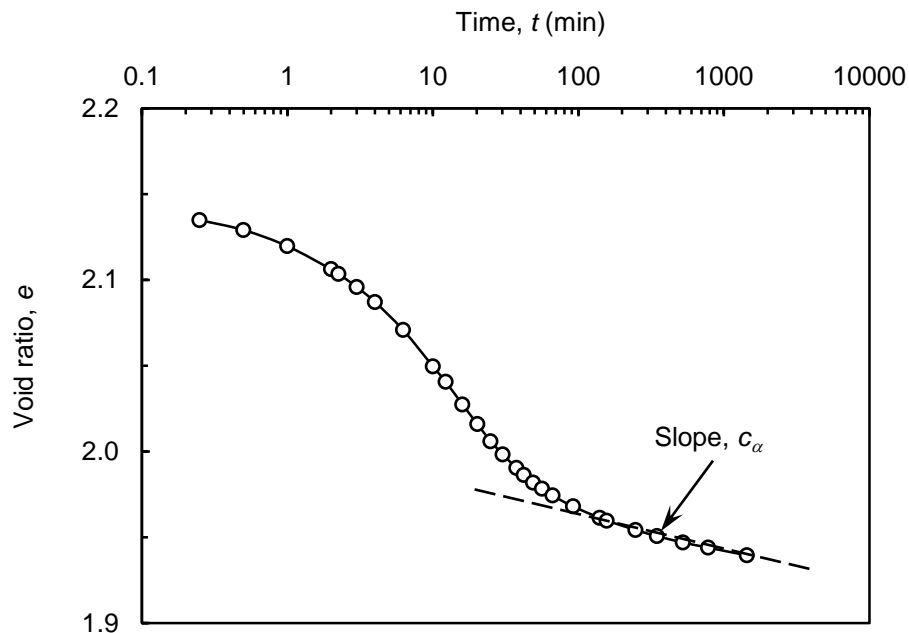


Figure 3.12: Typical  $e$ -log  $t$  curve for Bombay marine clay for the pressure range of 50-100 kPa

Table 3.3: Classification of soils based on secondary compressibility (Mesri, 1973)

Secondary compression (%)	Secondary compressibility	Secondary compression (%)	Secondary compressibility
< 0.2	Very low	1.6	High
0.4	Low	3.2	Very high
0.8	Medium	> 6.4	Extremely high

Table 3.4: Coefficient of secondary compression from the IL consolidation test

Sl. No.	Soil	Pressure, kPa						Average $c_\alpha$	Classification
		12.5-25	25-50	50-100	100-200	200-400	400-800		
1	Red soil 1	0.003	0.005	0.006	0.004	0.005	0.003	0.004	Low
2	Red soil 2	0.007	0.006	0.004	0.005	0.005	0.005	0.005	Medium
3	Gummudipoondi clay	0.010	0.009	0.012	0.014	0.014	0.013	0.012	High
4	Kaolinite	0.001	0.005	0.006	0.005	0.005	0.003	0.004	Low
5	Taramani clay	0.033	0.023	0.021	0.022	0.021	0.018	0.023	Very high
6	Siruseri clay	0.002	0.013	0.013	0.019	0.021	0.024	0.018	High
7	Bombay marine clay	0.047	0.025	0.018	0.012	0.019	0.020	0.023	Very high
8	Madhavaram clay (6 m)	0.0002	0.0005	0.0010	0.0014	0.0015	0.0016	0.001	Very low
9	Bombay marine clay (12 m)	0.002	0.006	0.005	0.025	0.031	0.029	0.028	Very high
10	Cochin marine clay (21 m)	0.005	0.008	0.015	0.024	0.027	0.028	0.026	Very high
11	Cochin marine clay (5 m)	--	0.001	0.006	0.016	0.020	0.023	0.020	Very high
12	Cochin marine clay (19.5 m)	0.018	0.030	0.065	0.076	0.054	0.045	0.048	Extremely high
13	Cochin marine clay (16 m)	0.010	0.014	0.027	0.047	0.051	0.048	0.048	Extremely high

Coefficient of permeability ( $k$ ) is a derived parameter from the IL consolidation test. By knowing the values of coefficient of consolidation ( $c_v$ ) and coefficient of volume compressibility ( $m_v$ ),  $k$  can be determined (Section 2.3.3). The variation of calculated  $k$  values with average void ratio from the IL consolidation test with 24 hours duration is plotted in Figure 3.13(a). In the present study,  $k$  was also measured at the end of each increment load with 24 hours duration test by performing a falling head permeability test. The measured permeability is plotted with void ratio as shown in Figure 3.13(b). Similarly, the coefficient permeability values were calculated from EOP test. The permeability variation with average void ratio from EOP test is shown in Figure 3.14. The values of coefficient of permeability for reconstituted soils from the control tests are compared in Figures 3.15 and 3.16. In Figure 3.15, the calculated and measured values of coefficient of permeability from the conventional IL test with 24 hours duration are compared with each other and the results are comparable. In Figure 3.16, the calculated values of coefficient of permeability obtained from IL test with 24 hours duration are compared with EOP test. It can be observed that the results are highly comparable with EOP test. These data will be used to evaluate the testing procedures developed in the present study.

### ***Total settlement parameters***

Total settlement parameters such as the compression index ( $c_c$ ), recompression index ( $c_r$ ) and the preconsolidation pressure ( $\sigma_c'$ ) were determined from the void ratio ( $e$ ) versus effective consolidation pressure ( $\sigma_v'$ ) curve. The  $e$ - $\log\sigma_v'$  curves for all the soils were obtained from the settlement data for each increment of load. The  $e$ - $\log\sigma_v'$  curve of the reconstituted soils from IL test with duration of 24 hours are compared with EOP test as shown in Figure 3.17(a-g). It can be observed that the soils with very high secondary compressibility (Table 3.4) show some variation in  $e$ - $\log\sigma_v'$  curve. Taramani clay and Bombay marine clay have very high secondary compressibility, therefore the EOP  $e$ - $\log\sigma_v'$  plot is shifted up from the IL test with 24 hours. Similarly, the  $e$ - $\log\sigma_v'$  plots from IL test with 24 hours and EOP tests for the undisturbed samples are shown in Figure 3.18 and Figure 3.19, respectively. Due to the unavailability of undisturbed samples, the EOP tests could not be performed on all the undisturbed soil samples.

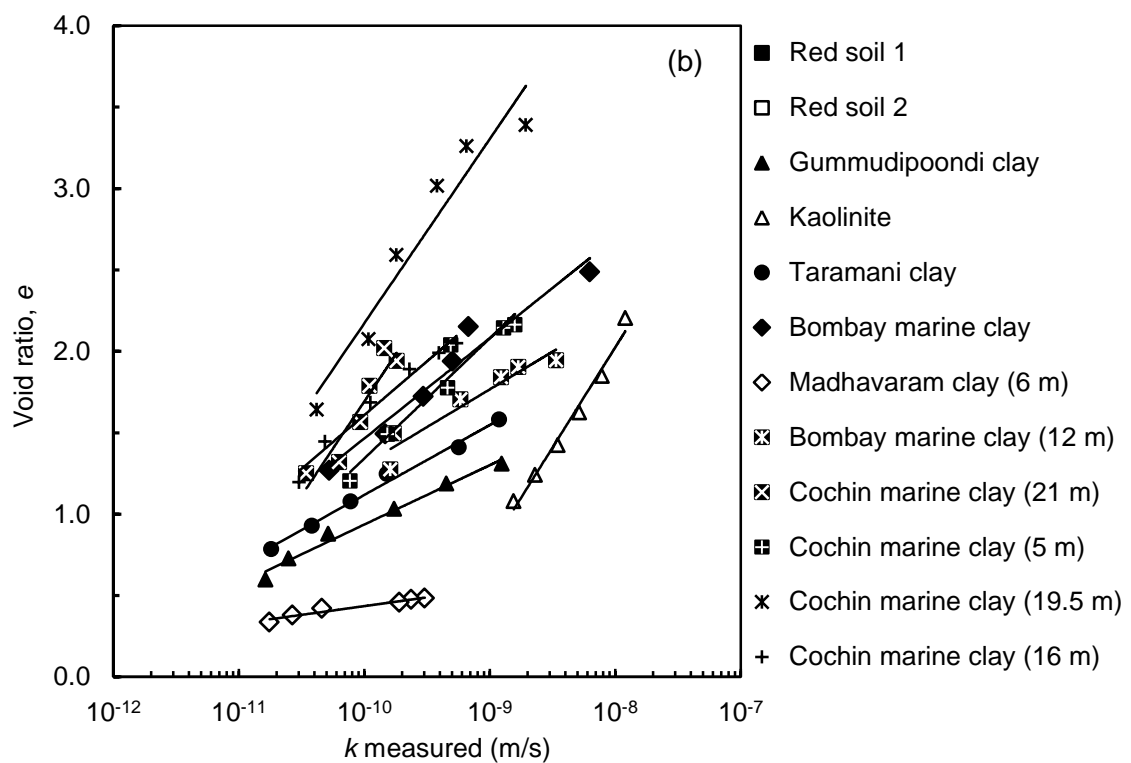
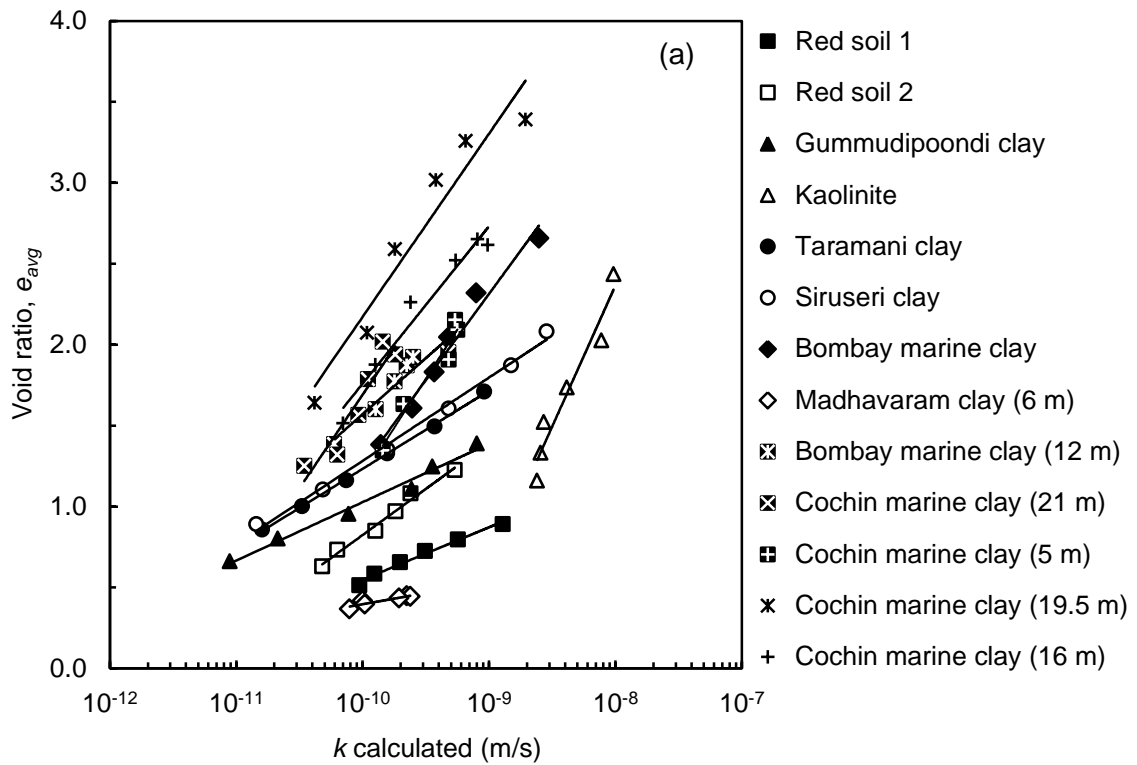


Figure 3.13: Coefficient of permeability from the IL test with 24 hours duration  
 (a) calculated and (b) measured

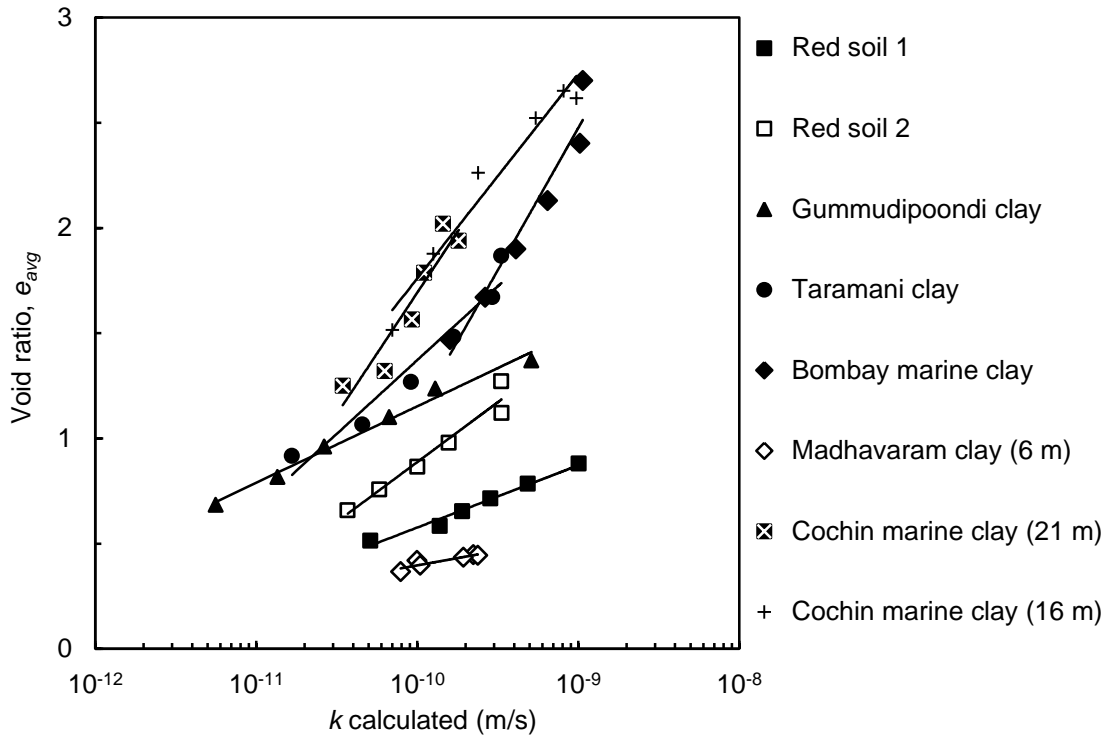


Figure 3.14: Coefficient of permeability calculated from the EOP test

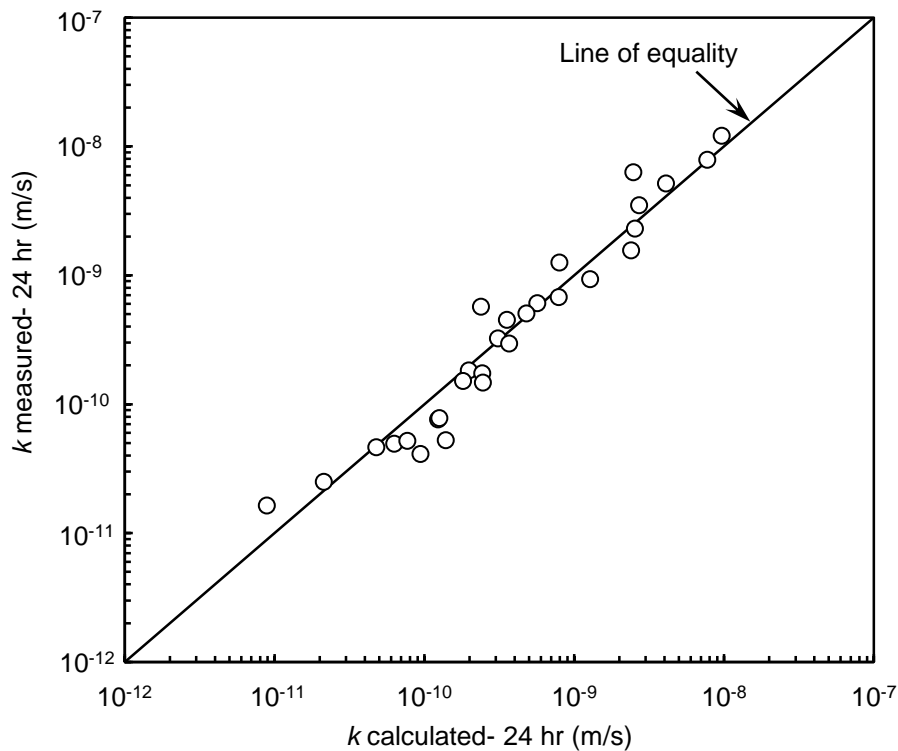


Figure 3.15: Comparison of coefficient of permeability calculated and measured from the conventional IL test with 24 hours duration

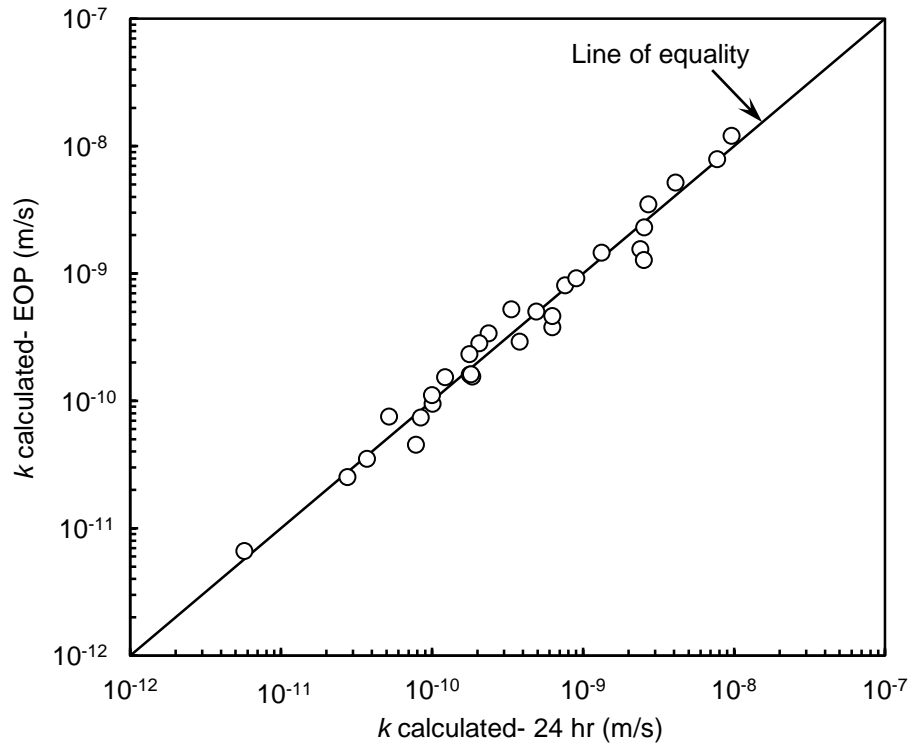


Figure 3.16: Comparison of coefficient of permeability calculated from the conventional IL test with 24 hours duration and the EOP test

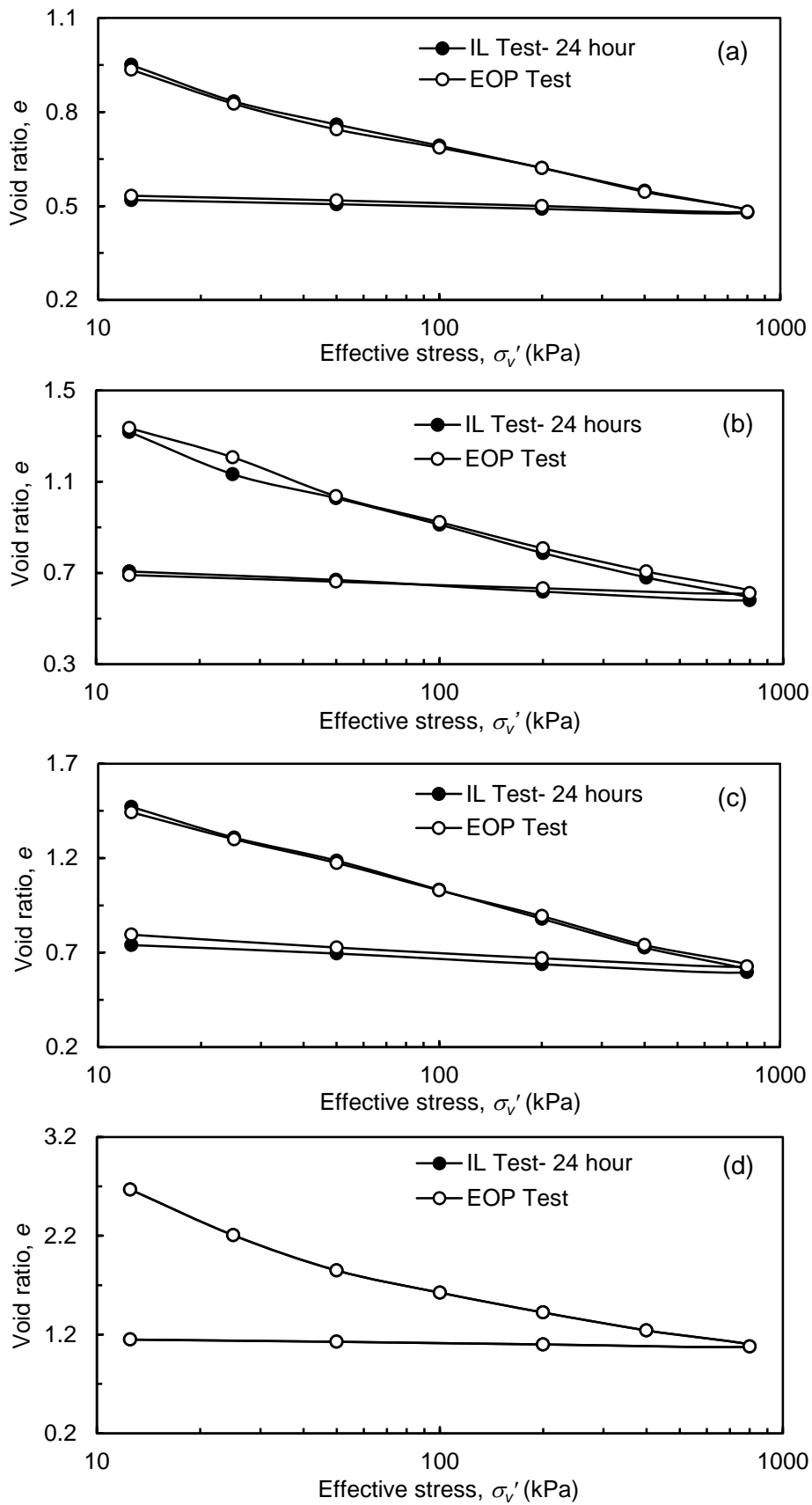


Figure 3.17 contd...



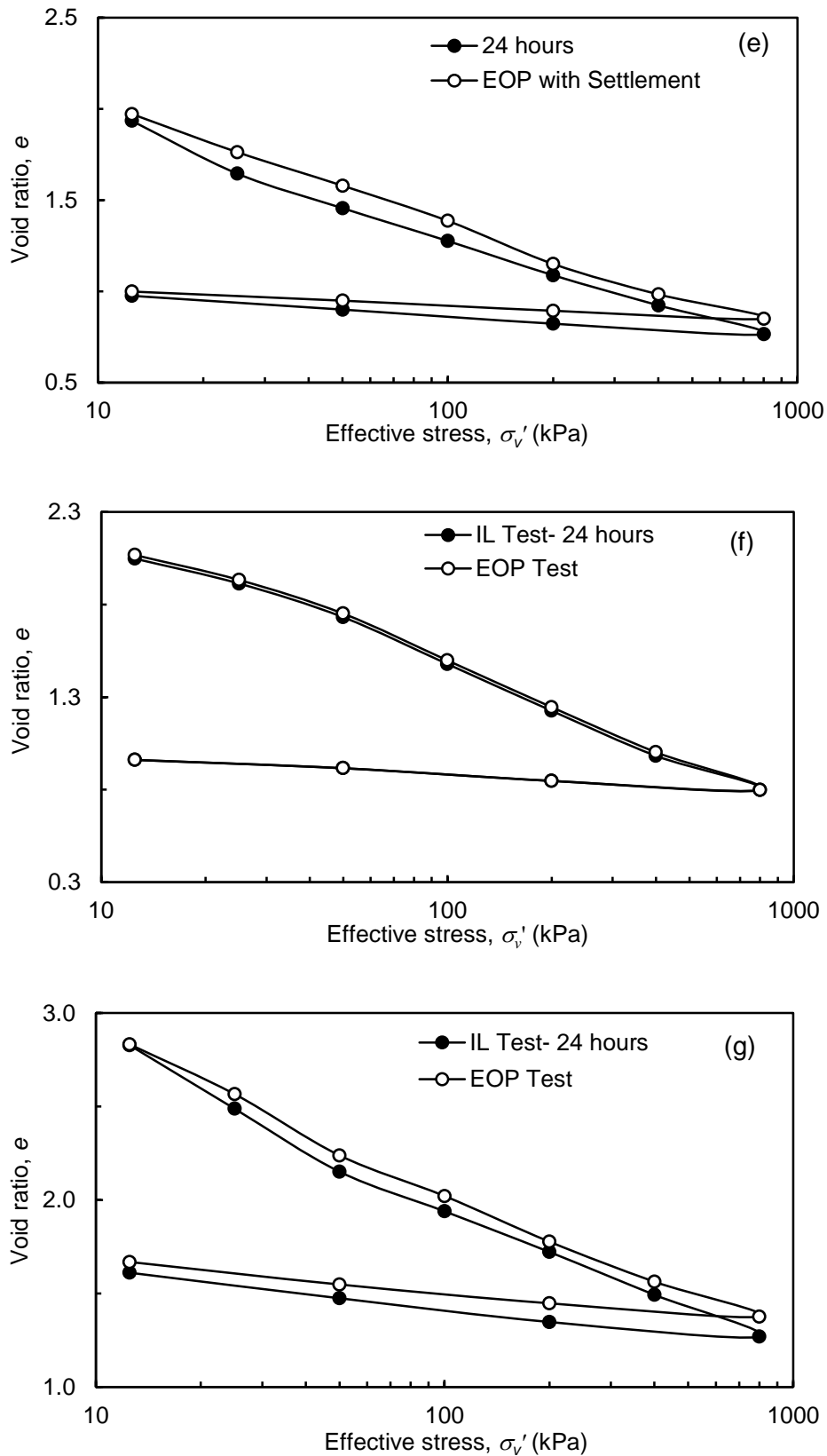


Figure 3.17:  $e$ - $\log \sigma'_v$  curves for (a) Red soil 1 (b) Red soil 2 (c) Gummudipoondi clay (d) Kaolinite (e) Taramani clay (f) Siruseri clay and (g) Bombay marine clay

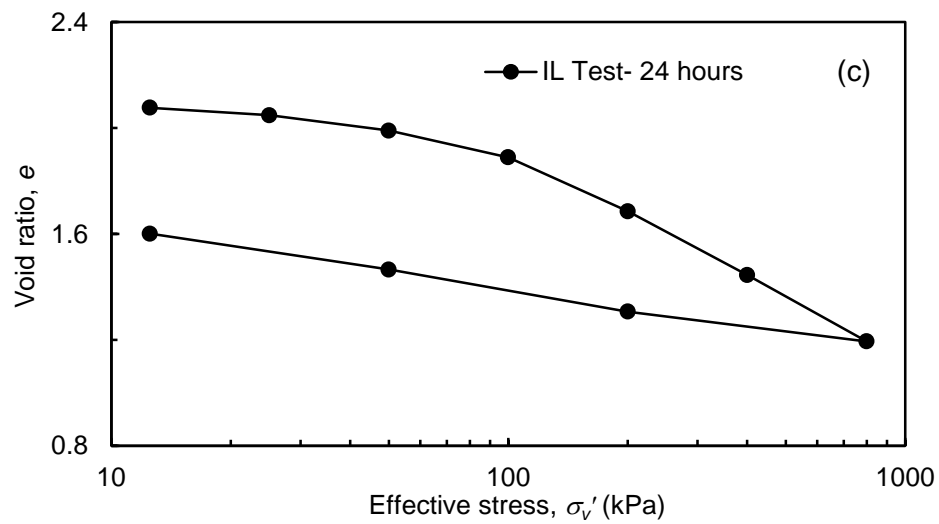
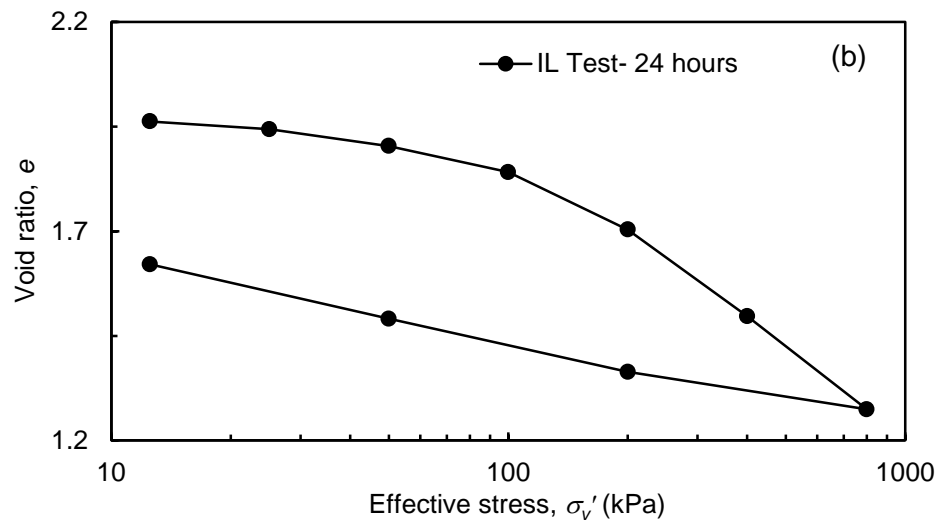
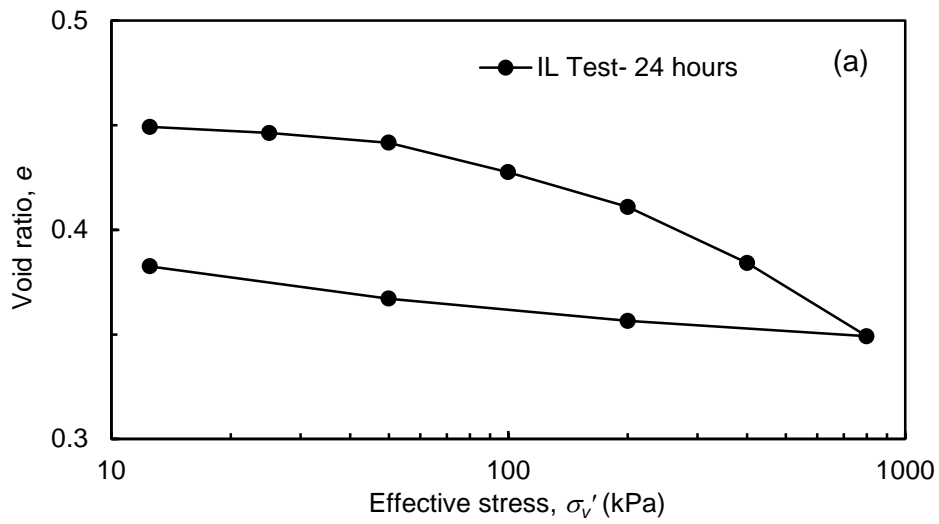


Figure 3.18 contd...

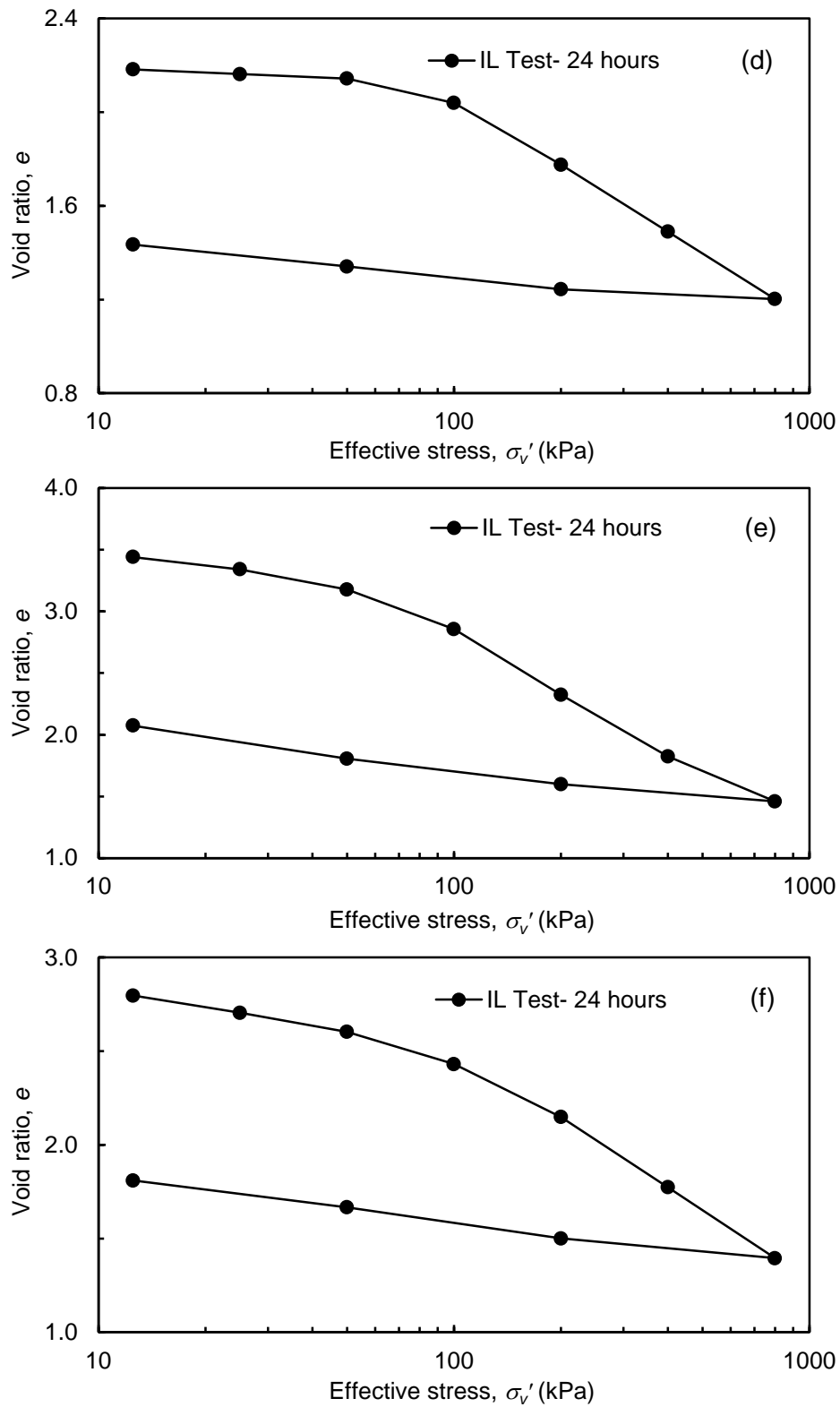


Figure 3.18:  $e$ - $\log \sigma_v'$  curves for Undisturbed clays from IL test with 24 hours (a) Madhavaram clay (6 m) (b) Bombay marine clay (12 m) (c) Cochin marine clay (21 m) (d) Cochin marine clay (5 m) (e) Cochin marine clay (19.5 m) and (f) Cochin marine clay (16 m)

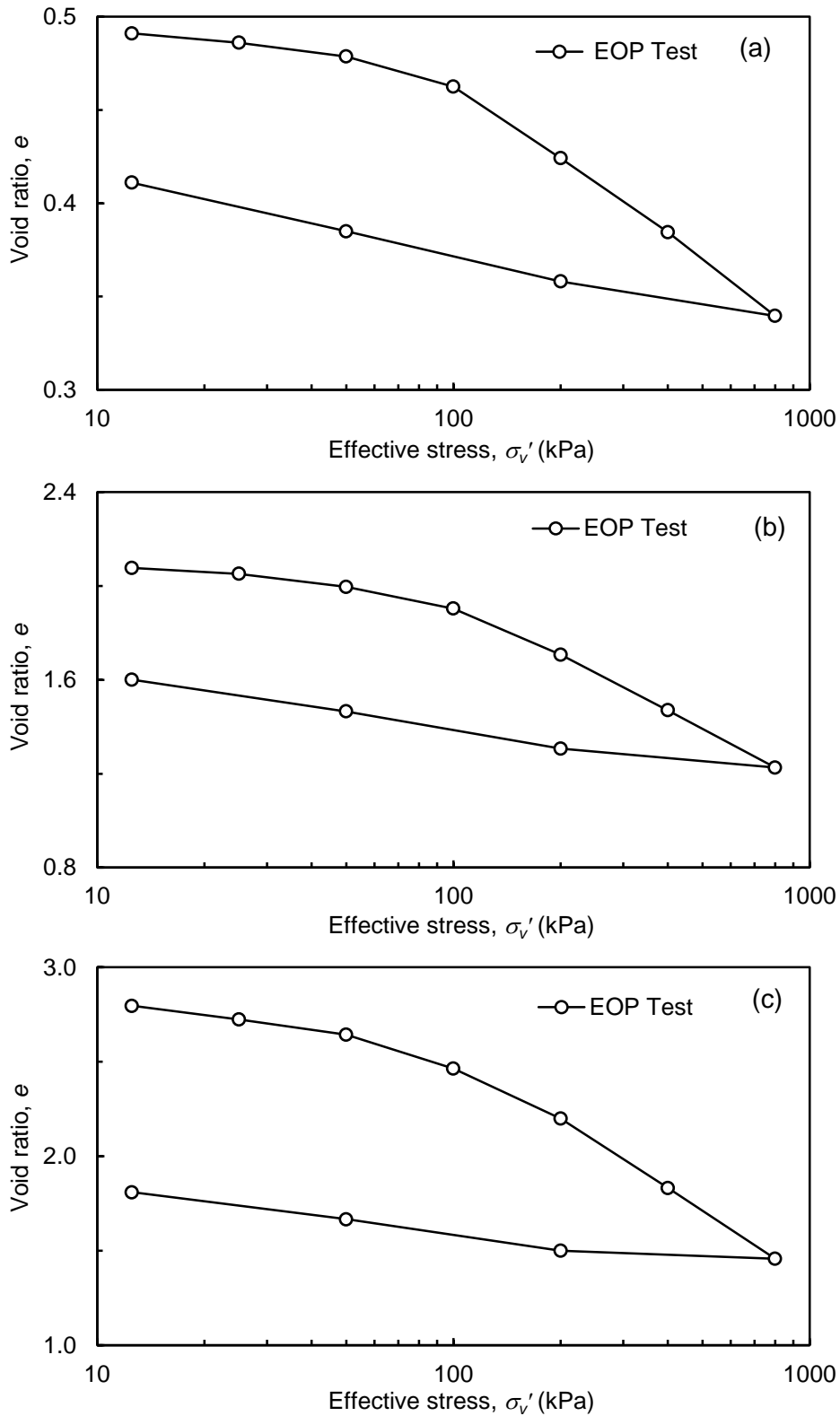


Figure 3.19  $e$ - $\log \sigma_v'$  curves for Undisturbed clays from EOP test (a) Madhavaram clay (6 m) (b) Cochin marine clay (21 m) and (c) Cochin marine clay (16 m)

The compression index ( $c_c$ ) and recompression index ( $c_r$ ) values were determined from the  $e$ - $\log \sigma_v'$  plots (Figure 3.17-3.19) and are summarized in Table 3.5. The values obtained from IL test with 24 hours duration is compared with EOP test as shown in Figure 3.20. It can be clearly seen that except one soil that the values are almost same from both test. The scattered point is for undisturbed Cochin marine clay sampled at 19.5 m that may be due to sample variability.

Table 3.5: Compression index and Recompression index of the soils

Sl. No.	Soil	Compression index, $c_c$		Recompression index, $c_r$	
		IL test	EOP test	IL test	EOP test
1	Red soil 1	0.262	0.259	0.021	0.030
2	Red soil 2	0.385	0.373	0.067	0.064
3	Gummudipoondi clay	0.468	0.482	0.077	0.073
4	Kaolinite	0.690	--	0.090	--
5	Taramani clay	0.522	0.530	0.071	0.092
6	Siruseri clay	0.697	--	0.087	--
7	Bombay marine clay	0.815	0.798	0.183	0.166
8	Madhavaram clay (6 m)	0.102	0.135	0.017	0.033
9	Bombay marine clay (12 m)	0.633	--	0.185	--
10	Cochin marine clay (21 m)	0.772	0.753	0.218	0.203
11	Cochin marine clay (5 m)	0.929	--	0.126	--
12	Cochin marine clay (16 m)	1.156	--	0.223	--
13	Cochin marine clay (19.5 m)	1.214	1.125	0.220	0.194

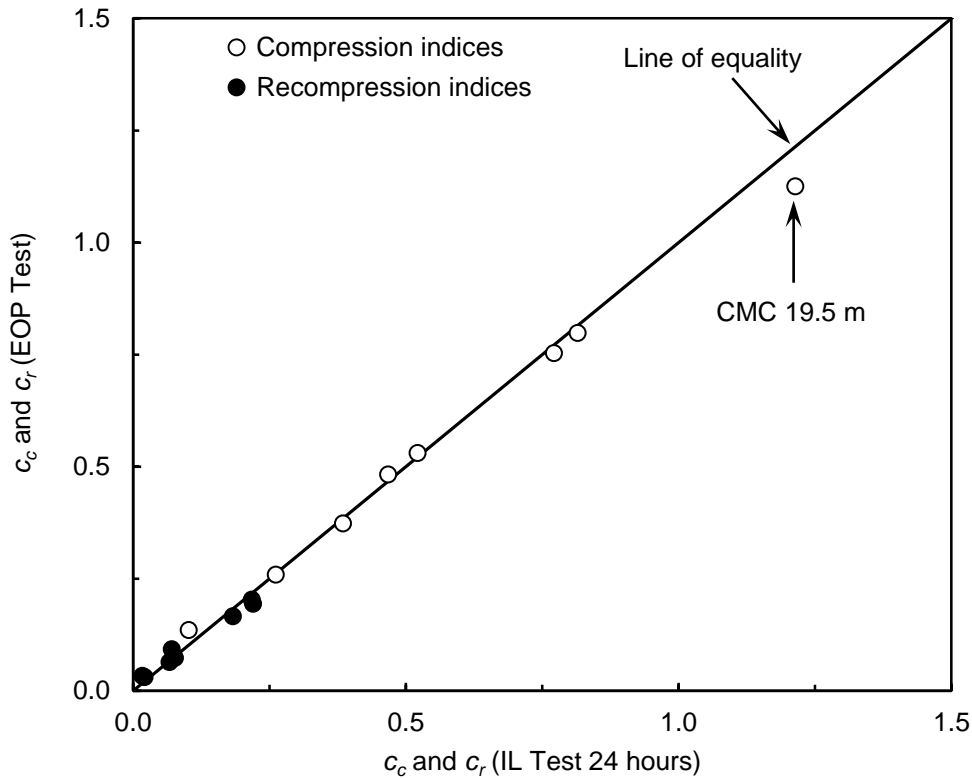


Figure 3.20: Comparison of compression indices and recompression indices from the IL test 24 hours and the EOP test

The preconsolidation pressure ( $\sigma_c'$ ) values were calculated for all the undisturbed soils. Sridharan *et al.* (1991) suggested a method to determine the preconsolidation pressure ( $\sigma_c'$ ) from the  $\log(1+e)$  versus  $\log\sigma_v'$  plot. Typical plot of  $\log(1+e)$  versus  $\log\sigma_v'$  plot for Cochin marine clay (19.5 m depth) is shown in Figure 3.21, in which the intersection point of the bi-linear plot gives the preconsolidation pressure. The values of preconsolidation pressure obtained from the IL test are given in Table 3.6. The in-situ effective overburden pressure was evaluated by knowing the sampling depth, the depth of water table and the unit weight of the specimen are also given in Table 3.6 along with OCR values. The overconsolidation ratio (OCR) values of undisturbed soils are nearly one. If the overconsolidation ratio is in the range of 0.8-1.2 then the soil is said to be normally consolidated (Coduto, 1998). Except Madhavaram clay, the OCR is in the range of 0.94-1.13. Therefore, the soils are in normally consolidated. For Madhavaram clay, OCR obtained is 0.83 which may be attributed to sample variability. The consolidation parameters obtained from the conventional IL test with duration and EOP test will be compared with new one-dimensional consolidation testing procedures.

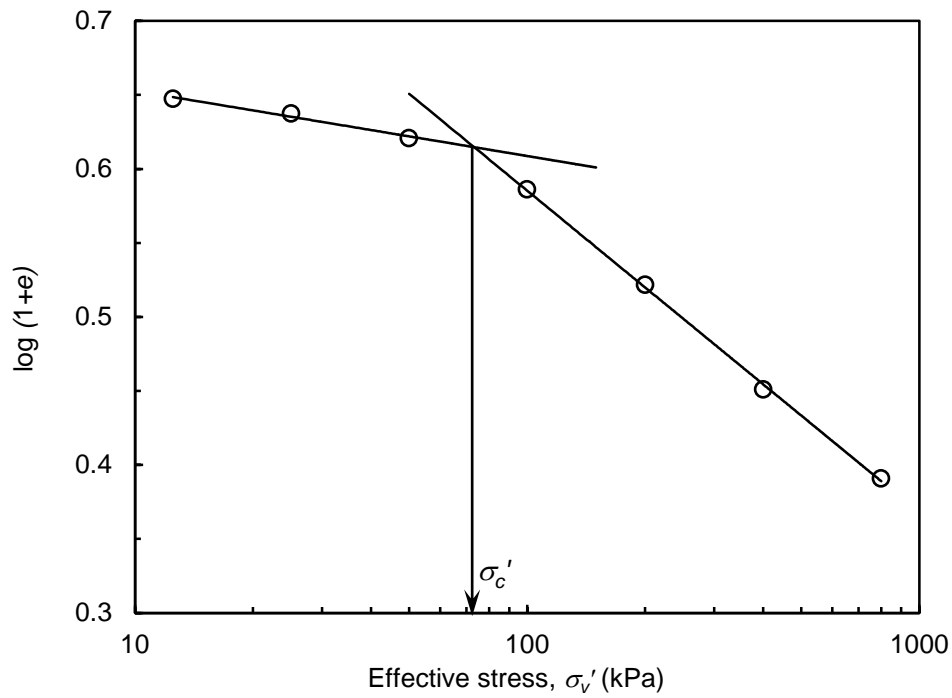


Figure 3.21:  $\log(1+e)$ - $\log \sigma_v'$  plot for Cochin marine clay (19.5 m)

Table 3.6: Preconsolidation pressure and OCR

Sl. No.	Soil	$w_n$ %	$\gamma_b$ , kN/m <sup>3</sup>	$\sigma_{vo}'$ , kPa	IL Test	
					$\sigma_c'$ , kPa	OCR
1	Madhavaram clay (6 m) 1	15	20.5	123	120	0.98
2	Madhavaram clay (6 m) 2	14	18.0	108	90	0.83
3	Bombay marine clay (12 m)	68	16.2	114	120	1.05
4	Cochin marine clay (21 m)	94	14.2	88	90	1.02
5	Cochin marine clay (5 m)	99	14.5	75	85	1.13
6	Cochin marine clay (19.5 m) 1	102	14.3	84	80	0.95
7	Cochin marine clay (19.5 m) 2	120	13.4	66	62	0.94
8	Cochin marine clay (16 m)	109	14.0	104	100	0.96

Note:  $\sigma_c'$  - Preconsolidation pressure,  $w_n$ - Natural water content,  $\gamma_b$ - Bulk unit weight,  $\sigma_{vo}'$  - In-situ effective stress and OCR- Overconsolidation ratio

### *Time taken to complete the control tests*

The testing time required to complete the conventional IL test with duration 24 hours under each pressure increment is 240 hours. The time taken to complete the EOP test are given in Table 3.7. The time taken to complete the test depends on the coefficient of consolidation ( $c_v$ ). For soils with  $c_v$  greater than  $1 \times 10^{-8}$  m<sup>2</sup>/s, the time taken is less one day. It can be clearly seen that by performing EOP test a considerable amount of time can be saved. However, it would be ideal if the test could be completed within the working hours of a day.

Table 3.7: Time taken to complete the EOP test

Sl. No.	Soil	$c_v$ (m <sup>2</sup> /s)	Time (hours)
1	Red soil 1	$3 \times 10^{-8}$ - $6 \times 10^{-8}$	12
2	Red soil 2	$1 \times 10^{-8}$ - $3 \times 10^{-8}$	21
3	Gummudipoondi clay	$4 \times 10^{-9}$ - $6 \times 10^{-8}$	54
4	Taramani clay	$8 \times 10^{-9}$ - $1 \times 10^{-8}$	40
5	Siruseri clay	$6 \times 10^{-9}$ - $8 \times 10^{-8}$	--
6	Bombay marine clay	$5 \times 10^{-8}$ - $6 \times 10^{-8}$	8.5
7	Madhavaram clay 6m	$3 \times 10^{-7}$ - $1 \times 10^{-8}$	15
8	Cochin marine clay 21m	$5 \times 10^{-8}$ - $2 \times 10^{-8}$	27
9	Cochin marine clay 16m	$4 \times 10^{-7}$ - $1 \times 10^{-8}$	23

### **3.5 SUMMARY**

Several fine grained soils were selected for the present study such that a wide range of plasticity characteristics are covered with liquid limit values of soils ranging from 32%-165%, which is expected to cover soils encountered in practice. Tests were conducted on both reconstituted and undisturbed soils. The basic properties of the selected soils were determined as per Indian standards, so as to identify and classify them. The reconstituted soil specimens were prepared from slurry with water content of 1.5 to 2 times the liquid limit water content.



The conventional IL consolidation and EOP tests were performed as the control tests. During each increment of load, the time-settlement data were recorded. From the time-settlement data, the one-dimensional consolidation parameters were obtained. The rate of settlement parameters and the total settlement parameters obtained from the conventional IL test with 24 hours duration and EOP test were reported in this chapter. The results obtained from the IL test with duration of 24 hours and EOP test were compared with each other. The results obtained from the control tests will be used in following chapters to validate the results obtained from the proposed methodologies.



## **CHAPTER 4**

### **METHOD TO FIX STRAIN RATE FOR CONTROLLED- STRAIN LOADING CONSOLIDATION TEST**

#### **4.1 INTRODUCTION**

As discuss in Chapter 2 (Literature Review), Constant Rate of Strain (CRS) consolidation test is one of the widely used testing methods to determine consolidation parameters of fine grained soils. ASTM D4186-12 (2012) suggests controlling the strain rate during the CRS test (Named as Controlled- Strain Loading (CSL) consolidation test), such a way that the pore pressure ratio ( $r_u$ ) shall be within the range of 0.03-0.015. The pore pressure ratio depends on the strain rate adopted for testing. Fixing proper strain rate to perform the CSL consolidation test is not well established in the literature, though automated testing devices are commercially available which can control the rate to obtain the required pore pressure ratio. In the present study, an attempt is made to develop a rational method for fixing the initial strain rate of the CSL test using a rapid permeability measurement prior to the test and an observational approach to control the strain rate during the CSL consolidation test. CRS tests were performed so as to validate the method to fix the initial strain rate of CSL consolidation test. Detailed experimental works was carried out to validate the proposed methodology. The experimental program and guidelines arrived to fix the strain rate of CSL tests are discussed in this chapter.

#### **4.2 EXPERIMENTAL PROGRAMME**

Seven reconstituted soils, namely Red soil 1, Red soil 2, Gummudipoondi clay, Kaolinite, Taramani clay, Siruseri clay, Bombay marine clay and four undisturbed samples were used for the study. The four undisturbed soil (UDS) samples were marine clays sampled from Cochin and Bombay, India. The Cochin marine clays were sampled from depths of 5 m, 16 m and 19.5 m. The Bombay marine clay was sampled from a depth of 12 m. The basic properties, determined as per the relevant Indian standards, are summarized in Chapter 3 (Section 3.3).

The one-dimensional consolidation tests were conducted on the reconstituted specimens in the normally consolidated (NC) state and few in the overconsolidated (OC) state with known preconsolidation pressure. The NC soil specimens were prepared by consolidating the slurry samples to an initial pressure of 12.5 kPa, which was already explained in Chapter 3 (Section 3.4.1). To study the OC behavior, three soils such as Gummudipoondi clay, Kaolinite and Taramani clay were selected. The OC soil specimens were prepared by consolidating the specimens to known preconsolidation pressures of 50 kPa, 100 kPa and 200 kPa. The required preconsolidation pressure was applied in steps and once the consolidation was over, it was unloaded to a seating pressure of 12.5 kPa in steps and allowed sufficient time for swelling. Three identical specimens were prepared for carrying out each set of experiments.

Conventional IL consolidation test was performed as control test on one of the specimens as per standard procedures (IS 2720-15 (1986)) in which the incremented load was maintained for 24 hours and the time-settlement data were recorded throughout the loading period. The testing procedure and the results obtained in the IL consolidation tests were described in Chapter 3 (Section 3.4.2-3.4.3). Strain controlled consolidation tests were performed on the other specimens as per the proposed procedure and also as per ASTM D4186-12 (2012) testing procedure.

To perform controlled-strain loading consolidation test, a CRS cell was fabricated as per ASTM D4186-12 (2012). The schematic of CRS cell used for the study is shown in Figure 4.1(a). The components and the assembled CRS cell are shown in Figure 4.1(b) and Figure 4.1(c), respectively. The important part of the CRS cell is the consolidation ring, which has a size of 60 mm diameter and 20 mm thickness and a collar is clamped to the ring using a four clamping screw, so as to keep the ring in fixed position. The CRS cell has a provision to measure the pore pressure at the base and a cell chamber to apply the back pressure to saturate the specimen. During the CSL consolidation test, the pore pressure developed at the base of the specimen is continuously measured. Therefore, before setting up the specimen in the CRS cell, it was ensured that the system is de-aired by flushing de-aired water through the back pressure line. After assembling the cell, the chamber was fully filled with de-aired water so as to saturate the specimen by applying a back pressure. A minimum back pressure of 200 kPa was used to saturate the specimen.

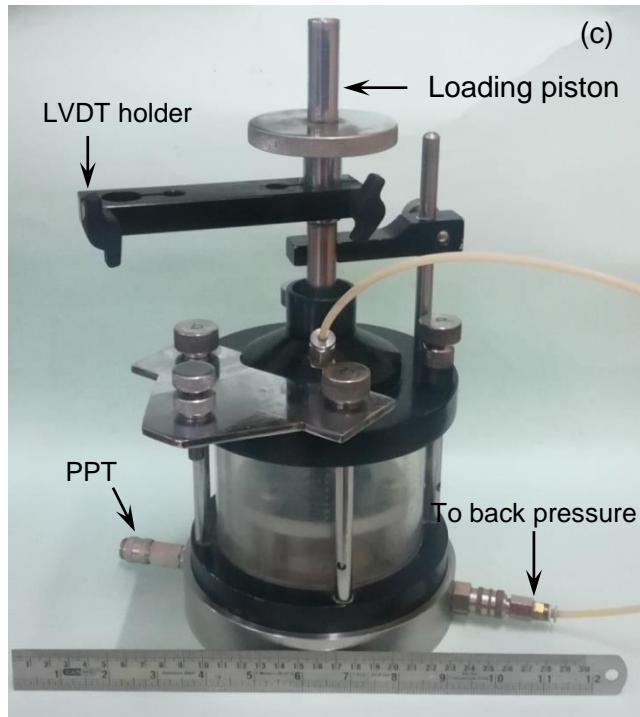
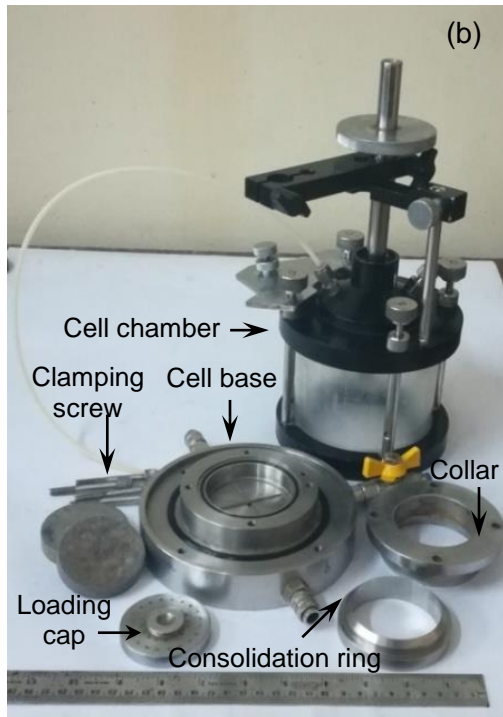
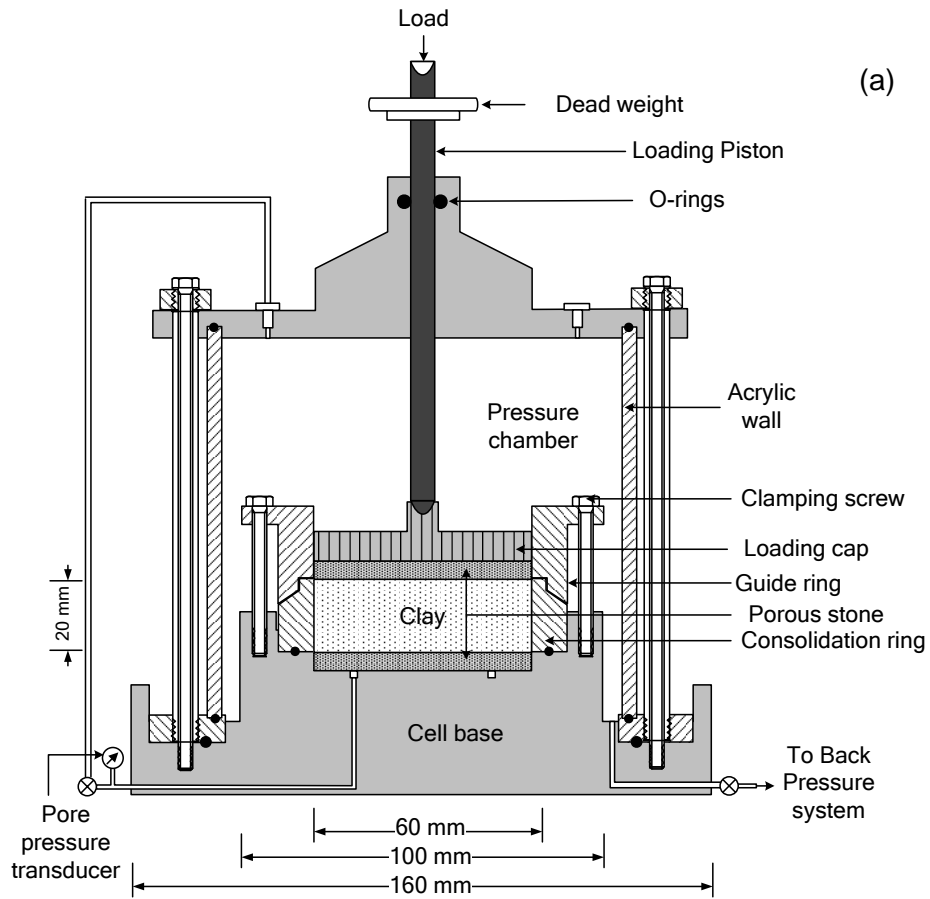


Figure 4.1: (a) Schematic diagram of the CRS cell (b) Components of the cell and (c) Assembled cell

A data acquisition unit (ADU) was used to log the data. Load cell, pore pressure transducer (PPT) and LVDT were used to measure the load coming on to the specimen, pore pressure developed at the base and settlement of the specimen, respectively. Before applying the back pressure, it was made sure that the loading ram is in contact with specimen and load cell, so as to account for the load coming on to the ram due to the applied back pressure. During consolidation phase, the drainage was allowed only from the top, as the pore pressure developed is to be measured at the base of the specimen. A strain controlled triaxial loading frame was used to apply the required deformation rate and once the required total stress is reached, the specimen was unloaded to the minimum seating pressure of 12.5 kPa with one-half of the loading strain rate. At the end of the test, the final height and final water content of the specimen were recorded.

### **4.3 PROPOSED METHOD TO FIX INITIAL STRAIN RATE OF CSL TEST**

The strain controlled consolidation tests were performed with a constant rate of strain (CRS), so as to fix the initial strain rate of CSL test. Preliminary studies were carried out as per ASTM D4186-12 (2012) testing procedure. ASTM standard recommends the initial strain rate based on soil classification and also suggest controlling the strain rate during the CSL test, such that the pore pressure ratio,  $r_u$  (defined as the ratio of excess pore water pressure ( $u_b$ ) at the base of the sample to total stress ( $\sigma_v$ )) is within the range of 0.03-0.15 (Chapter 2). In the present study, a rational method is proposed to fix the initial strain rate and further controlling it during CSL consolidation test. The theoretical consideration, experimental methodology and the results obtained are discussed along with the results obtained from tests conducted as per ASTM method.

#### **4.3.1 Theoretical Considerations**

As brought out in the literature review chapter (Section 2.4.1), the reliability of CRS test results depends on the rate of strain used in the test. The existing procedures in the literature have limitations, as discussed in Section 2.4.3. In the present study, it is proposed to fix the rate using initial permeability measurements. The proposed procedure is based on the theory of Wissa *et al.* (1971). Wissa *et al.* (1971) proposed the following expression for calculating the coefficient of permeability from a CRS test:

$$k = \frac{-0.434 \gamma_w r H^2}{2 \sigma_v' \log(1 - r_u)} \quad (4.1)$$

where,  $k$  is the coefficient of permeability,  $r$  is the strain rate,  $H$  is the initial thickness of sample,  $\sigma_v'$  is the present effective stress and  $r_u$  is the pore pressure ratio. Rearranging Eq. (4.1) for  $r$ ,

$$r = \frac{-2k \sigma_v' \log(1 - r_u)}{0.434 \gamma_w H^2} \quad (4.2)$$

By knowing the coefficient of permeability for an effective stress of  $\sigma_v'$ , the required strain rate can be evaluated for any required value of  $r_u$  from Eq. (4.2). The allowable range of  $r_u$  as per ASTM D4186-12 (2012) is in the range of 0.03- 0.15. The test could be completed faster if the value of  $r_u$  is maintained at the maximum allowable value of 0.15. Knowing the initial permeability ( $k_i$ ) under the seating pressure ( $\sigma_{vi}'$ ), the initial strain rate ( $r_i$ ) can be calculated for achieving the pore pressure ratio of 0.15 as

$$r_i = \frac{0.325 k_i \sigma_{vi}'}{\gamma_w H^2} \quad (4.3)$$

This approach is adopted in the present study, by measuring the permeability of the specimen under a seating pressure of 12.5 kPa before performing the CRS consolidation test. A permeability set-up which can measure the permeability within a short time is fabricated.

### 4.3.2 Experimental Methodology

As per the proposed procedure, the initial permeability is essential to determine the strain rate (Eq. 4.3). Typically, soil with low permeability ( $< 1 \times 10^{-9}$  m/s) will take very long time, if the commonly used falling head permeability set-up with stand pipes of larger diameter is used. Therefore, in the present study, a set-up was fabricated using a stand pipe with internal diameter of 3.0 mm. A burette of 11 mm diameter is connected in series to the stand pipe so as to fill the stand pipe and also to de-air the CRS cell. The schematic diagram and photograph of the permeability set up are shown in Figure 4.2(a) and Figure

4.2(b), respectively. Capillarity rise was observed (Figure 4.2(c)) in the smaller diameter stand pipe which was accounted for during the calculations.

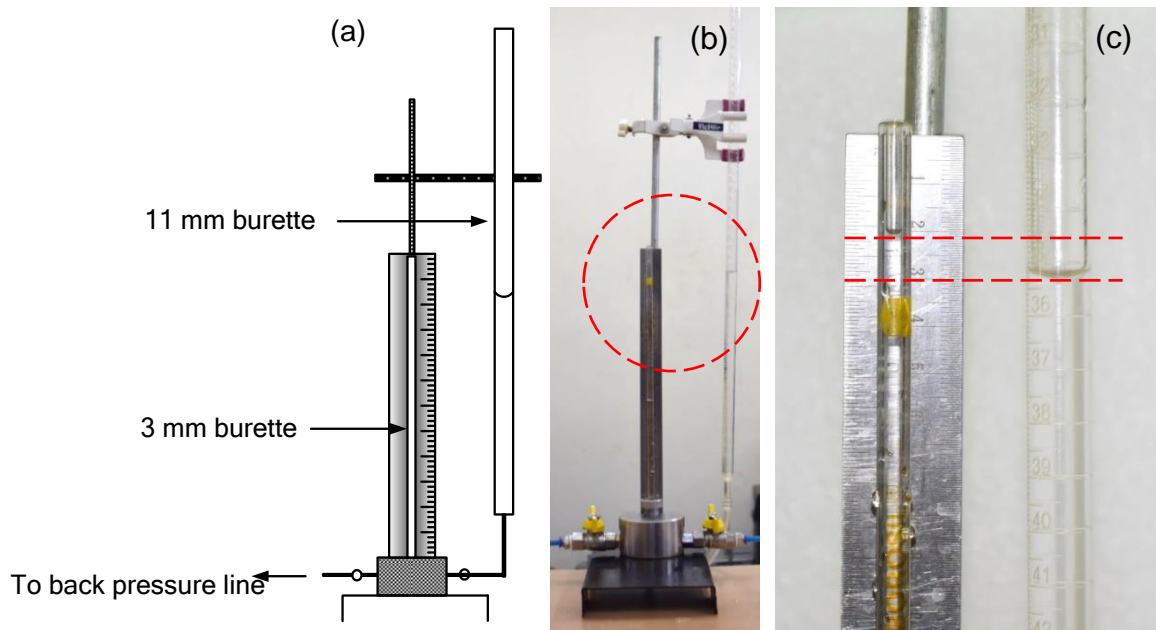


Figure 4.2: (a) Schematic diagram of the permeability set-up (b) Photograph of the permeability set-up and (c) Capillarity rise observed in the 3mm diameter burette

Schematic illustration of the permeability set-up connected to the base of the CRS cell is shown in Figure 4.3(a). The photograph of the complete set-up used for the study is shown in Figure 4.3(b). A dead weight (seating pressure) of 12.5 kPa was applied, before measuring the permeability. After applying the seating pressure of 12.5 kPa, water was filled in the cell and soaked overnight for saturation. The 3 mm diameter stand pipe was connected to the base of the specimen. The hydraulic gradient recommended by the standard procedure (ASTM D5084-10 (2010)) was adopted. Sufficient time was allowed to stabilize the flow of water through the sample and then measured the permeability. The permeability test results using the 3 mm diameter stand pipe and the standard pipe of 11 mm diameter, typically for Bombay marine clay 12 m (UDS) is shown in Figure 4.4. The results are highly comparable suggesting that the set-up using small diameter pipe is good enough to obtain reliable permeability values. The time taken for the test is typically about one hour for the soil with lowest initial permeability, used in the study, of about  $1 \times 10^{-10}$  m/s. The CRS test was then conducted using the calculated rate based on the measured initial permeability using Eq. (4.3).



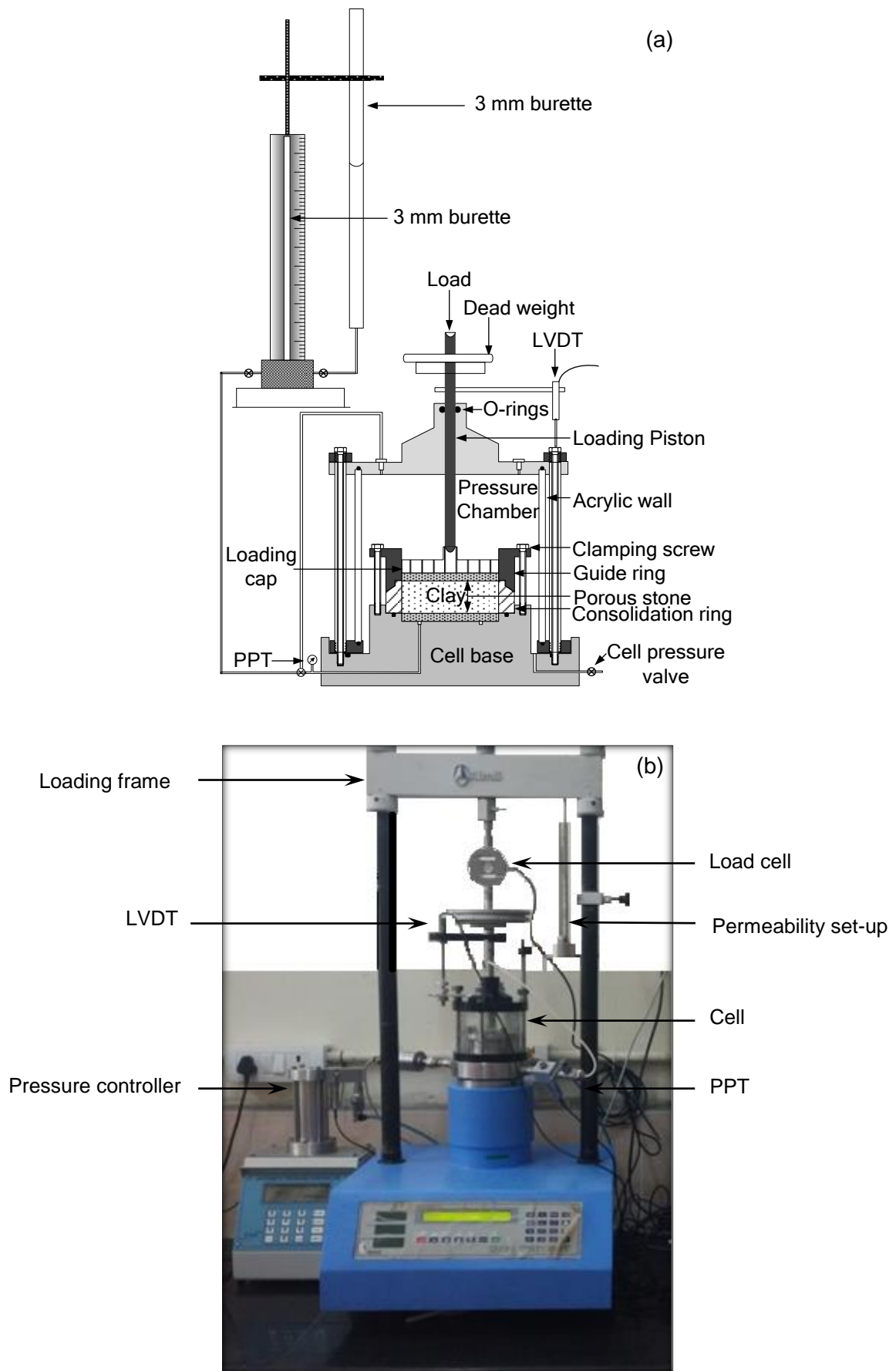


Figure 4.3: (a) Schematic diagram and (b) Photograph of CRS set-up used for the study

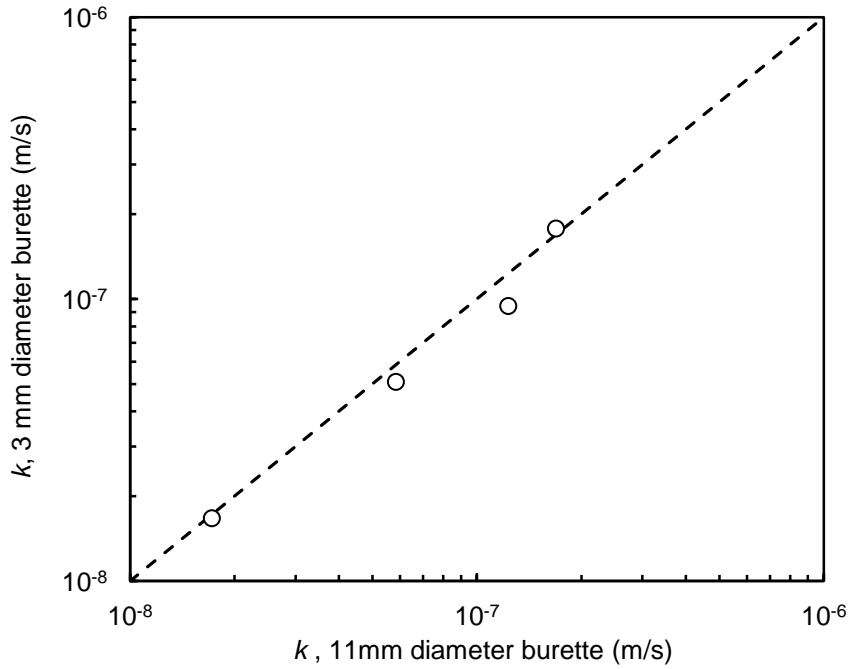


Figure 4.4: Validation of the 3 mm diameter burette used for measuring  $k$ , typically for Bombay marine clay 12 m (UDS)

The proposed procedure to fix the strain rate was validated by performing a series of experiments on reconstituted specimens with varying plasticity characteristics and on selected undisturbed specimens. The strain controlled consolidation test data were interpreted based on the theory suggested by Wissa *et al.* (1971). The interpretation of consolidation data are described in the next section.

#### 4.3.3 Interpretation of CRS Consolidation Test Data

Wissa *et al.* (1971) proposed the theory to interpret the CRS test, which includes the transient and steady state analysis, as already explained in Chapter 2 (Section 2.4.1). The term  $F_3$  is used to verify the presence of transient state (Eq. 2.22). If the term  $F_3 > 0.4$ , steady state exist. The steady state data were analyzed based on the non-linear theory of Wissa *et al.* (1971). To compute the total settlement consolidation parameters such as compression index ( $c_c$ ), recompression index ( $c_r$ ) and preconsolidation pressure ( $\sigma_c'$ ), require values of void ratio for the respective effective stresses. The void ratio can be directly determined from the settlement and swelling data by knowing the initial or final thickness and water content of the specimen. Knowing the load coming on to the

specimen and the pore water pressure ( $u_b$ ) developed at the base, the effective stress can be calculated using the Eq. (4.4) as:

$$\sigma_v' = (\sigma_v^3 - 2\sigma_v^2 u_b + \sigma_v u_b^2)^{1/3} \quad (4.4)$$

where,  $\sigma_v$  is the total stress and  $u_b$  is the base pore pressure. The values of  $c_c$  and  $c_r$  are the slopes of the  $e$ - $\log \sigma_v'$  compression curve and swelling curves, respectively. If the soil is overconsolidated, then the preconsolidation pressure,  $\sigma_c'$  are determined using  $\log(1+e)$  versus  $\log \sigma_v'$  method (Sridharan *et al.* 1991).

The coefficient of consolidation ( $c_v$ ) and coefficient of permeability ( $k$ ) are also evaluated using the following equations suggested by Wissa *et al.* (1971).

$$c_v = \frac{-0.434 r H^2}{2\sigma_v' m_v \log(1 - r_u)} \quad (4.5)$$

$$k = -\frac{0.434 \gamma_w r H^2}{2\sigma_v' \log(1 - r_u)} \quad (4.6)$$

where,  $r$  is the strain rate,  $H$  is the thickness of specimen,  $\gamma_w$  is the unit weight of water,  $\sigma_v'$  is the effective stress and  $r_u$  is the pore pressure ratio. The interpreted results from CRS tests are compared with the conventional IL test and are discussed in the next section.

#### 4.3.4 Results and Discussions

In order to evaluate the proposed procedure to fix the initial strain rate of CSL consolidation test, constant rate of strain (CRS) consolidation tests were conducted on the reconstituted soil specimens in NC state. The CRS tests were performed as per the recommendation of ASTM D4186-12 (2012) and as per the proposed method. The recommended strain rates in ASTM D4186-12 (2012) based on soil classification (USCS) are given in Table 4.1. As per the proposed procedure, the initial strain rates of CRS test was calculated based on the initial permeability at a consolidation pressure of 12.5 kPa, so

as to obtain the pore pressure ratio of 0.15 is also given in Table 4.1. The strain rate values obtained based on permeability measurements are more for some soils and less for other soils compared to those obtained based on soil classification as per ASTM D4186-12 (2012), even within the soil group.

Table 4.1: Strain rates as per ASTM D4186-12 (2012) and the proposed method

Sl. No.	Soils	ASTM D4186-12			Proposed method		
		Soil Classification	Rate of test	$(r_u)_{12.5}$	$k$ -measured	Rate of test	$(r_u)_{12.5}$
		(USCS)	(%/hour)	%	(m/s)	(%/hour)	%
1	Red soil 1	CL	1.0	50	$1.8 \times 10^{-9}$	0.60	14
2	Red soil 2	CL	1.0	30	$1.0 \times 10^{-9}$	0.45	15
3	Gummudipoondi clay	CH	0.1	5	$1.7 \times 10^{-9}$	0.35	16
4	Kaolinite	CH	0.1	0.1	$1.6 \times 10^{-8}$	7.00	13
5	Taramani clay	CH	0.1	3	$8.9 \times 10^{-10}$	0.30	15
6	Siruseri clay	CH	0.1	0.3	$3.7 \times 10^{-9}$	1.35	16
7	Bombay marine clay	MH	10	59	$1.5 \times 10^{-9}$	0.54	12

Note: USCS- Unified Soil Classification System,  $(r_u)_{12.5}$ - Pore pressure ratio at  $\sigma_v' = 12.5$  kPa

The pore pressure ratio obtained from both CRS test as per the rates obtained from ASTM D4186-12 (2012) method and the proposed methods as the test progresses is shown in Figure 4.5(a) and Figure 4.5(b). The pore pressure ratio obtained at consolidation pressure of 12.5 kPa, when the tests were conducted as per the rate specified in ASTM D4186-12 (2012) and as per the proposed procedure are also given in Table 4.1. It can be observed that the measured pore pressure ratio at  $\sigma_v' = 12.5$  kPa is too high for MH and CL types of soils and too low for CH type of soils, when the test is conducted as per the rate recommended in ASTM D4186-12 (2012). When the tests were conducted as per the rates calculated using the proposed procedure, the measured pore pressure ratio at 12.5 kPa varies from 12%-16% with an average value of 14.4%, suggesting that the proposed procedure can be used to fix the strain rate to achieve a pore pressure ratio of 0.15 at a seating pressure of 12.5 kPa.

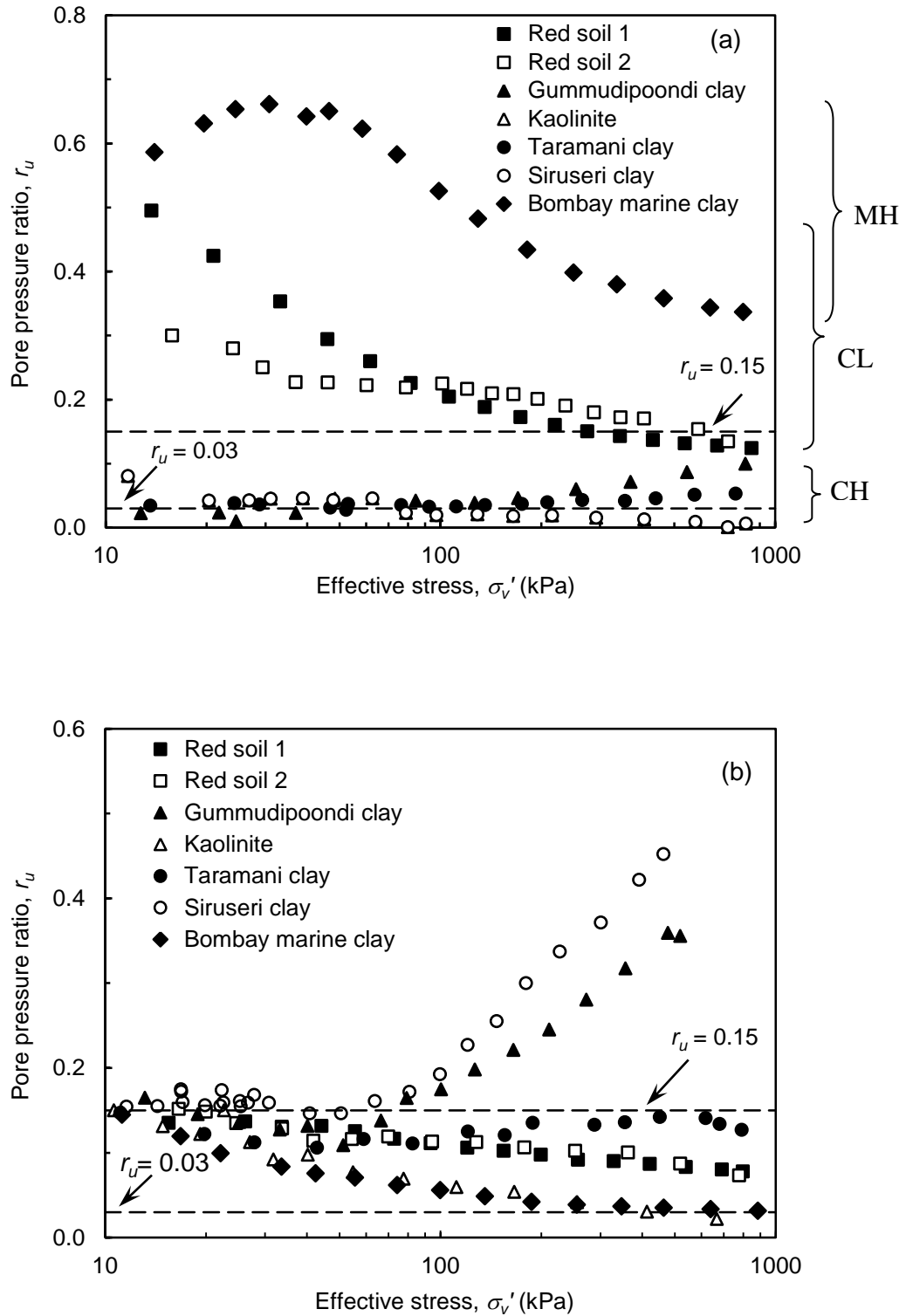


Figure 4.5: Pore pressure ratio variation with effective stress of reconstituted soils based on the (a) ASTM D4186-12 (2012) standard and (b) Proposed procedure

It is to be noted that the strain rate was not varied during the test for the data presented in Figures 4.5(a) and 4.5(b). The variation of pore pressure ratio as the test progress (consolidation pressure increment) is not constant after  $\sigma_v' = 12.5$  kPa. Typically, for Gummudipoondi clay and Siruseri clay the pore pressure ratio keeps on increasing as the test progresses but for kaolinite the pore pressure ratio decreases, and for Taramani clay  $r_u$  is nearly constant. Even though these soils belong to CH type of soils, the trend of variation of  $r_u$  is not similar. For the MH soil (Bombay marine clay) the rate recommended by ASTM D4186-12 (2012) is 19 times faster than that obtained from permeability measurements. The consequence is that the pore pressure ratio shoots up to very high value. The value then decreases as the test progresses.

The above results suggest that the strain rate based on soil classification is highly approximate. The variation of pore pressure ratio with consolidation pressure increase, as the test progress, may be related to the variation of  $c_v$  with consolidation pressure discussed in section 2.3.3 and 3.4.3. This is verified using nonlinear theory of Wissa *et al.* (1971). The equation of coefficient of consolidation ( $c_v$ ) suggested by Wissa *et al.* (1971) is as follows:

$$c_v = \frac{-0.434 rH^2}{2\sigma_v' m_v \log(1-r_u)} \quad (4.7)$$

where,  $m_v$  is the coefficient of volume compressibility of soils. Rearranging Eq. (4.7) for  $r_u$ ,

$$r_u = 1 - \exp\left(-\frac{rH^2}{2\sigma_v' m_v c_v}\right) \quad (4.8)$$

Expansion of the Eq. (4.8) is

$$r_u = \frac{rH^2}{2\sigma_v' m_v c_v} - \frac{\left(\frac{rH^2}{2\sigma_v' m_v c_v}\right)^2}{2!} + \frac{\left(\frac{rH^2}{2\sigma_v' m_v c_v}\right)^3}{3!} \dots \quad (4.9)$$

Eq. (4.9) can be simplified by neglecting higher order terms:

$$r_u = \frac{rH^2}{2\sigma'_v m_v c_v} \quad (4.10)$$

where,  $r_u$  is a function of  $H$ ,  $r$ ,  $m_v$ ,  $\sigma'_v$  and  $c_v$ . The error between the Eq. (4.8) and Eq. (4.10) is less than 10%.  $m_v$  and  $c_c$  can be related as follows:

$$c_c = \frac{de}{d \log \sigma'_v} = \frac{de}{d \ln \sigma'_v} \times 2.303 \quad (4.11)$$

$$= \frac{de}{d\sigma'_v} (2.303 \times \sigma'_v)$$

$$\frac{c_c}{1+e} = \frac{de}{(1+e)d\sigma'_v} (2.303 \times \sigma'_v) = m_v \times 2.303 \times \sigma'_v \quad (4.12)$$

By rearranging Eq. (4.10) for  $m_v \times \sigma'_v$ ,

$$m_v \times \sigma'_v = \frac{0.434 c_c}{1+e} \quad (4.13)$$

The term  $m_v \times \sigma'_v$  can be assumed as approximately constant, considering the change in void ratio is relatively small in small strain theory. The values of  $m_v \times \sigma'_v$  obtained from the CRS test is plotted with  $\sigma'_v$  as shown in Figure 4.6. The term  $m_v \times \sigma'_v$  can be approximated as constant for given soil. Hence, if  $m_v \times \sigma'_v$  is approximately constant, the pore pressure ratio ( $r_u$ ) is directly proportional to the rate of strain ( $r$ ) and inversely proportional to  $c_v$ , as per Eq. (4.10). Thus, if  $r$  is constant, the coefficient of consolidation ( $c_v$ ) controls the variation of pore pressure ratio with effective stress. Therefore, the trend of variation of  $c_v$  with consolidation pressure and the variation of  $r_u$  with consolidation pressure (for the constant  $r$ ) are directly linked. For the soils Kaolinite, Red soil and Bombay marine clay (Figure 4.7) the values of  $c_v$  increases with consolidation pressure. Therefore, as expected, the pore pressure ratio decreases as the test progresses (Figure 4.5). For Taramani clay, the pore pressure ratio is nearly constant due to the fact that the variation of  $c_v$  with pressure is not significant. For Gummudipoondi clay and Siruseri clay the values of  $c_v$  decreases with  $\sigma'_v$  resulting in increase in pore pressure ratio.

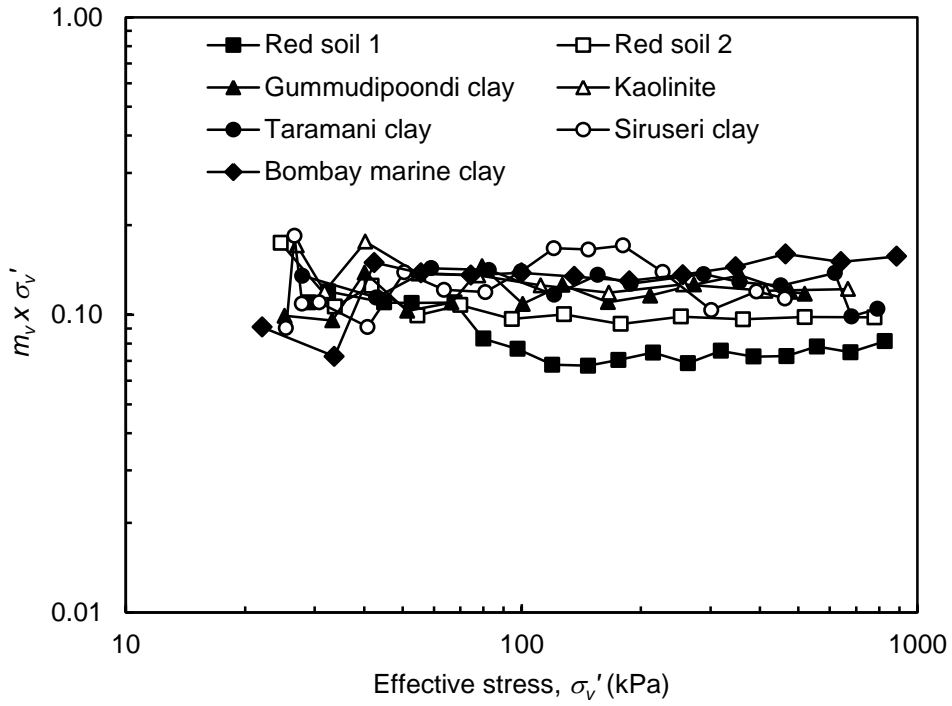


Figure 4.6 : Variation of  $m_v \times \sigma'_v$  with effective stress

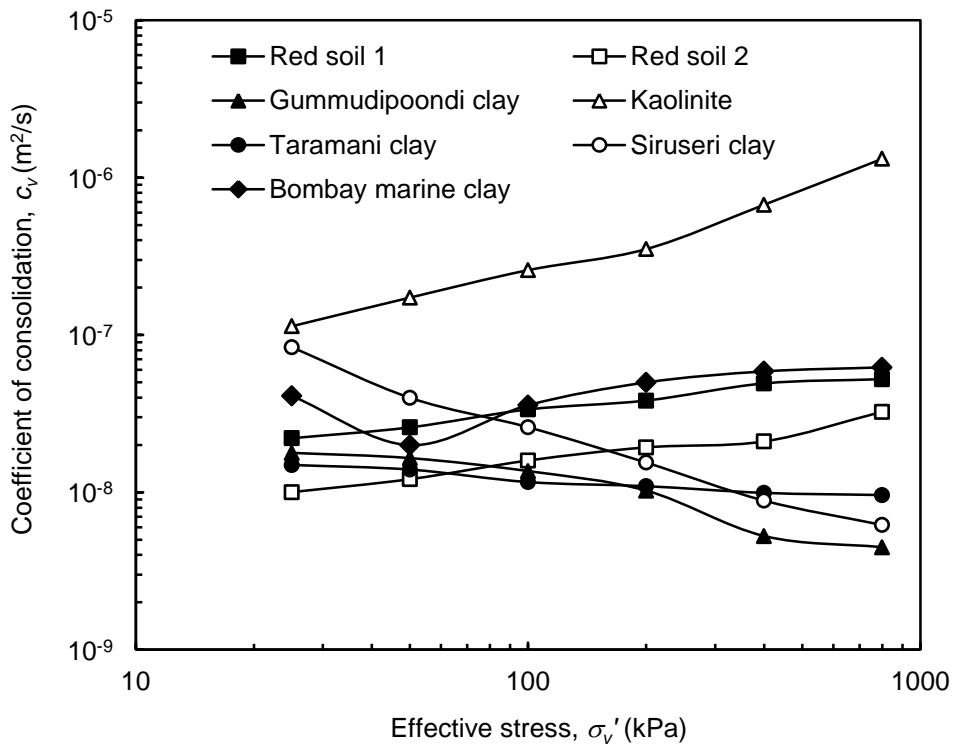


Figure 4.7: Coefficient of consolidation variation with effective stress from the IL test



The pore pressure ratio obtained at a consolidation pressure of 12.5 kPa is nearly 0.15 when the test conducted as per proposed method (Figure 4.5(b)). However, the pore pressure ratio is not constant during CRS tests, as the coefficient of consolidation varies with consolidation pressure. The pore pressure ratio can be maintained constant by controlling the strain rate.

Similarly, to study the variation of pore pressure ratio of overconsolidated (OC) soils, the CRS test was performed on reconstituted soil specimen in OC state and on undisturbed Bombay marine clay sampled at a depth of 12 m. Kaolinite and Taramani clay were the selected reconstituted soils to study the OC behaviour, in which Kaolinite was preconsolidated at 100 kPa and Taramani clay was preconsolidated to 50 kPa. The initial strain rate of CRS test was calculated at the preconsolidation pressure. The  $r_u$ - $\log \sigma_v'$  plots for overconsolidated soils are shown in Figure 4.8. The preconsolidation pressures of the respective soils are also marked in Figure 4.8. It can be observed that the measured pore pressure ratio of OC soils for the virgin compression phase is within the allowable limit, but the values of pore pressure ratio are more than the allowable value for the initial recompression region. Therefore, the strain rate is different for recompression phase and virgin compression phase. Hence, the strain rate needs to be properly controlled for the recompression region also.

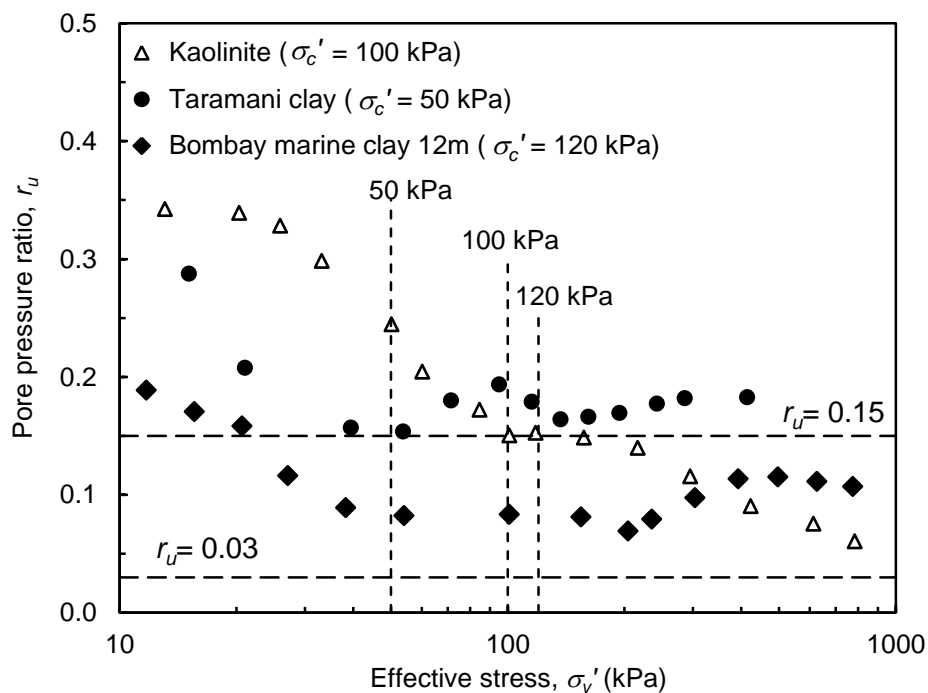


Figure 4.8: Pore pressure ratio variation with effective stress of the overconsolidated soils

From the previous results, it is concluded that fixing the initial strain rate of strain controlled consolidation test based on permeability measurements provides the required pore pressure ratio at the desired  $\sigma_v'$  value of 12.5 kPa. If constant rate is adopted  $r_u$  varies as the test progresses depending on the variation  $c_v$  with consolidation pressure. Therefore, the strain rate needs to be controlled during CSL consolidation test, such a way that the  $r_u$  values will be maintained nearly 0.15 throughout the test and also to make the test faster. For overconsolidated soils, the strain rate needs to be controlled for the recompression region, to obtain consistent results with IL consolidation test. An observational approach to control the strain rate during CSL consolidation test is discussed in the next section.

#### **4.4 OBSERVATIONAL APPROACH TO CONTROL THE STRAIN RATE**

As brought out in the previous section, the pore pressure ratio is directly proportional to the strain rate and inversely proportional to the coefficient of consolidation,  $c_v$  (Eq. 4.10). If the test is conducted at constant rate of strain, the variation of  $r_u$  depends on the variation of  $c_v$  as the test progresses. In other words depending upon the variation in  $c_v$  values, the pore pressure ratio may increase or decrease as the test progresses. Therefore, the value of pore pressure ratio can be maintained within the allowable limits during the entire duration of the test, preferably close to the upper limit of 0.15 by controlling the strain rate. This will also help to complete the test faster. Similarly, in the overconsolidated soils, the pore pressure ratio needs to be maintained for the recompression region.

##### **4.4.1 Theoretical Considerations**

The initial strain rate of CSL consolidation test is fixed based on the permeability measurements, such a way that the pore pressure ratio is 0.15. As the test progresses, the pore pressure ratio can be maintained by controlling the strain rate to obtain a pore pressure of close to the targeted pore pressure ratio of 0.15, by knowing the current pore pressure ratio  $r_{uc}$  as discussed below.

Let  $r_c$  be the current strain rate which yielded a pore pressure ratio of  $r_{uc}$ . As per Eq. (4.2), the relationship between  $r_c$  and  $r_{uc}$  can be approximated as

$$r_c = \frac{-2k\sigma'_v \log(1-r_{uc})}{0.434\gamma_w H^2} \quad (4.14)$$

The strain rate required to produce a pore pressure ratio of 0.15 is given by

$$r_{0.15} = \frac{-2k\sigma'_v \log(1-0.15)}{0.434\gamma_w H^2} \quad (4.15)$$

Taking  $k\sigma'_v$  as approximately constant in Eq. (4.14) and (4.15), the rate ( $r_{0.15}$ ) required to generate the pore pressure ratio of 0.15 can be obtained as

$$r_{0.15} = \frac{\log(1-0.15)}{\log(1-r_{uc})} r_c = \frac{-0.706 \times r_c}{\log(1-r_{uc})} \quad (4.16)$$

As the test progresses, the rate can be controlled to the required strain rate to obtain pore pressure ratio of 0.15 using Eq. (4.16).

For overconsolidated soils, the strain rate required will be different in the recompression and normally consolidated phases. In the recompression phase, the change in void ratio is small and the coefficient of permeability is approximately constant. Therefore, as per Eq. (4.3), the rate required is expected to increase as  $\sigma'_v$  increases from the seating pressure of  $\sigma'_{vi}$  to the preconsolidation pressure  $\sigma'_p$ . The rate ( $r_p$ ) required when the specimen reached the preconsolidation pressure is derived as follows:

$$r_p = \frac{0.325k_i\sigma'_p}{\gamma_w H^2} \quad (4.17)$$

By taking  $k$  as approximately constant in the recompression phase and equating Eq. (4.17) with the Eq. (4.3), the Eq. (4.17) can be simplified as

$$r_p = \left( \frac{r_i}{\sigma'_s} \right) \sigma'_p \quad (4.18)$$

As the preconsolidation pressure is not known for the intact samples taken from the field, the in-situ effective stress may be taken as the preconsolidation pressure for the estimate. The strain rate is applied 2-4 increments from  $r_i$  to  $r_p$  in the recompression phase. In the normally consolidated phase, the rate required is expected to be  $r_p$ .

The effectiveness of the observational approach is validated by performing tests on six reconstituted soils in NC state, two soils in OC state with known preconsolidation pressure and three undisturbed soils.

#### **4.4.2 Results and Discussions**

##### *Normally consolidated soils*

The recommended range of pore pressure ratio as per ASTM D4186-12 (2012) is 0.03-0.15. Tests could be performed faster if the pore pressure ratio is maintained close to 0.15. A typical result for kaolinite is shown in Figure 4.9. When the test was conducted at constant rate, the pore pressure ratio was found to decrease as the test progresses due to the fact that  $c_v$  increases with consolidation pressure for kaolinitic soils. Therefore, the strain rate was controlled as per Eq. (4.16) to the target pore pressure ratio of 0.15. For  $c_v$  increasing soils the test can be completed faster by increasing the strain rate so as to maintain the pore pressure ratio as 0.15. The  $c_v$  variation with effective stress is very high for the Kaolinite. In addition, the coefficient of consolidation is also quite high. Therefore, maintaining the pore pressure ratio manually was found to be little difficult. Therefore, the pore pressure ratio observed is in the range of 12%-8%. If constant rate of 7%/hour is used, during loading and 3.5%/hour during unloading, the time required to complete the test is 8.5 hours. However, with controlling the rate, the total duration required is only 3.5 hours. Therefore, by controlling the rate so as to obtain  $r_u$  close to 0.15 the test can be completed much faster. The results compare well with IL test results. There is a discrepancy in the results of  $c_v$  upto  $\sigma_v' \approx 50$  kPa, probably due to transient state. The  $e$ - $\log \sigma_v'$ ,  $c_v$ - $\sigma_v'$  and  $e$ - $\log k$  curves obtained when the rate is adjusted are shown in Figures 4.9(b-d), respectively, along with one-dimensional IL consolidation test results. The CSL tests by controlling strain rate for other soils are presented in Appendix D.

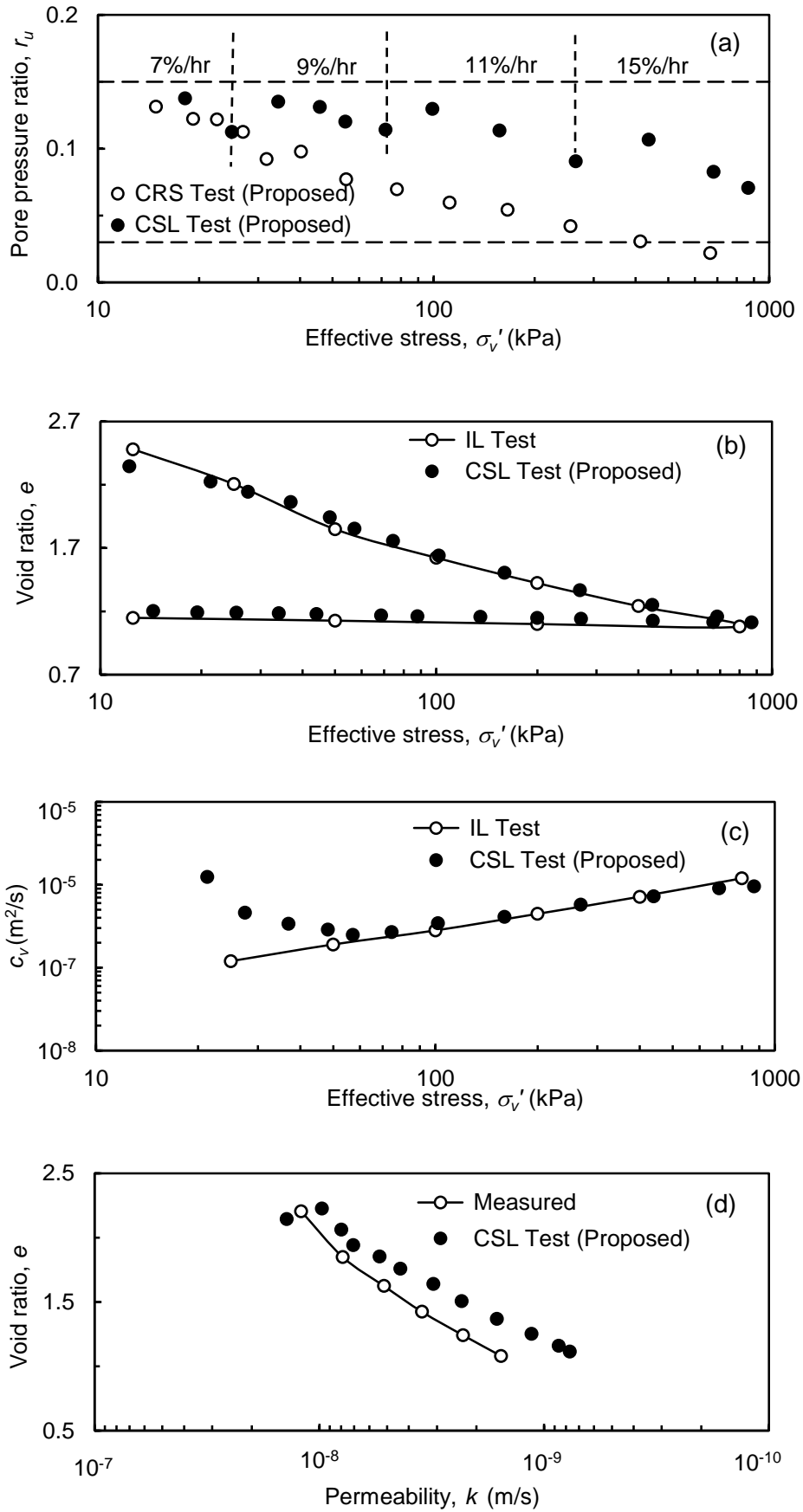


Figure 4.9: Comparison of CSL Test with IL Test results for Kaolinite

Typical plot for Gummudipoondi clay for which  $c_v$  decrease with pressure is shown in Figures 4.10(a)-(d). When the strain rate was not controlled the pore pressure ratio keeps on increasing beyond 0.15 (Figure 4.10(a)) warranting the need to control the rate. Therefore, the rate was reduced every time the rate shoots-up above 0.15. The results obtained from the proposed CSL test is plotted along with the results from the conventional IL test in Figures 4.10(b-d). The results from CSL test matches very well with IL test.

The total settlement parameters such as the compression index ( $c_c$ ) and recompression index ( $c_r$ ) were obtained from the  $e$ - $\log \sigma_v'$  plots and are shown in Figure 4.11. The values obtained from CSL consolidation test are highly comparable with conventional IL test with a coefficient of variance of 6%.

The time required for performing the CSL test as per the proposed observational method during the loading and unloading for all the reconstituted soils are given in Table 4.2 along with the range of pore pressure ratio observed. It can be clearly seen that the duration required for completing the CSL test depends on the coefficient of consolidation and also the trend of variation with consolidation pressure. For soils for where  $c_v$  values increase with consolidation pressure, the rate can be increased so that the test is completed faster. However, for low permeable soils with  $c_v$  decreasing with consolidation pressure, the time required for the CSL test is high. Hence, it can be concluded that for low permeable soils with  $c_v$  decreasing with pressure, time required is high. This is consistent with the results in the literature (Table 2.4) that low permeable soils require more time.

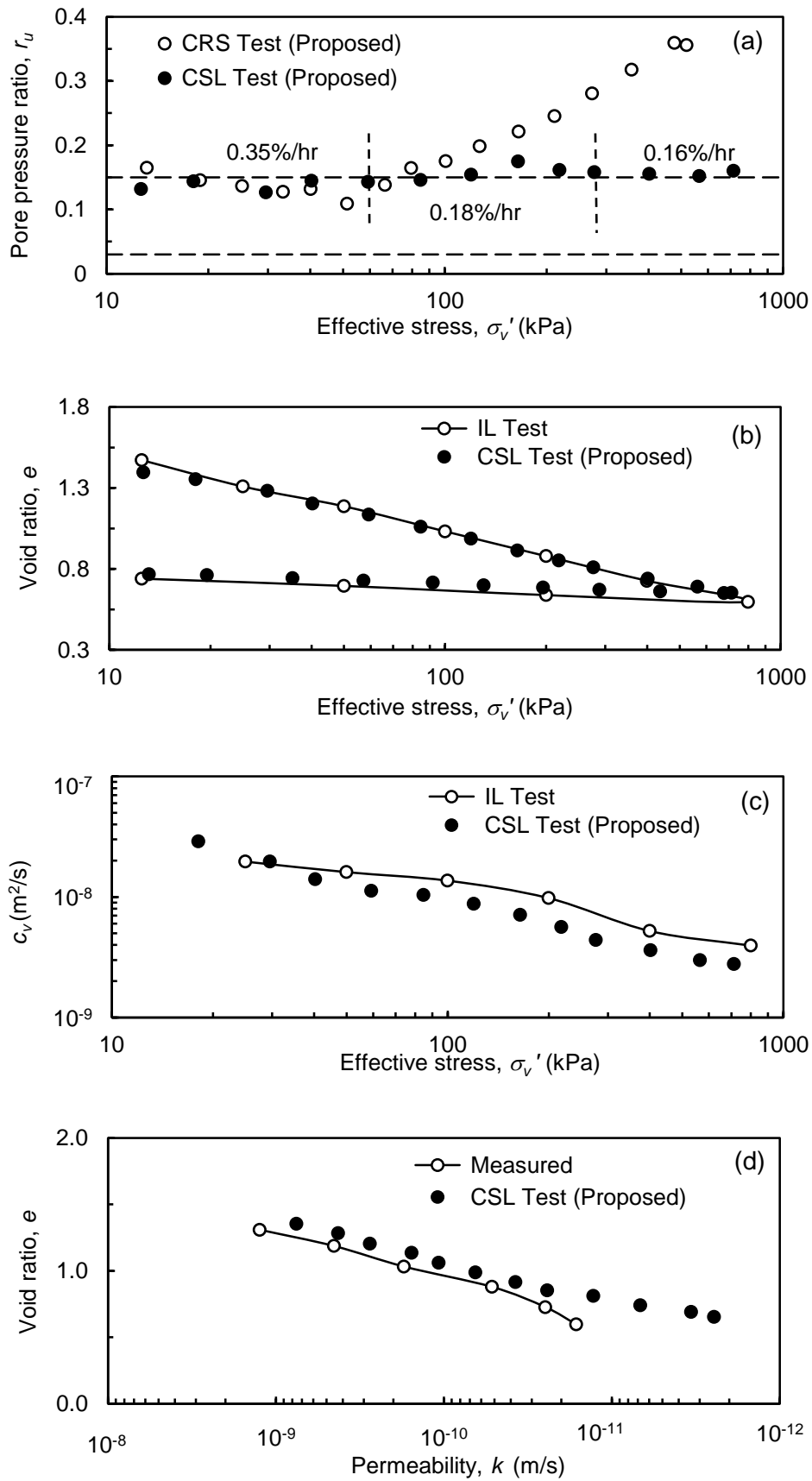


Figure 4.10: Comparison of CSL Test with IL Test results for Gummudipoondi clay

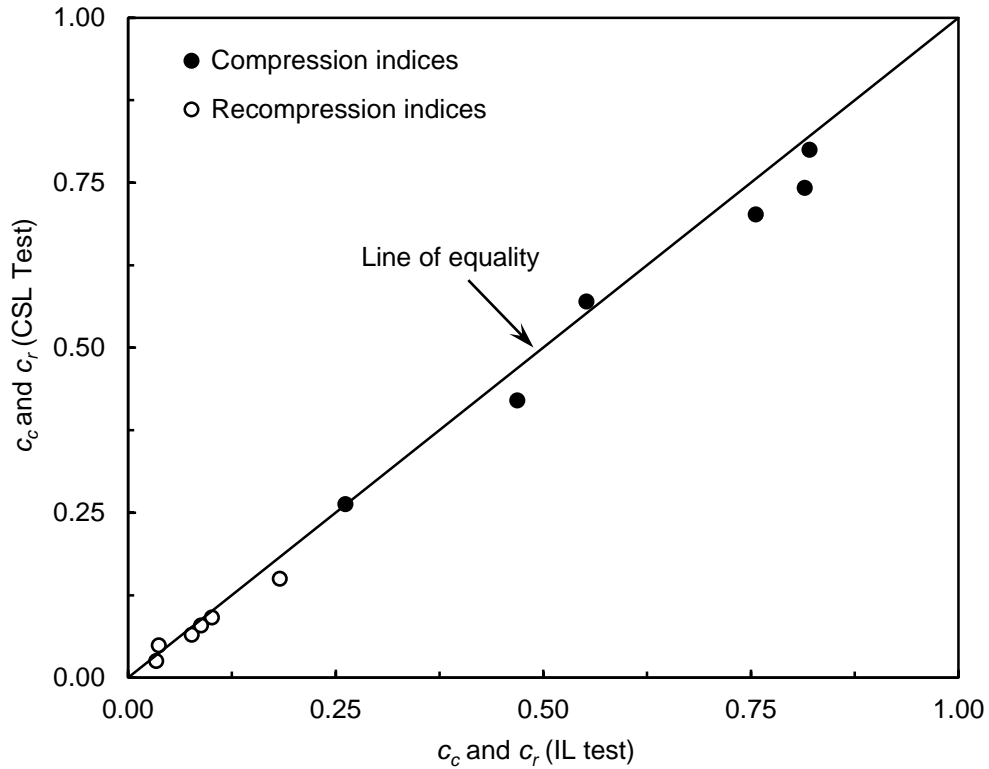


Figure 4.11: Comparison of  $c_c$  and  $c_r$  from the CSL Test and IL test for the reconstituted normally consolidated soils

Table 4.2: Time required for the CSL test as per the proposed method

Sl. No.	Soil Type	Range of $c_v$ , $m^2/s$	$r_u$ (%)	Time taken, hours		
				Loading	Unloading	Total
1	Red soil 1	$3 \times 10^{-8}$ - $6 \times 10^{-8}$	15-12	30	7	37
2	Gummudipoondi clay	$4 \times 10^{-9}$ - $6 \times 10^{-8}$	15-12	130	110	240
3	Kaolinite	$2 \times 10^{-7}$ - $1 \times 10^{-6}$	12-08	3	0.5	3.5
4	Taramani clay	$8 \times 10^{-9}$ - $1 \times 10^{-8}$	15-13	135	42	177
5	Siruseri clay	$6 \times 10^{-9}$ - $8 \times 10^{-8}$	15-16	60	67	127
6	Bombay marine clay	$5 \times 10^{-8}$ - $6 \times 10^{-8}$	15-10	34	9	43



### ***Overconsolidated soils and undisturbed soils***

The proposed observational method was further validated on the reconstituted soils in the OC state of known preconsolidation pressure. Kaolinite was preconsolidated to 200 kPa and Gummudipoondi clay was preconsolidated to 50 kPa in the oedometer itself. The preconsolidated specimens were tested as per the proposed procedure. Three undisturbed samples such as Cochin marine clay (16 m), Cochin marine clay (5 m) and Cochin marine clay (19.5 m) were selected to validate the proposed procedure. The results obtained are shown in Figures 4.12-4.16 along with IL test. It can be clearly seen that the pore pressure ratio is maintained nearly 0.15 for the recompression region as shown in Figures 4.12(a)-4.16(a). The  $e$ - $\log \sigma'_v$ ,  $c_v$ - $\sigma'_v$  and  $e$ - $\log k$  curves obtained are shown in Figures 4.12(b-d)-4.16(b-d), respectively, along with one-dimensional IL consolidation test results and the curves obtained from the CSL test matches well with the IL test.

The total settlement parameters such as the compression index ( $c_c$ ) and recompression index ( $c_r$ ) obtained from the proposed method are compared with those obtained from the one-dimensional IL consolidation test in Table 4.3. The values obtained are comparable with the IL test results. The preconsolidation pressure for the soils was determined by the  $\log(1+e)$  versus  $\log \sigma'_v$  method suggested by Sridharan *et al.* (1991) and the values obtained are listed in Table 4.4. It can be seen that the preconsolidation pressure obtained from the proposed method is almost the same as the conventional test for reconstituted soils in OC state. The preconsolidation pressure for undisturbed soils shows some difference, which may be attributed to sample variability. The comparison with the one-dimensional consolidation test is very good suggesting that the proposed method for controlling the strain rate of CSL test is valid.

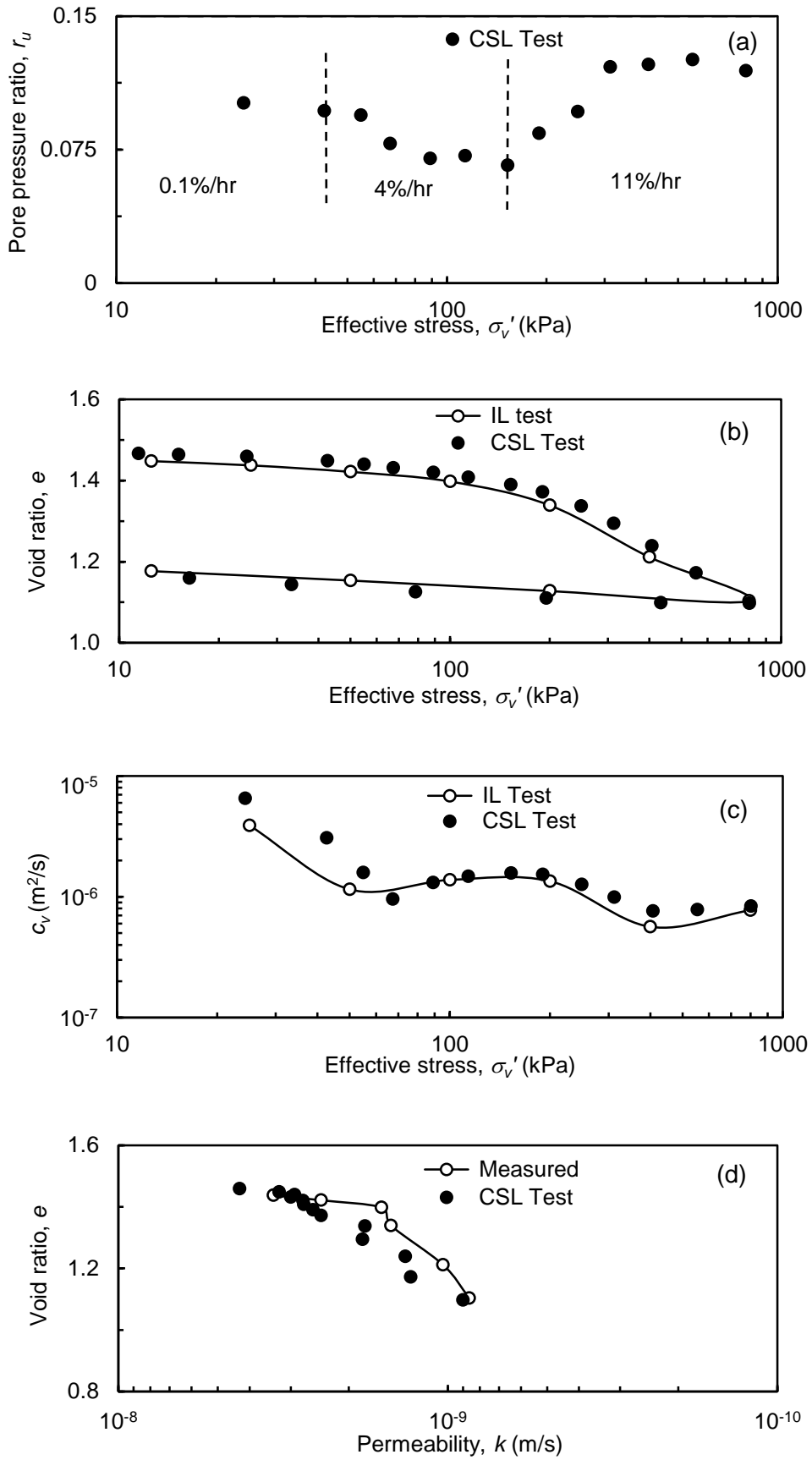


Figure 4.12: Comparison of CSL Test and IL Test results for the overconsolidated Kaolinite specimen with  $\sigma'_c = 200$  kPa

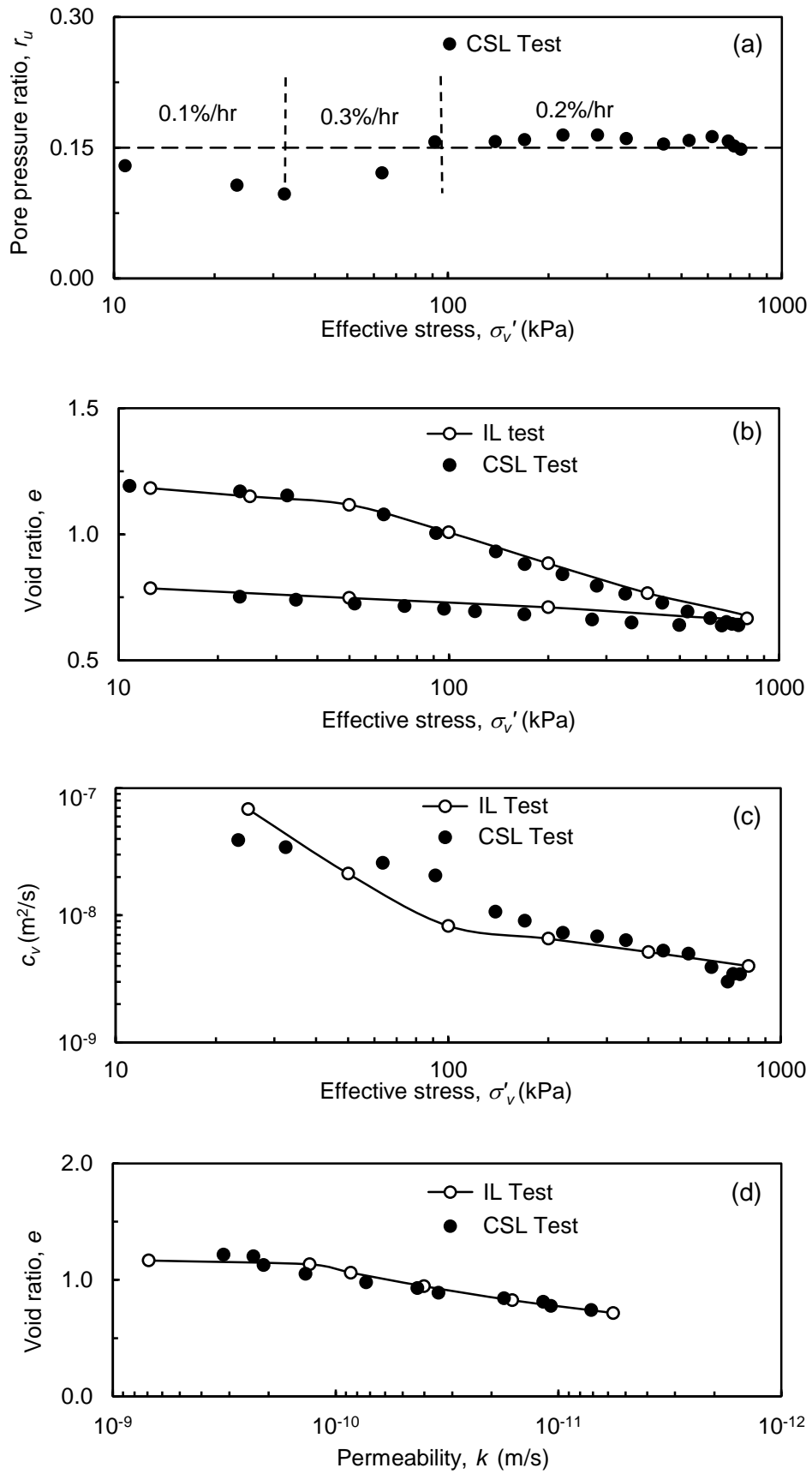


Figure 4.13: Comparison of CSL Test and IL Test results for the overconsolidated Gummudipoondi clay specimen with  $\sigma'_c = 50$  kPa

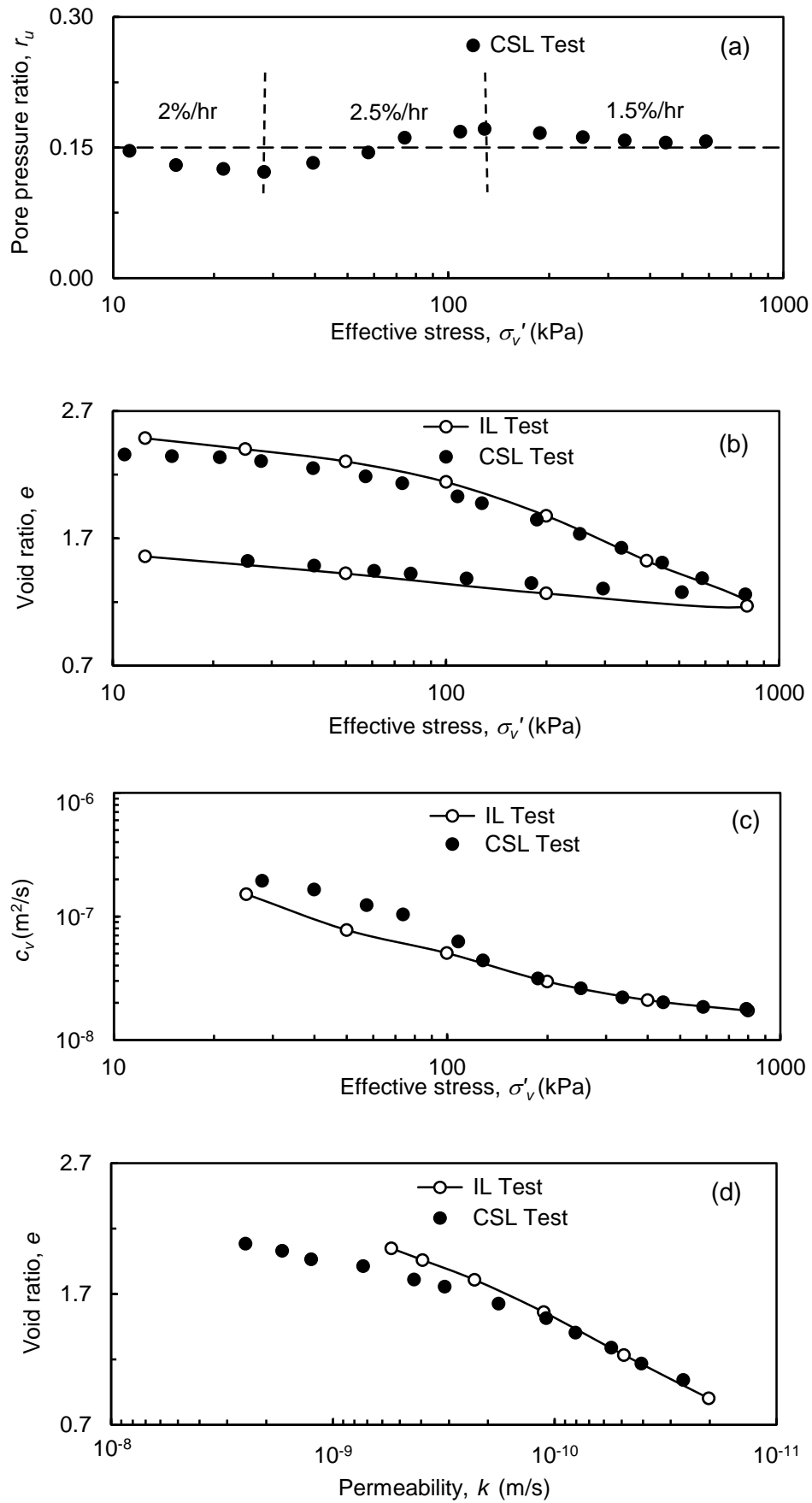


Figure 4.14: Comparison of CSL Test and IL Test results for CMC (16 m)

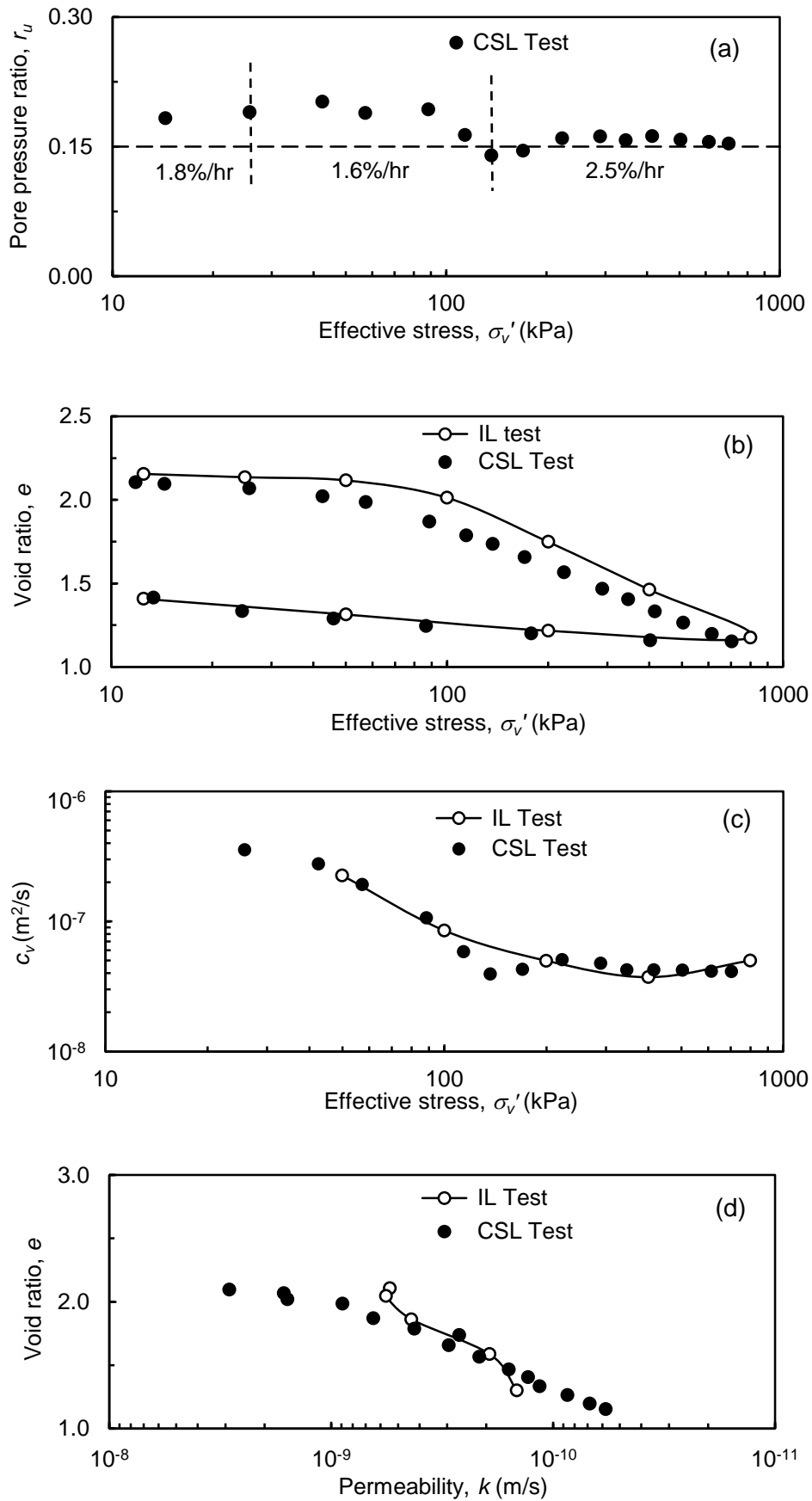


Figure 4.15: Comparison of CSL Test and IL Test results for CMC (5 m)

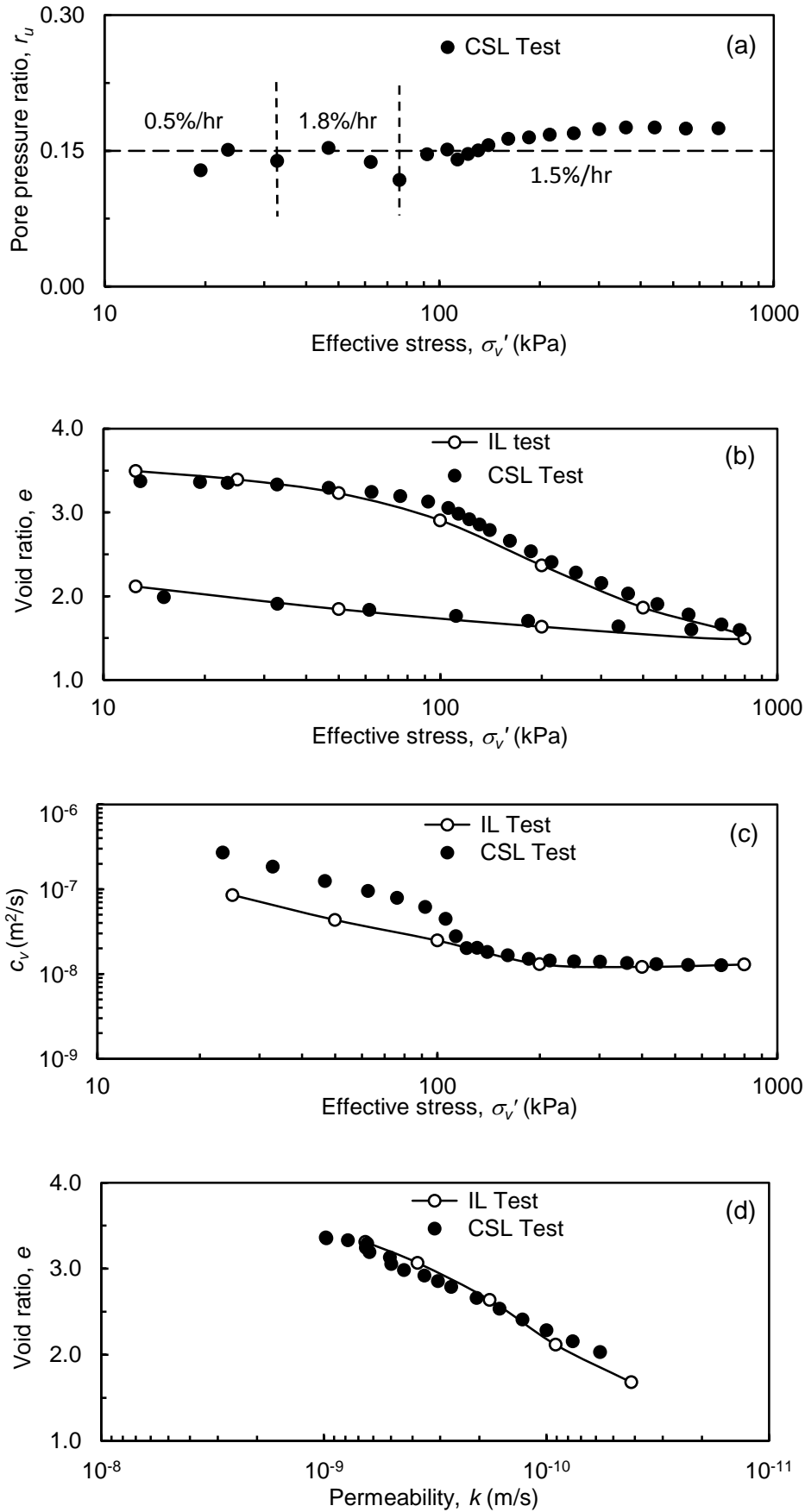


Figure 4.16: Comparison of CSL Test and IL Test results for CMC (19.5 m)

Table 4.3: Compression indices and Recompression indices from IL test and CSL test

Sl. No.	Soils	Compression Index, $c_c$		Recompression index, $c_r$	
		IL Test	CSL Test	IL Test	CSL Test
		1	Kaolinite	0.40	0.47
2	Gummudipoondi clay	0.47	0.40	0.077	0.080
3	Cochin marine clay (16 m)	1.09	0.91	0.210	0.195
4	Cochin marine clay (5 m)	0.929	0.817	0.126	0.166
5	Cochin marine clay (19.5 m)	1.22	1.21	0.221	0.192

Table 4.4: Values of preconsolidation pressure from IL test and CSL test

Sl. No.	Soils	Applied or $\sigma_{v0}'$ (kPa)	$\sigma_c'$ (kPa)	
			IL Test	CSL Test
1	Kaolinite	200	190	199
2	Gummudipoondi clay	50	50	48
3	Cochin marine clay (16 m)	70*	104	71
4	Cochin marine clay (5 m)	75*	95	85
5	Cochin marine clay (19.5 m)	74*	90	75

Note:  $\sigma_{v0}'$  - Effective overburden pressure.

#### 4.5 SUMMARY

In this chapter, a rational method of fixing the strain rate for controlled-strain loading consolidation test is proposed, so as to obtain a pore pressure ratio of nearly 0.15. The proposed method is suggested based on the theory of Wissa *et al.* (1971). The initial strain rate is determined by measuring the permeability of the specimen for a particular effective stress of 12.5 kPa. A permeability set-up was designed and fabricated so as to measure the permeability faster. The proposed method for fixing the initial strain rate was validated by performing a series of CRS tests on the reconstituted soils in NC state and OC state and the results obtained were compared with the recommendations in ASTM D4186-12 (2012). Tests were also performed on three undisturbed soil specimens. The experimental results show that the initial strain rate based on permeability measurement is

more appropriate than based on soil classification. It was observed that the pore pressure ratio changes during CRS test. Therefore, it is essential to maintain the pore pressure ratio close to 0.15 during the test, so as to make the test faster.

Hence, an observational approach was suggested for controlling the strain rate of Controlled strain loading consolidation test. The method was validated by performing a series of CSL consolidation tests on seven reconstituted soil specimens in NC state, two soil specimens in OC state and three undisturbed soil specimens. The CSL test results were compared with the incremental loading (IL) consolidation test. The values of compression index ( $c_c$ ), recompression index ( $c_r$ ), coefficient of consolidation ( $c_v$ ) and coefficient of permeability ( $k$ ) obtained from the CRS test and CSL test compare very well with incremental loading (IL) oedometer test.



## **CHAPTER 5**

# **DESIGN AND DEVELOPMENT OF SIMPLIFIED CRS APPARATUS**

### **5.1 INTRODUCTION**

Several types of CRS consolidation apparatus were developed in the literature (Chapter 2). In Chapter 4, the guidelines to perform controlled strain loading (CSL) consolidation test was proposed, where CRS apparatus recommended by ASTM D4186-12 (2012) was used. ASTM D4186-12 (2012) provided the protocol for CRS apparatus, which is based on the apparatus proposed by Wissa *et al.* (1971). The commercially available CRS cell, meeting the requirements of ASTM standards is generally expensive. Therefore, developing a simplified and cost effective CRS apparatus will be useful to the teaching and research laboratories.

In this chapter, details of a simplified CRS consolidation cell are given. In addition, it is also attempted to use the conventional oedometer cell for performing CRS test. The slight modifications required in the conventional cell to perform CRS test is described. The CRS test results obtained using the proposed apparatus is compared with those obtained from the standard apparatus.

### **5.2 SIMPLIFIED CRS APPARATUS**

#### **5.2.1 Details of the Apparatus**

The schematic diagram of the standard CRS apparatus, meeting the requirements of ASTM D4186-12 (2012) is shown in Figure 5.1. The apparatus is similar to the standard triaxial cell with provisions for applying cell pressure and back pressure. Provision for fixing the pore pressure transducer at the base is also provided. A pressure chamber is an essential component of the cell, which is provided to apply the back pressure, so as to ensure that the sample is saturated throughout the test. The top draining boundary of the

specimen is in direct contact with the pressure chamber. The specimen holder (consolidation ring) is properly affixed at the base via an O-ring so as to make it watertight enabling accurate pore pressure measurements.

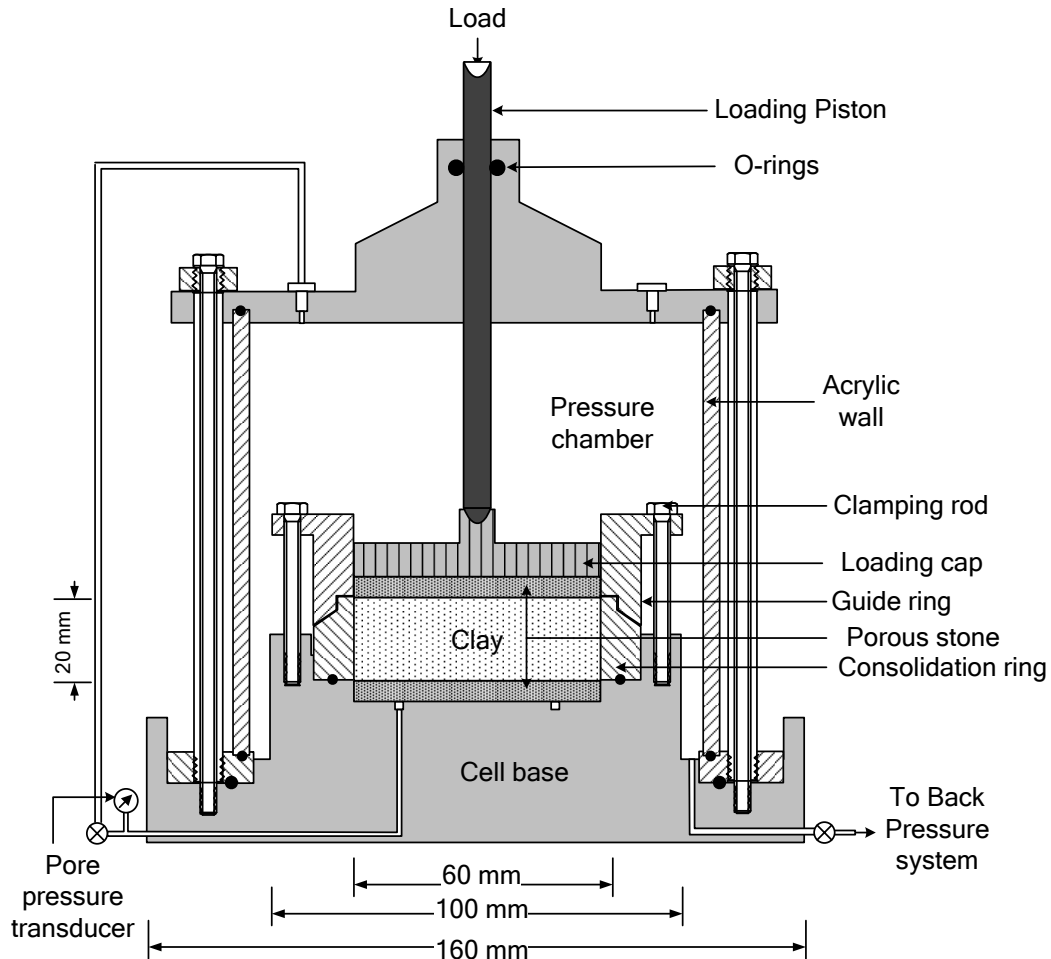


Figure 5.1: Schematic diagram of the standard CRS cell

In the proposed simplified CRS apparatus, the pressure chamber is eliminated and a piston type loading cap is used directly to apply the load on the soil specimen. The schematic diagram of the simplified CRS apparatus is shown in Figure 5.2. The other major components are the base, specimen ring and a top platen. The photographic view of the components of the simplified CRS apparatus and the assembled apparatus are shown in Figures 5.3(a) and 5.3(b), respectively. The apparatus can be fabricated to test any size of specimen. In the present study, the apparatus is designed to test specimens of 60 mm diameter and 20 mm thickness. The inner diameter and height of the specimen ring are 60 mm and 60 mm, respectively. The diameter and thickness of the cell base are 120 mm and

25 mm, respectively. The cell base is provided with a porous stone at its center for bottom drainage and also has provisions for the measurement of pore water pressure. A bottom O-ring is provided in the base to prevent leakage from the bottom of the specimen. The outer and inner diameters of the top platen are 120 mm and 70 mm, respectively. The thickness of the top platen is 12 mm. The specimen ring is clamped between the base and the top platen by tie-bolts. The important feature of the cell is the piston cum loading cap. The diameter of the loading cap is 59.8 mm and two O-rings are provided along its sides, to prevent leakage. A 50 mm diameter and 5 mm thick porous stone is fixed at the center of the loading cap for top drainage. The loading cap has provision for the application of back pressure as shown in Figure 5.2.

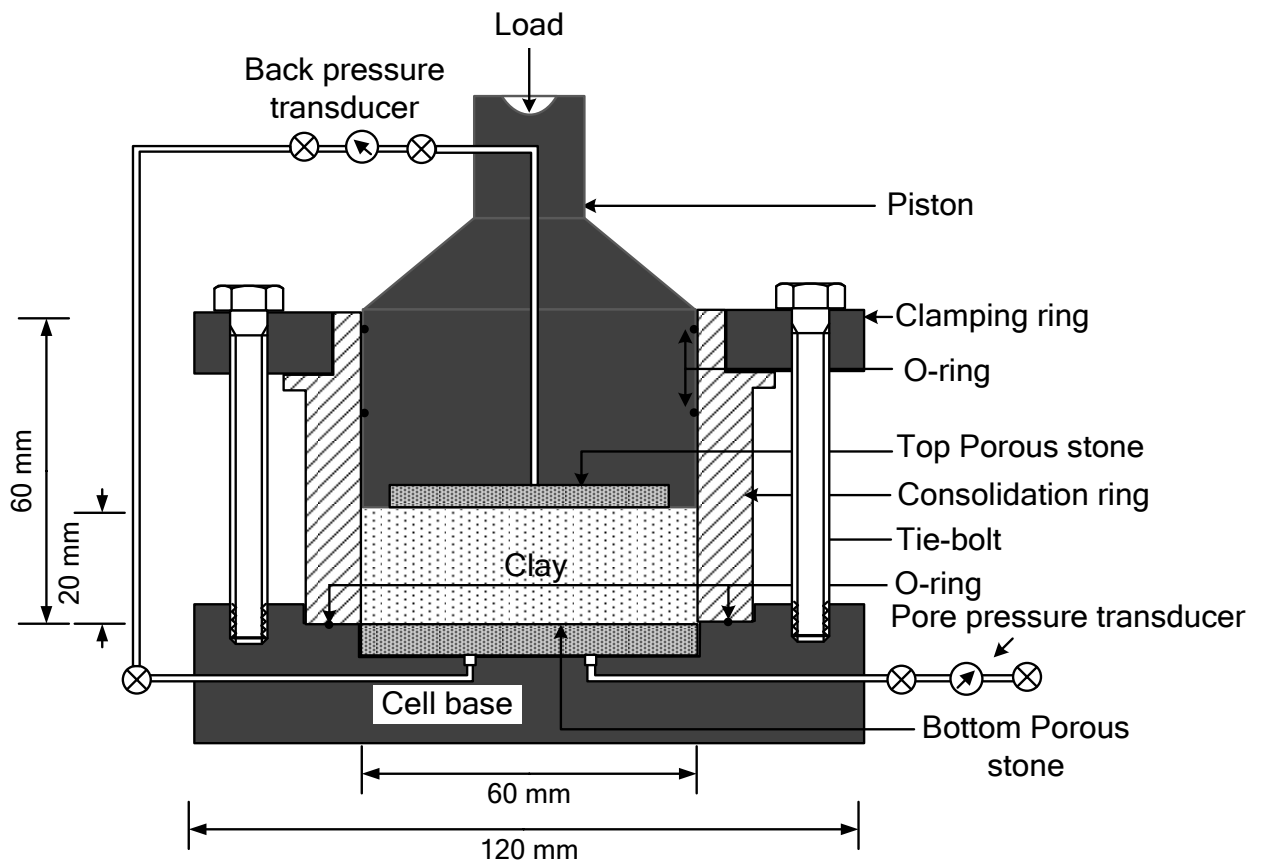


Figure 5.2: Schematic diagram of the simplified CRS Cell

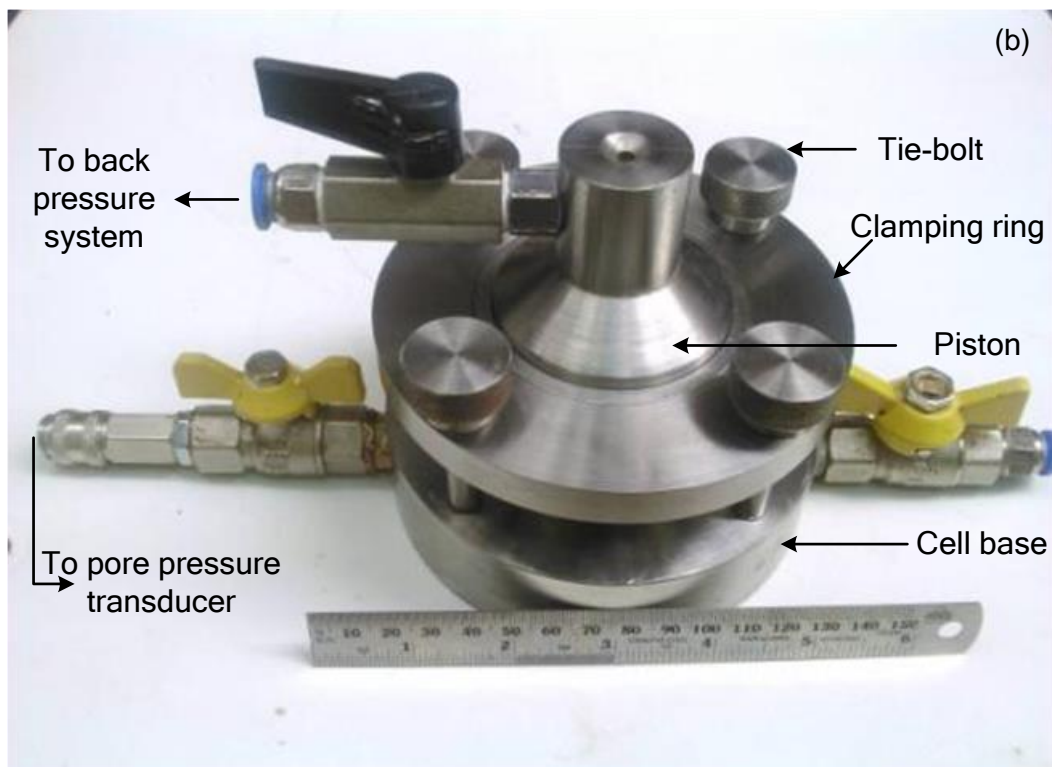
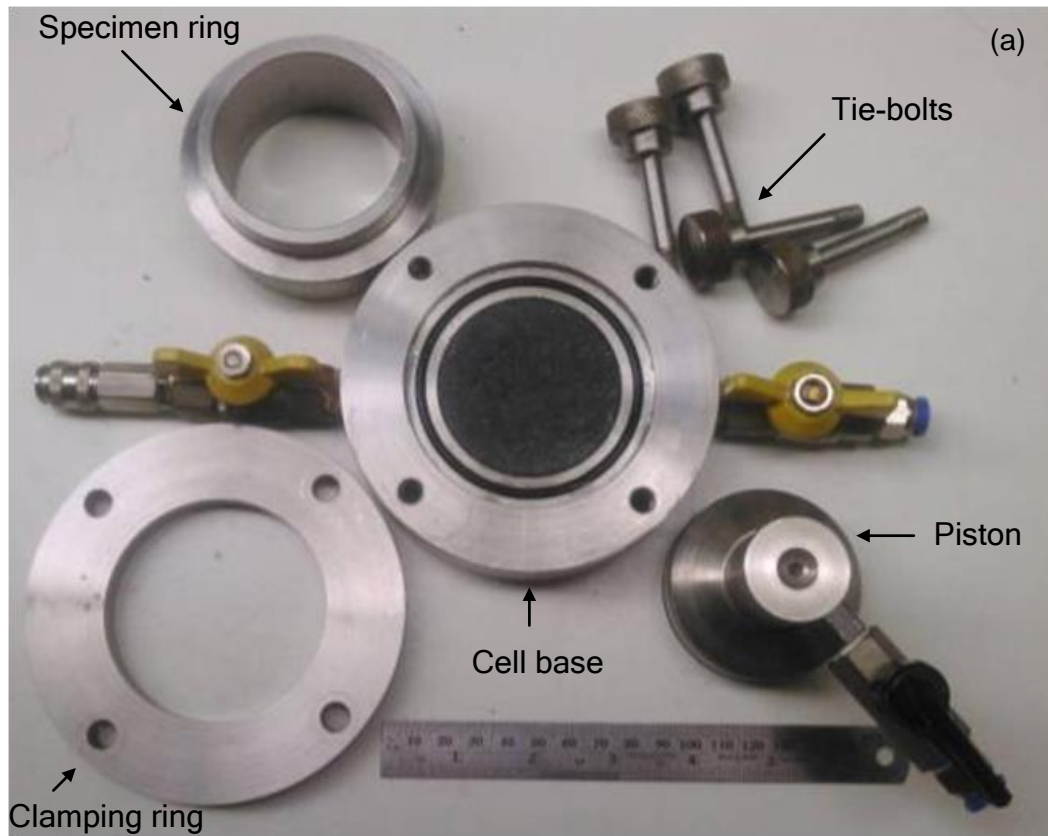


Figure 5.3: Photographic view of the proposed CRS apparatus (a) Components of the cell and (b) Assembled cell

During the CRS test, the loading cap slides along the inner wall of the specimen ring. As the loading cap snugly fits in the specimen ring and provided with two O-rings, friction between the specimen ring and loading cap is inevitable. The friction developed was measured by pushing the loading cap in to the specimen ring without soil specimen. The friction was found to be 20 N (7 kPa for 60 mm diameter ring). This value was deducted while calculating the vertical stress on the soil specimen.

The apparatus was fabricated at the Department Workshop facility, Department of Civil Engineering, Indian Institute of Technology Madras. It can be fabricated in any mechanical engineering workshops. The cost of fabrication is about (1/10)<sup>th</sup> the cost of commercially available apparatus. The performance of the proposed CRS apparatus was validated by performing a series of experiments on four reconstituted soils with varying plasticity characteristics and one undisturbed soil. The experimental program and the results obtained are discussed in the next section.

### **5.2.2 Experimental Programme**

The performance of the proposed CRS apparatus was validated by conducting consolidation tests on four reconstituted soil samples namely, Red soil 1, commercially available Kaolinite, Taramani clay and Bombay marine clay and on one undisturbed soil. Cochin marine clay, sampled at a depth of 19.5 m was the selected undisturbed soil. The basic properties of the soils were given in Chapter 3 (Table 3.1).

The reconstituted specimens were directly prepared in the specimen ring to reduce disturbance. The inner wall of the specimen ring was smeared with Silicone grease to avoid side wall friction. The slurry was placed in the consolidation ring to a thickness of 35 mm and consolidated to an initial pressure of 12.5 kPa under double drainage. Once the consolidation was completed, the consolidation ring with the soil was carefully detached from the consolidation cell base. Using a spacer block of 59.8 mm diameter and 40 mm thickness, the excess soil in the ring was pushed out and trimmed so that a specimen height of 20 mm (= 60-40, 60 mm is the height of the specimen ring) was obtained.

As the pore water pressure is measured at the base of the specimen, the bottom drainage lines were de-aired by flushing with de-aired water. A filter paper was placed over the bottom porous stone. The specimen ring with the specimen was placed in the CRS cell base. After placing the top filter paper, the loading cap with the top porous stone was then placed. The whole set-up was placed on a standard digital triaxial loading frame for applying the deformation to the specimen (Figure 5.4). Back pressure of 200 kPa was applied through the loading cap to saturate the specimen. After equilibration of the applied back pressure in the specimen, the test was started. The strain rate was selected based on the proposed method discussed in Chapter 4, such that the base pore pressure ratio (defined as the ratio of base excess pore pressure to the axial stress) was obtained as nearly 15%. The rates adopted for Red soil 1, Kaolinite, Taramani clay, Bombay marine clay and Cochin marine clay (19.5 m) were 0.6, 6.0, 0.3, 0.9 and 1.5 %/hour, respectively.

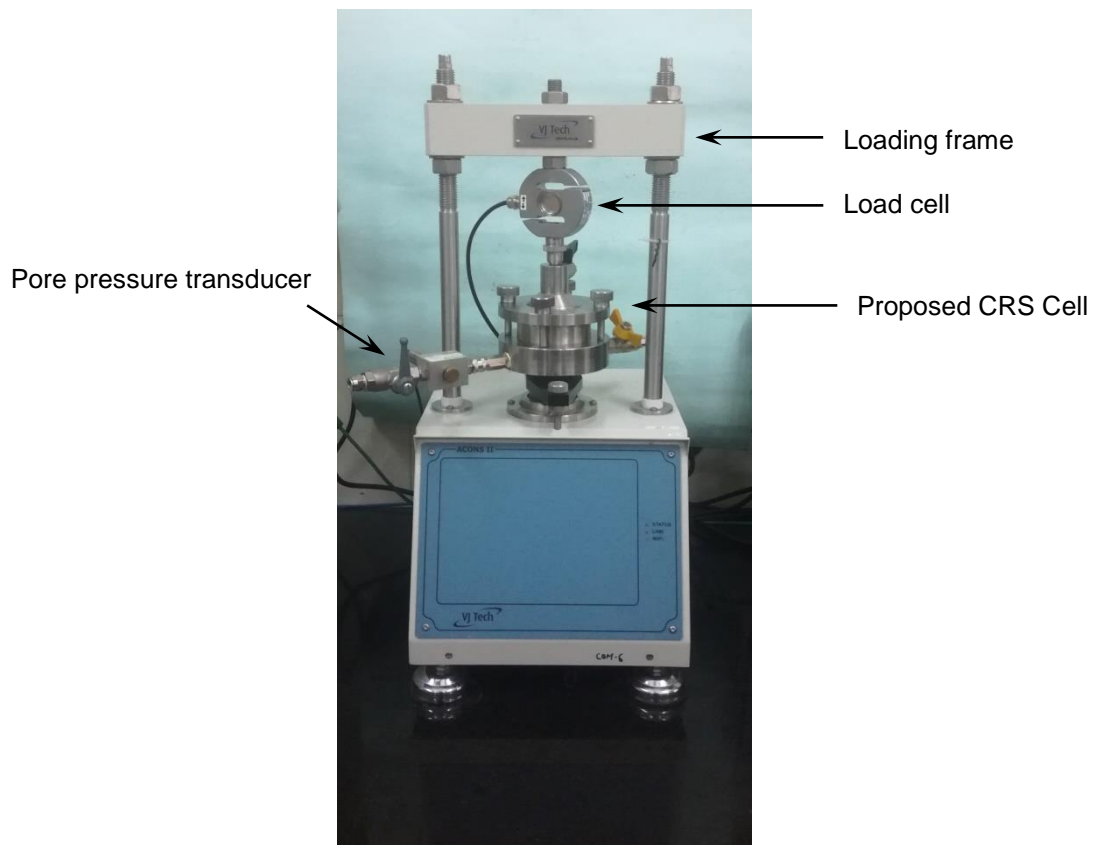


Figure 5.4: Photograph of CRS set-up used for the study

The axial force, axial deformation and base pressure were monitored continuously. Once the required axial force was reached, the specimen was unloaded to one-half of the rate used during the loading phase, to a seating pressure of 12.5 kPa. At the end of the test, the final water content and the final thickness of the specimens were measured. The CRS test data obtained from the simplified apparatus was interpreted using the theory of Wissa *et al.* (1971). The CRS test results obtained using the proposed CRS apparatus is compared with the conventional IL consolidation test with 24 hours incremental load duration and the CRS test using the standard CRS apparatus.

### 5.2.3 Results and Discussions

#### *Results from reconstituted soils*

The variation of total stress and pore pressure with axial strain obtained from the standard and the proposed CRS apparatus are compared in Figures 5.5(a), 5.5(b), 5.5(c) and 5.5(d) for Red soil 1, Kaolinite, Taramani clay and Bombay marine clay, respectively. The results are highly comparable and the pore pressure ratio obtained for Red soil 1, Kaolinite, Taramani clay and Bombay marine clay are in the range of 0.05-0.13, 0.03-0.15 0.07-0.13 and 0.05-0.15, respectively, which are well within the range of 0.03 to 0.15. As the objective of this part of the study is to evaluate the performance of the proposed apparatus, tests were carried out with constant rate of strain only.

The data were analysed to obtain the consolidation parameters as per ASTM D4186-12 (2012). The void ratio ( $e$ )-effective consolidation pressure ( $\sigma_v'$ ) plots are shown in Figures 5.6(a)-(d), for all the soils tested. The results from the standard CRS apparatus and the proposed apparatus compare very well. The results from IL consolidation tests also match well with the CRS test results. The compression index ( $c_c$ ) and recompression index ( $c_r$ ) values obtained from the different apparatuses for different soil types tested are shown in Table 5.1. From Table 5.1, it can be observed that the  $c_c$  and  $c_r$  values obtained from the proposed apparatus compare well with those obtained from the standard CRS apparatus and the IL consolidation test. Error analysis was carried out with the IL consolidation results as the control. With reference to the IL consolidation test, the average coefficient of variance (COV) of  $c_c$  for the standard CRS apparatus and the proposed apparatus are 4% and 3%, respectively.

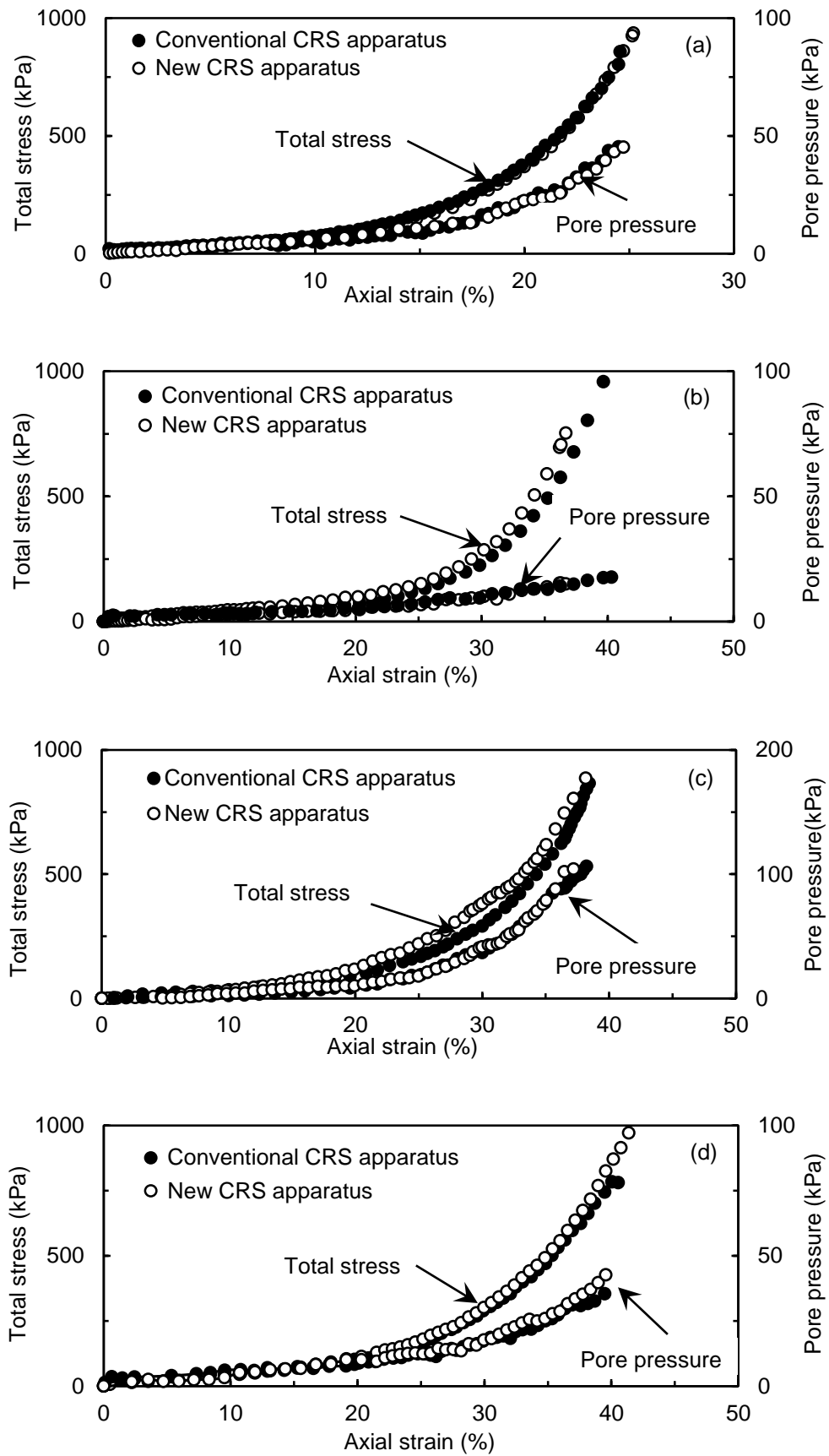


Figure 5.5: Total stress and Pore pressure –Axial strain plot for (a) Red Soil 1 (b) Kaolinite (c) Taramani clay and (d) Bombay marine clay



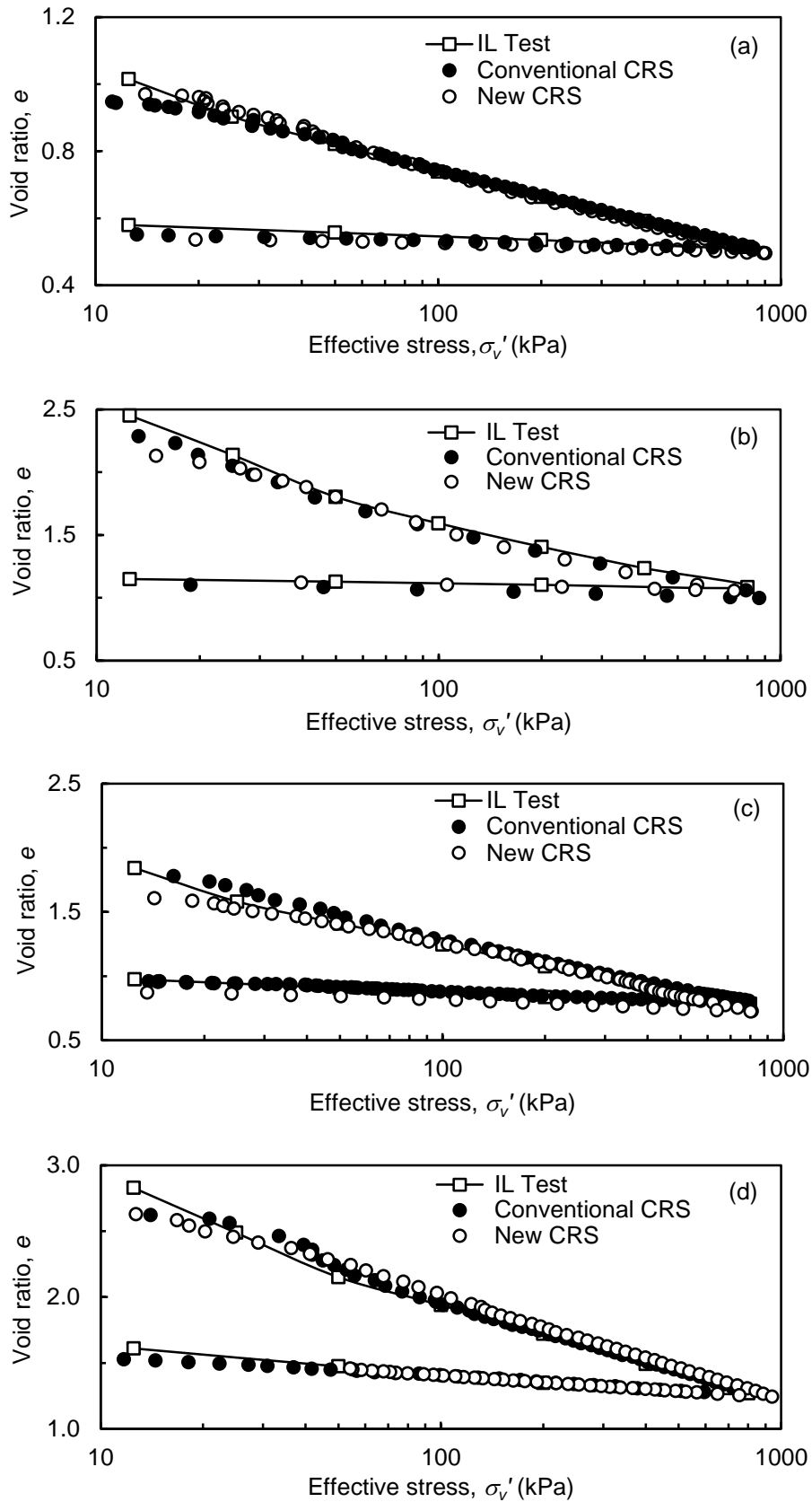


Figure 5.6:  $e$ - $\log \sigma'_v$  plot for (a) Red Soil 1 (b) Kaolinite (c) Taramani clay and (d) Bombay marine clay

Table 5.1: Comparison of Compression index and Recompression Index values of the reconstituted soils

Sl. No	Soils	Compression Index ( $c_c$ )			Recompression Index ( $c_r$ )		
		IL test	Standard CRS	New CRS	IL test	Standard CRS	New CRS
1	Red soil 1	0.26	0.25	0.28	0.03	0.02	0.03
2	Kaolinite	0.69	0.65	0.68	0.09	0.07	0.06
3	Taramani clay	0.55	0.58	0.54	0.10	0.10	0.09
4	Bombay marine clay	0.81	0.81	0.80	0.18	0.16	0.17

The other important parameter derived from the consolidation test is the coefficient of consolidation ( $c_v$ ). The values of coefficient of consolidation obtained from the CRS consolidation tests using the standard CRS apparatus and the simplified CRS apparatus are shown in Figures 5.7 (a)-(d). The  $c_v$  values obtained from the CRS tests, using the standard and the proposed apparatus, shows high values below 25-30 kPa. However, the trend shows convergence beyond 25-30 kPa. This is attributed to the transient conditions at low stress levels in the early stages of the test. Similar results were reported by Gorman *et al.* (1978) and Jia *et al.* (2010). The values are also compared with those obtained from IL consolidation test using Taylor's  $\sqrt{t}$  method (Taylor, 1942). The values are of the same order. With reference to the IL consolidation test, the average coefficient of variance (COV) of  $c_v$  for the standard CRS apparatus and the proposed apparatus are 36% and 31%, respectively.

The variation of coefficient of permeability ( $k$ ) with void ratio ( $e$ ) determined using the proposed CRS consolidation apparatus, standard CRS consolidation apparatus and those measured during the IL consolidation test for the four soil types are shown in Figures 5.8 (a)-(d). The values match very well lending support to the validity of the proposed CRS consolidation apparatus for evaluating the consolidation parameters. Very similar to  $c_v$ , the COV for the standard CRS apparatus and the proposed apparatus are 36% and 31%, respectively.

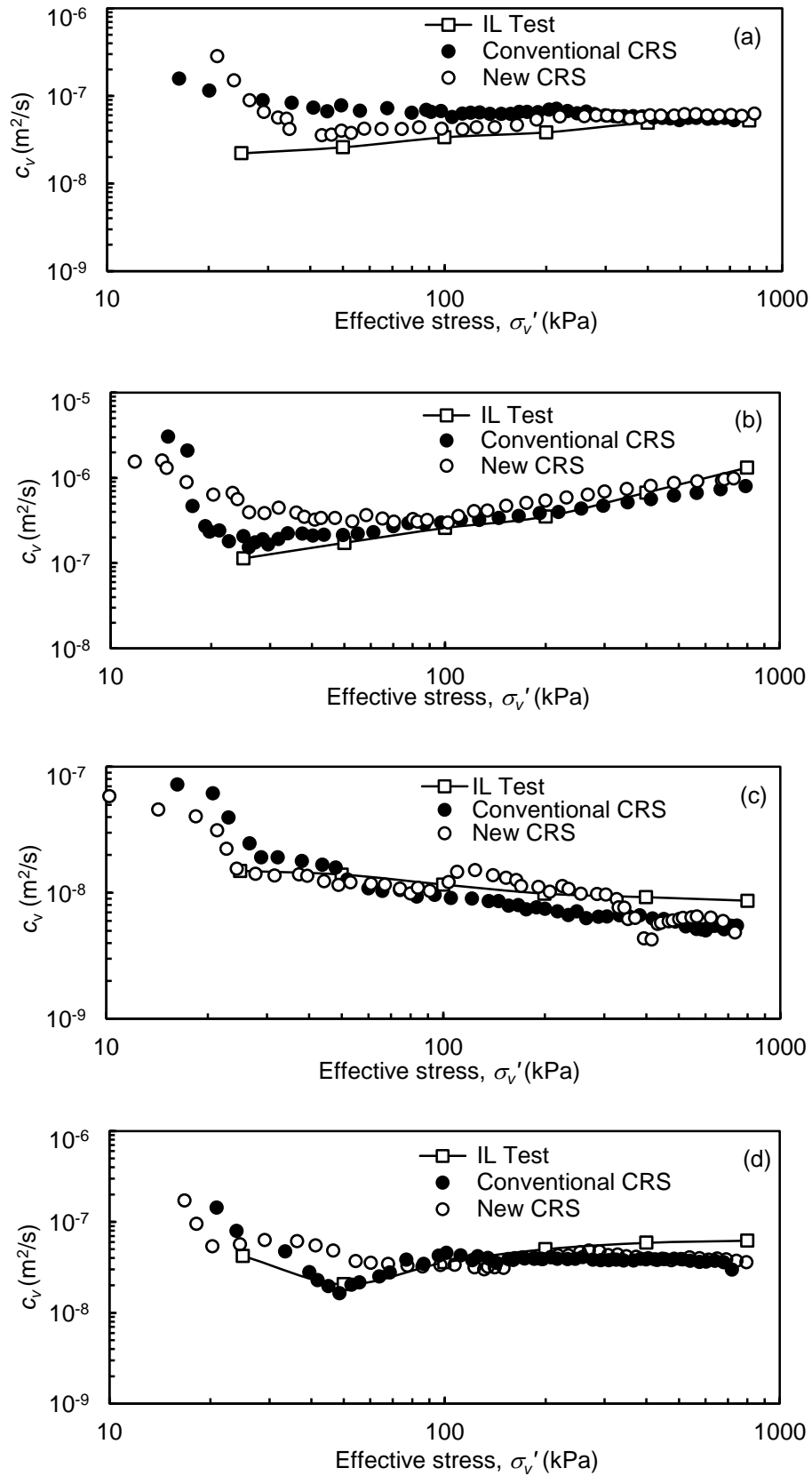


Figure 5.7:  $c_v$ - $\log\sigma'_v$  plot for (a) Red Soil 1 (b) Kaolinite (c) Taramani clay and (d) Bombay marine clay

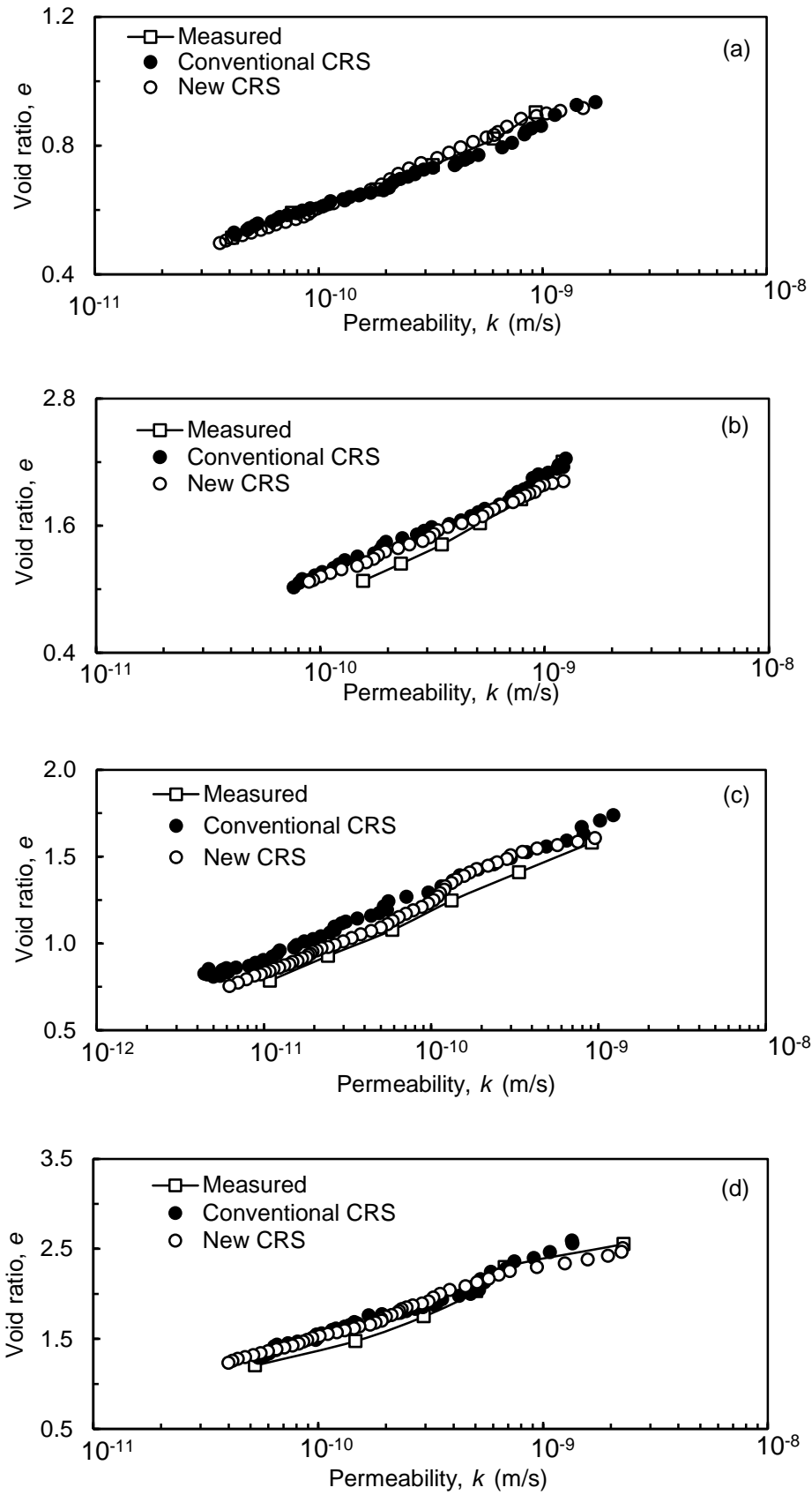


Figure 5.8:  $e$ - $\log k$  plot for (a) Red Soil 1 (b) Kaolinite (c) Taramani clay and (d) Bombay marine clay

### ***Results from undisturbed soils***

The CRS test results obtained for the undisturbed soil sample using the proposed CRS cell were compared with those obtained from the standard CRS cell and the IL test in Figures 5.9 (a-d). Similar to the reconstituted specimens, the results tally well. The values of  $c_c$  and  $c_r$  obtained are listed in Table 5.2, which are comparable. The values of preconsolidation pressure were determined by using the  $\log(1+e)$  versus  $\log\sigma_v'$  method (Sridharan *et al.* 1991). The values obtained from the IL test, standard CRS test and CRS test from the new CRS apparatus are also presented in Table 5.2. The results are highly comparable proving that the proposed CRS consolidation apparatus can be conveniently used to perform CRS tests for determining the consolidation properties of soils.

Table 5.2: Compression index, recompression Index and preconsolidation values of undisturbed Cochin marine clay (19.5 m)

Properties	IL test	Standard CRS	New CRS
Compression index	1.57	1.69	1.70
Recompression index	0.32	0.27	0.27
Preconsolidation pressure	62	65	61

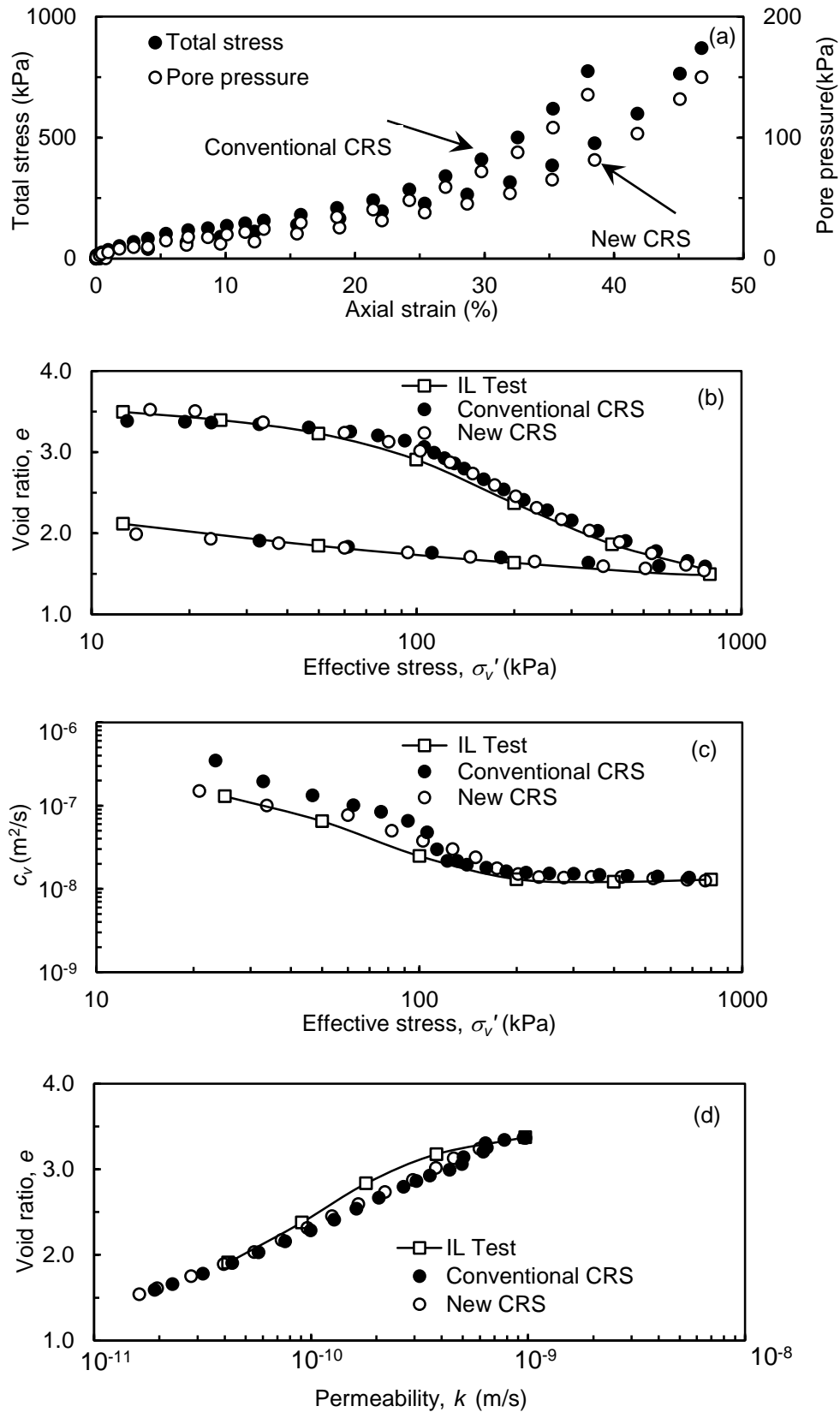


Figure 5.9: (a) Total stress and pore pressure–axial strain plot (b)  $e$ - $\log \sigma_v'$  plot (c)  $c_v$ - $\log \sigma_v'$  plot and (d)  $e$ - $\log k$  plot for the undisturbed Cochin marine clay (19.5 m)

### **5.3 MODIFIED FIXED RING CONSOLIDOMETER TO PERFORM CRS TEST**

The basic components of the CRS cell are similar to a conventional one-dimensional consolidation cell with the difference that a pressure chamber, similar to a triaxial cell chamber is provided to apply back pressure to the soil specimen for saturation. Due to this requirement of back pressure application, a constant pressure system is essential to apply the required back pressure. Though back pressure saturation is ideal to saturate soil specimens within a shorter period of time, the authors believe that overnight soaking of the specimens in a consolidation cell, with double drainage, is sufficient to saturate the specimens as is done in the conventional consolidation testing. This is due to the fact that the thickness of the usual soil specimens for conventional consolidation testing is about 20 mm only. Therefore, the conventional cell with a simple modification to measure the pore water pressure at the base of the soil specimen may be sufficient to carry out a CRS test, without resorting to back pressure application. The details of the modification required in the conventional cell are described in the following sections.

#### **5.3.1 Details of the Modified Consolidation Cell**

Several configurations of conventional one-dimensional consolidation cells (Oedometer cells) are available in the literature. The most common types of one-dimensional consolidation cells in the market are shown in Figure 5.10(a) and (b), which are denoted as Type-1 and Type-2 in the subsequent discussions. Both models are fixed ring type consolidation cells. The following modifications are required to measure the pore water pressure developed at the base of the soil specimen during the CRS consolidation test

- (i) A sealed base to prevent water leakage so that the consolidation takes place under one-way drainage at the top and pore water pressure develops at the base.
- (ii) A drainage line in the base plate to aid de-airing of pore water pressure transducer, allowing water from a burette during saturation stage and for connecting the pore pressure transducer and the sample.
- (iii) Connections for ball valve and pore pressure transducer at the ends of the drainage line.

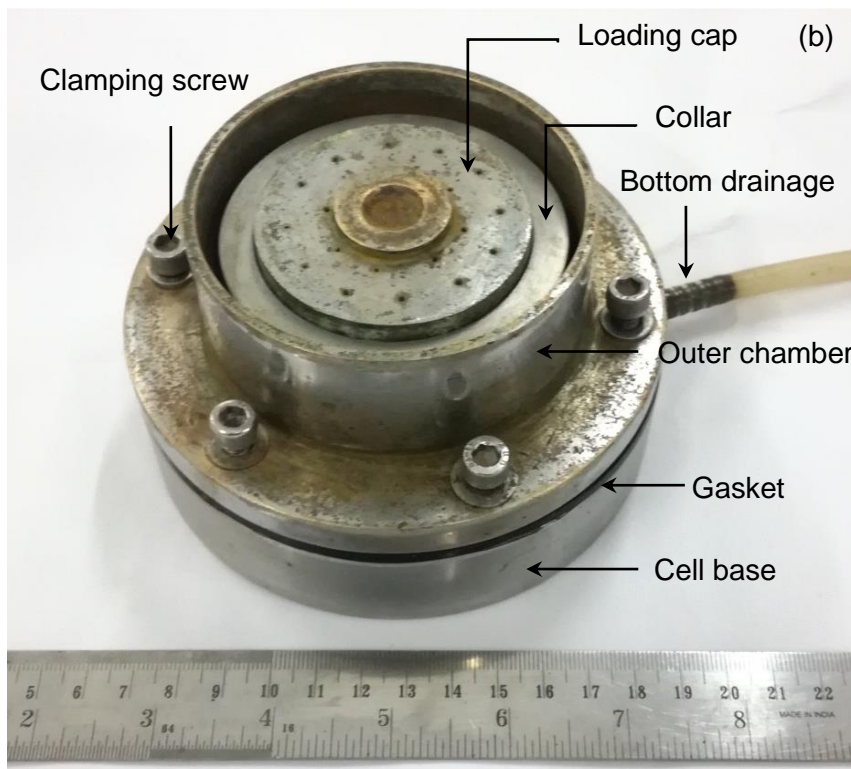
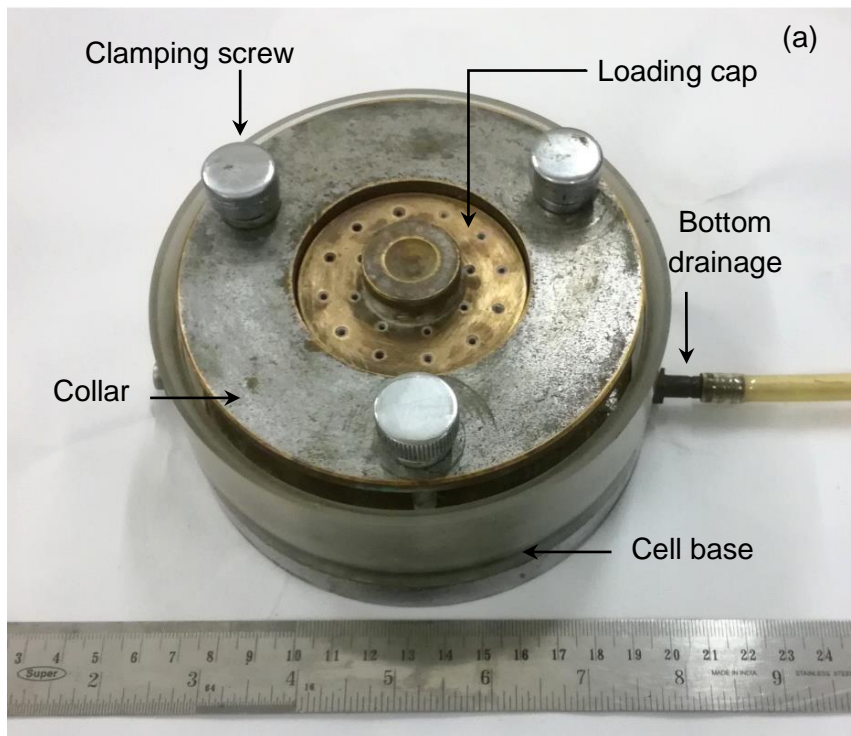


Figure 5.10: Photographs of (a) Type-1 and (b) Type-2 consolidation cells



The modifications can be easily carried out in any mechanical engineering workshop. In the present study, Type-1 consolidation cell, after modification, was used. The schematic illustration of the modifications required is shown in Figure 5.11. The photographic view of the components of the CRS apparatus and the assembled apparatus are shown in Figures 5.12(a) and 5.12(b), respectively. The apparatus was designed to test soil specimens of 60 mm diameter and 20 mm thickness. The cell base is provided with a porous stone at its center for bottom drainage. An O-ring of 66 mm outer diameter and 2 mm thickness is placed in the groove made in the base plate to prevent leakage from the soil specimen. The consolidation ring is pressed over the O-ring by clamping the flange of the collar using the screws. Therefore, no drainage occurs through the base during consolidation. The drainage line extends on either side of the base plate, which will facilitate proper de-airing. One end is connected to the pore pressure transducer while the other to a burette to flush the drainage line. A saturated porous stone is provided on the top of the soil specimen for vertical drainage. A perforated loading cap is placed over the top porous stone for the application of vertical load.

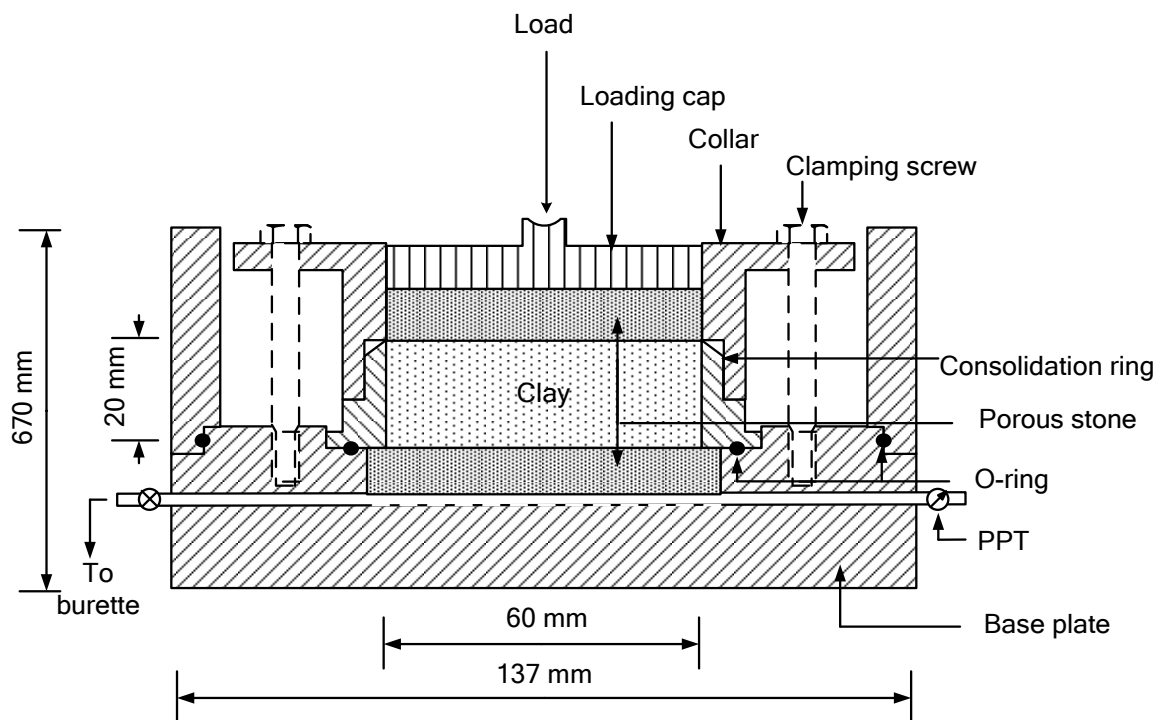


Figure 5.11: Schematic diagram of type-1 consolidation cell after modification

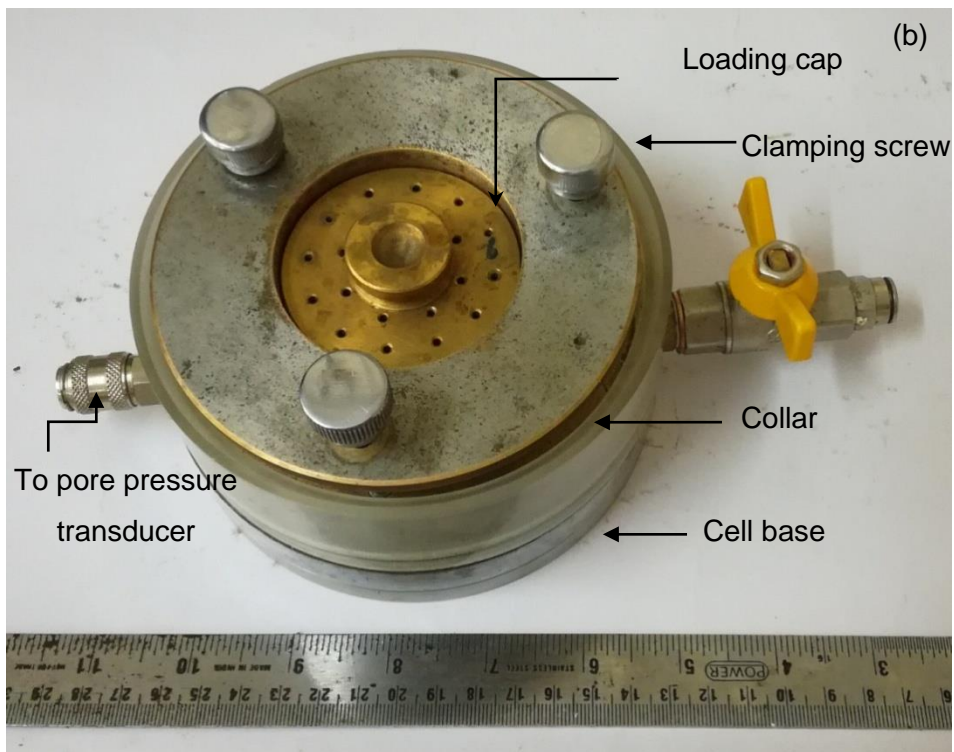
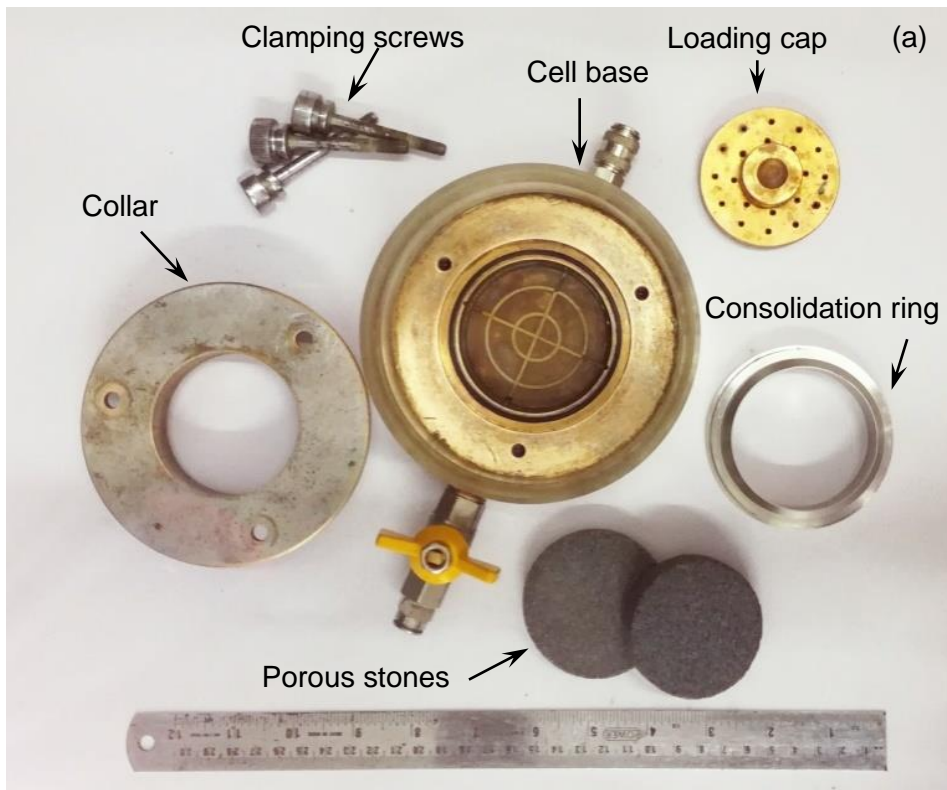


Figure 5.12: Photographic view of (a) components of the proposed CRS apparatus and (b) assembled apparatus

The modifications required in the base plate for Type-2 consolidation cell is schematically shown in Figure 5.13. Very similar to Type-1 consolidation cell, the base is provided with an O-ring to prevent leakage during consolidation and drainage line with provisions for connecting the pore pressure transducer and the burette at the ends. When the outer chamber is clamped to the base, the consolidation ring gets pressed which in turn gets snugly seated over the O-ring. The dimensions marked in the schematic diagrams (Figure 5.11 and 5.13) pertain to consolidation cells for testing 60 mm diameter and 20 mm thickness soil specimens. Consolidation cells of any size can be used, but in the present study consolidation cells for testing 60 mm diameter and 20 mm thick soil specimens are used.

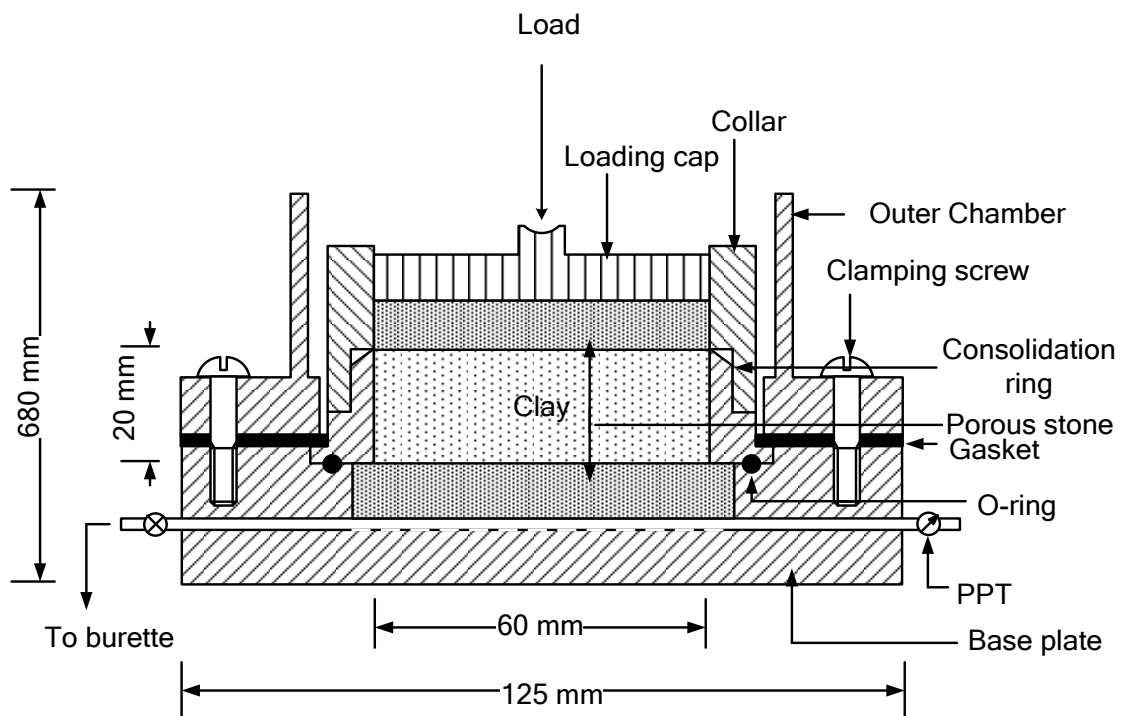


Figure 5.13: Schematic diagram of type-2 consolidation cell after modification

### 5.3.2 Experimental Programme

Four reconstituted and one undisturbed soil samples were used to validate modified conventional cell to perform CRS test. The reconstituted samples used are Red soil 1, commercially available Kaolinite, Taramani clay and Bombay marine clay. Cochin marine clay sampled at depth of 19.5 m was selected as the undisturbed sample. The basic characterization was already explained in chapter 3 (Table 3.1). Two identical soil

specimens were prepared, one for the IL consolidation test and other for CRS consolidation test using the modified consolidation apparatus. The CRS test was conducted as per ASTM D4186-12 (2012), with the exception that back pressure was not applied.

As the pore water pressure is measured at the base of the soil specimen, the bottom drainage line needs to be properly de-aired. This was achieved by flushing the cell base with de-aired water. Once the flushing of drainage line and the pore water pressure transducer were done, a filter paper was placed over the bottom porous stone. The consolidation ring with the soil specimen was placed in the modified oedometer cell base. After placing the top filter paper, the top porous stone was placed in contact with the filter paper. The loading cap was then placed over the top porous stone and the set-up was assembled as shown in Figure 5.12(b). As the back pressure was not applied, the saturation of the soil specimen was done by soaking the specimen in water. The assembled set-up was placed in the conventional consolidation loading frame and a seating pressure of 12.5 kPa was applied. Water was poured into the cell so that the top of the soil specimen was in contact with water. In order to saturate the soil specimen from the top surface, water was poured into the consolidation cell. As the bottom of the consolidation ring is sealed with an O-ring, the water from the cell will not be in contact with the base of the soil specimen. Therefore, to saturate the soil specimen from the bottom surface, in addition to the top, a burette filled with water was connected to the bottom drainage line. Therefore, saturation can take place from both the top and bottom surfaces. The change in thickness of the soil specimen during saturation process was monitored. Once no further change in the thickness of the soil specimen was noted, it was assumed that the soil specimen was saturated. Overnight soaking is generally sufficient to saturate most of the field specimens of 20 mm thickness. However, some unsaturated soil specimens may take more time up to 24 hours.

The consolidation cell was then placed on the triaxial loading frame (Figure 5.14). The deformation rate was fixed such that the developed pore water pressure ratio (defined as the ratio of base excess pore water pressure to the axial stress) was within the limit of 0.03-0.15 (ASTM D4186-12 (2012)). The deformation rates used for Red soil 1, Kaolinite, Taramani clay and Bombay marine clay were 0.6, 6.0, 0.3 and 0.9 %/hour, respectively. These rates were arrived based on permeability measurements and

preliminary CRS tests. For the undisturbed soil specimen, a rate of 1.5%/hour was used. The strain rate was not controlled during the test as objective was to evaluate the performance of the apparatus with IL test. During the test, the axial force, axial deformation and the pore water pressure at the base of the soil specimens were recorded continuously using a data logger. After reaching the required axial force, the specimen was unloaded at one-half of the rate used for loading, to a minimum seating pressure of 12.5 kPa. The final water content and the final thickness of the soil specimens were measured after the completion of the test. The CRS test data were analysed as per ASTM D4186-12 (2012) for determining the consolidation parameters. The results obtained from the CRS tests are discussed in the next section.

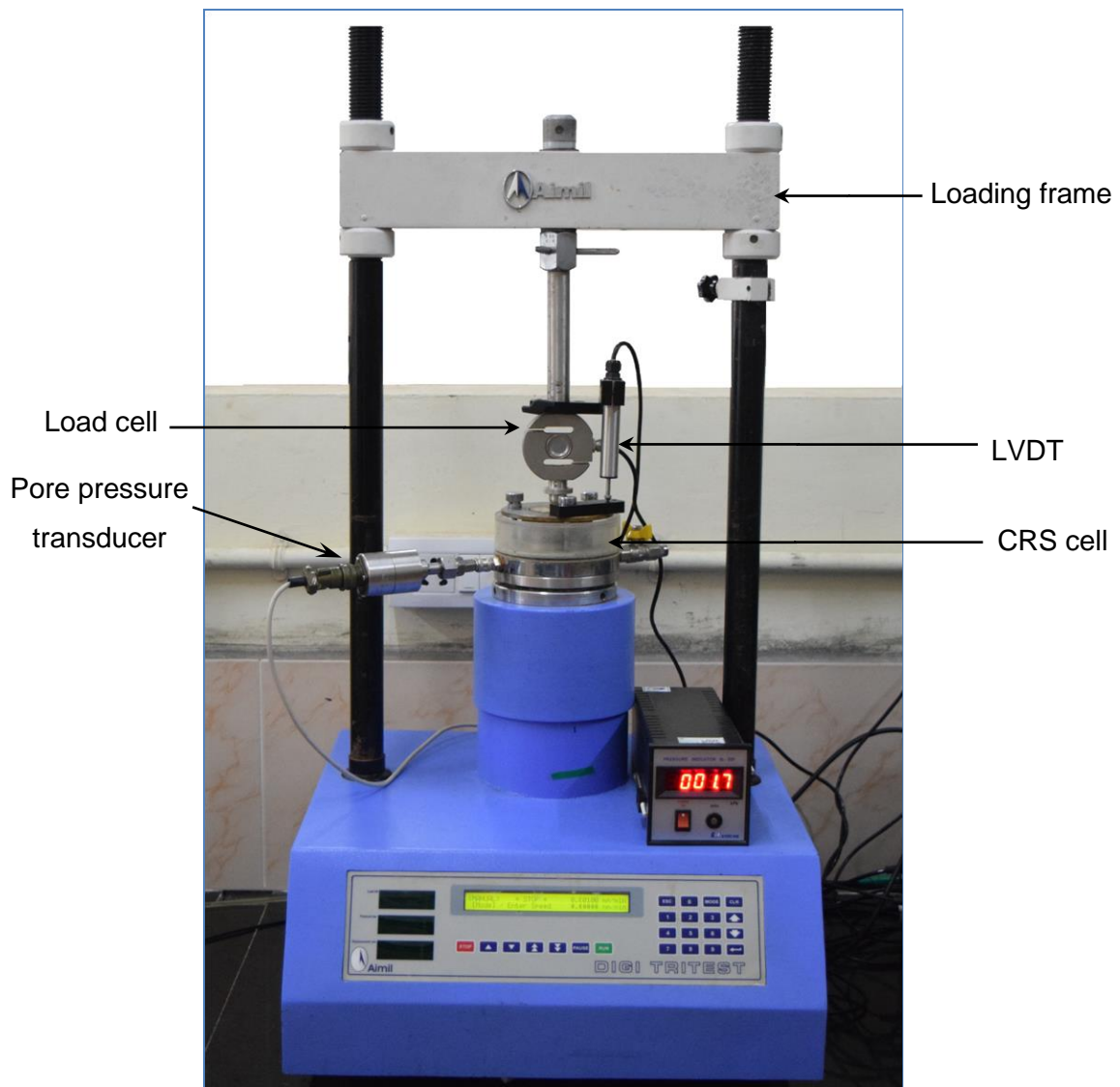


Figure 5.14: Modified consolidation cell for CRS test assembled in the triaxial loading frame

### 5.3.3 Results and Discussions

The variation of total stress and the pore water pressure with axial strain obtained from the CRS test using the modified apparatus are shown in Figures 5.15(a-d) for the reconstituted soil specimens of Red soil 1, Kaolinite, Taramani clay and Bombay marine clay, respectively. The results clearly show that pore water pressure gets developed at the base of the soil specimens, even without the application of back pressure. The variation of pore pressure ratio with effective stress is presented in Figure 5.16 for all the soil specimens tested. For the Bombay marine clay, the pore water pressure ratio is slightly higher than 0.15 at the start of the test corresponding to a consolidation pressure of about 12.5 kPa and for the kaolin clay the pore water pressure ratio is marginally lower than 0.03 towards the end of the test corresponding to a consolidation pressure of about 800 kPa. However, the pore water pressure ratio lies within the range of 0.03 to 0.15 over a wide range of effective stress values for all the soils used.

The consolidation parameters obtained for the reconstituted soil specimens from the CRS test using the proposed modified consolidation cell were compared with the conventional IL consolidation test. The void ratio ( $e$ )-effective consolidation pressure ( $\sigma_v'$ ) plot from the CRS test and IL test are shown in Figures 5.17(a-d), for all the reconstituted soils tested. The results match very well. The compression index ( $c_c$ ) and the recompression index ( $c_r$ ) values obtained from the  $e$ -log  $\sigma_v'$  plots are listed in Table 5.3. It can be observed that the  $c_c$  and  $c_r$  obtained from the CRS test compare very well with the IL consolidation test. The coefficient of variance in  $c_c$  and  $c_r$  are 4% and 15%, respectively.

The other important parameter derived from one-dimensional consolidation test is the coefficient of consolidation ( $c_v$ ). Taylor's  $\sqrt{t}$  method (Taylor, 1942) was used to determine  $c_v$  from the IL consolidation test in the present study. The values of,  $c_v$  obtained from the CRS test and IL test are shown in Figures 5.18 (a)-(d). It can be observed that the  $c_v$  values obtained from the CRS test matches reasonably well with the IL consolidation test. With reference to IL test, the average COV of  $c_v$  is 36%, which is acceptable in case of  $c_v$  (Sridharan *et al.* 1994).

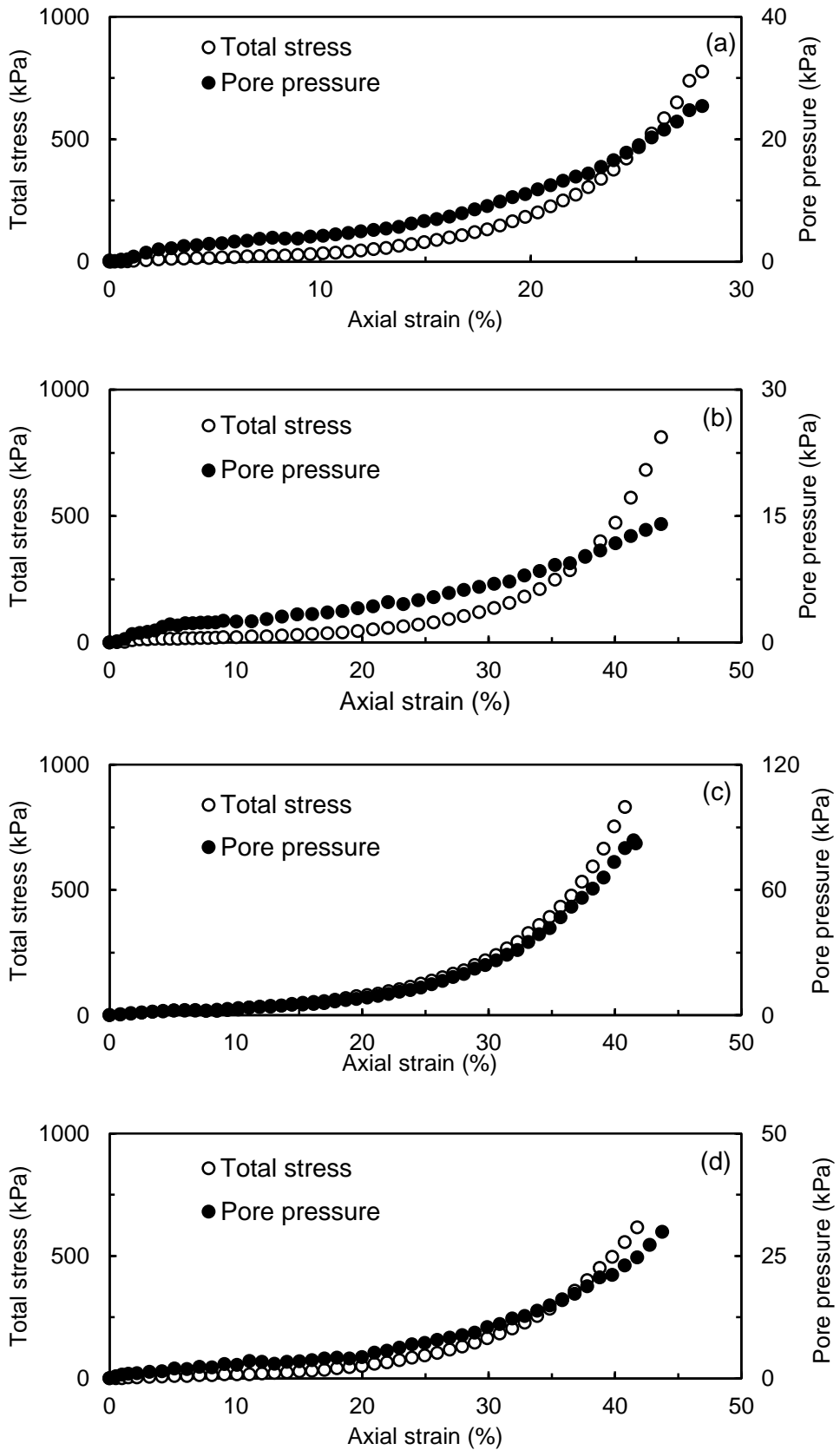


Figure 5.15: Total stress and pore pressure –axial strain plot for reconstituted specimens of (a) Red Soil 1 (b) Kaolinite (c) Taramani clay and (d) Bombay marine clay

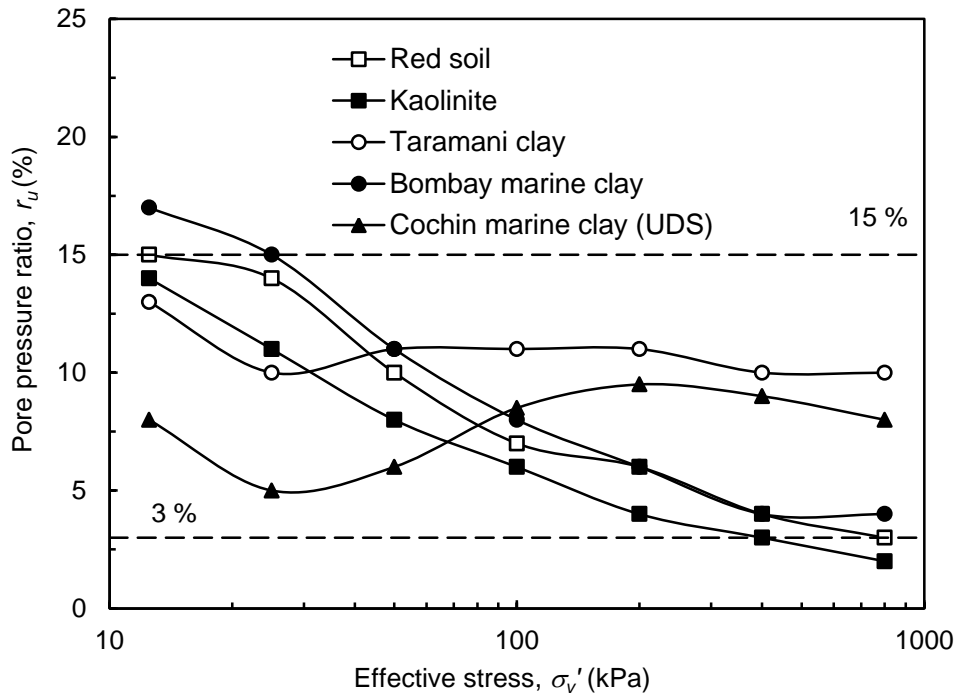


Figure 5.16: Pore pressure ratio versus effective stress

Table 5.3: Comparison of compression index and recompression index values

Sl. No.	Soils	Compression Index ( $c_c$ )		Recompression Index ( $c_r$ )	
		IL Test	CRS Test	IL Test	CRS Test
1	Red soil	0.26	0.25	0.03	0.03
2	Kaolinite	0.69	0.68	0.09	0.06
3	Taramani clay	0.55	0.58	0.10	0.13
4	Bombay marine clay	0.78	0.73	0.18	0.18

The value of coefficient of permeability ( $k$ ) is measured by falling head method during conventional IL test after each increment of load. The variation of coefficient of permeability ( $k$ ), with void ratio from CRS test and the calculated coefficient of permeability from IL consolidation test are shown in Figures 5.19(a)-(d) for the four reconstituted soil samples. The average COV of  $k$  with reference to IL test is 35%. The values match very well lending support to the validity of the proposed modified consolidometer for evaluating the consolidation parameters by conducting CRS test.



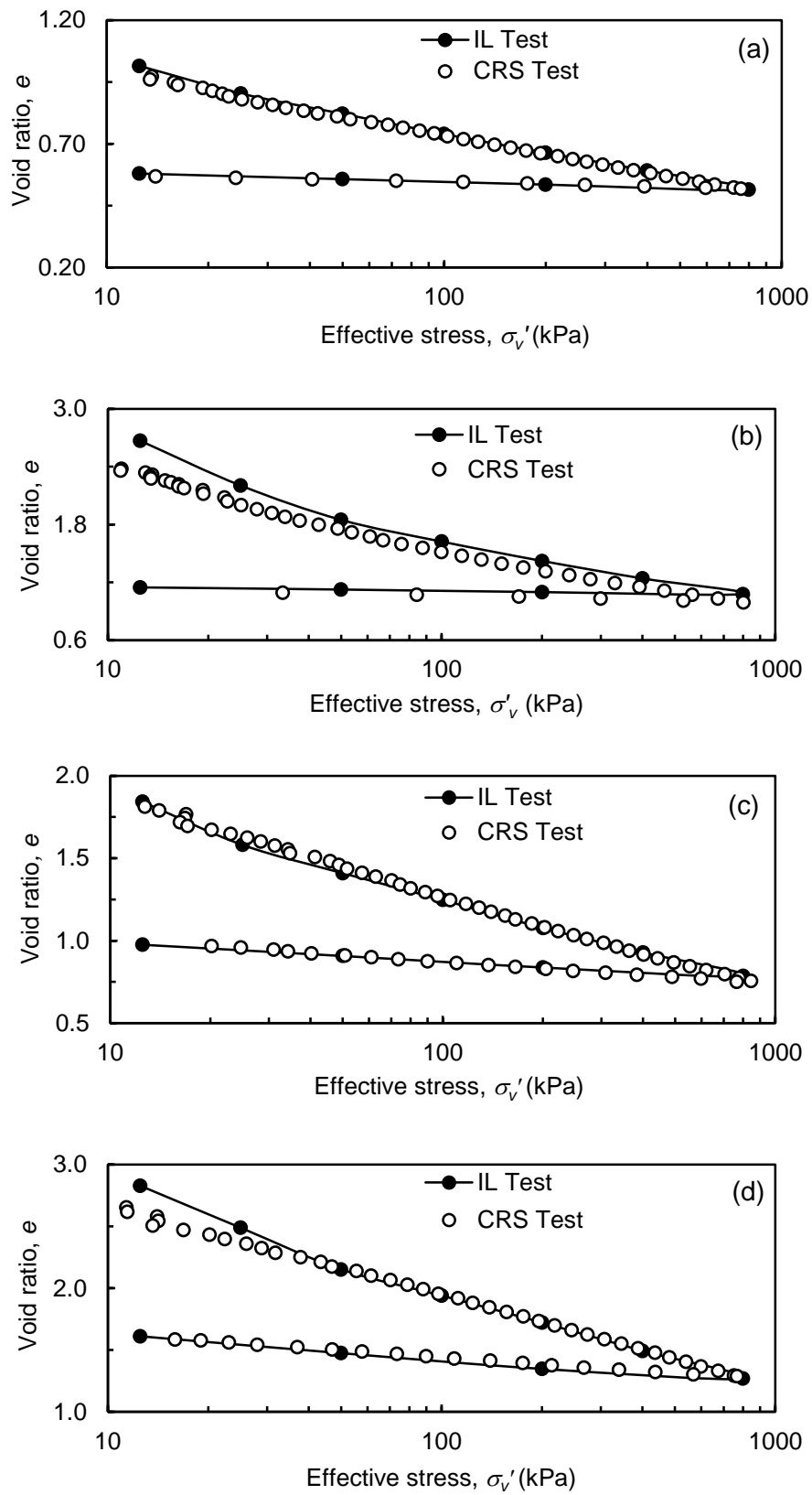


Figure 5.17:  $e$ - $\log \sigma'_v$  plot for (a) Red Soil 1 (b) Kaolinite (c) Taramani clay and (d) Bombay marine clay

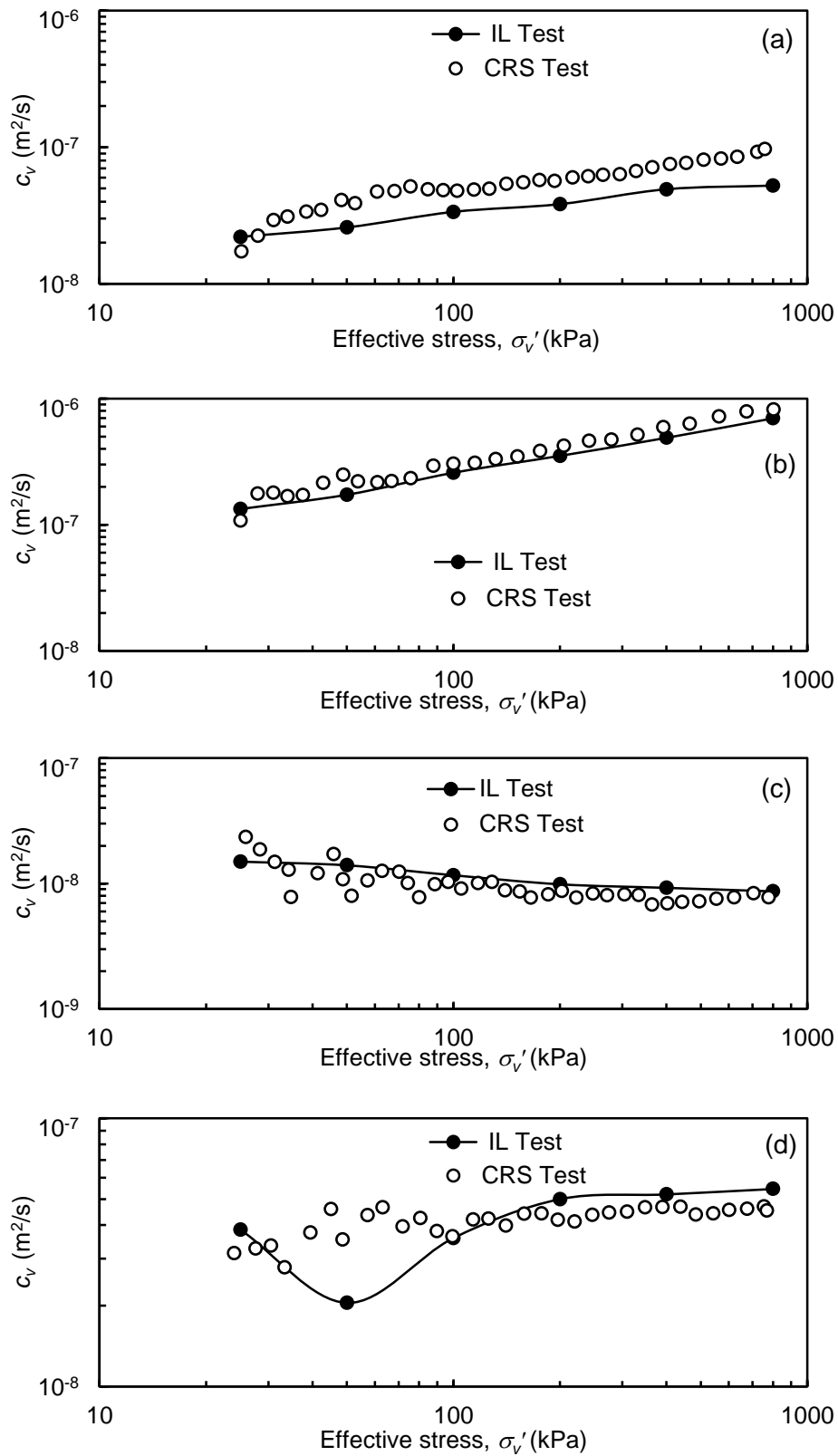


Figure 5.18:  $c_v$ - $\log\sigma'_v$  plot for (a) Red Soil 1 (b) Kaolinite (c) Taramani clay and (d) Bombay marine clay

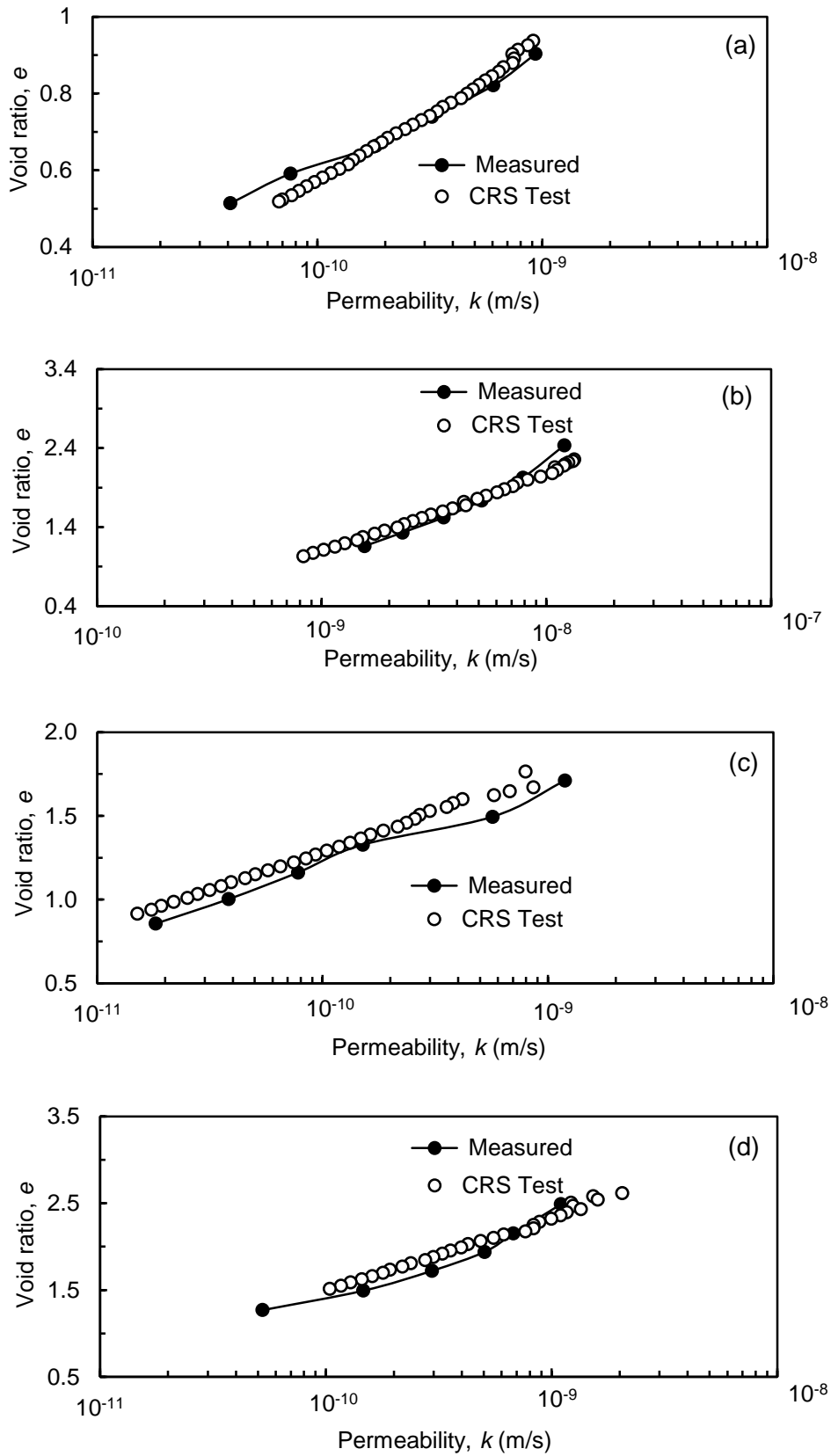


Figure 5.19:  $e$ -log  $k$  plot for (a) Red Soil 1 (b) Kaolinite (c) Taramani clay and (d) Bombay marine clay

Similarly, the CRS test results obtained for the undisturbed soil specimen (Cochin marine clay at a depth of 19.5 m) using the modified consolidometer were compared with the conventional IL test results in Figures 5.20 (a-d). Similar to the reconstituted specimens, the CRS test results compare very well with the IL consolidation test results, for the UDS soil specimen as well. The values of the compression index and the recompression index obtained are listed in Table 5.4, which are highly comparable. Considering the effective unit weight of Cochin Marine Clay as  $4.3 \text{ kN/m}^3$ , the effective overburden pressure at the depth of sampling is 84 kPa. The preconsolidation pressure ( $\sigma_c'$ ) was determined using the  $\log(1+e)$  versus  $\log \sigma_v'$  method (Sridharan *et al.* 1991). The values of  $\sigma_c'$  obtained from the CRS test and IL test are also given Table 5.4. These results validate the modified conventional consolidation cell to perform CRS test.

Table 5.4: Compression index, recompression Index and preconsolidation values of undisturbed Cochin marine clay (19.5 m)

Properties	IL test	Standard CRS
Compression index	1.214	1.251
Recompression index	0.22	0.23
Preconsolidation pressure	85	80

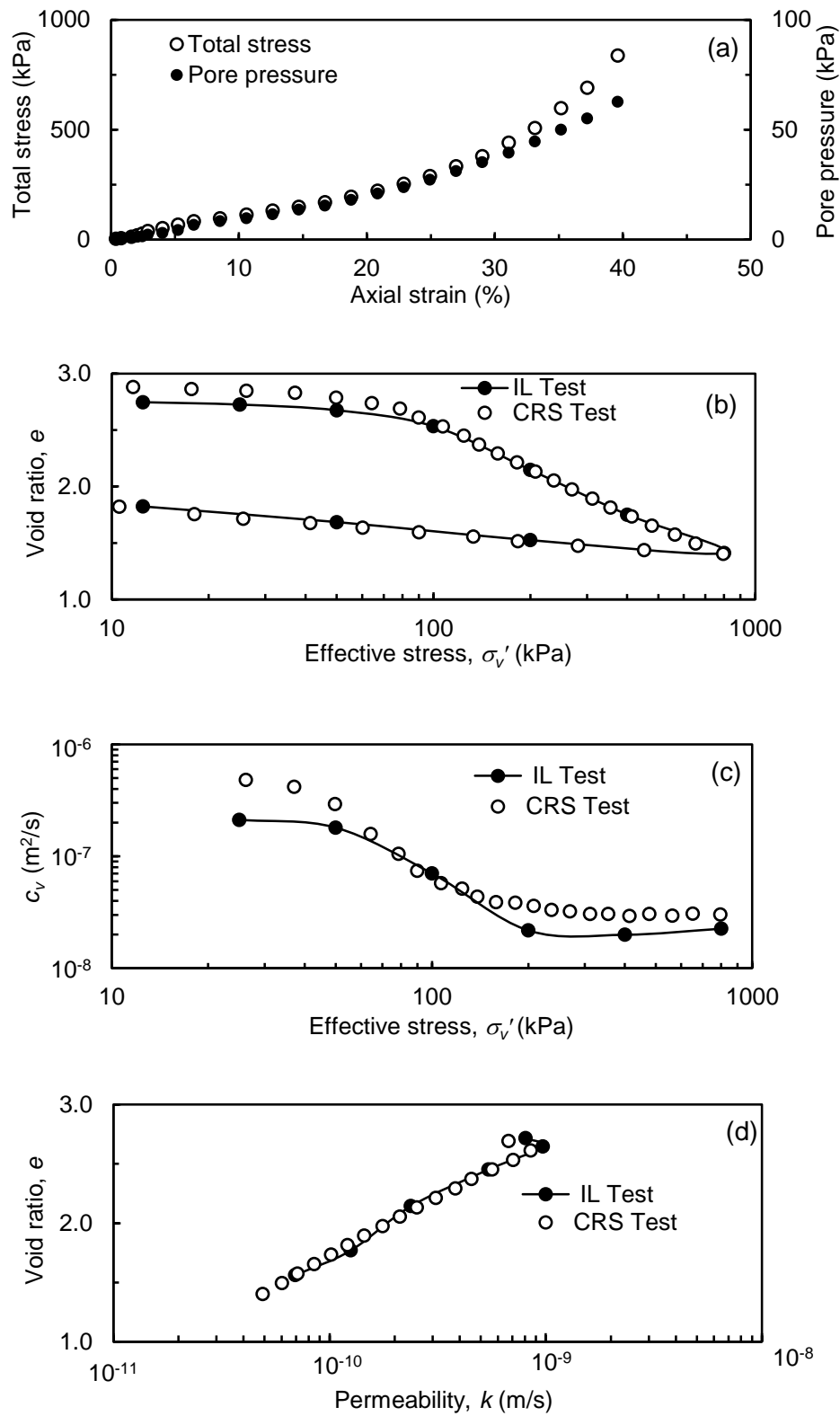


Figure 5.20: (a) Total stress and pore pressure –axial strain plot (b)  $e$ - $\log \sigma'_v$  plot (c)  $c_v$ - $\log \sigma'_v$  plot and (d)  $e$ - $\log k$  plot for the undisturbed Cochin marine clay

## 5.4 SUMMARY

In this chapter, two apparatus that were developed to perform CRS test were described. The first apparatus is a simplified CRS apparatus. The pressure chamber in the standard CRS apparatus (ASTM D4186-12 (2012)) was removed and the back pressure is directly applied through a piston type loading cap. The excess pore water pressure developed during the consolidation test can be measured at the base of the specimen. The apparatus configuration is very simple and can be easily fabricated in any mechanical engineering workshop. The performance of the apparatus was validated by carrying out CRS consolidation tests on four reconstituted soil specimens of varying plasticity characteristics and on one undisturbed soil. The results from the proposed apparatus were compared with those obtained from the consolidation tests conducted using the conventional incremental loading (IL) oedometer apparatus and CRS test using standard CRS apparatus. The test results prove that the proposed simplified CRS consolidation apparatus can be conveniently used to perform CRS tests for determining the consolidation properties of soils.

The other apparatus was the modified form of the conventional fixed ring consolidation cell to perform Constant Rate of Strain (CRS) consolidation test. The proposed CRS apparatus is similar to the conventional oedometer cell except that an extra drainage line is provided in the base of consolidation cell to connect a pore pressure transducer for measuring pore water pressure at the base of the soil specimen and a burette to de-air in addition to an O-ring to seal the base. Detailed description about the modifications required in the commonly available conventional consolidation cells is presented in this chapter. The modified consolidometer was validated by performing CRS consolidation tests on four reconstituted soil specimens and one undisturbed soil specimen. The test results were compared with incremental loading (IL) consolidation test results conducted on identical soil specimens. The test results prove that the conventional consolidation cell is very well suited after simple modification for performing CRS tests to determine the consolidation properties of soils.

## CHAPTER 6

# STRESS CONTROLLED TEST WITH PORE PRESSURE MEASUREMENTS

### 6.1 INTRODUCTION

As discussed in the literature review chapter (Chapter 2), constant rate of strain (CRS) consolidation test, currently called as CSL consolidation test in ASTM D4186-12 (2012), is one of the widely used strain controlled consolidation tests. CSL test gained popularity mainly because of the faster rate of testing compared to IL test with 24 hours loading duration between successive load increments. In addition, several data points can be gathered to plot the  $e$ - $\log \sigma_v'$  plot, which facilitates better estimation of preconsolidation pressure. However, low permeable soils will take long time to complete the test, as discussed in section 2.4.5 and 4.4.2. Hence, in the present study, it is attempted to develop a faster stress controlled consolidation testing procedure with pore pressure measurements, where duration of increment of load is controlled by the dissipation of excess pore pressure and allowed only to pore pressure ratio ( $r_u$ ) of 15% of the total stress. Detailed experimental programme was devised to validate the proposed methodology. The experimental methodology and the results obtained are discussed in this chapter.

### 6.2 THEORETICAL CONSIDERATIONS

During the stress controlled test with pore pressure measurement, the pore pressure developed in the specimen is allowed to dissipate only through the top. When the excess pore pressure at the base dissipates to 15% of the total stress applied (which is the maximum allowable pore pressure in a CRS test) for each increment of loading and unloading the next increment is applied. Hence, by assuming the pore pressure distribution is parabolic within the specimen, the average effective stress for each increment is determined using the measured base pore water pressure ( $u_b$ ) as follows:

$$\sigma_v' = \sigma_v - \frac{2}{3}u_b \quad (6.1)$$

where,  $\sigma_v$  is the applied total stress. As the base pore pressure is 15% of the total stress applied at the end of each increment, Eq. (6.1) can be simplified as:

$$\sigma_v' = \frac{9}{10}\sigma_v \quad (6.2)$$

Coefficient of consolidation can be determined by knowing the time ( $t_{0.15\sigma_v}$ ) required for the dissipation of pore pressure to  $r_u = 0.15$  from the equation:

$$c_v = \frac{(T_v)_{0.15\sigma_v} d^2}{t_{0.15\sigma_v}} \quad (6.3)$$

where,  $d$  is the length of drainage path.  $(T_v)_{0.15\sigma_v}$  is the time factor corresponding the  $t_{0.15\sigma_v}$ . As the base pore pressure ( $u_b$ ) was continuously monitored during the test, the degree of dissipation at the base of the specimen can be obtained as

$$U_b = 1 - \frac{u_b}{u_0} \quad (6.4)$$

where,  $u_0$  is the initial pore pressure, which is the sum of the current pressure increment ( $\Delta\sigma_{vi}$ ) and the average undissipated excess pore pressure in the previous increment ( $u_{ri}$ ), which is given by

$$u_0 = \Delta\sigma_{vi} + u_{ri} \quad (6.5)$$

The base pore pressure at any time  $t$  can be obtained using Terzaghi's theory as:

$$u_b = \sum_{m=0}^{m=\infty} \frac{2u_0}{M} \sin M \exp(-M^2 T_v) \quad (6.6)$$



Hence, by knowing the degree of dissipation ( $U_b$ ), the corresponding time factor ( $T_v$ ) can be obtained using Eq. (6.7) based on Terzaghi's theory of one-dimensional consolidation as:

$$U_b = 1 - \sum_{n=0}^{n=\infty} \frac{2}{M} \sin M \exp(-M^2 T_v) \quad (6.7)$$

where,  $M = \frac{(2m+1)\pi}{2}$

The average degree of consolidation ( $U$ ) and time factor ( $T_v$ ) are related as:

$$U = 1 - \sum_{n=0}^{n=\infty} \frac{2}{M^2} \exp(-M^2 T_v) \quad (6.8)$$

The variation of  $U_b$  and  $U$  are shown in Figure 6.1.

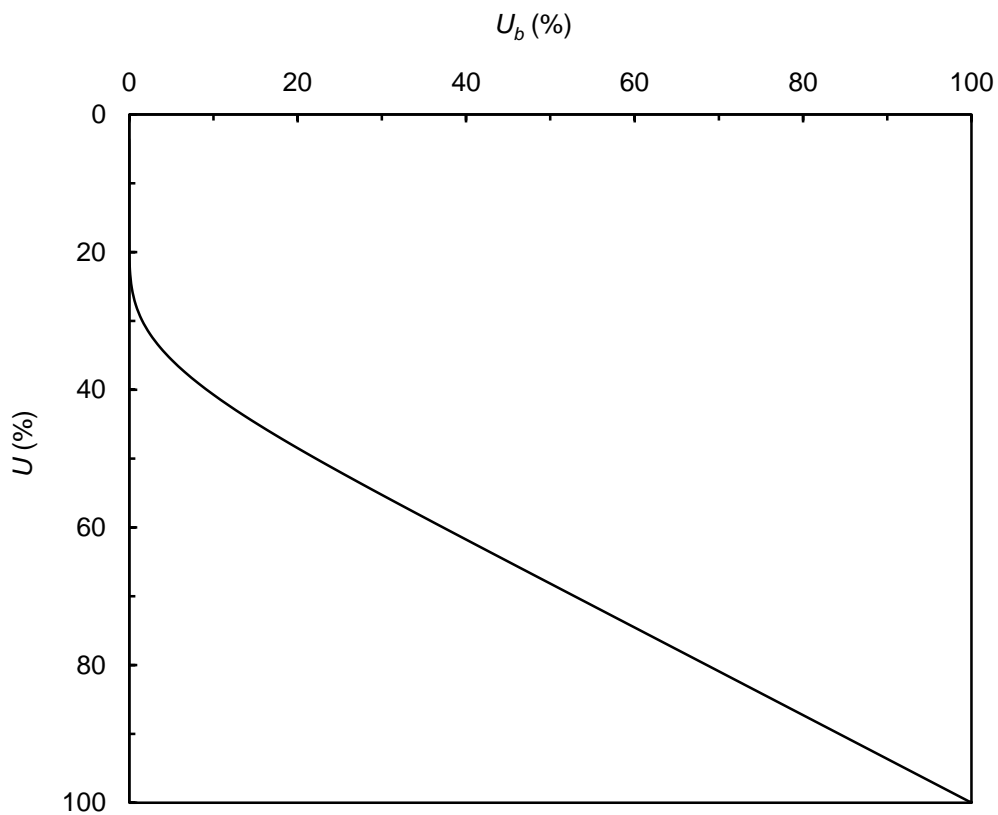


Figure 6.1 Variation of degree of dissipation with degree of consolidation

For  $r_u = 0.15$ , the degree of dissipation ( $U_b$ ), time factor  $(T_v)_{0.15\sigma_v}$  and the degree of consolidation ( $U$ ) are given in Table 6.1. It can be seen that the average degree of consolidation for  $r_u = 0.15$  is 83% except for the first increment, which is 81% and the corresponding time factor ( $T_v$ ) for each incremental load is also given in Table 6.1.

Table 6.1: Typical calculation of effective stress and average degree of consolidation

Stage	Total stress, $\sigma_v$ (kPa)	Stress increment, $\Delta\sigma_v$ (kPa)	Base PwP, $u_b$ (kPa)	Initial PwP, $u_0$ (kPa)	Effective stress, $\sigma_v'$ (kPa)	$U_b$ (%)	$U$ (%)	$T_v$
Loading	12.5	12.5	0.00	12.5	12.5	--	--	--
	25	12.5	3.75	12.5	22.5	70.0	80.9	0.586
	50	25	7.5	27.5	45	72.7	82.6	0.624
	100	50	15.0	55	90	72.7	82.6	0.624
	200	100	30.0	110	180	72.7	82.6	0.624
	400	200	60.0	220	360	72.7	82.6	0.624
	800	400	120.0	440	720	72.7	82.6	0.624
Unloading	200	-600	-30	-520	220	94.2	--	--
	50	-150	-7.5	-170	55	95.6	--	--
	12.5	-37.5	-1.875	-32.5	13.75	95.6	--	--

Note: PwP- Pore water pressure,  $U_b$ - Degree of dissipation,  $U$ - Average degree of consolidation

### 6.3 EXPERIMENTAL PROGRAMME

Seven reconstituted soils and three undisturbed soils were used to validate the proposed methodology. The reconstituted soils were Red soil 1, Red soil 2, Gummudipoondi clay, Kaolinite, Taramani clay, Siruseri clay and Bombay marine clay. The undisturbed soil (UDS) samples were marine clays collected from Cochin and Bombay, India. The Cochin marine clay samples were sampled at depths of 19.5 m and 5 m. The Bombay marine clay was sampled at depth of 12 m. The basic characterization of the selected soils were done as per the relevant Indian standards and are summarised in Chapter 3 (Section 3.3).

The specimen preparation technique is the same as that explained in Chapter 3. The reconstituted specimens were prepared under a consolidation pressure of 12.5 kPa and are considered as normally consolidated soil. The overconsolidated (OC) specimens were prepared by consolidating them to known preconsolidation pressure. Three reconstituted soils such as Gummudipoondi clay, Kaolinite and Taramani clay were selected for preparing OC soils of known preconsolidation pressure. Preconsolidation pressure adopted for Gummudipoondi clay, Kaolinite and Taramani clay are 200 kPa, 100 kPa and 50 kPa, respectively. The required preconsolidation pressure was applied in steps and once the consolidation was over, it was unloaded to a seating pressure of 12.5 kPa in steps and allowed sufficient time for swelling. Undisturbed soil specimens were directly trimmed into the consolidation ring. Three identical specimens were prepared from each reconstituted and undisturbed soils for carrying out the experiments.

Conventional incremental loading (IL) consolidation test was performed as control test on one of the specimens. The incremental load was maintained for 24 hours and the time-settlement data were recorded throughout the loading period. The results obtained from IL test with 24 hours duration were discussed in Chapter 3. One of the other specimens was subjected to controlled strain loading (CSL) consolidation test, where the strain rate was fixed as per the proposed methodology discussed in Chapter 4. The other specimen was subjected to the proposed methodology. The proposed stress controlled test requires pore pressure for computing average effective stress. Therefore, accurate measurement of pore pressure is essential during the consolidation tests. This can be achieved by applying back pressure to the specimen. Therefore, consolidation cell with provision for measuring pore pressure and application of back pressure are essential. A consolidation cell, similar to CRS cell was designed and fabricated. Figure 6.2 shows the schematic diagram of the cell. The components of consolidation cell are shown in Figure 6.3(a) and the assembled set-up is shown in Figure 6.3(b). The cell was designed to a small size, so that it can be accommodated in the conventional consolidation loading frame, as the test is a stress controlled test. The conventional loading frame was suitably modified, by raising the connecting rods in the consolidation apparatus as shown in Figure 6.3(c). A pore pressure transducer (PPT) and LVDT were connected to a data logging unit to record the pore pressure and settlement data, respectively.

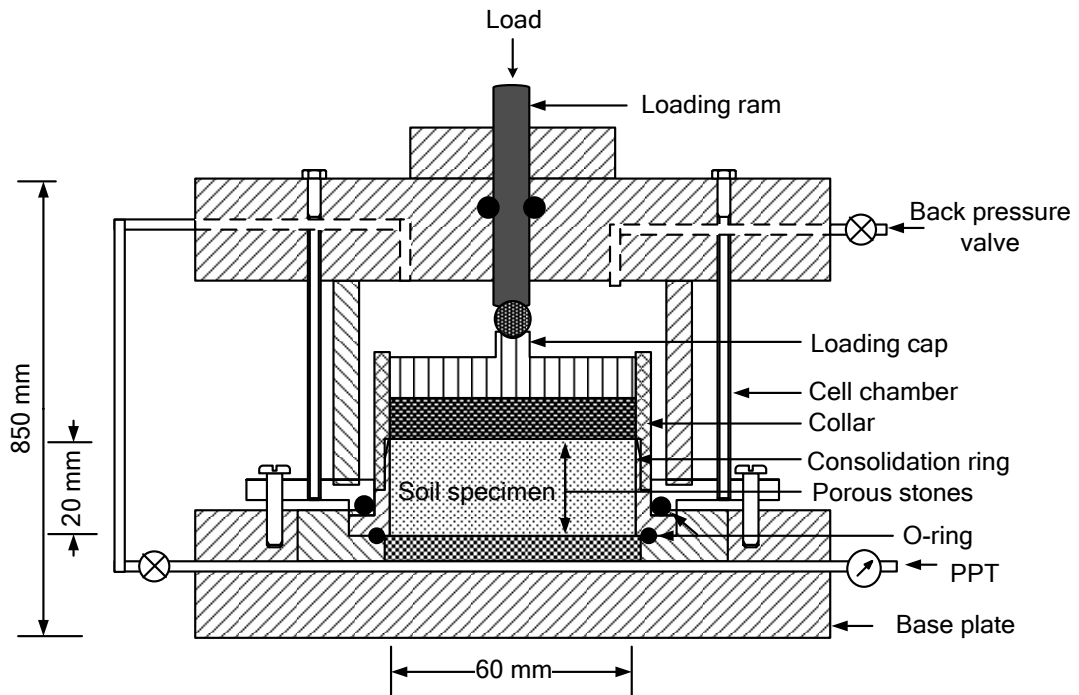


Figure 6.2: Schematic diagram of the cell

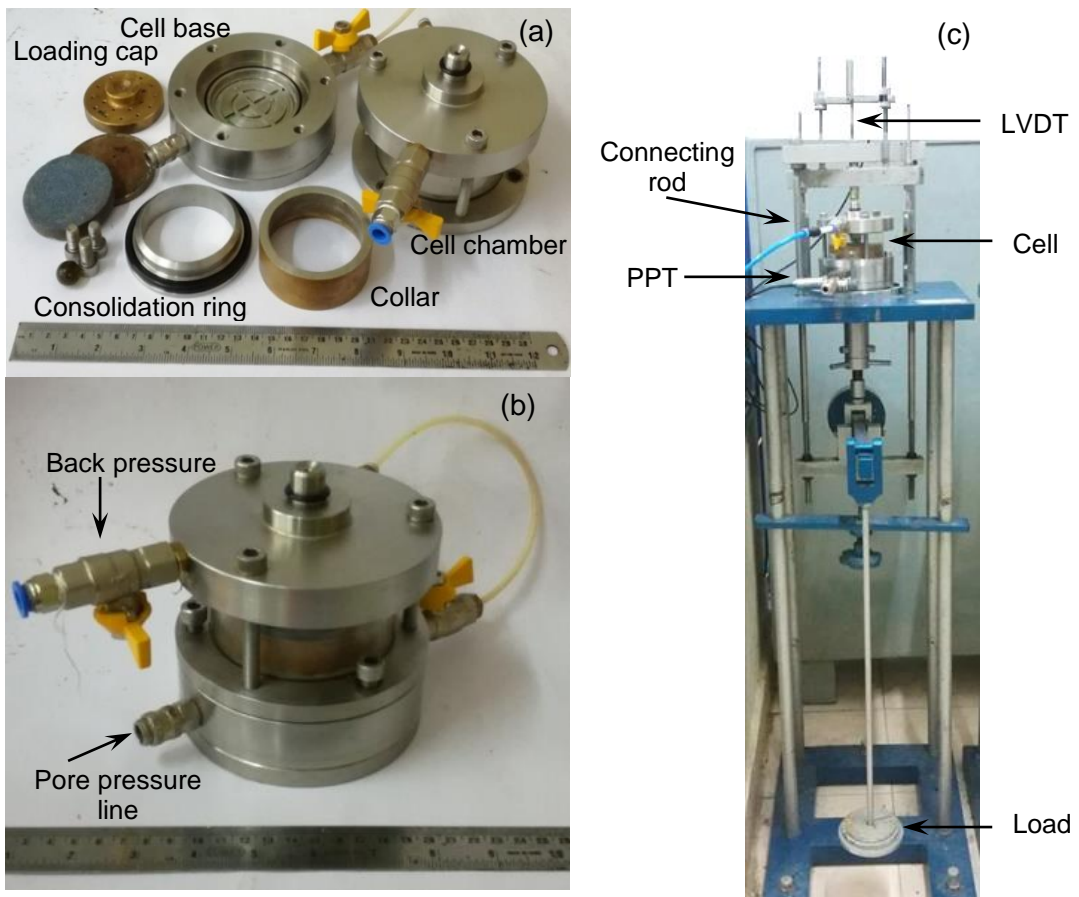


Figure 6.3: (a) Components of the cell (b) Assembled cell and (c) Complete set-up

The test is similar to the conventional incremental loading (IL) consolidation test, with the exception that the test is drained through the top so that the pore pressure developed at the base can be measured. The duration of load under each increment was controlled by the dissipation of pore pressure, which is allowed up to 15% of total stress. Similarly, the unloading stages are controlled based on the dissipation of negative pore pressure. A minimum back pressure of 200 kPa was applied to saturate the specimen and also to measure the negative pore pressure accurately. The results from the proposed method are compared with IL test with 24 hours duration with CSL consolidation test, so as to understand the reduction in the duration of test.

#### 6.4 RESULTS AND DISCUSSIONS

The proposed testing procedure was validated using seven reconstituted soils with varying plasticity characteristics and three undisturbed soil samples. Typical plot of time-pore pressure at the base of the specimen of Gummudipoondi clay for the pressure range of 100-200 kPa is shown in Figure 6.4 along with the theoretical curve. The theoretical time-pore pressure distribution is plotted using Terzaghi's theory of one-dimensional consolidation. The theoretical curve is obtained by assuming that the initial pore pressure developed at time,  $t = 0$  is equal to the sum of the applied increment of stress and the average residual pore pressure in Eq. (6.6).

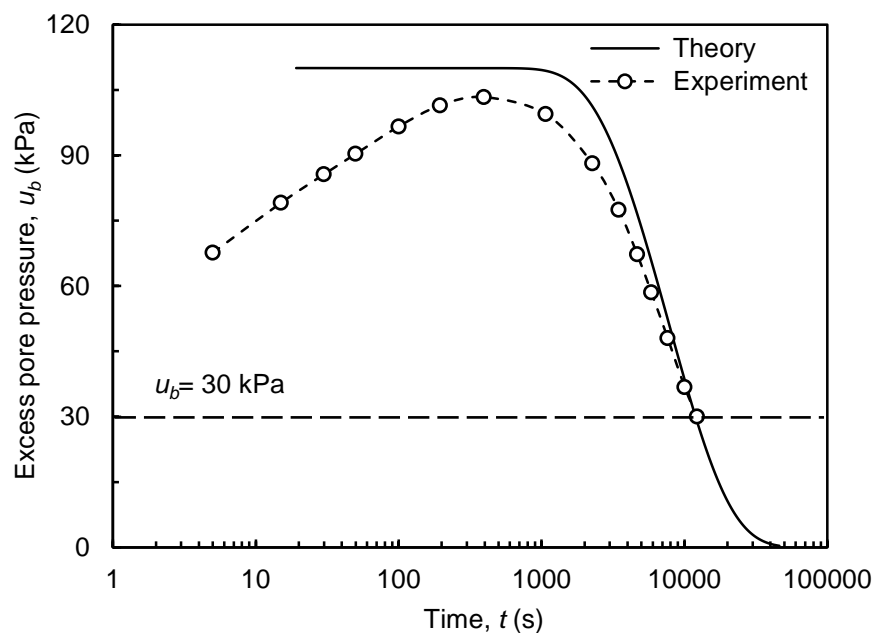


Figure 6.4: Pore pressure versus time of Gummudipoondi clay (100-200 kPa)

In Figure 6.4, it can be seen that there is a time lag to develop the maximum excess pore pressure at the base, which is not instantaneous. The time lag may be attributed to the stiffness of the measuring system relative to that of soil skeleton (Gibson, 1963; Perloff *et al.* 1965) and due to the top drainage that was allowed right from the time load was applied. However, the experimental curve merges with the theoretical curve at the later stages of consolidation. Similar results were observed for all soils.

#### 6.4.1 Normally Consolidated Soils

A typical time-pore pressure and time- settlement data obtained from the proposed test on reconstituted soil (Red Soil 2) is shown in Figure 6.5(a) and Figure 6.5(b), respectively. The soil specimen was loaded incrementally from 12.5 kPa-800 kPa and unloaded back to 12.5 kPa. From Figure 6.5 (b), it can be seen that the primary consolidation is not completed. Therefore, the consolidation parameters need to be determined based on the base pore water pressure.

By knowing the base pore pressure at the end of each increment of load, the average effective stress was computed using the Eq. (6.1). Void ratio ( $e$ ) was computed from the total settlement of each increment of load. The  $e$ - $\log \sigma_v'$  curves for all reconstituted soils are shown in Figures 6.6 along with IL test with 24 hours duration and CSL test. The results of IL test with 24 hours were interpreted based on the theory of one-dimensional consolidation by Terzaghi (1925) and CSL consolidation test are interpreted using theory of Wissa *et al.* (1971) and were already discussed in Chapter 3 and Chapter 4, respectively.

The total settlement parameters such as the compression index ( $c_c$ ) and recompression index ( $c_r$ ) values are determined from the  $e$ - $\log \sigma_v'$  plot. The values of  $c_c$  and  $c_r$  from the proposed SC test are compared with IL test with duration of 24 hour as shown in Figure 6.7. The values are comparable with IL test. With reference to IL test with 24 hours, the error analysis was carried out on the total settlement parameters obtained from proposed test. The average coefficient of variance (COV) of  $c_c$  is 7% and of  $c_r$  is 15%.

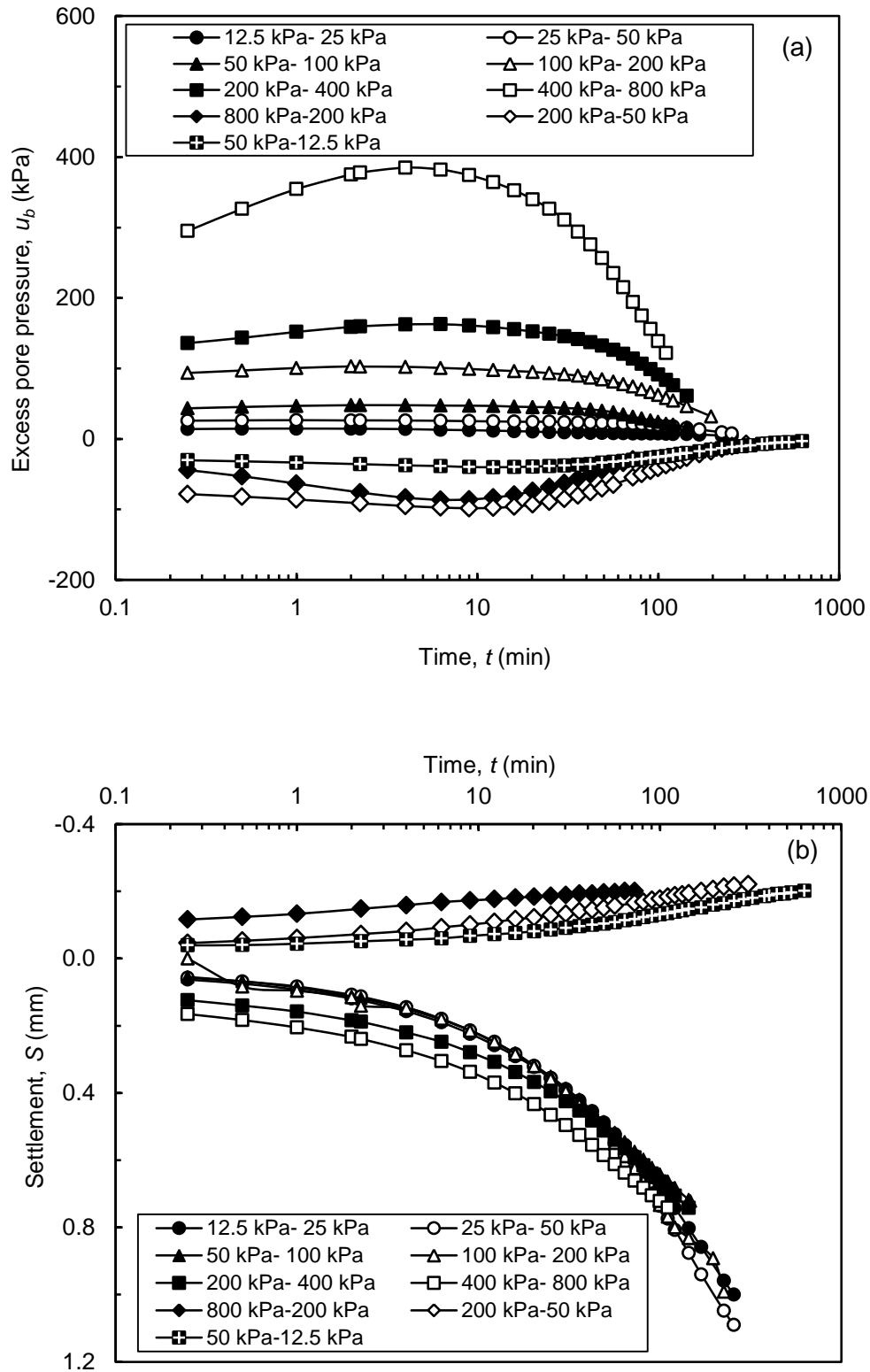


Figure 6.5: (a)Time-excess pore pressure and (b)Time-settlement/swell data for Red soil 2

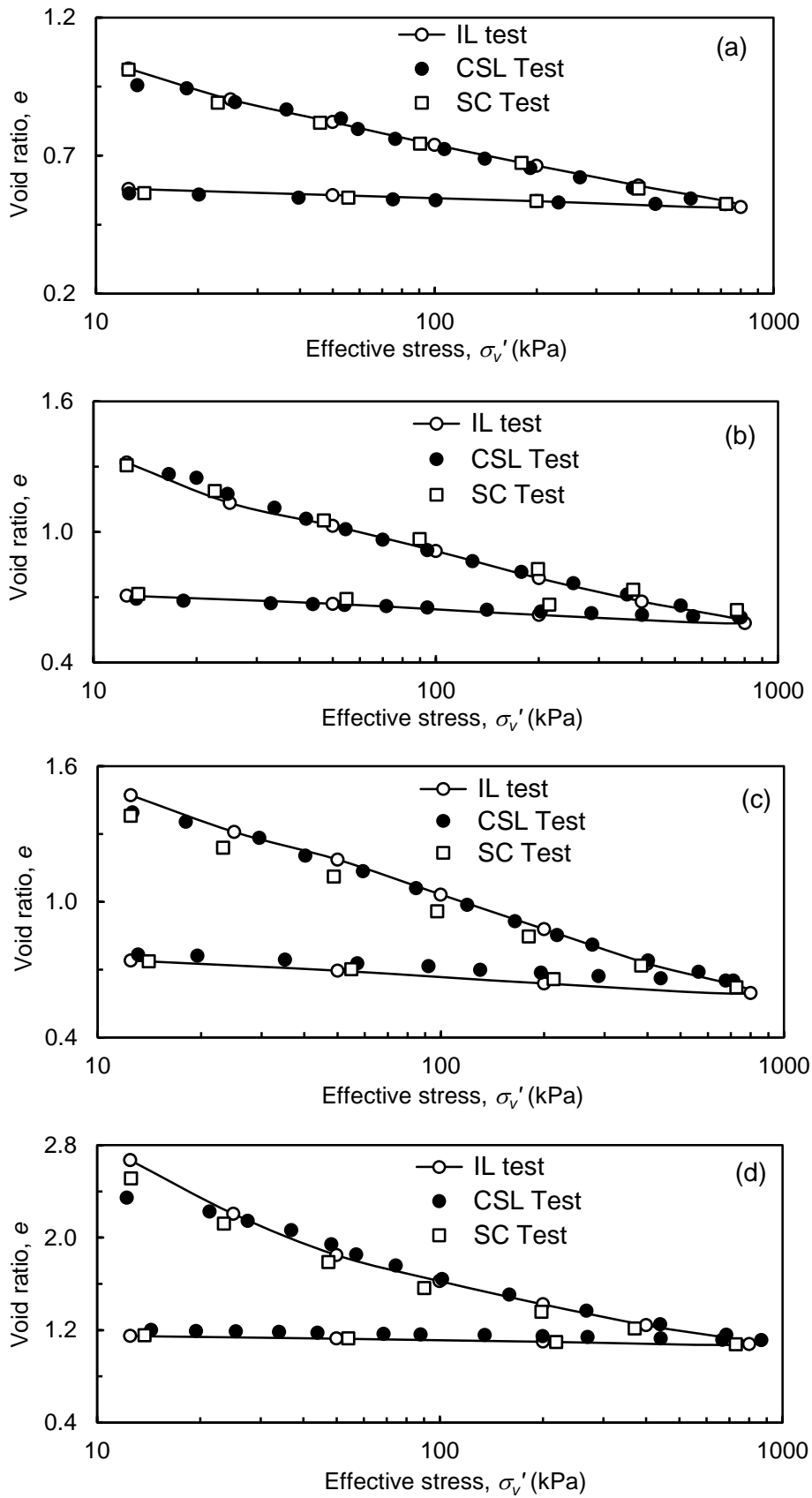


Figure 6.6 contd...



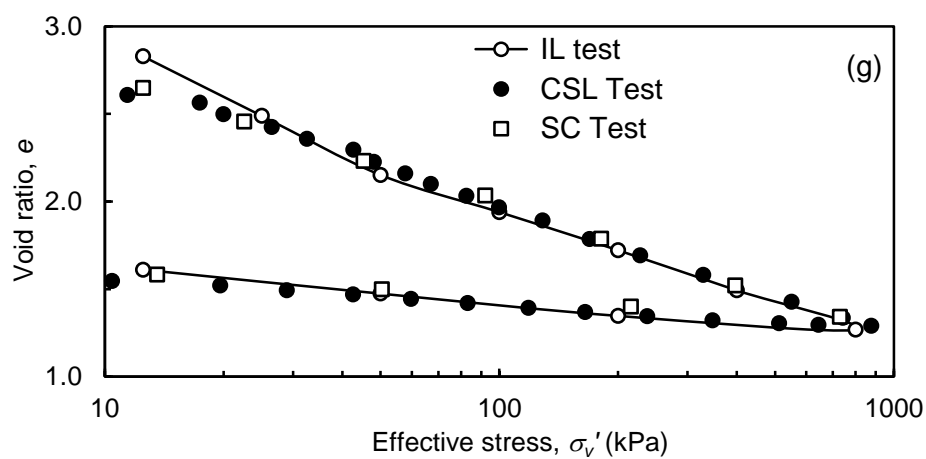
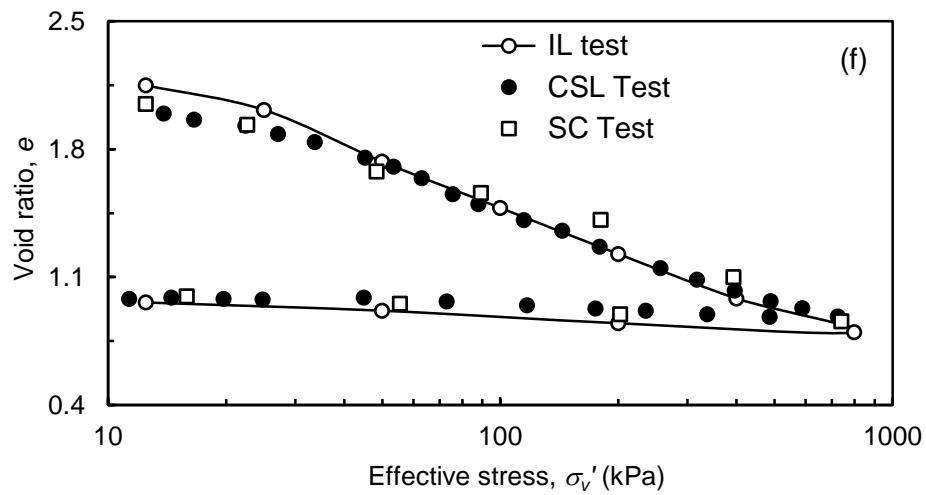
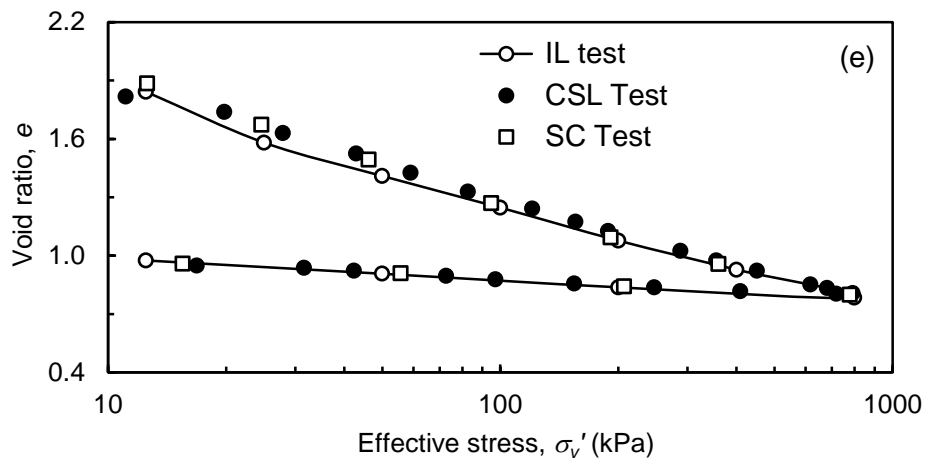


Figure 6.6: Comparison of  $e$ - $\log \sigma'_v$  plot from SC test, IL test and CSL test of the reconstituted soils in NC state for (a) Red soil 1 (b) Red soil 2 (c) Gummudipoondi clay (d) Kaolinite (e) Taramani clay (f) Siruseri clay and (g) Bombay marine clay

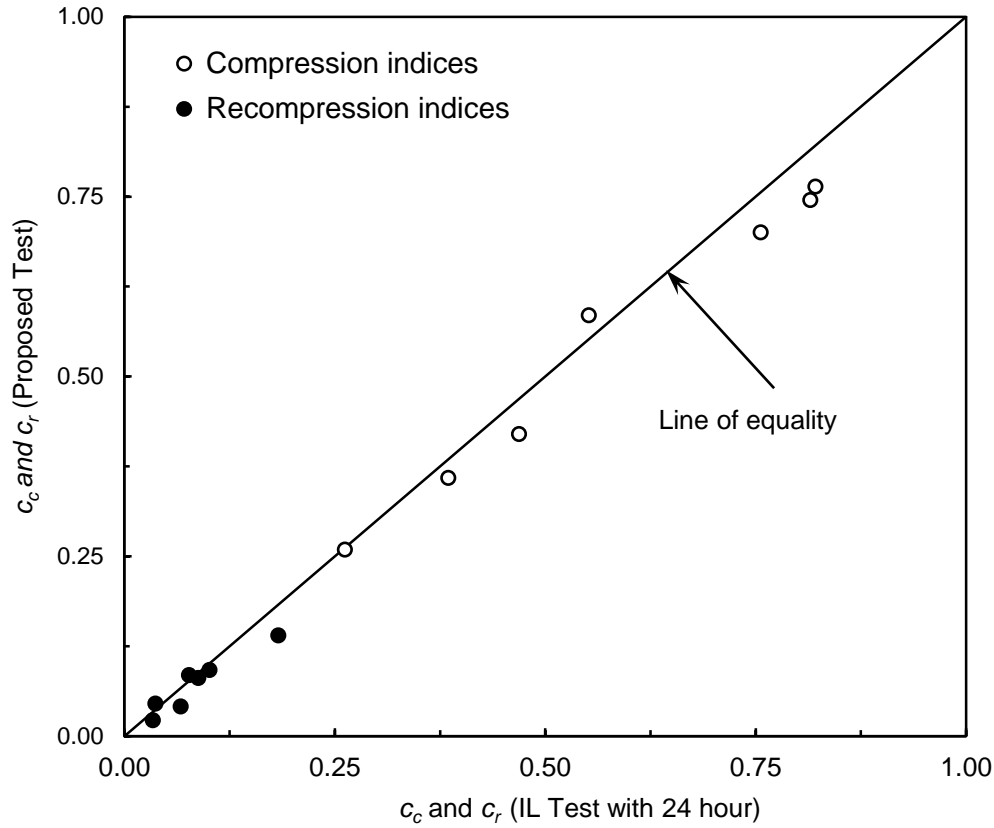


Figure 6.7: Comparison of Compression index and Recompression index from proposed test with IL test

The coefficient of consolidation ( $c_v$ ) from the proposed method was calculated using Eq. (6.3). The  $c_v$  variation with effective stress of reconstituted soils in NC state is shown in Figure 6.8, compared with IL test with 24 hours and CSL consolidation test. The values of  $c_v$  from IL test was calculated using the inflection point method (Robinson, 1997) and CSL test is based on Wissa *et al.* (1971). The trend of  $c_v$ - $\sigma'_v$  shows reasonably good match with IL test with 24 hours duration and CSL consolidation. To understand the percent of error in the result from the IL test with 24 hours, the results of the proposed methodology are compared with IL test as shown in Figure 6.9. The average COV of  $c_v$  values is nearly 30% with reference to IL test with 24 hours duration. Reanalysis of data in the literature, error of 33% is also reported in case of  $c_v$  (Leonard and Ramiah, 1959; Sridharan *et al.* 1994; Jia *et al.* 2010). Therefore, the coefficient of consolidation ( $c_v$ ) values obtained are reasonable.

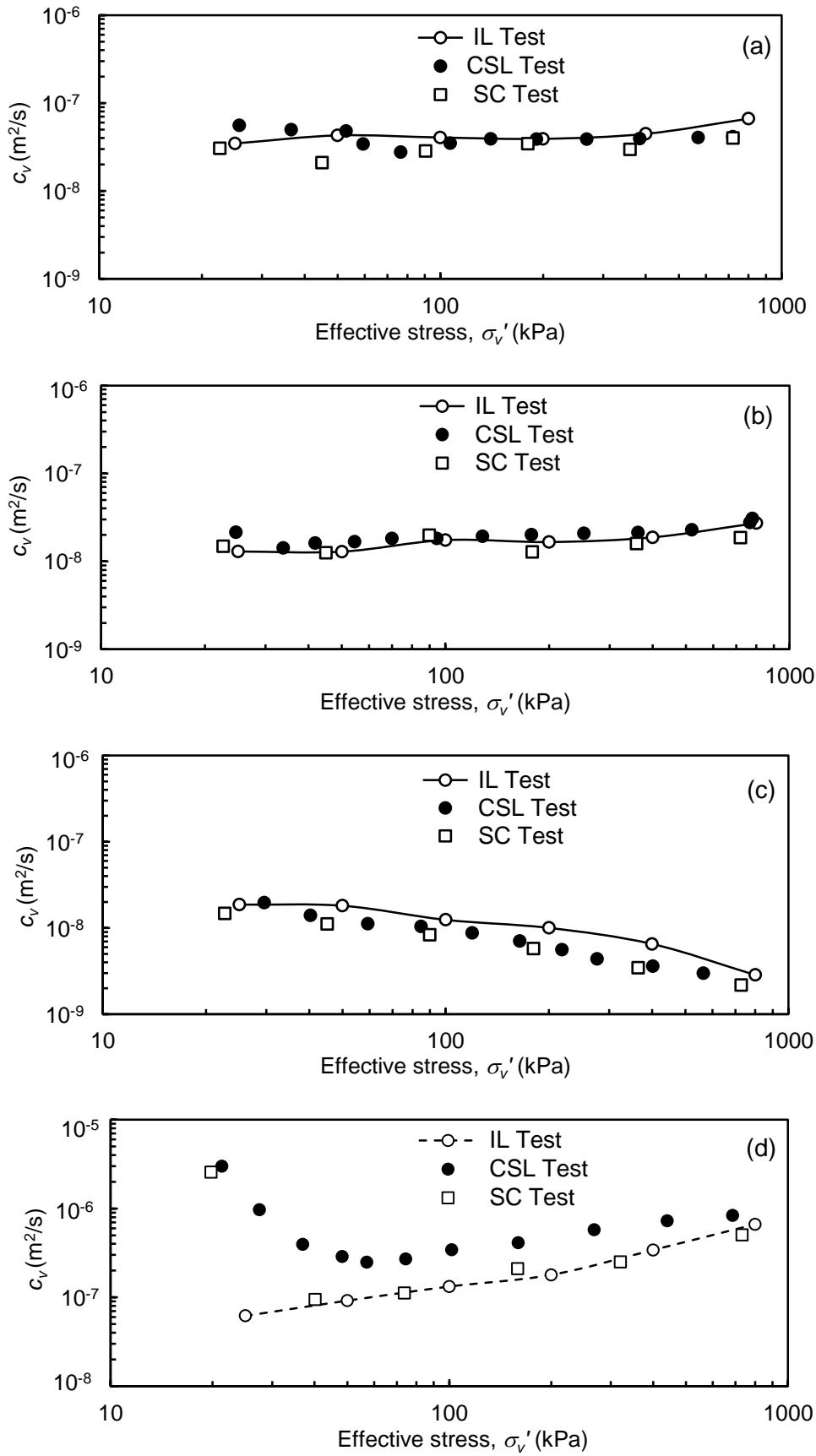


Figure 6.8 contd...

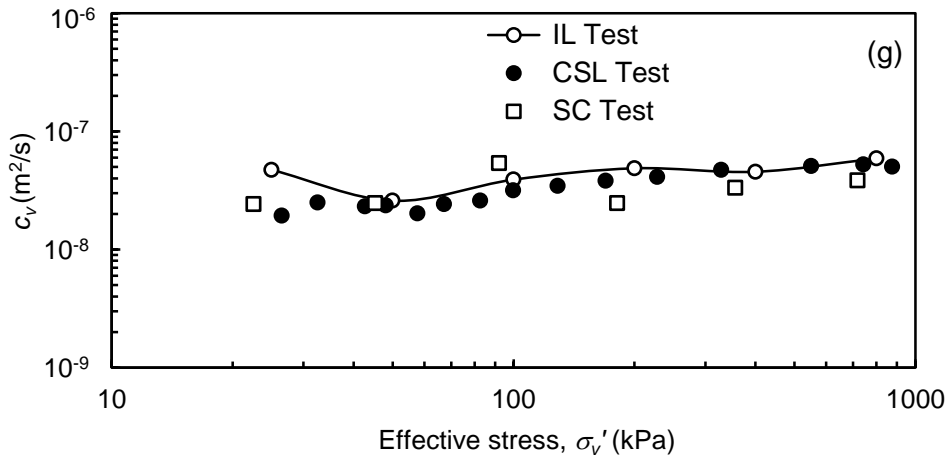
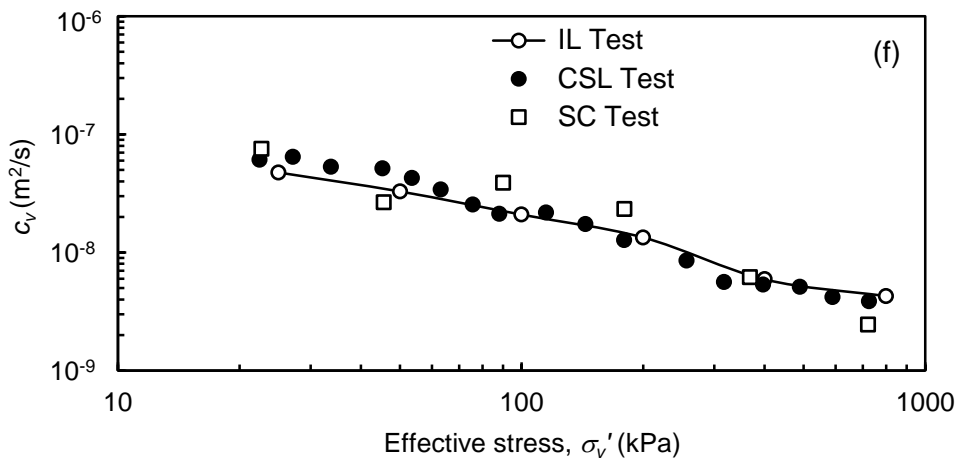
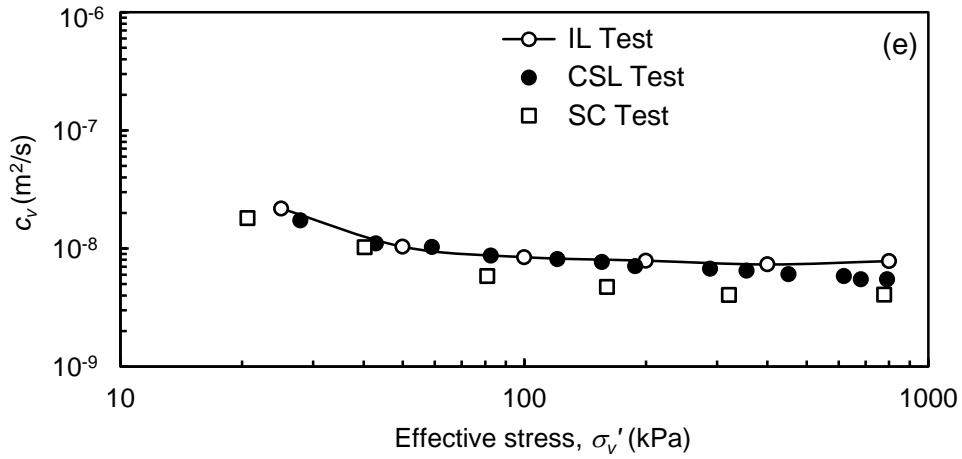


Figure 6.8: Comparison of  $c_v$ - $\sigma_v'$  variation from SC test, IL test and CSL test of reconstituted soils in NC state for (a) Red soil 1 (b) Red soil 2 (c) Gummudipoondi clay (d) Kaolinite (e) Taramani clay (f) Siruseri clay and (g) Bombay marine clay

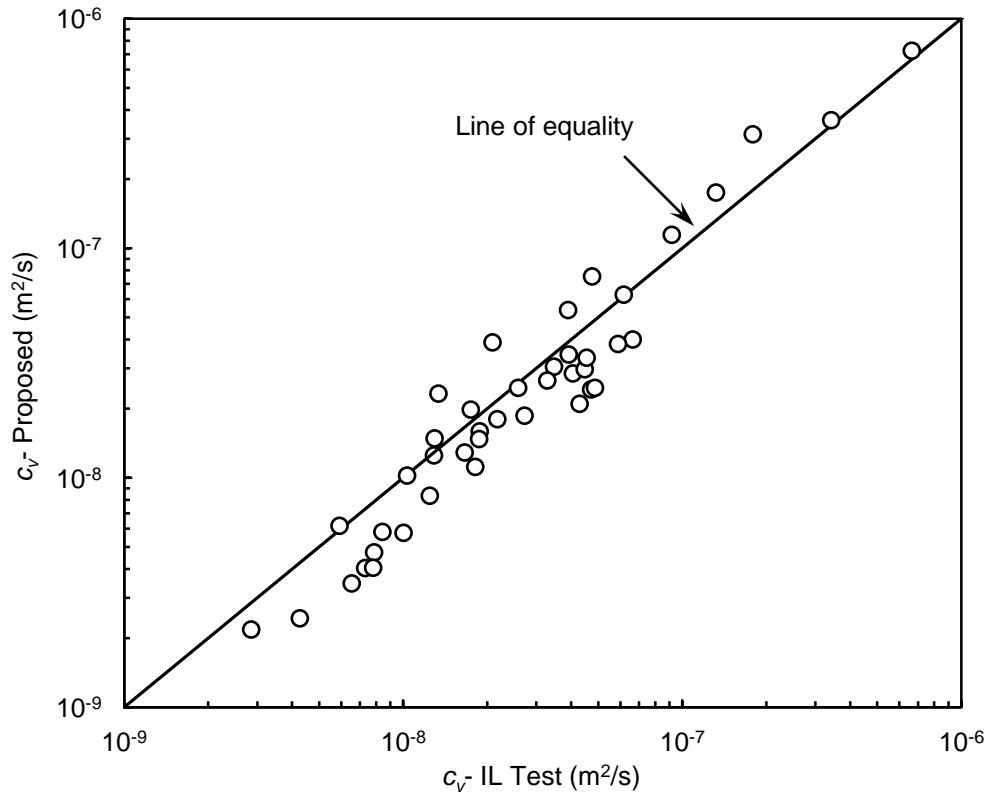


Figure 6.9: Comparison of coefficient of consolidation from the proposed test with IL test

Coefficient of permeability ( $k$ ) was also determined using the value of  $c_v$  and  $m_v$ . The results from the proposed SC test were compared with IL test with 24 hours duration and CSL consolidation test. The coefficient of permeability ( $k$ ) variation with effective stress ( $\sigma_v'$ ) of reconstituted soils in NC state are shown in Figure 6.10. The results obtained from reconstituted soils in NC state shows a very good match with the IL test results. Hence, the proposed method is valid to determine the consolidation parameters.

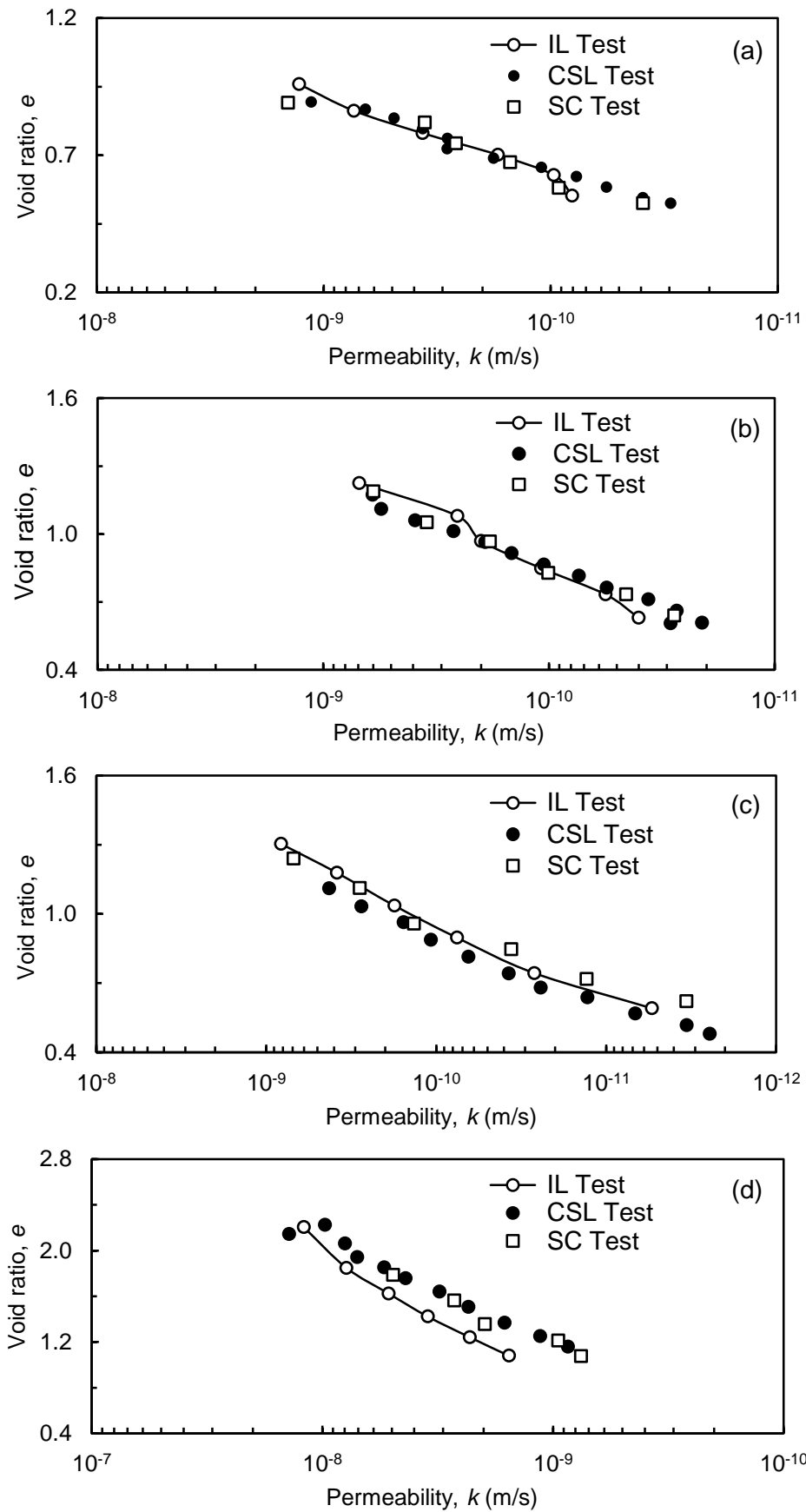


Figure 6.10 contd...

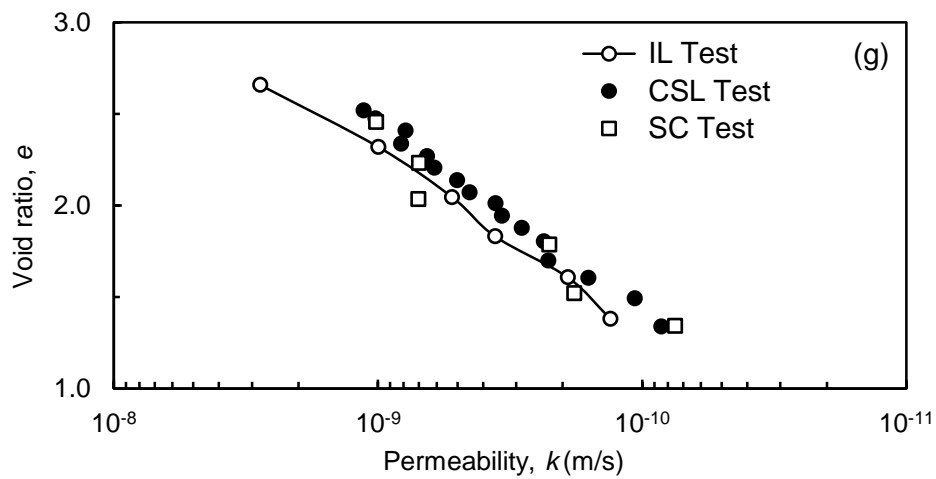
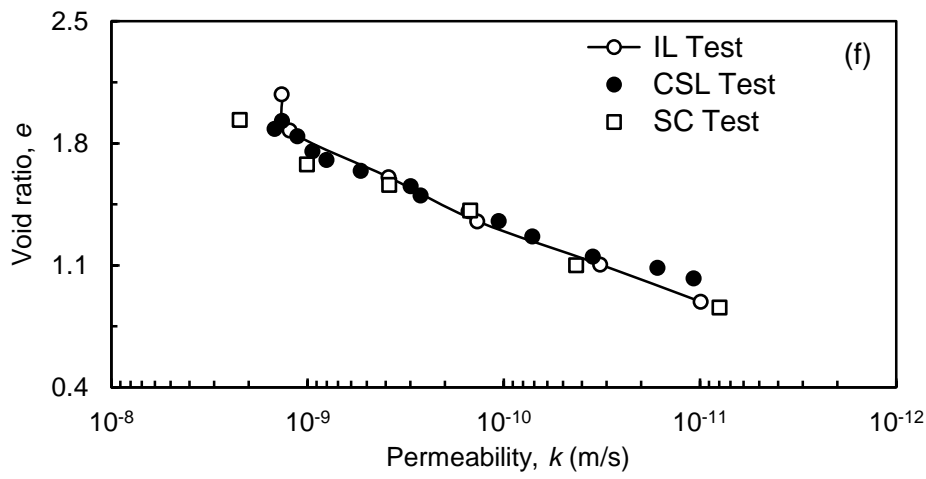
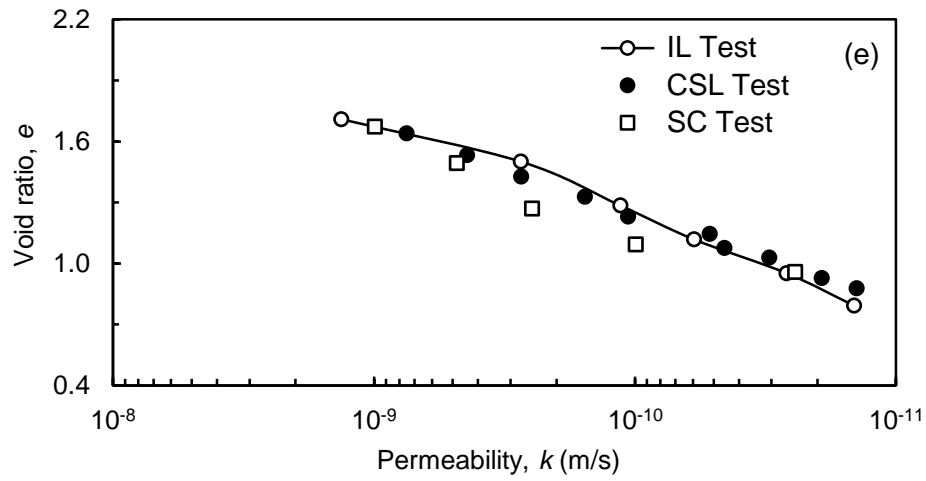


Figure 6.10: Comparison of  $e$ - $\log k$  curve from SC test, IL test and CSL test of reconstituted soils for (a) Red soil 1 (b) Red soil 2 (c) Gummudipoondi clay (d) Kaolinite (e) Taramani clay (f) Siruseri clay and (g) Bombay marine clay

## 6.4.2 Overconsolidated Soils

A typical time-pore pressure and time settlement/swell data of undisturbed soil (Cochin marine clay 19.5 m) is shown in Figure 6.11(a) and Figure 6.11(b), respectively. The specimen was loaded the same way as reconstituted soils in NC state. The consolidation parameters are determined based on the base pore water pressure data.

The  $e$ - $\log \sigma_v'$  curves of the reconstituted soils in OC state and undisturbed soils are shown in Figure 6.12 and 6.13, respectively. The  $e$ - $\log \sigma_v'$  plot obtained from the proposed test shows a good match with IL test with 24 hours duration. The total settlement parameters such as compression index ( $c_c$ ) and recompression index ( $c_r$ ) values are determined from the  $e$ - $\log \sigma_v'$  plot. The values of  $c_c$  and  $c_r$  from the proposed SC test are compared with IL test with duration of 24 hour as shown in Figure 6.14. With reference to IL test with 24 hours duration, the error analysis was carried out on the total settlement parameters obtained from the proposed test. The average coefficient of variance (COV) of  $c_c$  is less than the 6% and of  $c_r$  is about 10%.

The preconsolidation pressure of overconsolidated soils was determined using the  $\log(1+e)$  versus  $\log \sigma_v'$  method suggested by Sridharan *et al.* (1991). A typical plot for Cochin marine clay (19.5 m) is shown in Figure 6.15. The bi-linear plot directly gives the preconsolidation pressure. The preconsolidation pressure values from the proposed (SC) test are shown in Table 6.2 along with IL test and CSL test. The applied preconsolidation pressure of reconstituted soils and in-situ effective stress (effective overburden pressure) of undisturbed soils are also given in Table 6.2. The effective overburden pressure was calculated by knowing the effective unit weight of the soil, sampling depth and depth of water table. The results of the reconstituted soils in the OC state shows a good match and the undisturbed soils despite slight variation for the case of undisturbed soil due to soil variability.



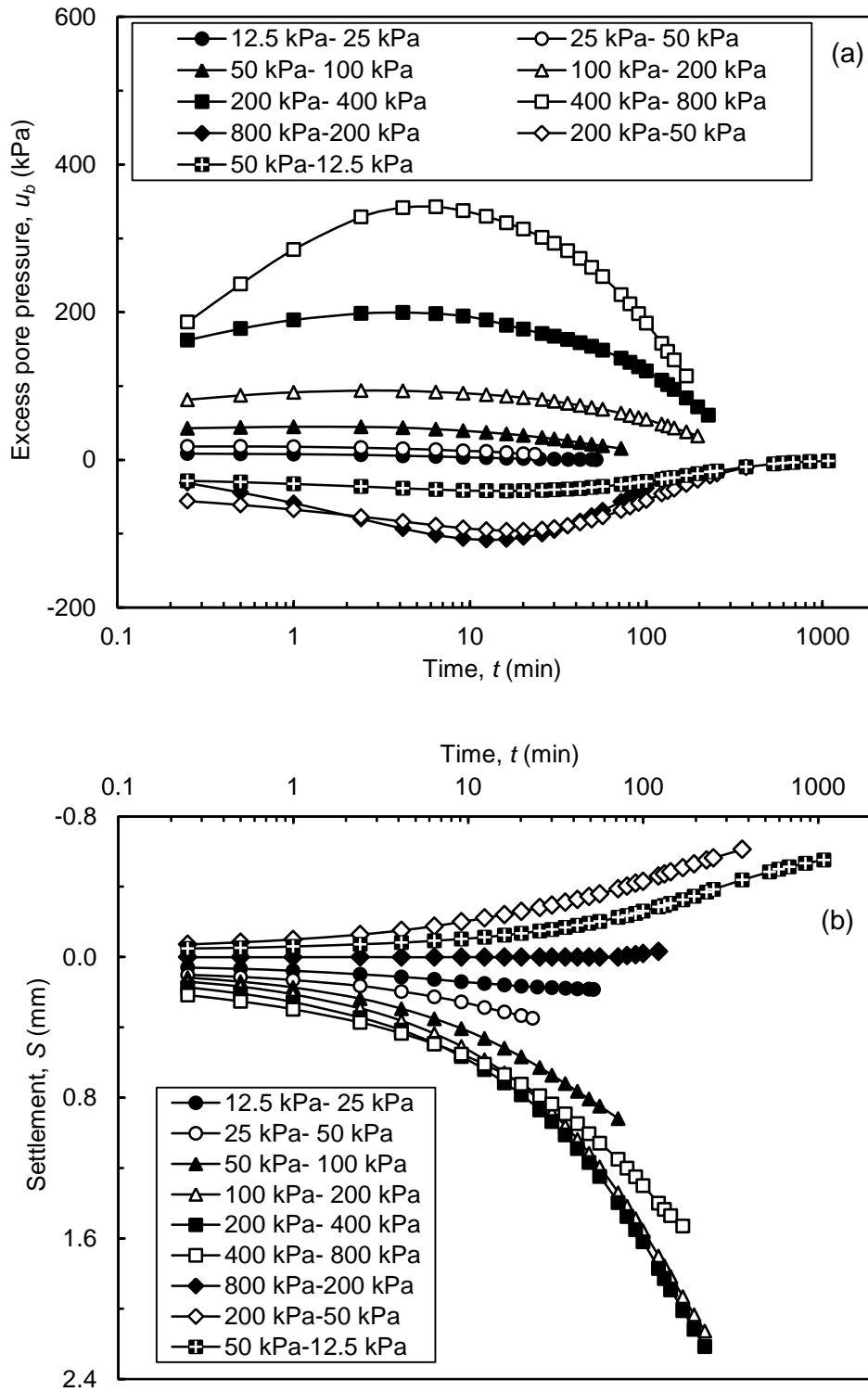


Figure 6.11: (a) Time- excess pore pressure and (b) Time-settlement data from proposed test of undisturbed soil (CMC 19.5 m)

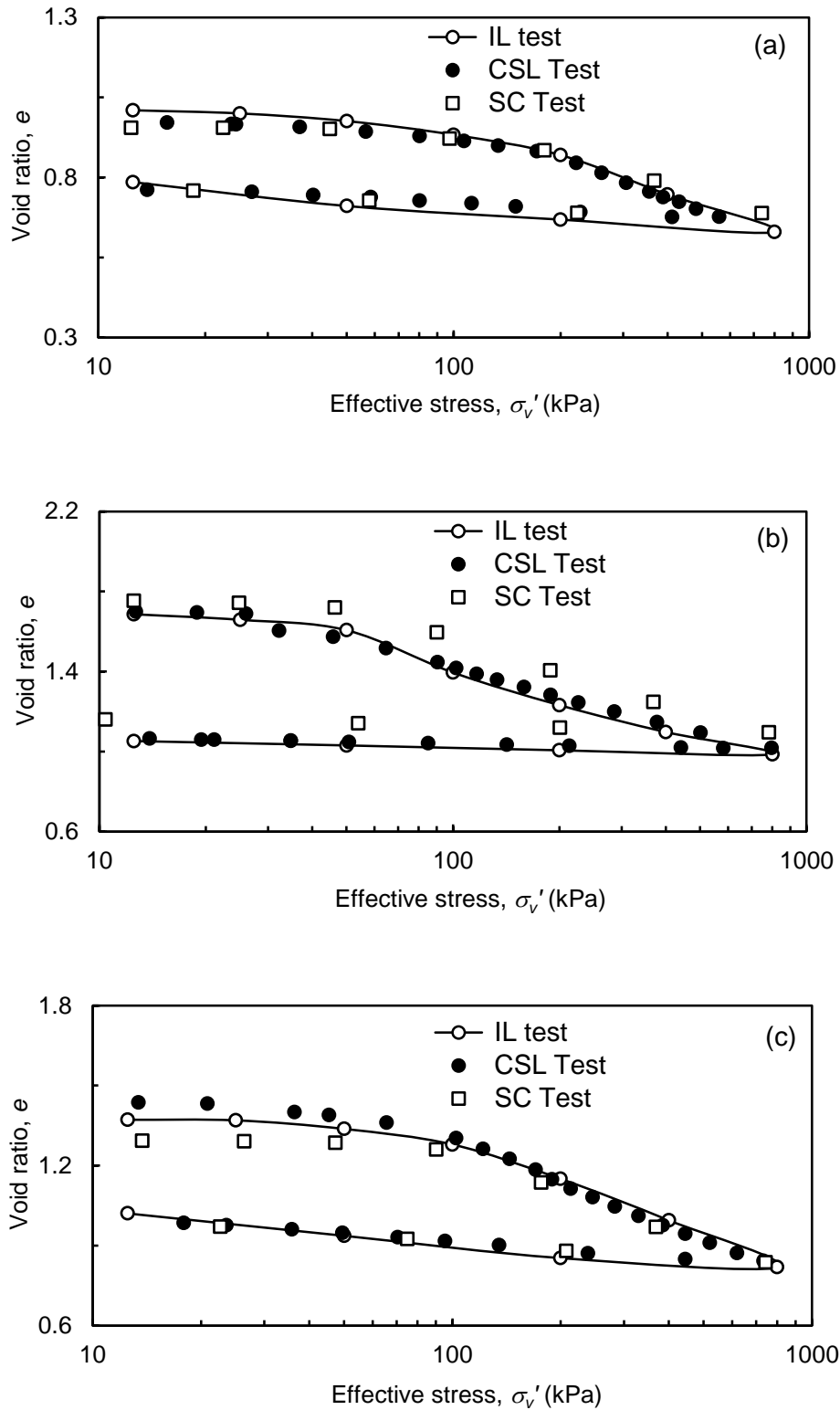


Figure 6.12: Comparison of  $e$ - $\log \sigma'_v$  plot from SC test, IL test and CSL test of reconstituted soils in OC state (a) Gummudipoondi clay (b) Kaolinite and (c) Taramani clay

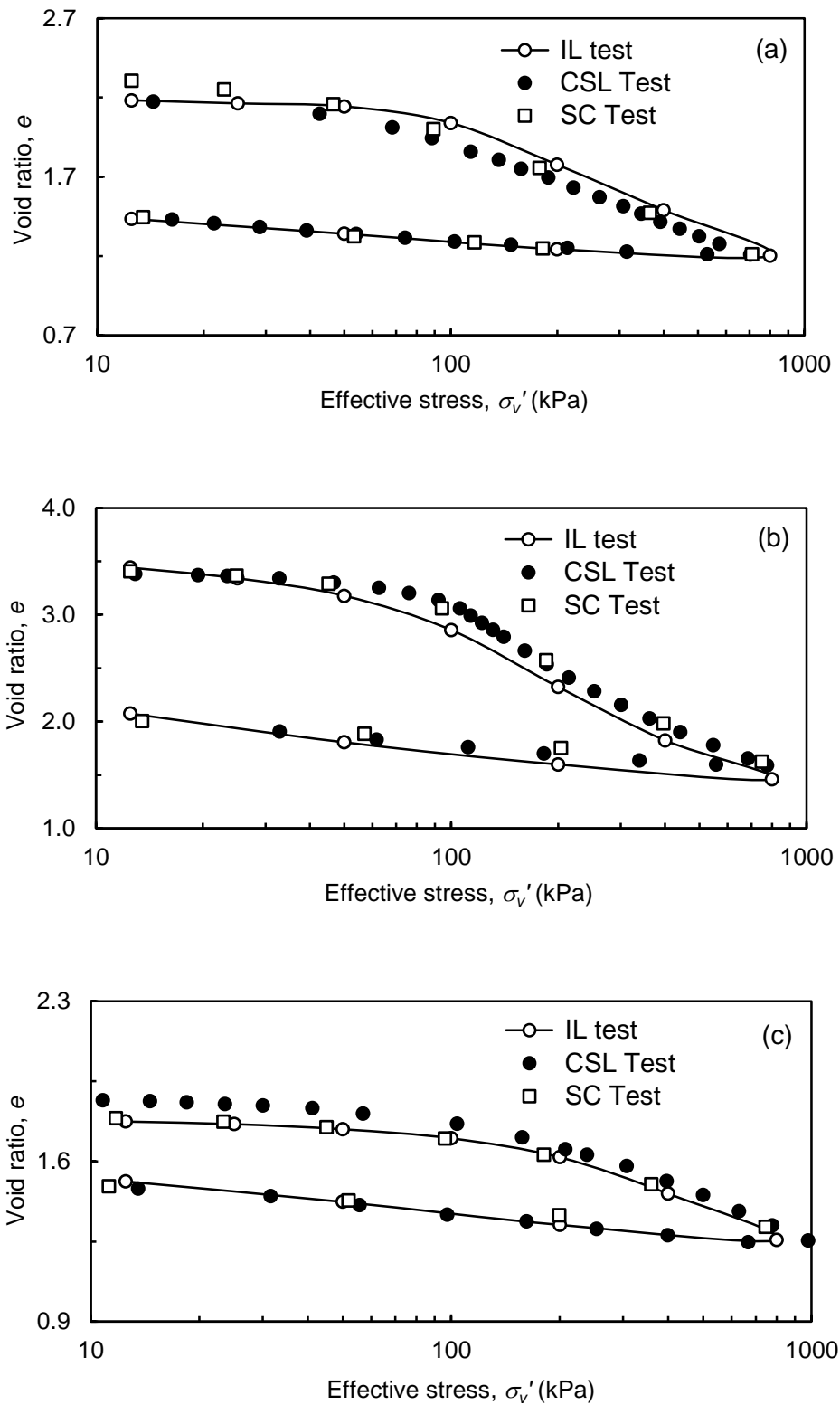


Figure 6.13: Comparison of  $e$ - $\log \sigma'_v$  plot from SC test, IL test and CSL test of undisturbed soils (a) Cochinchinese marine clay (5 m) (b) Cochinchinese marine clay (19.5 m) and (c) Bombay marine clay (12 m)

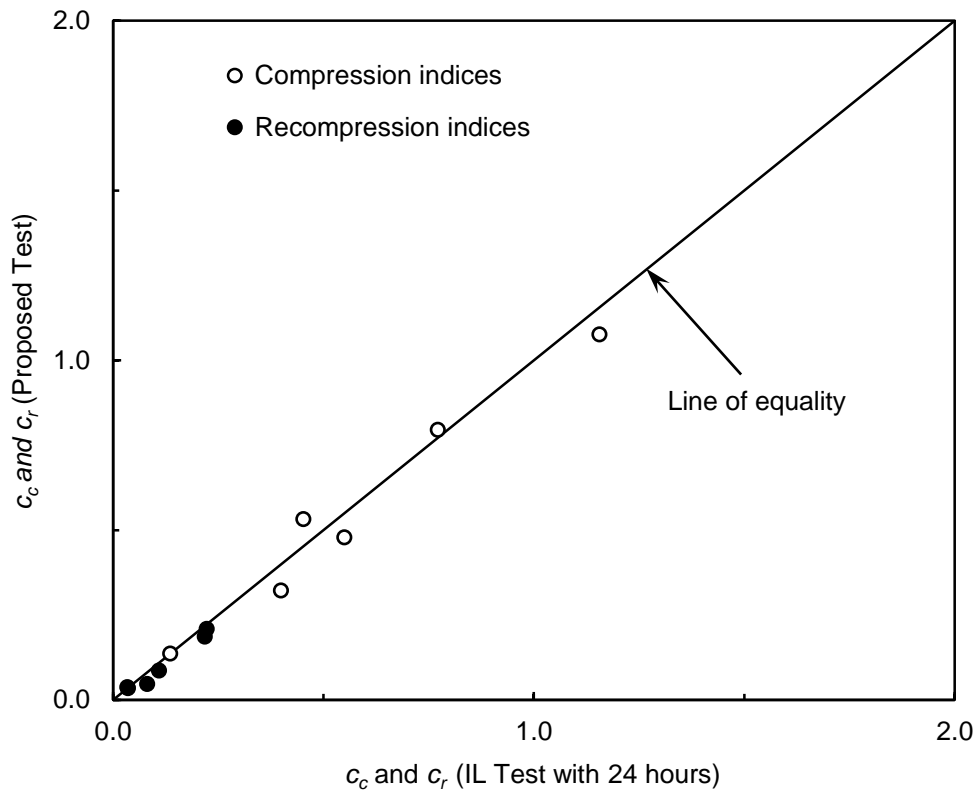


Figure 6.14: Comparison of Compression index and Recompression index from proposed test with IL test

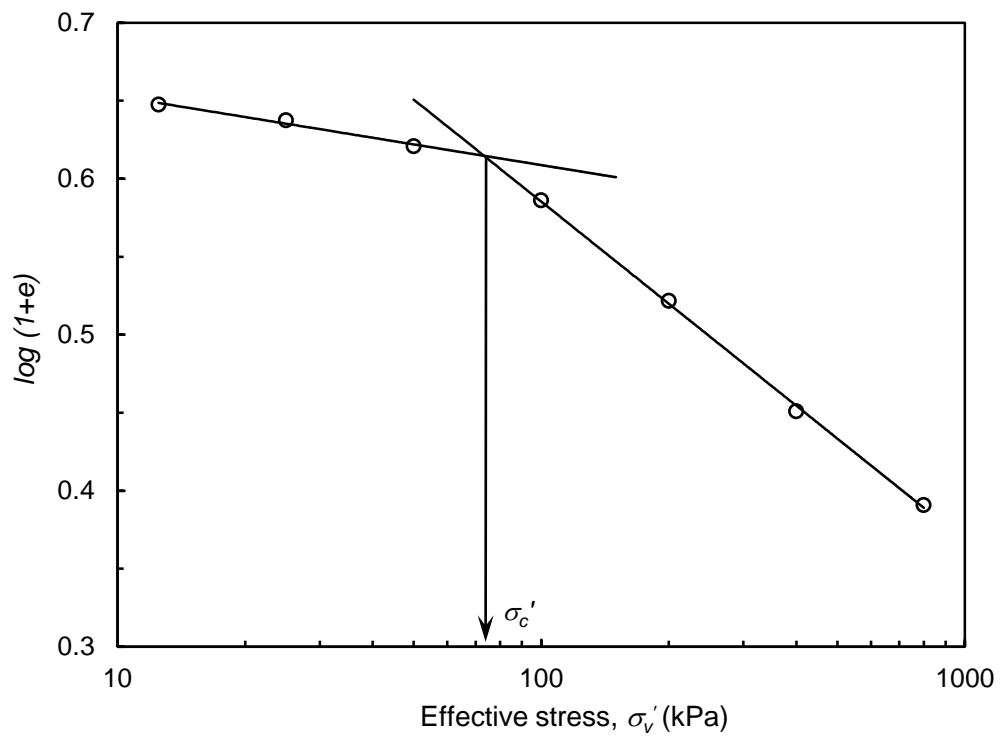


Figure 6.15: Typical  $\log(1+e)$  versus  $\log \sigma'_v$  plot for Cochin marine clay (19.5 m)

Table 6.2: Values of preconsolidation pressure

Sl. No.	Soils	Applied or $\sigma_{vo}'$ (kPa)	Preconsolidation pressure, $\sigma_c'$ (kPa)		
			IL Test	CSL Test	SC Test
<i>Reconstituted soils</i>					
1	Gummudipoondi clay	200	195	195	199
2	Kaolinite	50	50	45	50
3	Taramani clay	100	100	100	100
<i>Undisturbed soils</i>					
4	Cochin marine clay (5 m)	99	85	92	93
5	Cochin marine clay 19.5 m)	66	62	65	70
6	Bombay marine clay (12 m)	--	120	125	130

The variation of coefficient of consolidation with effective stress of the reconstituted soils in OC state and undisturbed soils are shown in Figure 6.16 and 6.17, respectively, along with IL consolidation test with 24 hours duration and CSL consolidation test. The trend of  $c_v$ - $\sigma_v'$  variation is in good agreement with IL test with 24 hours and CSL consolidation. Similarly, variation of coefficient of permeability ( $k$ ) variation void ratio of reconstituted soils in OC state and undisturbed soils are shown in Figure 6.18 and 6.19, respectively. The results obtained from the reconstituted soils in OC state shows a good match with the IL test results. However, there is little variation in the trend of  $e$ -  $\log k$  for undisturbed soils that may be due to the sample variability.

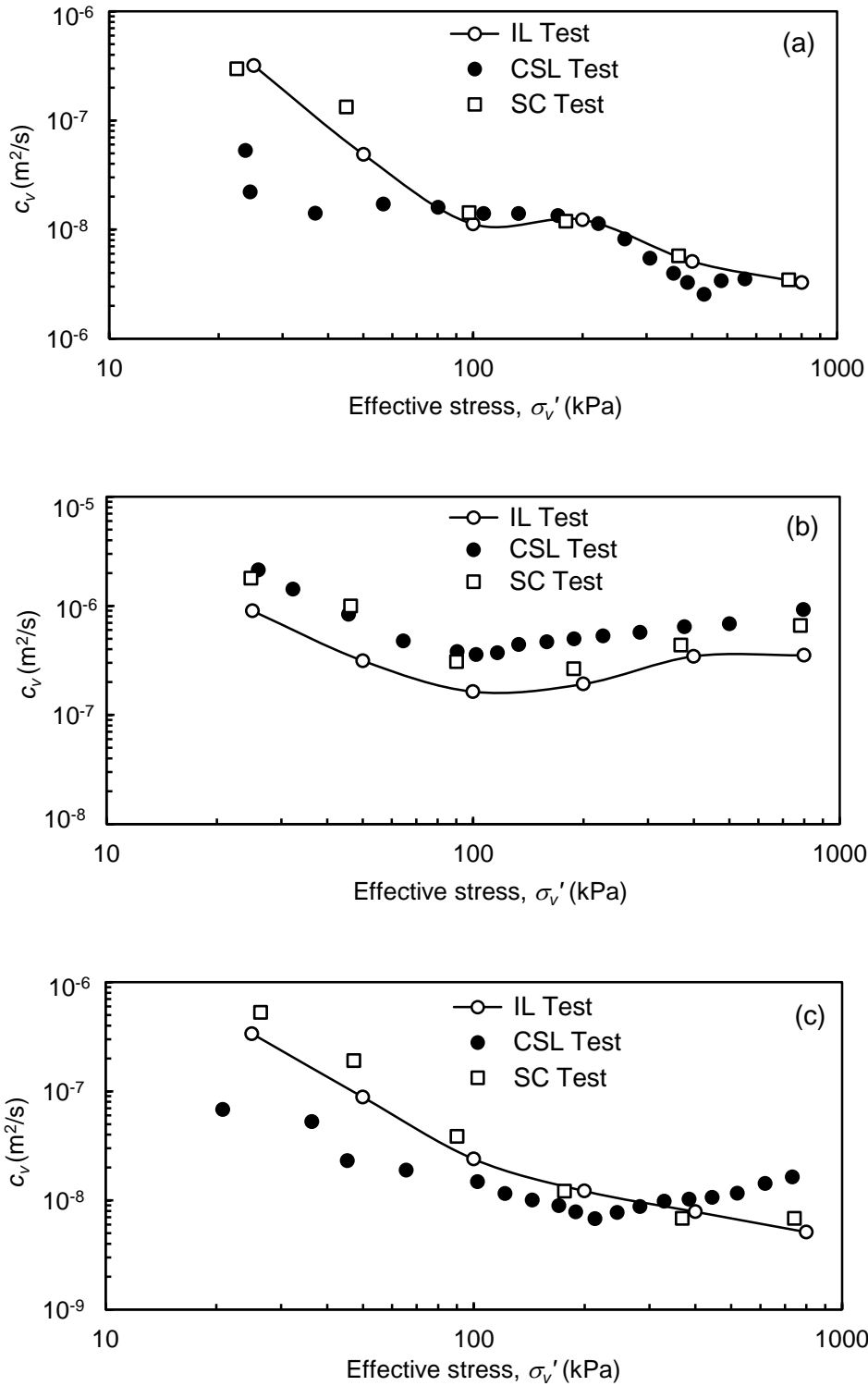


Figure 6.16: Comparison of  $c_v$ - $\sigma'_v$  variation from SC test, IL test and CSL test of reconstituted soils in OC state (a) Gummudipoondi clay (b) Kaolinite and (c) Taramani clay

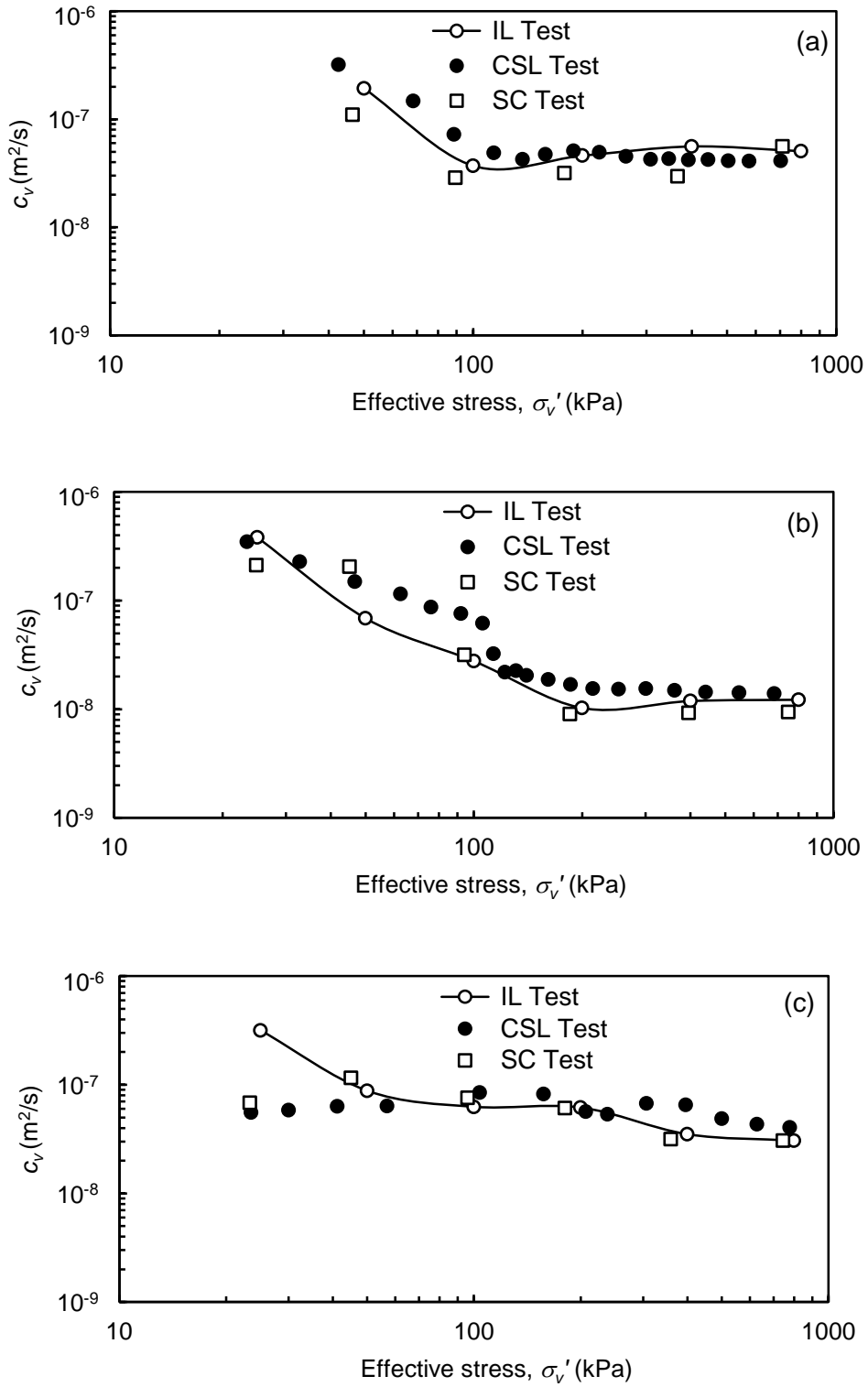


Figure 6.17: Comparison of  $c_v$ - $\sigma'_v$  variation from SC test, IL test and CSL test of undisturbed soils (a) Cochin marine clay (5 m) (b) Cochin marine clay (19.5 m) and (c) Bombay marine clay (12 m)

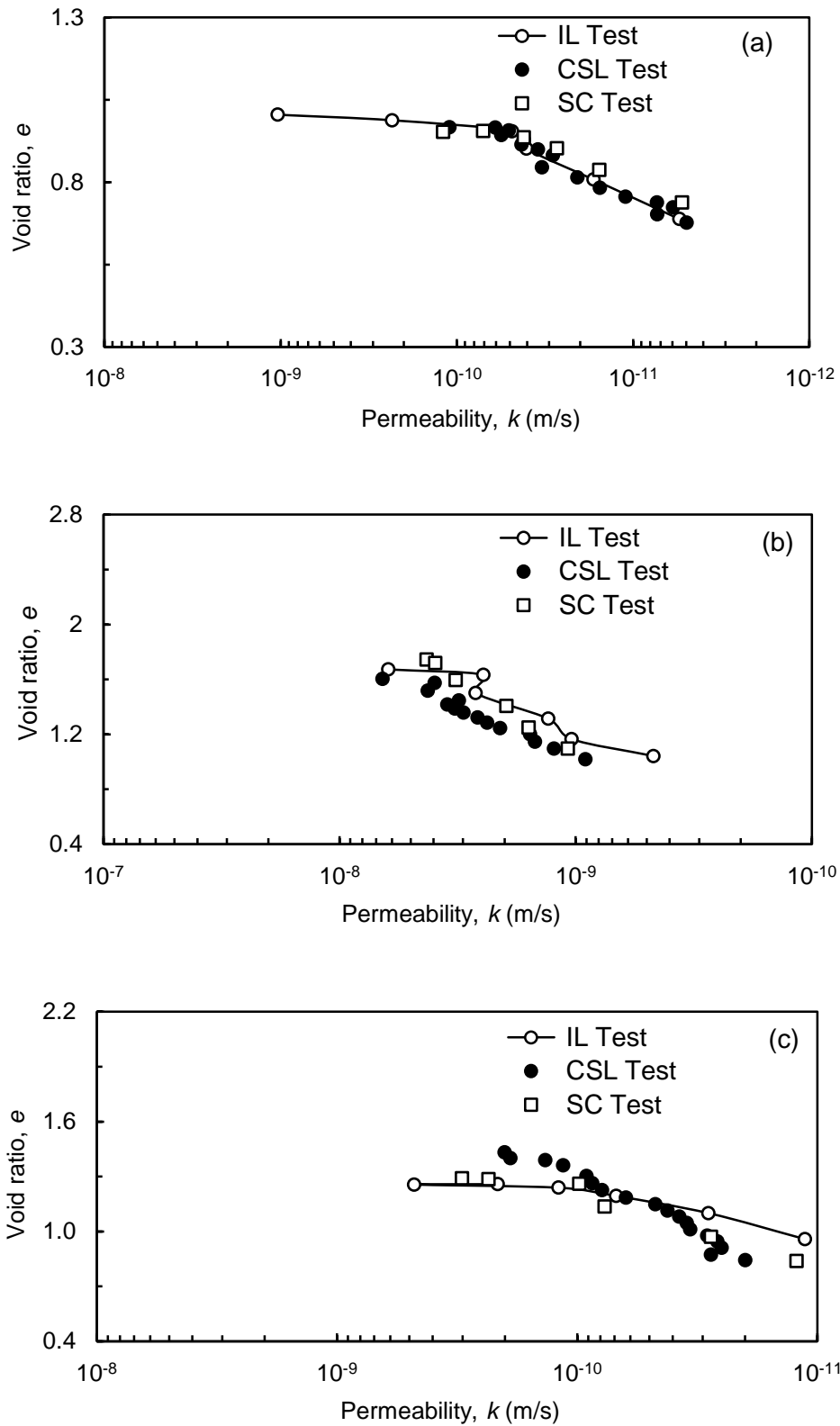


Figure 6.18: Comparison of  $e$ -log  $k$  curve from SC test, IL test and CSL test of reconstituted soils (a) Gummudipoondi clay (b) Kaolinite and (c) Taramani clay



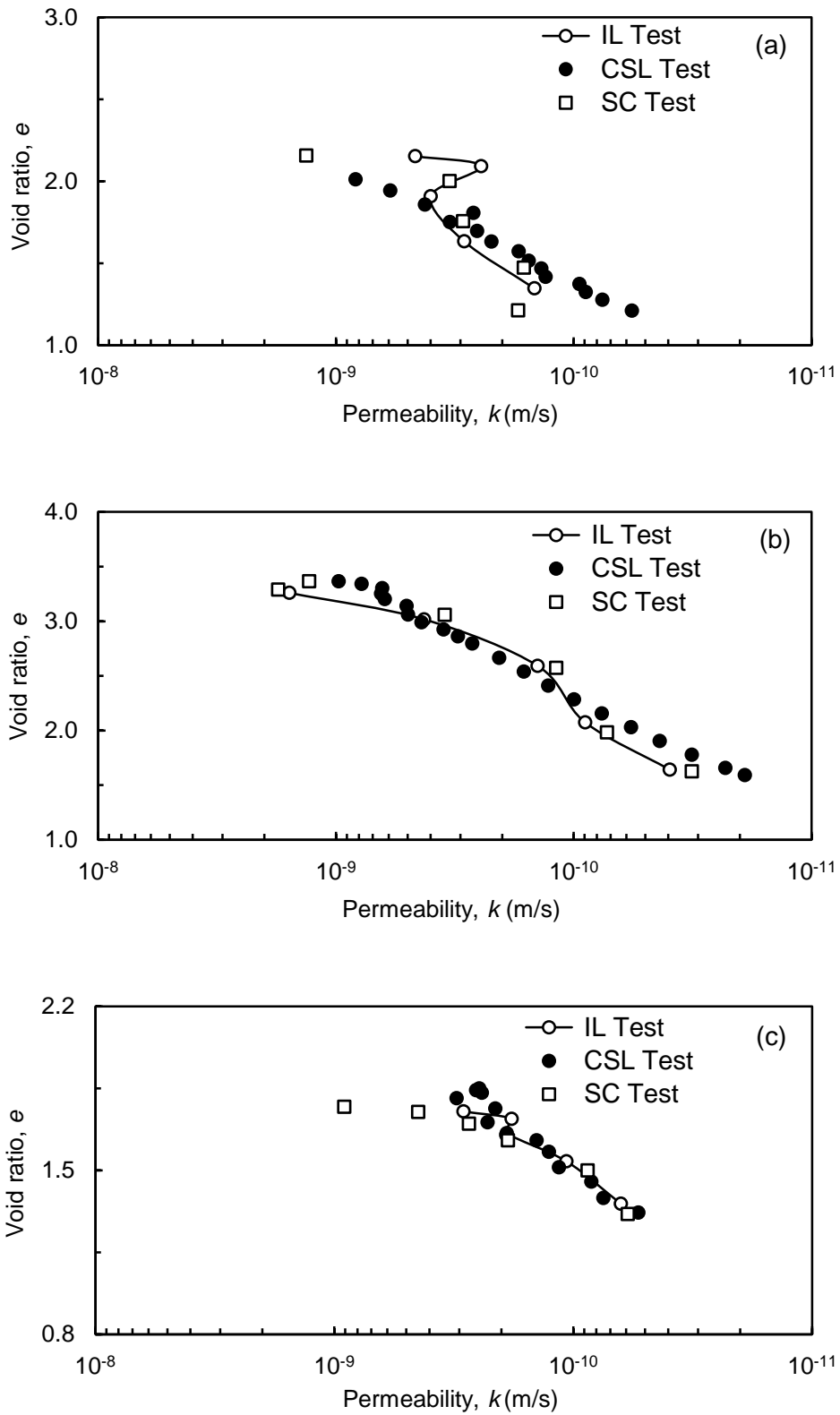


Figure 6.19: Comparison of  $e$ -log  $k$  curve from SC test, IL test and CSL test of undisturbed soils (a) Cochin marine clay (5 m) (b) Cochin marine clay (19.5 m) and (c) Bombay marine clay (12 m)

### **6.4.3 Time Required for Complete the Test**

The duration required for performing the SC test with pore pressure measurement, during loading and unloading stages for all the soils are given in Table 6.3 along with duration required for CSL consolidation test. It is seen that the duration required to complete the test depends on the coefficient of consolidation of the soil. For soils with low  $c_v$  values, the time taken for unloading is also quite high. In general, soils with values of coefficient of consolidation greater than about  $3 \times 10^{-8} \text{ m}^2/\text{s}$  requires less than 20 hours to complete the test. For low permeable soils, with  $c_v < 10^{-8} \text{ m}^2/\text{s}$ , the duration required is higher. When compared with the time required for CSL consolidation test, the proposed method is much faster by about 1.5-2.5 times for natural soils. Clearly, the proposed procedure saves considerable time for one-dimensional consolidation testing.

### **6.5 SUMMARY**

This chapter discussed about a stress controlled consolidation test with pore pressure measurements, where the dissipation of pore pressure was allowed from the top only upto 15% of the total stress applied. Series of experiments were performed to validate the proposed methodology on soils with varying plasticity characteristics. The results obtained are compared with IL test with 24 hours and CSL consolidation test. The results obtained matches well with IL test, confirming the validity of the proposed method. The duration required to complete the SC test are nearly 1.5-2.5 times faster than the CSL consolidation test for natural soils.

One of the limitations of the method is that continuous data points are not available compared to CSL test.

Table 6.3: Time required for the CSL test and the SC Test

Sl. No.	Soil Type	Range of $c_v$ , $m^2/s$	Time taken, hours					
			CSL Test			SC Test		
			Loading	Unloading	Total	Loading	Unloading	Total
1	Red soil 1	$3 \times 10^{-8}$ - $6 \times 10^{-8}$	28	7	35	8	9	16
2	Red soil 2	$1 \times 10^{-8}$ - $3 \times 10^{-8}$	62	13	75	18	16	34
3	Gummudipoondi clay	$4 \times 10^{-9}$ - $6 \times 10^{-8}$	126	88	214	42	79	121
4	Kaolinite	$6 \times 10^{-8}$ - $6 \times 10^{-7}$	3	1	4	0.75	0.25	1
5	Taramani clay	$8 \times 10^{-9}$ - $1 \times 10^{-8}$	126	43	169	32	66	98
6	Siruseri clay	$4 \times 10^{-9}$ - $4 \times 10^{-8}$	56	67	123	19	48	67
7	Bombay marine clay	$5 \times 10^{-8}$ - $6 \times 10^{-8}$	33	8	41	9	8	17
8	Cochin marine clay 19.5m (UDS)	$4 \times 10^{-7}$ - $1 \times 10^{-8}$	28	22	50	13	20	33
9	Cochin marine clay 5m (UDS)	$1 \times 10^{-7}$ - $5 \times 10^{-8}$	13	8	21	9	2	11
10	Bombay marine clay 12m (UDS)	$5 \times 10^{-8}$ - $2 \times 10^{-8}$	33	19	52	7	12	19



## CHAPTER 7

### ACCELERATED INCREMENTAL LOAD (AIL) CONSOLIDATION TEST USING CURVE FITTING METHODS

#### 7.1 INTRODUCTION

The one-dimensional consolidation testing methods discussed in the previous chapters (Chapter 4 and Chapter 6) require special testing procedures. The testing also requires the measurement of pore pressure during the consolidation process. In the conventional consolidation tests, pore pressures are not usually measured. Moreover, conventional incremental loading (IL) consolidation test with two-way drainage is always preferred, as it is simple and familiar to practicing geotechnical engineers. The proposed SC test discussed in the previous Chapter is faster than CSL test, as the specimen is not allowed to consolidate fully and only about 83% degree of consolidation is permitted. However, the consolidation is under one-way drainage. Therefore, the test takes longer time. Low permeable soils may take as much as 5 days (Table 6.3). If the test is conducted under two-way drainage, the test can be completed much faster.

This chapter describes two types of accelerated IL consolidation testing procedures using the curve fitting methods so as to obtain the void ratio-consolidation curve at the end-of-primary (EOP) and the coefficient of consolidation. The testing procedure is similar to the conventional incremental load (IL) consolidation test with the only difference that the subsequent loading is applied once the degree of consolidation is identified using the curve fitting procedures before the EOP. The standard  $\sqrt{t}$  method (Taylor, 1942) and the inflection point method (Cour, 1971; Robinson, 1997; Mesri *et al.* 1999) are the selected curve fitting procedures used to develop the accelerated incremental load consolidation test which were originally developed for the determination of only coefficient of consolidation ( $c_v$ ). Using the accelerated incremental load consolidation test method, considerable amount of time can be saved. The testing procedures and theory of the accelerated IL consolidation testing methods are validated by performing a series of tests and the results obtained are described in the subsequent sections.

## 7.2 ACCELERATED IL TEST USING THE $\sqrt{t}$ METHOD

The accelerated incremental load test is an incremental load test. The duration of load increment is reduced by applying the subsequent load increment, once the 90% degree of consolidation is reached. Taylor's  $\sqrt{t}$  method is used to identify the 90% degree of consolidation from the time-settlement data.

### 7.2.1 Theoretical Considerations

In the proposed method, the sample is allowed to consolidate up to a degree of consolidation ( $U$ ) of 90%. When  $U = 90\%$  is reached, the next pressure increment is applied. Degree of consolidation of 90% is identified using the Taylor's  $\sqrt{t}$  method. Hence, the applied stress is not equal to the effective stress. Therefore, the effective stress is corrected for the excess mid plane pore water pressure developed in the specimen to obtain EOP consolidation parameters. The corresponding average effective stress is evaluated by assuming the distribution of pore water pressure with depth as parabolic (Figure 7.1), the average effective stress ( $\sigma_v'$ ) within the specimen can be obtained from:

$$\sigma_v' = \sigma_v - \frac{2}{3} u_m \quad (7.1)$$

where,  $\sigma_v$  is the total stress acting on the specimen and  $u_m$  is the mid plane pore pressure. The excess pore water pressure developed at the middle of the clay specimen under double drainage at any time is estimated using Terzaghi's one-dimensional consolidation theory (Terzaghi, 1925) using Eq. (7.2) as

$$u_m = \sum_{m=0}^{m=\infty} \frac{2u_0}{M} \sin M \exp(-M^2 T_v) \quad (7.2)$$

where,  $M = \frac{(2m+1)\pi}{2}$ ,  $u_0$  = initial pore pressure at time  $t = 0$ , and  $T_v$  is the time factor given by

$$T_v = \frac{c_v t}{d^2} \quad (7.3)$$

where,  $c_v$  is the coefficient of consolidation. The values of  $c_v$  can be determined from Eq. (7.3) by knowing the time factor  $T_v = 0.848$  corresponding to degree of consolidation  $U = 90\%$ . The pore pressure ratio ( $u/u_0$ ) with depth factor (depth ( $z$ )/ drainage path ( $d$ )) for double drainage case is obtained by substituting the time factor in Eq. (7.2) as shown in Figure 7.1.

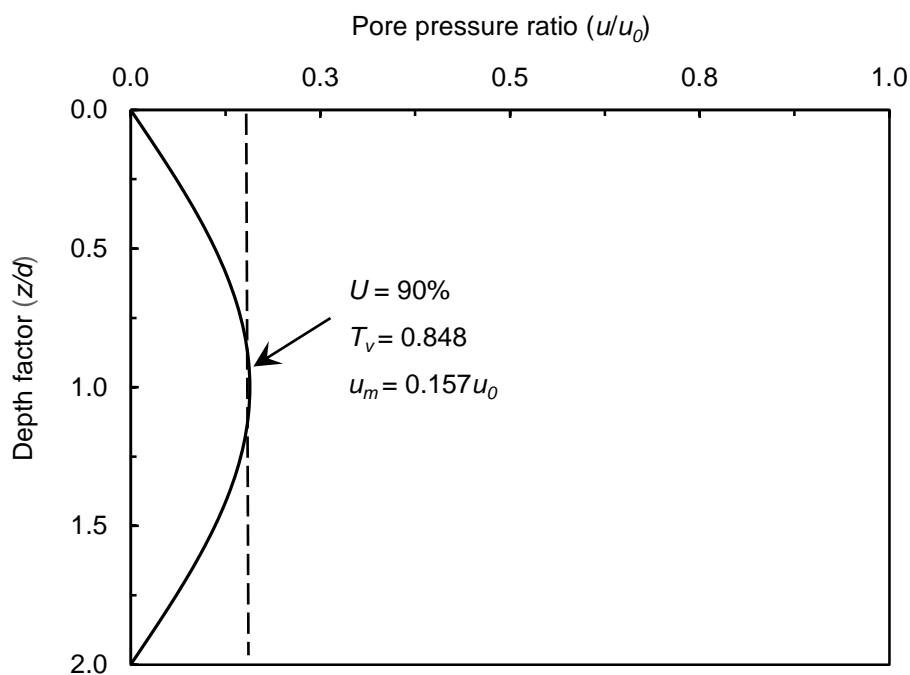


Figure 7.1: Variation of pore pressure ratio ( $u/u_0$ ) with ( $z/d$ )

From Figure 7.1 the pore pressure ratio ( $u_m/u_0$ ) at the mid-plane of the specimen for the degree of consolidation of 90% is 0.157. The initial excess pore pressure is generally taken as the applied pressure increment ( $\Delta\sigma_v$ ) in the conventional oedometer test with 24 hours duration test. However, in the proposed method the pore pressure is not allowed to dissipate fully in the previous increment. The pore pressure has not dissipated in the previous increment, referred to as residual pore pressure, need to be considered to obtain  $u_0$ . The residual pore pressure distribution is taken as parabolic, as shown in Figure 7.1.

Knowing the mid-plane pore pressure ( $u_{m_{i-1}}$ ) in the previous increment, the average residual pore pressure in the current pressure increment ( $u_{ri}$ ) is taken as:

$$u_{ri} = \frac{2}{3}u_{m(i-1)} \quad (7.4)$$

The initial pore pressure is the sum of the current pressure increment ( $\Delta\sigma_{vi}$ ) and the average residual pore pressure ( $u_{ri}$ ), which is given by

$$u_0 = \Delta\sigma_{vi} + u_{ri} \quad (7.5)$$

By knowing the excess pore water pressure developed at the mid-plane ( $u_m$ ), the average effective stress can be determined using Eq. (7.1). Therefore, it is essential that the value of  $u_m$  is minimum so that the error in  $\sigma_v'$  is minimum. ASTM D4186-12 (2012) recommends the maximum allowable pore pressure at the base during loading phase in CSL test as 15% of the total stress so that the error in effective stress calculated using Eq. (7.1) is minimum. The expected residual pore water pressure and mid plane pore water pressure under different pressure increments for sample thickness of 20 mm are computed and summarized in Table 7.1. It can be clearly observed from Table 7.1 that the mid plane pore pressure developed, for all the load increments, is about 8.3% of  $\sigma_v$ , which is well within the maximum allowable value of 15%. The load increment ratio (LIR), calculated as the ratio of applied effective stress increment to the existing effective stress, is also given in the Table 7.1. Except for the pressure increment of 12.5 kPa, the value of LIR is equal to 1. It may be also noted that the effective consolidation pressure ( $\sigma_v'$ ) is about 5% less than the applied total stress ( $\sigma_v$ ). If the effective consolidation pressure required is similar to the conventional one-dimensional consolidation test, the total stress can be suitably applied so as to obtain the required values like 12.5, 25, 50, 100 kPa etc. In other words, if the total stress values of 13.1, 26.3, 52.8, 105.5, 211.0, 422.0, 844.1 kPa are applied, the expected average effective consolidation pressures at  $U = 90\%$  are 12.5, 25, 50, 100, 200, 400 and 800 kPa, respectively.

In the unloading phase, the mid plane pore pressure developed at the base are also shown in Table 7.1. Usually in IL consolidation test an unloading decrement is one fourth



of the previous pressure, but the first unloading in the accelerated IL test using  $\sqrt{t}$  method it is only one third of the previous pressure and other decrements are nearly equal to the one fourth of it.

Table 7.1: Typical calculation of mid plane pore pressure and effective stress at  $U=90\%$

Stage	Total stress, $\sigma_v$	Stress increment, $\Delta\sigma_v$	Residual PwP, $u_{ri}$	Initial PwP, $u_0$	Mid plane PwP, $u_m$	Effective stress, $\sigma_v'$	LIR	$\frac{u_m}{\sigma_v} \times 100$ (%)
Loading	6.25	6.25	0	0	0.00	6.3	-	-
	12.5	6.25	0.00	6.25	0.98	11.8	0.9	7.85
	25	12.5	0.98	13.15	2.07	23.6	1.0	8.26
	50	25	2.07	26.38	4.14	47.2	1.0	8.28
	100	50	4.14	52.76	8.28	94.5	1.0	8.28
	200	100	8.28	105.52	16.57	189.0	1.0	8.28
	400	200	16.57	211.04	33.13	377.9	1.0	8.28
	800	400	33.13	422.09	66.27	755.8	1.0	8.28
Unloading	200	-600	66.27	-555.82	-87.26	258.2	0.34	-
	50	-150	-87.26	-208.18	-32.68	71.8	0.28	-
	12.5	-37.5	-32.68	-59.29	-9.31	18.7	0.26	-

Note: PwP-Pore water pressure, LIR-Load increment ratio, Pressure units are in kPa

## 7.2.2 Experimental Programme

The selected reconstituted soils were Red soil 1, Red soil 2, Gummudipoondi clay, Taramani clay and Bombay marine clay. Three undisturbed soils were also used, namely Cochin marine clay (sampled at 5 m), Bombay marine clay (sampled at 12 m) and Madhavaram clay (sampled at 6 m). The basic properties of the selected soils and the specimen preparation procedure were reported in the Chapter 3 (section 3.3). Two identical specimens were prepared for carrying out the experiments.

One-dimensional consolidation test with loading duration up to the end-of-primary (EOP) consolidation was conducted on the first specimen, as the control test. The testing procedure and results were already explained in Chapter 3. The second specimen was subjected to the proposed procedure. The testing procedure is the same as that adopted for the first specimen, except that the subsequent load was applied only upto a degree of consolidation of 90%. The 90% degree of consolidation was identified by continuously monitoring the time-settlement data for each increment of load and simultaneously plotting the data with  $\sqrt{t}$  in the X-axis and settlement in the Y-axis as shown in Figure 7.2. In the  $\sqrt{t}$ -settlement (Figure 2) plot, establish the initial linear portion (OB) based on the data obtained in the early stage of consolidation. Construct line OC such that its slope is (1/1.15) times OB. Continue to plot the test data till the experimental curve touches the line OC at D, which is the point at which the degree of consolidation of 90% is reached. Apply the next load increment once 90% degree of consolidation is reached and continue the procedure upto the required pressure. The same procedure is adopted for unloading stages also.

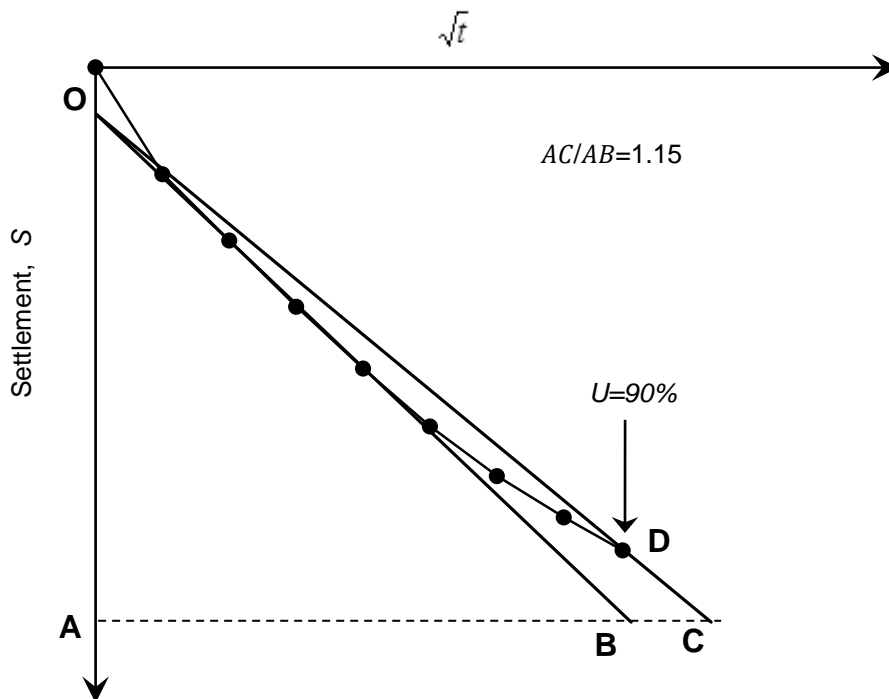


Figure 7.2: Evaluation of degree of consolidation- $\sqrt{t}$  method

The applicability of the  $\sqrt{t}$  method is validated by conducting a series of experiments on the selected reconstituted soils and undisturbed soils. The results of the proposed  $\sqrt{t}$  procedure were compared with EOP test results discussed in Chapter 3.

### 7.2.3 Results and Discussions

#### *Results from reconstituted soils*

Typical  $\sqrt{t}$ –settlement data for reconstituted specimen of Gummudipoondi clay is shown in Figure 7.3. As mentioned earlier, the subsequent increment was applied before the end of primary consolidation. The  $\sqrt{t}$ –settlement data for other reconstituted soils are given in Appendix E. The void ratio ( $e$ )-effective stress ( $\sigma_v'$ ) curves of the reconstituted soil specimens obtained from the EOP test and the accelerated IL test using the  $\sqrt{t}$  method are shown in Figures 7.4(a-e). The effective stresses were corrected for the excess mid-plane pore pressure. As it can be seen in the plots, the proposed method is able to yield  $e$ - $\log \sigma_v'$  curves comparable to the EOP test.

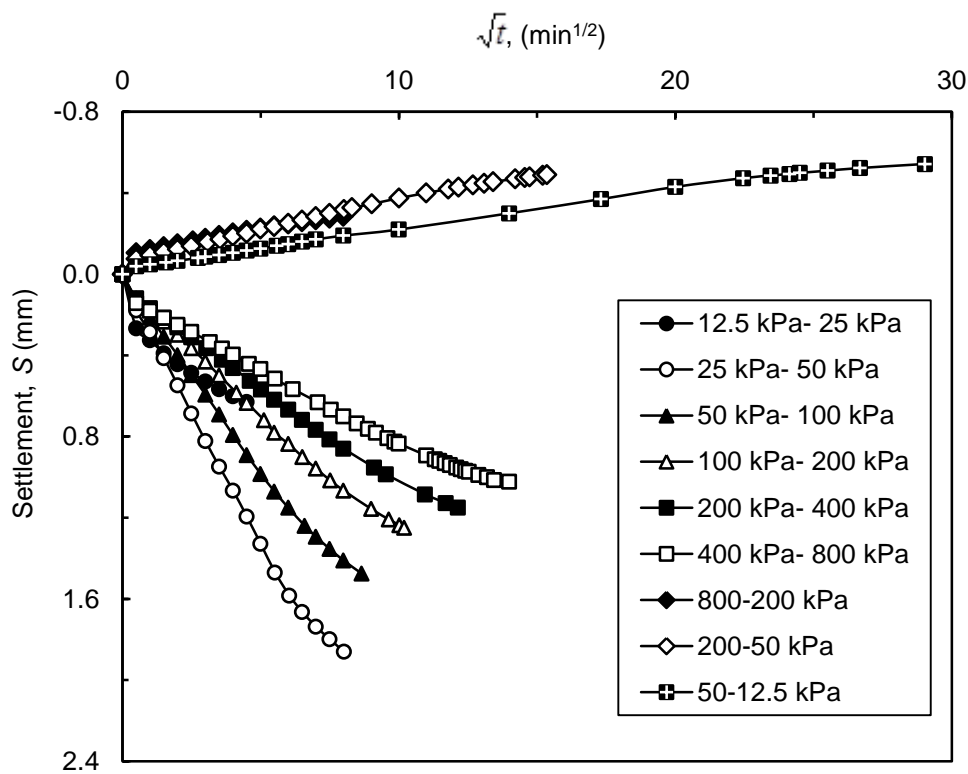


Figure 7.3:  $\sqrt{t}$ –settlement plot for Gummudipoondi clay

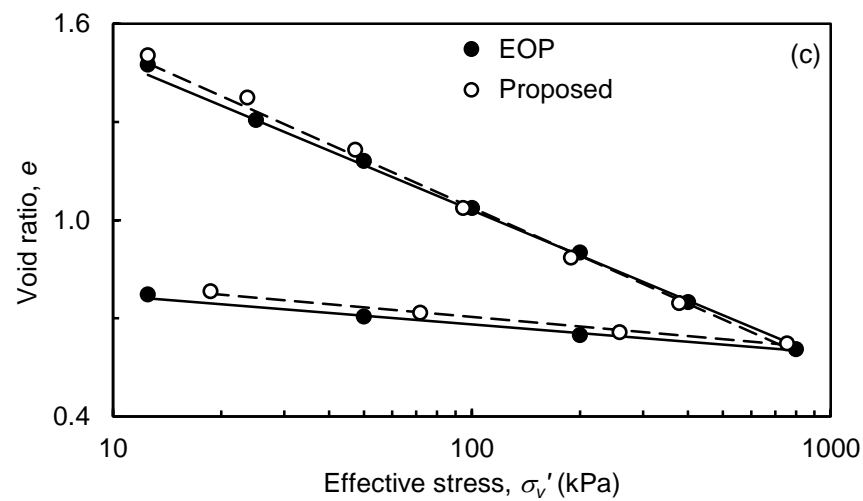
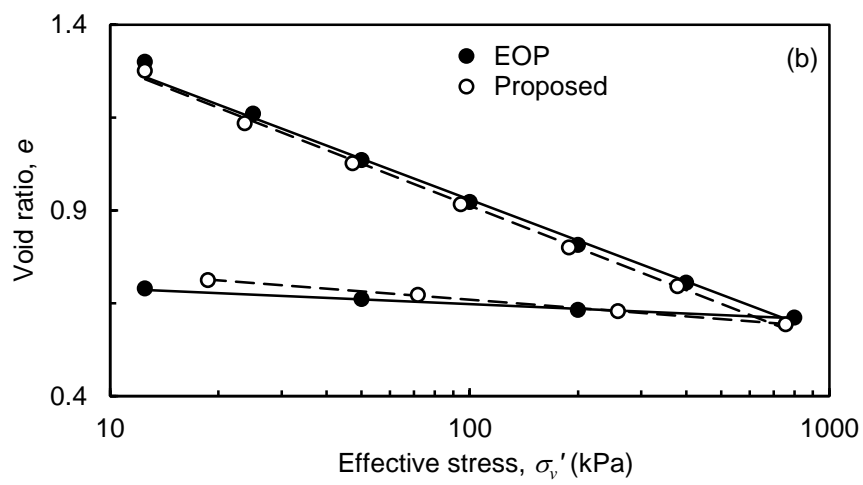
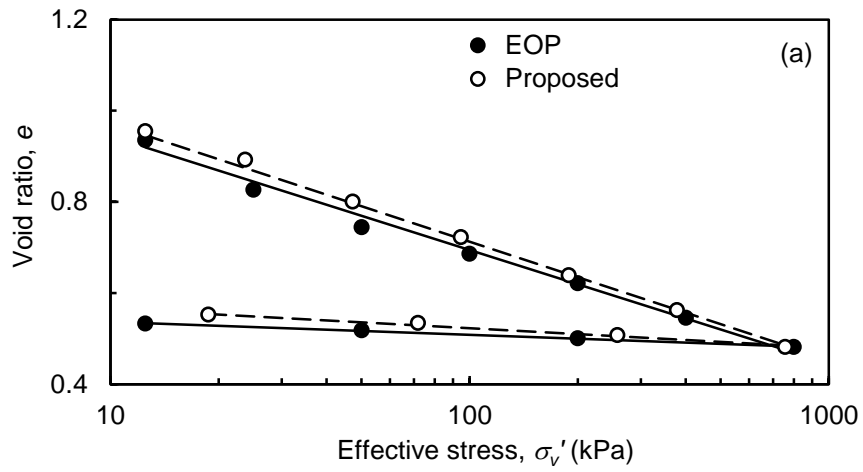


Figure 7.4 contd...

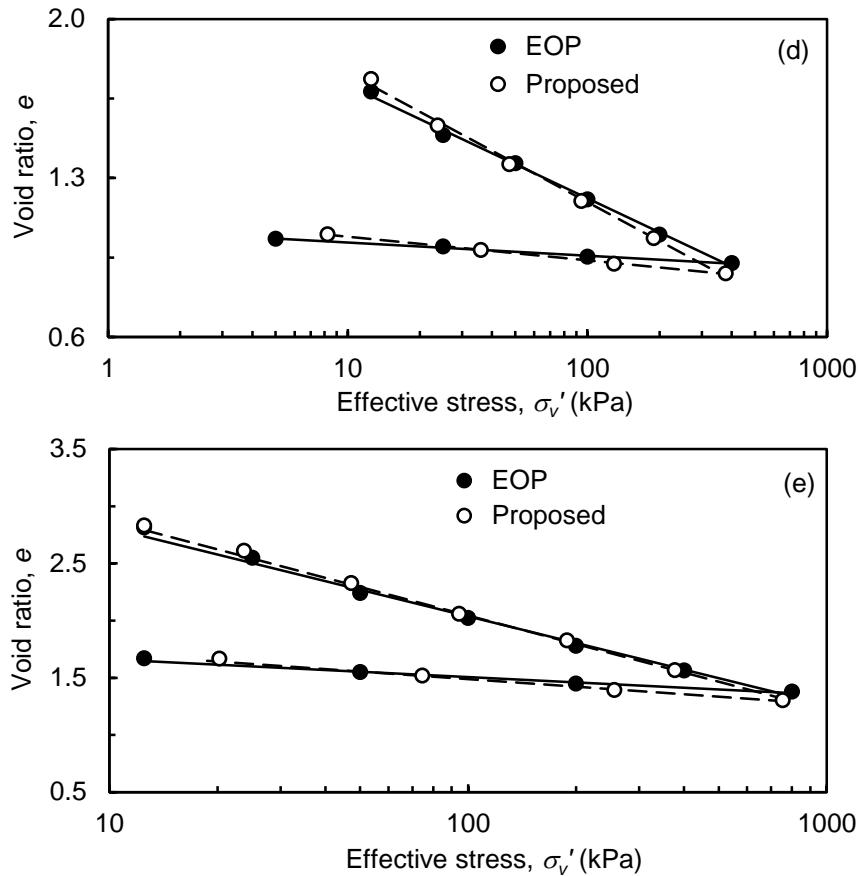


Figure 7.4: Comparison of  $e$ - $\log \sigma'_v$  curves of reconstituted soils obtained from the EOP and the proposed methods for (a) Red soil 1 (b) Red soil 2 (c) Gummudipoondi clay (d) Taramani clay and (e) Bombay marine clay

The total settlement parameters such as compression index ( $c_c$ ) and recompression index ( $c_r$ ) are obtained from the  $e$ - $\log \sigma'_v$  curves and are compared in Figure 7.5. Error analysis was carried out with reference to EOP test results. The average coefficient of variance (COV) of  $c_c$  is 3% but for  $c_r$  it is nearly 50%. Hence, it can be concluded that the compression index from both tests are practically the same for all the soils. But the values of recompression index obtained from the accelerated IL using the  $\sqrt{t}$  method is quite high that may be due to error in estimation of negative pore water pressure (Mair, 1979). An alternate procedure will be discussed in the later sections.

The values of coefficient of consolidation of reconstituted soils were determined using Taylor's  $\sqrt{t}$  curve fitting procedure for both EOP and accelerated tests and the values are compared in Figure 7.6. The plot clearly shows that the values are highly comparable. The average COV of  $c_v$  with reference to EOP test is 24%.

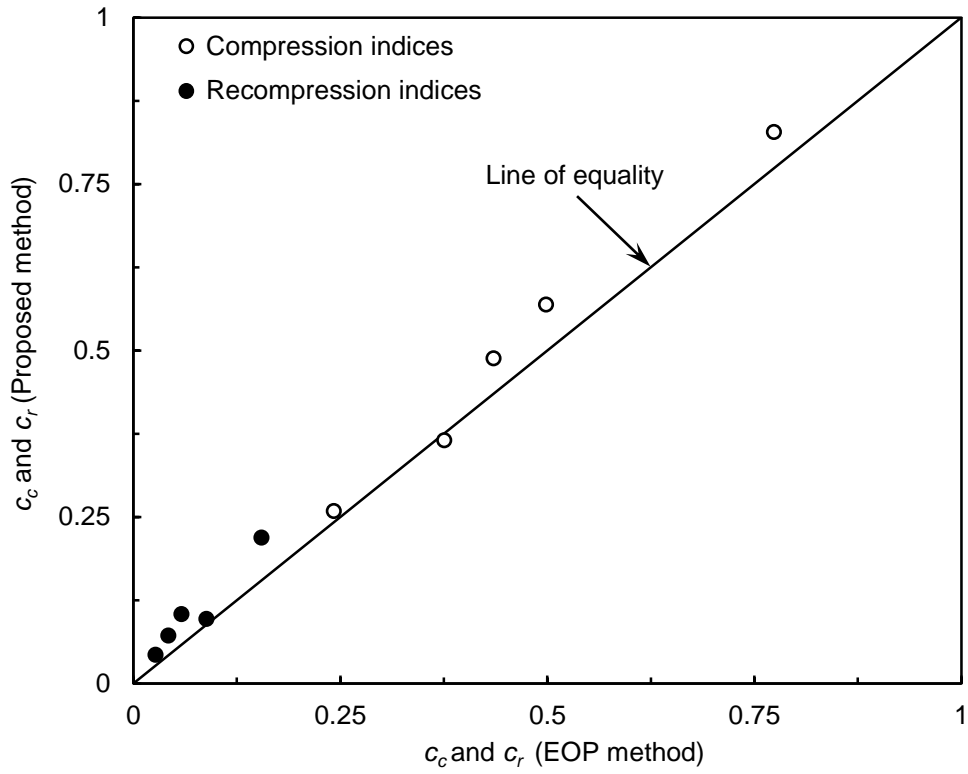


Figure 7.5: Comparison of values of compression index and recompression index obtained from the EOP and the  $\sqrt{t}$  methods

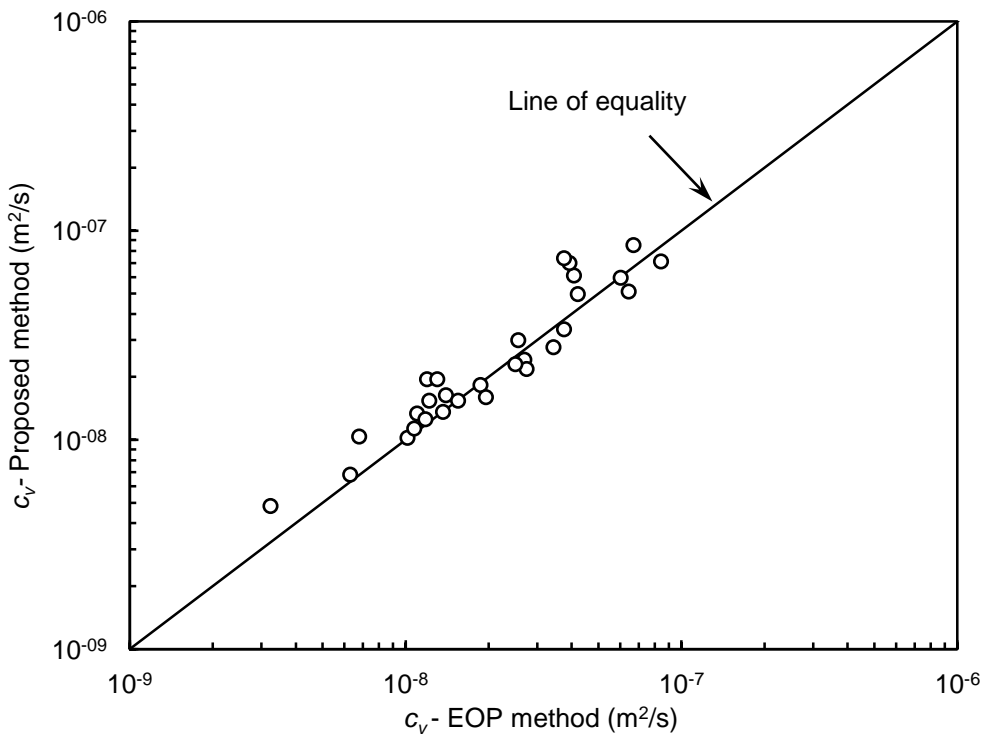


Figure 7.6: Comparison of  $c_v$  values from the EOP and the  $\sqrt{t}$  tests of reconstituted soils

### ***Results from undisturbed soils***

The proposed method was also validated for the selected undisturbed soils. The  $e$ - $\log \sigma_v'$  curves from the proposed method and EOP method are shown in Figures 7.7(a-c) and the comparison is reasonable. The slight variation in the results is attributed to the sample variability. The total settlement parameters such as compression index ( $c_c$ ) and recompression index ( $c_r$ ) are obtained from the  $e$ - $\log \sigma_v'$  curves and are summarized in Table 7.2. The values of preconsolidation pressure ( $\sigma_c'$ ) of the undisturbed soils were determined using the  $\log(1+e)$  versus  $\log \sigma_v'$  plot proposed by Sridharan *et al.* (1991). The values of preconsolidation pressure are also summarized in Table 7.2. The  $c_c$ ,  $c_r$  and  $\sigma_c'$  values are comparable, lending support to the validity of the accelerated IL test using Taylor's  $\sqrt{t}$  method. The values of coefficient of consolidation of undisturbed soils were also determined using Taylor's  $\sqrt{t}$  curve fitting procedure for both EOP and accelerated tests and the values are compared in Figure 7.8. The plot clearly shows that the values are highly comparable.

### ***Time required for completion of test***

The time required for performing the accelerated test during loading and unloading stages for all the soils are given in Table 7.3. It is seen that the duration required to complete the test depends on the coefficient of consolidation of the soil, as is expected. The duration required for completion of test for soils with values of coefficient of consolidation greater than about  $3 \times 10^{-8} \text{ m}^2/\text{s}$  requires only about 2 to 5 hours. For low permeable soils, with  $c_v < 3 \times 10^{-8} \text{ m}^2/\text{s}$ , the duration required is higher. Even for such soils, the total duration required for both loading and unloading stages is only about 30 hours compared to 10 to 14 days. The time required during unloading stage is quite high for soils with very low values of coefficient of consolidation. If tests are conducted with emphasis on loading part alone, the tests could be completed within about 7 hours even for very low permeable soils. It may be noted that some soils may not show initial straight line portion in the  $\sqrt{t}$  plot. For such soils the method is not applicable.

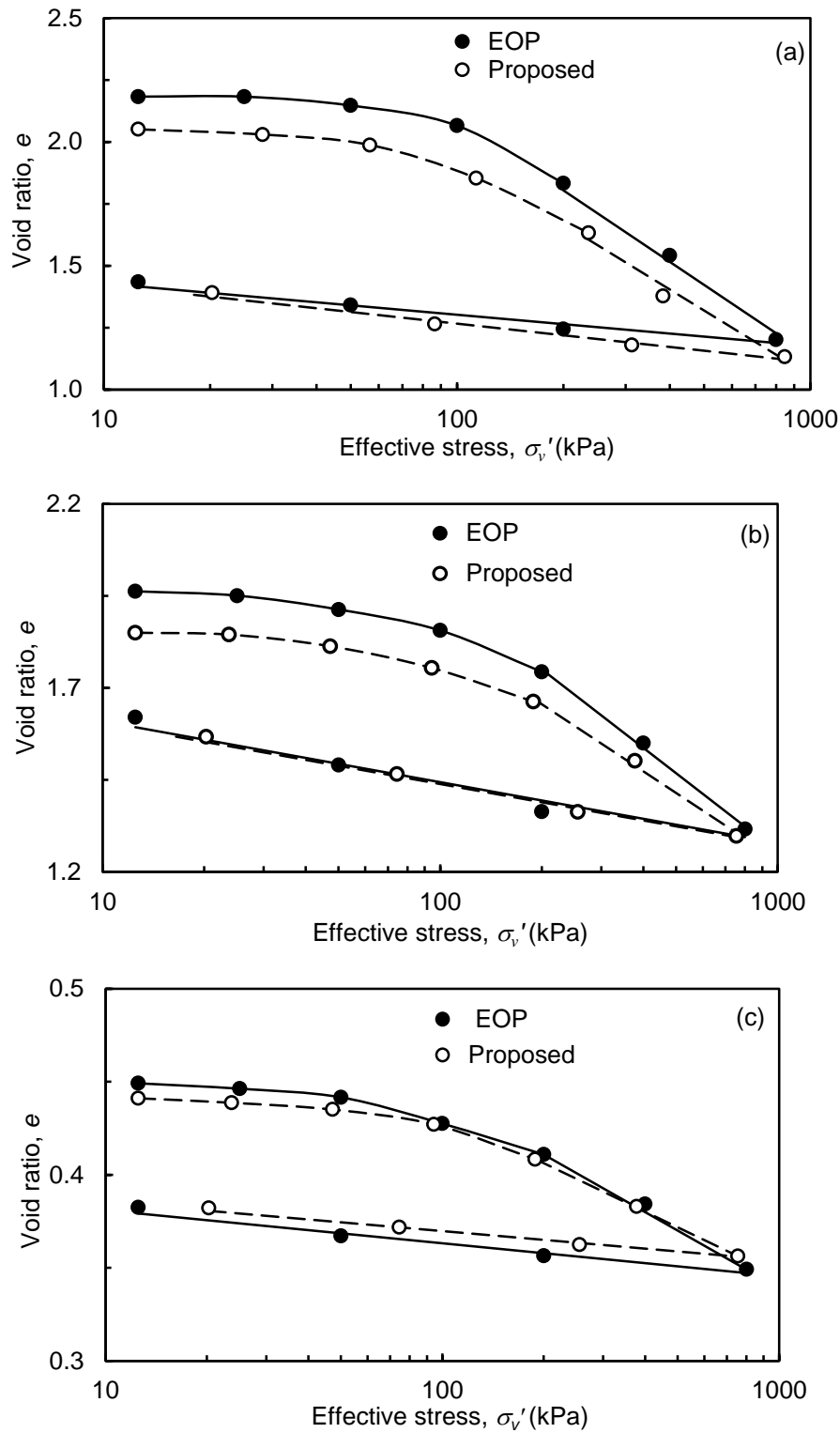


Figure 7.7: Comparison of  $e$ - $\log \sigma'_v$  curves of undisturbed soils obtained from the conventional IL consolidation test and the  $\sqrt{t}$  method for (a) Cochin marine clay (5 m) (b) Bombay marine clay (12 m) and (c) Madhavaram clay (6 m)



Table 7.2: Values of compression index, recompression index and preconsolidation pressure from the EOP test and proposed test

Sl. No.	Soil	$c_c$		$c_r$		$\sigma_c'$ (kPa)	
		EOP	Proposed	EOP	Proposed	EOP	Proposed
1	CMC (5 m)	0.957	0.881	0.126	0.156	85	90
2	BMC (12 m)	0.709	0.606	0.165	0.164	120	120
3	MC (6 m)	0.087	0.081	0.017	0.016	120	100

Note: CMC-Cochin marine clay, BMC- Bombay marine clay, MC- Madhavaram clay

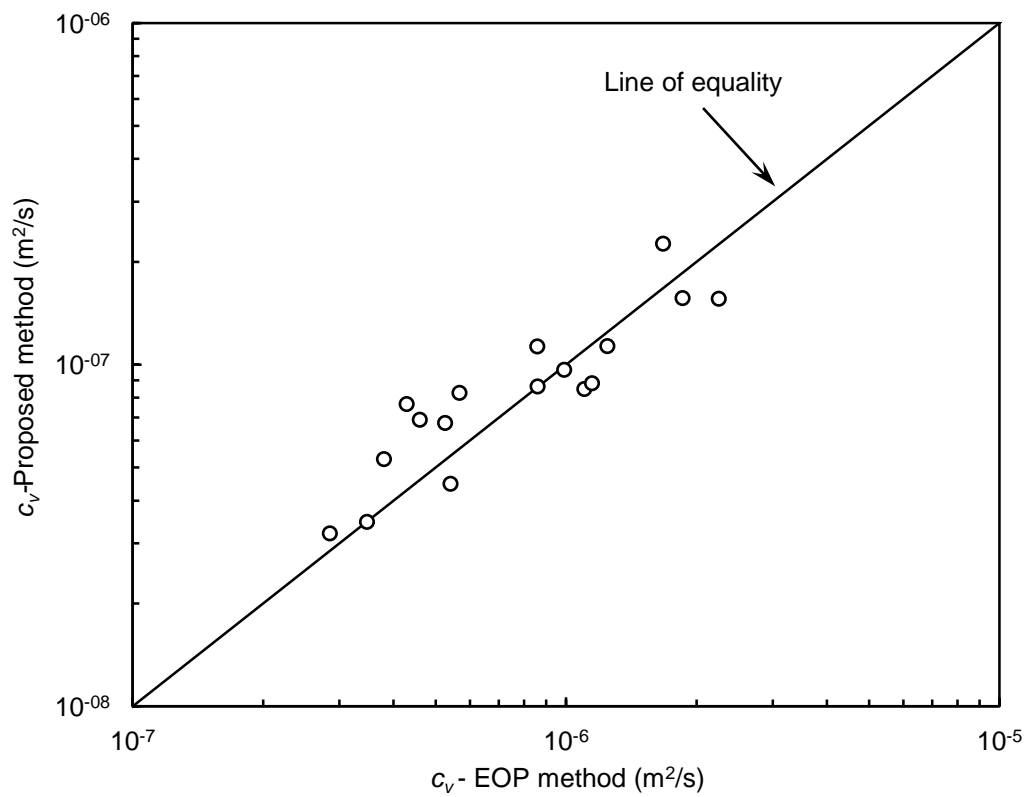


Figure 7.8: Comparison of  $c_v$  values from the EOP and  $\sqrt{t}$  methods for undisturbed soils

Table 7.3: Time required for the consolidation test as the proposed  $\sqrt{t}$  method

Sl. No.	Soil Type	Range of $c_v$ , $m^2/s$	Number of increments		Time taken, hours		
			Load	Unload	Load	Unload	Total
1	Red soil 1	$3 \times 10^{-8}$ - $9 \times 10^{-8}$	6	3	2.5	0.5	3.0
2	Red soil 2	$1 \times 10^{-8}$ - $3 \times 10^{-8}$	6	3	7.0	1.5	8.5
3	Gummudipoondi Clay	$2 \times 10^{-8}$ - $5 \times 10^{-9}$	6	3	11	19	30
4	Taramani Clay	$2 \times 10^{-8}$ - $1 \times 10^{-8}$	5	3	7.0	6.0	13
5	Bombay marine clay	$2 \times 10^{-8}$ - $7 \times 10^{-7}$	6	3	3.25	1.25	4.5
6	Cochin marine clay (5 m)	$2 \times 10^{-7}$ - $5 \times 10^{-8}$	6	3	1.75	1.75	3.5
7	Bombay marine clay (12 m)	$9 \times 10^{-8}$ - $3 \times 10^{-8}$	6	3	2.5	2.5	5.0
8	Madhavaram clay (6 m)	$2 \times 10^{-7}$ - $1 \times 10^{-7}$	6	3	1.5	0.5	2.0

### 7.3 ACCELERATED IL TEST USING INFLECTION POINT METHOD

It was noted in the previous section that the time taken to complete the accelerated consolidation test using the  $\sqrt{t}$  method can be as high as 30 hours for soils with very low permeability. It would be ideal if the consolidation test is completed within the working hours of a day (8 to 9 hours) itself. Review of the literature shows that for inflection point method (Cour, 1971; Robinson, 1997; Mesri *et al.* 1999) the characteristic feature can be identified at a degree of consolidation of  $U = 70.15\%$ . In other words, the test using inflection point method can be about two times faster than the  $\sqrt{t}$  method as the ratio of time factors corresponding to  $U = 90\%$  and  $U = 70.15\%$  is 2.09 ( $=0.848/0.405$ ). Therefore, the applicability of the inflection point method as rapid consolidation test method is also explored in this chapter.

Mesri *et al.* (1999) reported that most soils show the inflection point, both during the recompression and compression ranges, for tests conducted at a pressure increment ratio of unity. Therefore, inflection point method is selected for further reducing the testing time of the IL consolidation test. The validity of the testing procedure is verified by performing series of tests on six reconstituted soils and three undisturbed soils.

#### 7.3.1 Theoretical Considerations

In the inflection point method, the subsequent pressure increment is applied once the sample reached the inflection point in the Settlement ( $S$ )-logarithm of time ( $t$ ) plot. From the time required to reach the inflection point ( $t_i$ ) and the length of drainage path ( $d$ ), the value of the coefficient of consolidation  $c_v$  can be obtained from Eq. (7.6) as

$$c_v = \frac{T_i d^2}{t_i} \quad (7.6)$$

where,  $T_i$  is the time factor corresponding to the inflection point which is equal to 0.405.

The specimen is consolidated to degree of consolidation of upto 70.15% only. Therefore, there will be excess pore pressure within the specimen, which is required to

correct the effective stress. The excess pore pressure can be estimated as per Terzaghi's one-dimensional consolidation theory (Terzaghi, 1925). The detailed estimation of excess pore pressure developed at the mid plane of the specimen is discussed in section 7.2.2 for the  $\sqrt{t}$  method. In the similar way, the pore pressure distribution when the specimen reached the inflection point is shown in Figure 7.9.

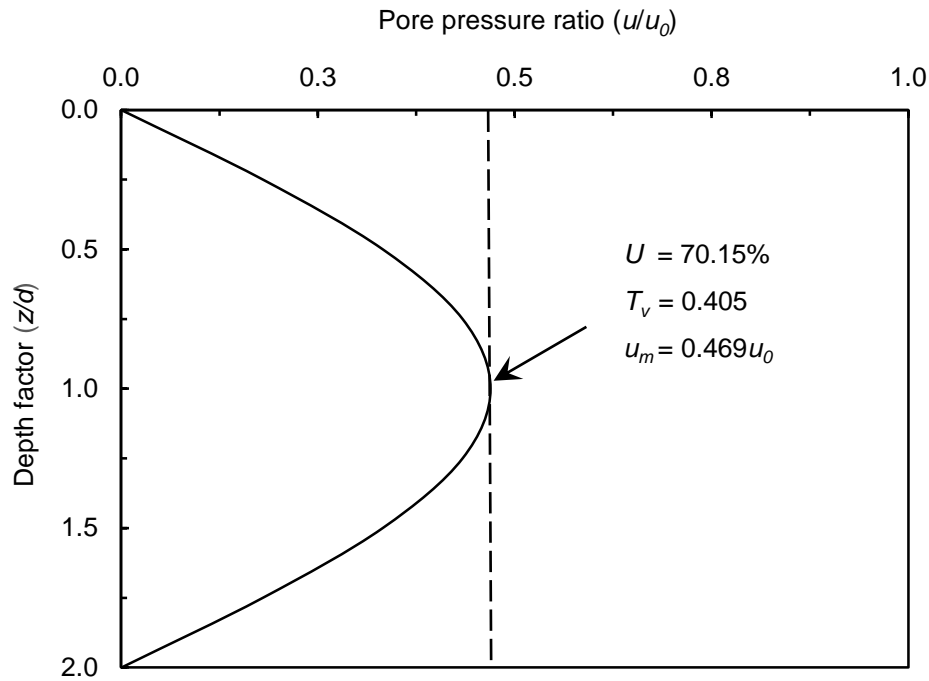


Figure 7.9: Variation of pore pressure ratio ( $u/u_0$ ) with ( $z/d$ )

The mid-plane pore pressure at  $U = 70.15\%$ , for double drainage condition is obtained as

$$u_m = 0.469u_0 \quad (7.7)$$

where, the initial pore pressure ( $u_0$ ), includes the sum of the current pressure increment ( $\Delta\sigma_{vi}$ ) and the average residual pore pressure ( $u_{ri}$ ) that was present in the previous increment due to partial dissipation of pore pressure. By knowing the mid-plane pore pressure at  $U = 70.15\%$ , the effective stress can be calculated using Eq. (7.1).

### 7.3.2 Experimental Programme

Five reconstituted and three undisturbed soil samples (UDS) were selected for the study. The reconstituted soils selected were Red soil 1, Red soil 2, Gummudipoondi clay,

Taramani clay and Bombay marine clay. Three undisturbed soils were also collected, namely Cochin marine clays (sampled at 19.5 m and 16 m) and Madhavaram clay (sampled at 6 m). The basic properties of the selected soils and the sample preparation procedure were discussed in Chapter 3 (section 3.3). The one-dimensional consolidation tests were conducted using the conventional consolidation cell with a ring size of 60 mm diameter and 20 mm thickness under double drainage. Two identical reconstituted soil specimens were prepared for each soil. The undisturbed soil specimens were directly placed in the consolidation ring.

One-dimensional consolidation test with loading duration up to the end-of-primary (EOP) consolidation was conducted on the first specimen, as the control test. The EOP testing procedure and the results were already discussed in Chapter 3. The second specimen was subjected to the proposed inflection point method. The inflection point occurs at a degree of consolidation of 70.15% which can be obtained from the time-settlement data (Robinson, 1997) from a plot of  $(\Delta S/\Delta \log t)$  versus  $\log t$  as shown in Figure 7.10. Inflection point is the peak point where the slope changes. Once the inflection point was identified the subsequent load increment was applied. The same procedure was adopted for unloading stages also.

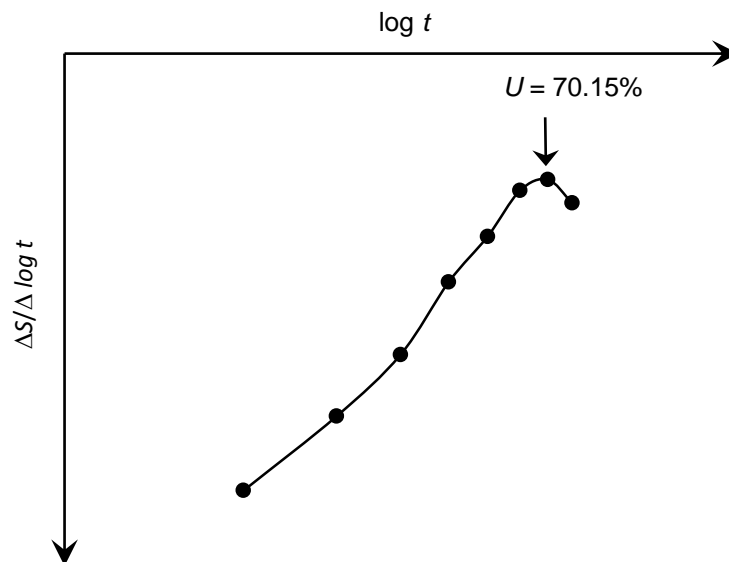


Figure 7.10: Identification of inflection point

### 7.3.3 Results and Discussions

#### *Results from reconstituted soils*

The time-settlement data for the selected reconstituted soils for accelerated IL test using inflection point method are given in Appendix F. The coefficient of consolidation ( $c_v$ ) values were obtained from the time-settlement data. The  $c_v$  values from the EOP consolidation test and the proposed procedure are compared in Figure 11. The values from the proposed method are comparable with the EOP consolidation test. With reference to EOP consolidation test, the coefficient of variance of  $c_v$  is 21%.

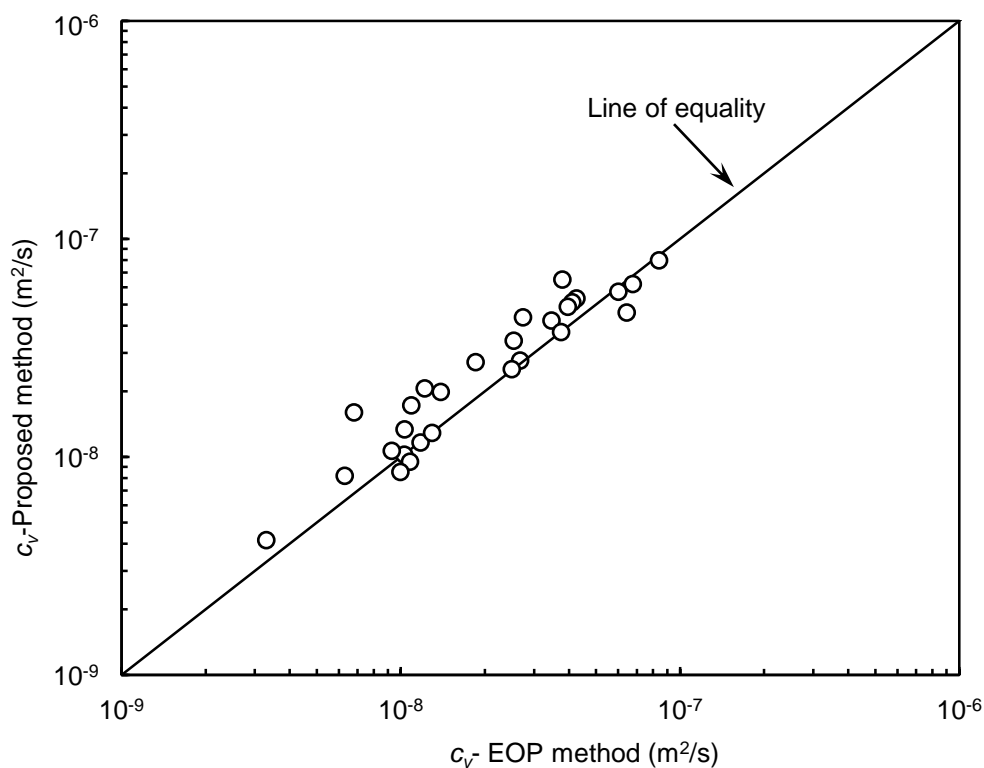


Figure 7.11: Comparison of coefficient of consolidation from the EOP and the proposed methods

The  $e$ - $\log \sigma'_v$  curves of the reconstituted soil specimens are shown in Figures 7.12(a-e). The comparison of the results in the loading phases is very good. However, the unloading curve is steeper than those obtained from the EOP test results similar to the  $\sqrt{t}$  method. The values of the compression index and recompression index obtained from the  $e$ - $\log \sigma'_v$  curves are compared in Figure 7.13. The average COV of  $c_c$  from the proposed method is only 4% with reference to EOP test. However, the average COV of  $c_r$  is nearly 65%. This

suggests that the estimated negative pore pressure based on Terzaghi's one-dimensional consolidation theory may not be appropriate. In order to further evaluate the accuracy of estimating the mid-plane pore pressure using the proposed procedure using Eq. (7.8), further experiments were carried out using Row cell (Rowe and Barden, 1966) with pore pressure measurements.

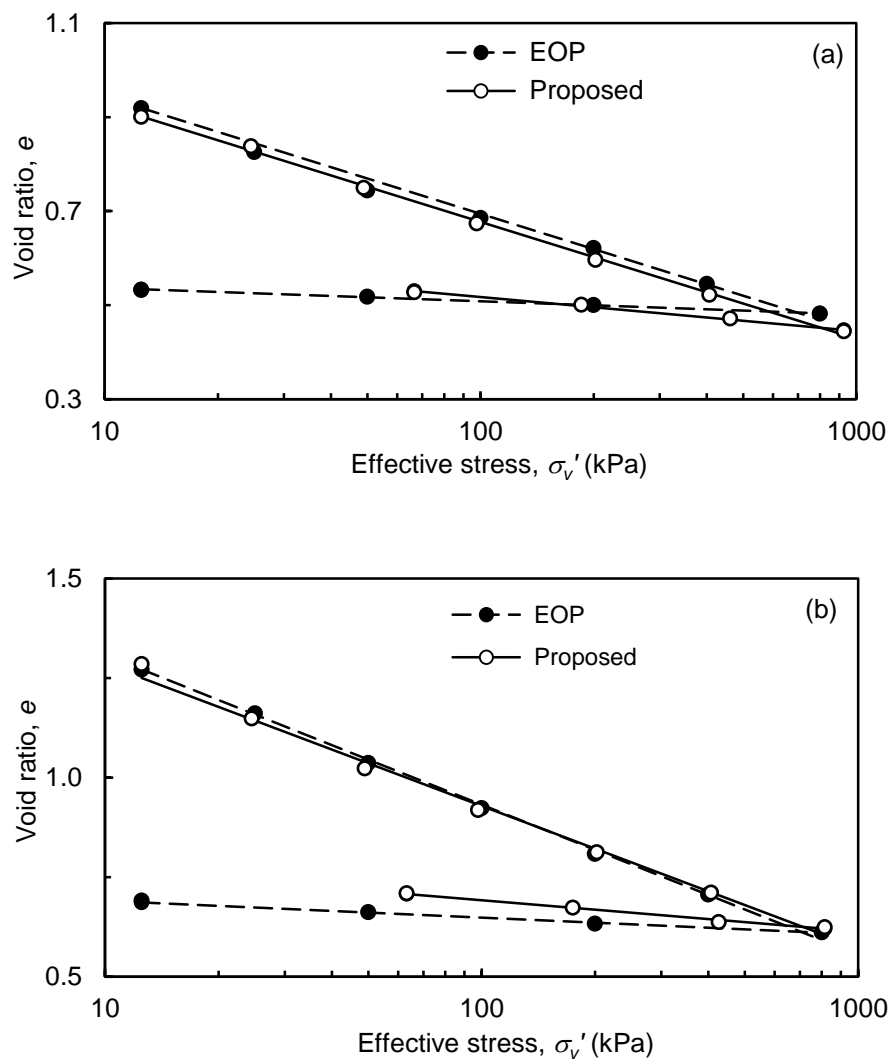


Figure 7.12 contd...

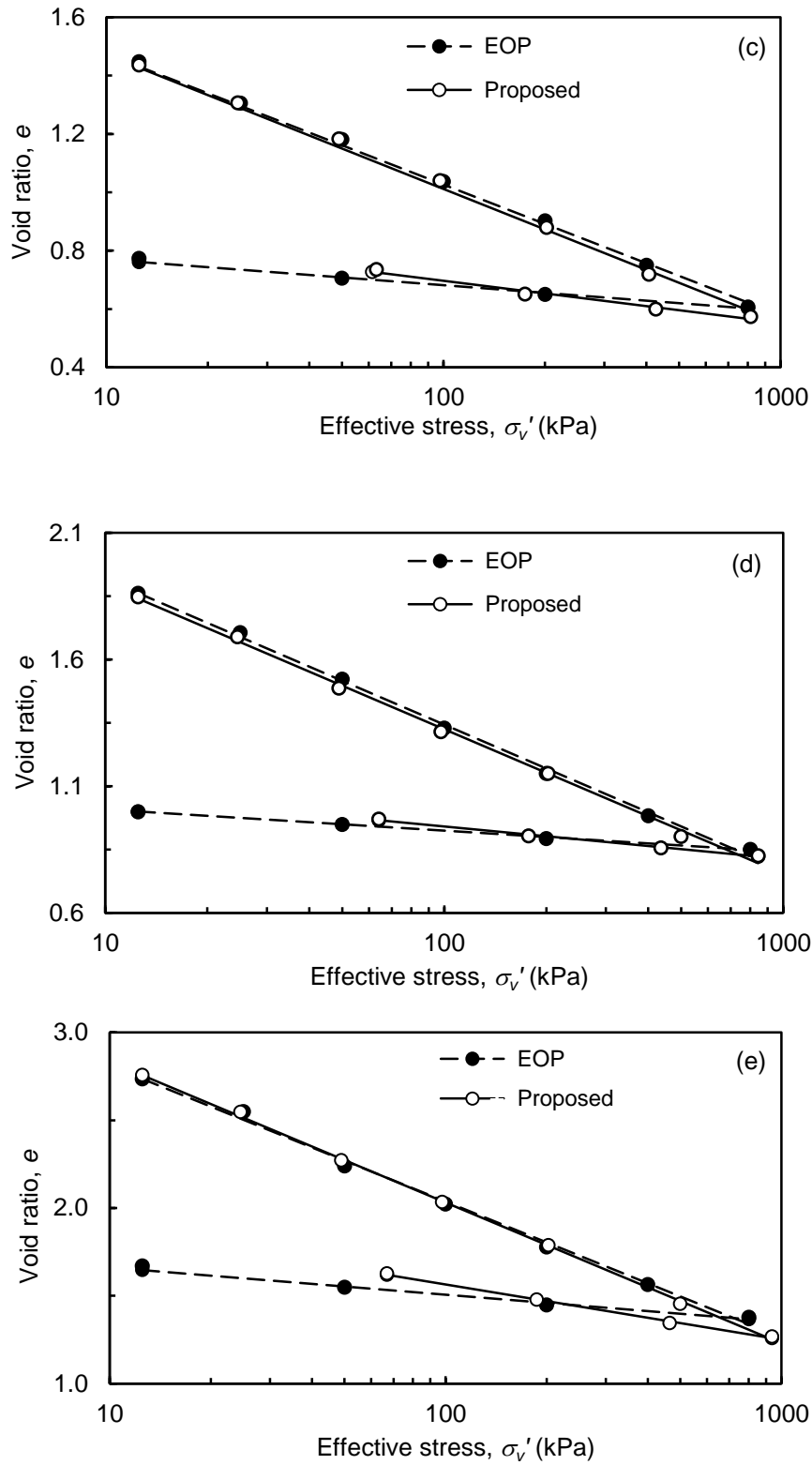


Figure 7.12: Comparison of  $e$ - $\log \sigma_v'$  curves of reconstituted soils from the EOP and the proposed tests for (a) Red soil 1 (b) Red soil 2 (c) Gummudipoondi clay (d) Taramani clay and (e) Bombay marine clay



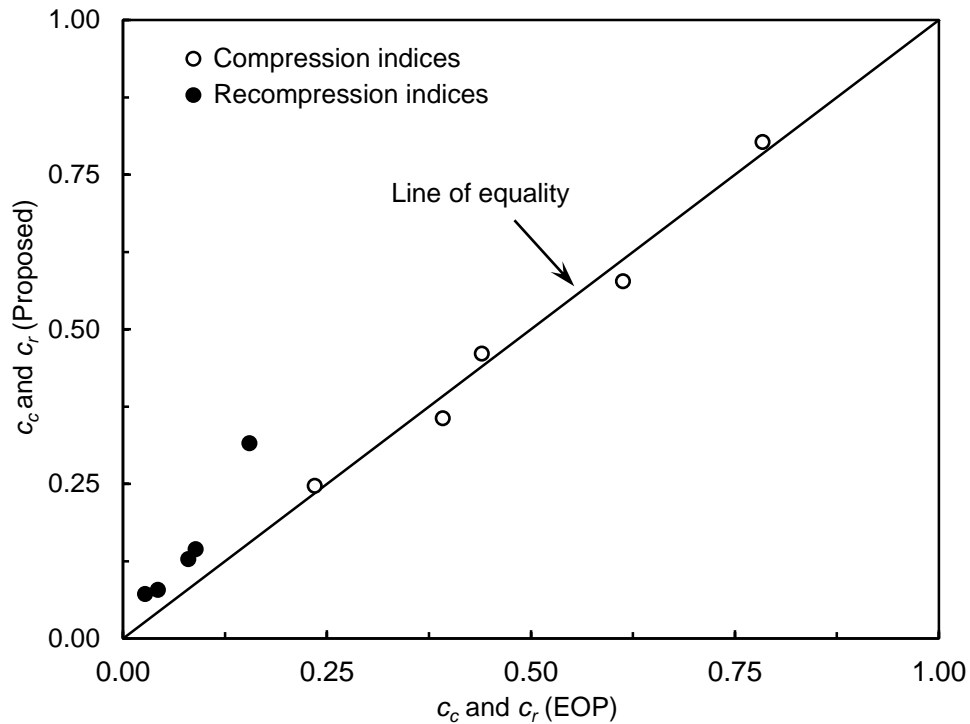


Figure 7.13: Comparison of Compression index and Recompression index obtained from the EOP and the proposed methods of reconstituted soils

#### *Tests Using Rowe Cell*

In order to validate the estimated pore pressure using Eq. (7.8), a set of experiments was conducted using Rowe cell (Rowe and Barden, 1966) of 100 mm diameter in which base pore pressure can be measured during the test. In the Rowe cell, tests will be conducted in one way drainage condition so as to measure the pore pressure at the bottom of the specimen. The thickness of the specimen used was 32 mm. In other words, the pore pressure measured at the base of the specimen is equivalent to the mid-plane pore pressure in a specimen of 64 mm thickness. The specimen of kaolinite, which has relatively high permeability, was selected as a representative soil so that the tests could be completed within a reasonable time. Tests were conducted for pressure increments of 25-50, 50-100 and 100-200 kPa and then unloaded to pressure range of 200-50 and 50-12.5 kPa. A back pressure of 100 kPa was applied through the top drainage line. Initially, the drainage valves were closed and the pressure increment was applied for pore pressure equilibration. Then, the specimen was allowed to consolidate through the top drainage and the settlement ( $S$ ) and base pore pressure ( $u_b$ ) were continuously monitored.

Two identical specimens were prepared for the test. The first specimen was used as the control sample, in which IL consolidation test was conducted so as to obtain the EOP consolidation parameters as per Terzaghi *et al.* (1996). The pore pressure at the bottom of the specimen was continuously monitored during consolidation. When the excess pore pressure dissipates to zero or to a very small value of about 1 kPa, the specimen state is said to be at the end-of-primary (EOP) consolidation (Terzaghi *et al.* 1996). Once EOP consolidation was identified, the next increment was applied. Similar procedure was adopted during unloading stages also. The second specimen was subjected to the proposed procedure with one-way drainage, in which the subsequent increment was applied once the specimen reached the inflection point. In this test also the pore pressure developed at the base of the specimen was continuously monitored.

The time–settlement and time–pore water pressure curves obtained during loading from the proposed method (second specimen) are shown in Figures 7.14(a) and 7.14(b), respectively. The predicted time-settlement curve using Terzaghi’s theory closely matches with the observed curve. The predicted base pore pressure during loading, corresponding to the inflection point, also matches very well with the measured data (Table 7.4). The average coefficient of variance of measured base pore pressure with reference to predicted base pore pressure is only 6%. As seen in Figure 7.14(c), the  $e$ - $\log \sigma_v'$  curves obtained from the proposed procedure matches very well with the end-of-primary consolidation test (control test) in the loading phase. The values of compression index ( $c_c$ ) are practically the same (Table 7.5), confirming the validity of the proposed method.

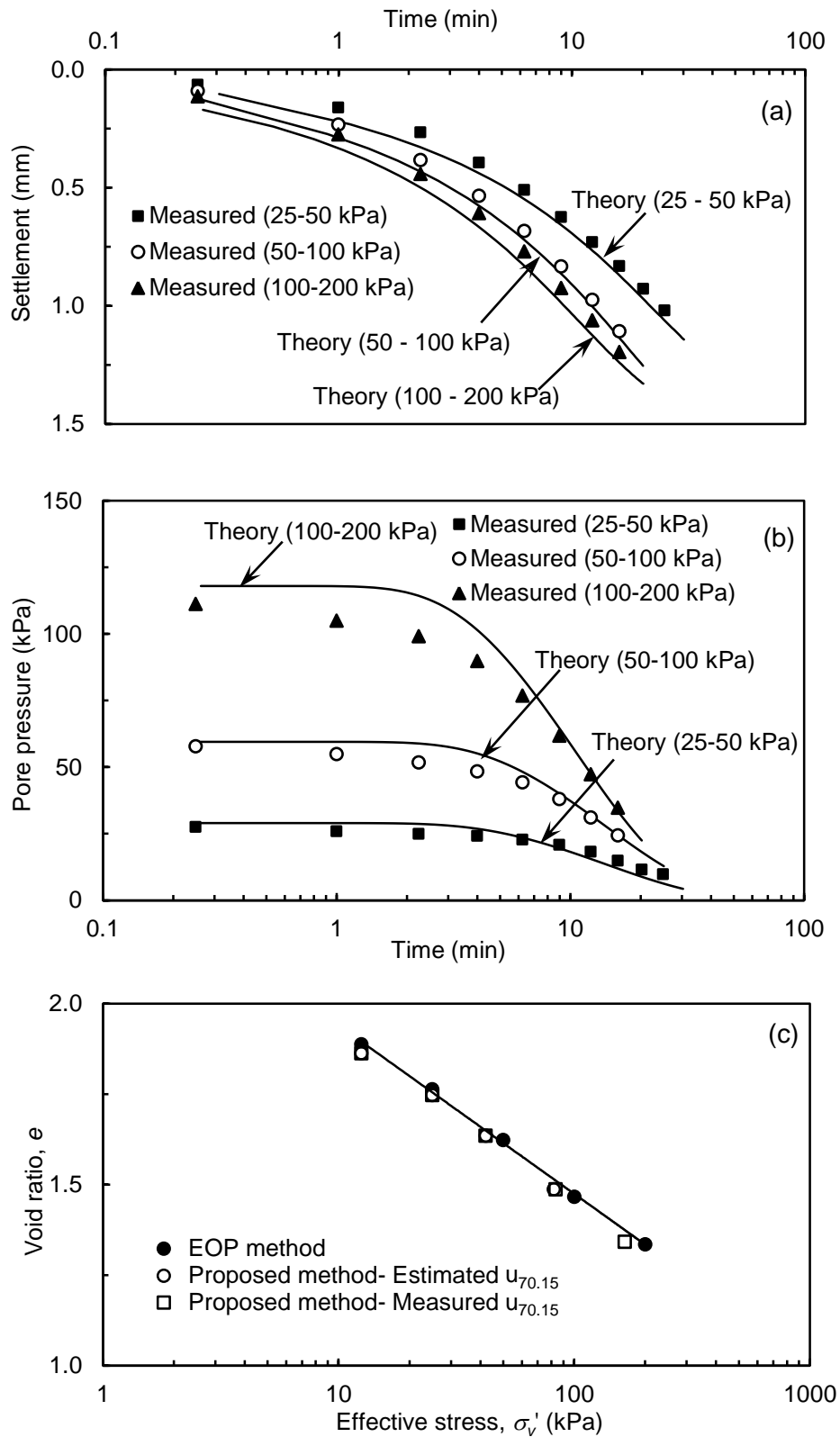


Figure 7.14: (a) Time-settlement curve (b) Time-pore pressure curve and (c)  $e$ - $\log \sigma'_v$  for Kaolinite during loading stages

Table 7.4: Details of Pore water pressure measurements and estimate

Stage	Applied pressure	Pore pressure, kPa			
	range, kPa	Measured		Predicted	
	$\sigma_v$	$u_0$	$u_{70.15}$	$u_0$	$u_{70.15}$
Loading	12.5-25	13	-	-	-
	25-50	24	11.9	25	11.7
	50-100	54.9	24.9	57.8	27.1
	100-200	109.0	54.3	118.1	55.4
Unloading	200-50	-43.5	-6.2	-113.0	-53.0
	50-12.5	-32	-2.4	-72.8	-34.2

Table 7.5: Compression index and recompression index values for Kaolinite

Method	$c_c$	$c_r$
EOP consolidation method	0.481	0.019
Proposed method with measured $u_{70.15}$	0.496	0.017
Proposed method with estimated $u_{70.15}$	0.499	0.027
Proposed method based on swell estimation	---	0.018

Similarly, the time-swelling and time-negative pore pressure curves during the unloading stages are shown in Figures 7.15(a) and 7.15(b), respectively. Terzaghi's theory is able to predict the time-swelling behaviour during the unloading stages reasonably well. However, the measured pore pressure values deviate significantly from the theoretical predictions. The coefficient of variance of the measured negative pore pressure with reference to predicted pore pressure is nearly 75%. The initial pore pressure measured is also lower than the predicted pore pressure. In addition, the measured pore pressure dissipates much faster than the predicted values. The predicted value of negative pore pressure at the inflection point is very different as seen in Table 7.4. The  $e$ - $\log \sigma_v'$  plot during the unloading stages are shown in Figure 7.15(c).

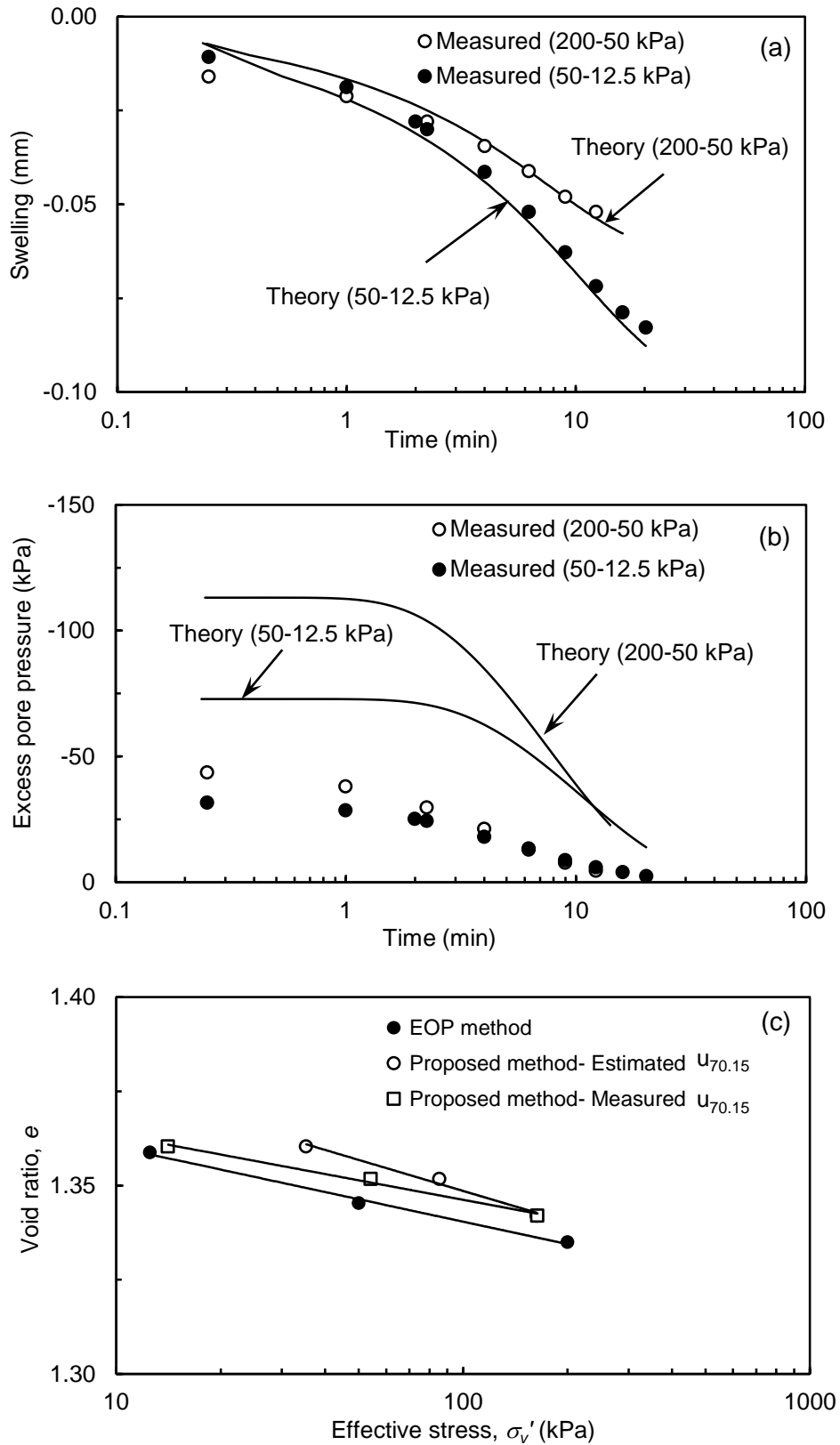


Figure 7.15: (a) Time-swelling curve (b) Time-negative pore pressure curve and (c)  $e$ - $\log \sigma'_v$  for Kaolinite during unloading stages

The recompression index ( $c_r$ ) values based on the estimated pore pressure is considerably higher while that based on the pore pressure measurement is closer to the values from the conventional test (Table 7.4). This suggests that the estimated negative pore pressure based on Terzaghi's one-dimensional consolidation theory is not appropriate. Mair (1979) studied the unloading response of a laterally confined sample and reported that the swelling is not always one-dimensional. During unloading, if the total vertical stress is zero, the total horizontal stress ( $\sigma_{hu}$ ) can be determined as (Mair, 1979):

$$\sigma_{hu} = \sigma'_{v0}(K_0 - 1) \quad (7.8)$$

where,  $K_0$  is the coefficient of earth pressure at rest. The value of  $K_0$  is less than unity for normally consolidated soils. Therefore, the total horizontal stress becomes negative leading to the development of a tensile stress between the clay and the consolidometer walls. If the pore pressure at the boundary cannot sustain the tensile stress, the specimen will separate from the consolidometer. Once separation occurs, the specimen deformation during unloading is no longer one-dimensional. Therefore, the magnitude of initial pore pressure developed will not be equal to the unloading decrement ( $\Delta\sigma'_v$ ) but will be equal to the change in mean effective stress,  $\Delta p'$  given as (Mair, 1979):

$$\Delta p' = \frac{(1 + 2K_0)}{3} \Delta\sigma'_v = -\Delta u \quad (7.9)$$

Assuming  $K_0 = (1 - \sin\phi')$ , the initial pore pressure is predicted as -77 kPa and -42 kPa for the pressure range of 200-50 kPa and 50-12.5 kPa, respectively. Even though the magnitude of the initial pore pressure predicted based on Eq. (7.7) is improved, the values are considerably higher than the measured values. This may be attributed to the fact that due to separation, water can enter through the side of the cell resulting in lesser development of negative pore pressure and faster dissipation. This could be the possible reason for the mismatch between the predicted and the observed negative pore pressure during unloading stages.

In order to avoid this complexity, another approach based on ultimate swelling estimation is proposed as explained below:

Let  $\sigma_i$  be the present consolidation pressure and  $\sigma_{i-1}$  be the pressure after unloading. If  $(\delta_{70.15})_{i-1}$  is the magnitude of swelling corresponding to the inflection point for the unloading pressure range of  $(\sigma_i - \sigma_{i-1})$ , the expected ultimate swelling  $(\delta_{100})_{i-1}$  under  $\sigma_{i-1}$  is,

$$(\delta_{100})_{i-1} = \frac{(\delta_{70.15})_{i-1}}{70.15} \times 100 \quad (7.10)$$

If  $H_i$  is the thickness of the specimen under consolidation pressure of  $\sigma_i$ , the expected thickness of the specimen  $H_{i-1}$  at the end of swelling under  $\sigma_{i-1}$  is

$$H_{i-1} = H_i + (\delta_{100})_{i-1} \quad (7.11)$$

By knowing  $H_{i-1}$ , the void ratio corresponding to  $\sigma_{i-1}$  is calculated and plotted in Figure 7.16. The value of  $c_r$  obtained based on swelling estimation is 0.018 (Table 7.5) which is very close to the value of 0.019 obtained from the EOP test. Guided by this, all the swelling data obtained in the present study were analysed based on ultimate swelling estimate as discussed in the next section.

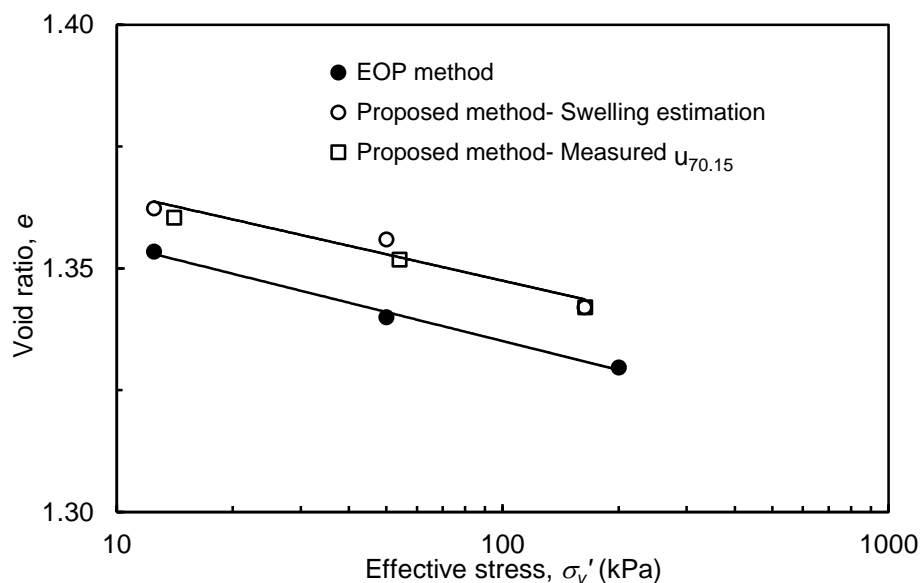


Figure 7.16: Swelling curve based on the ultimate swelling estimate for kaolinite

*Swelling curves of reconstituted samples using ultimate swelling estimation*

Based on the ultimate swelling estimation, the swelling curves of the reconstituted samples were calculated and plotted in Figure 7.17. The comparison is much better compared to those presented in Figure 7.12(a-e). The values of  $c_r$  obtained are compared with EOP test in Figure 7.18. The comparison is very good and the coefficient of variance (COV) of  $c_r$  is reduced to 10% from 65%. Therefore, the values of  $c_r$  obtained based on ultimate swelling are better than those based on the pore pressure estimation.

Similarly, the swelling estimation is done for the  $\sqrt{t}$  method, discussed in the previous section and the  $c_r$  values were computed in Figure 7.19. The average COV got reduced to 3% from 50%.

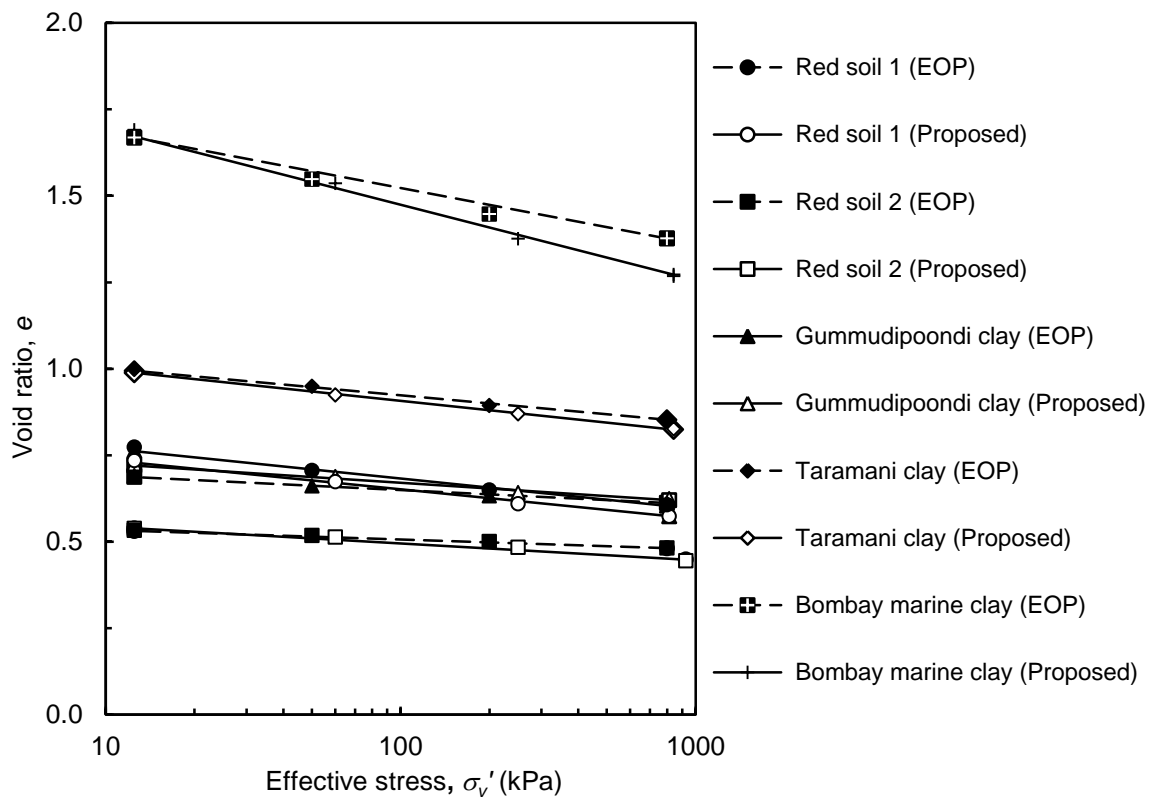


Figure 7.17: Swelling curves from the EOP method and the proposed method using inflection point method based on the ultimate swelling



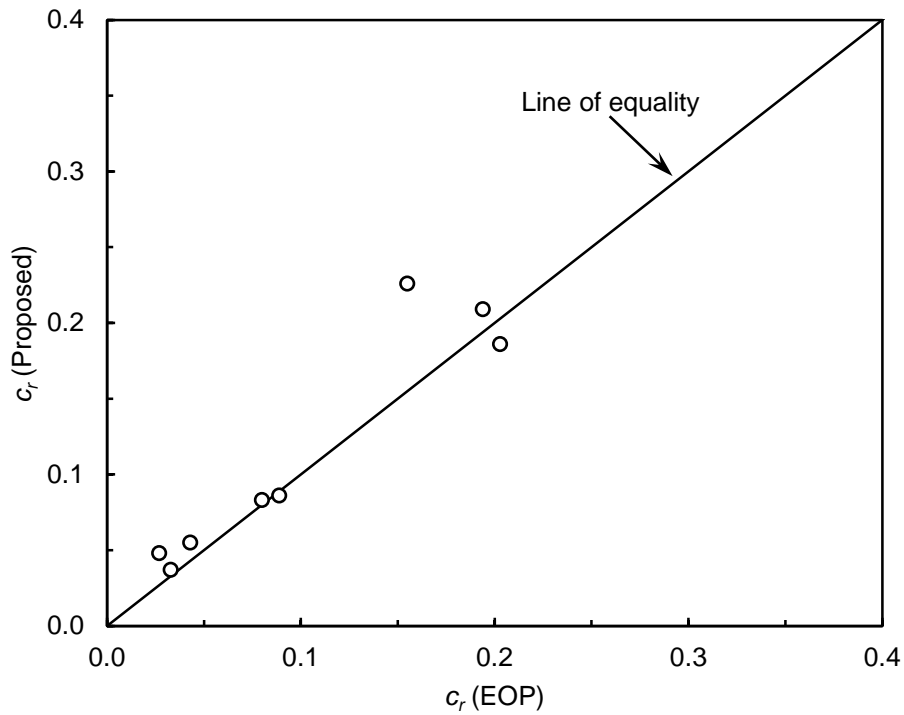


Figure 7.18: Recompression index obtained from the EOP method and the proposed method (Inflection point method) based on the ultimate swelling estimation of reconstituted soils

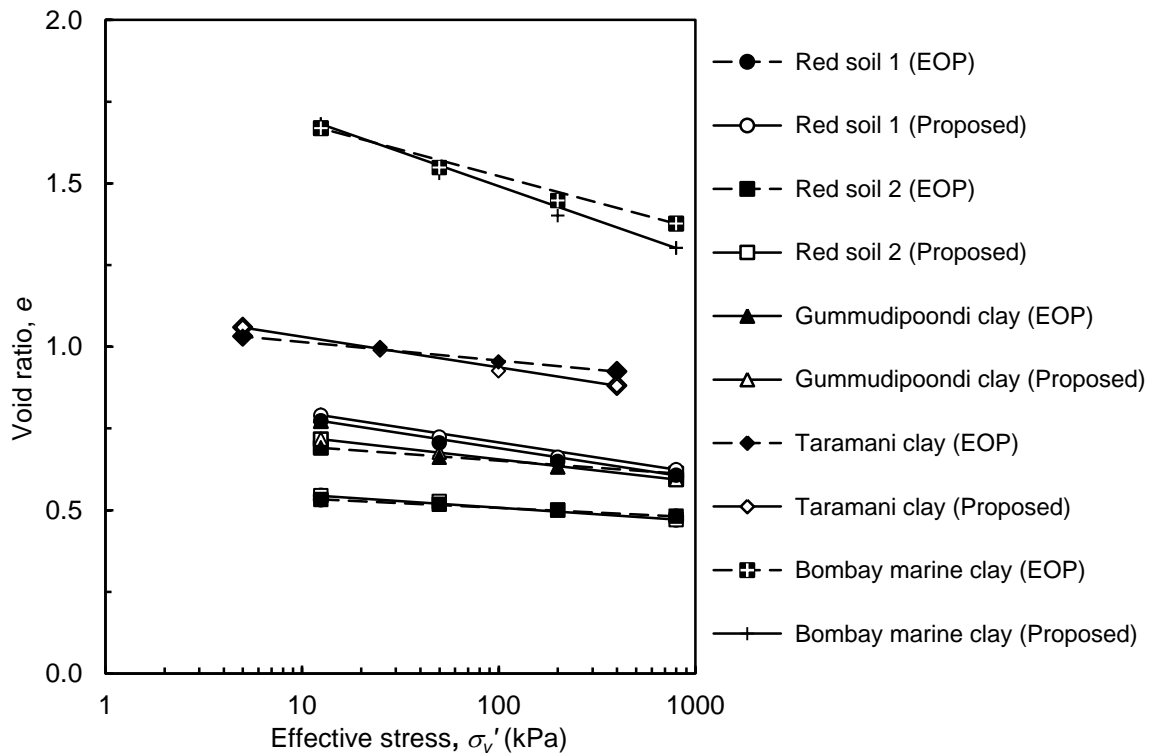


Figure 7.19: Swelling curves from the EOP method and the proposed method using  $\sqrt{t}$  method based on the ultimate swelling estimation of reconstituted soils

### **Results from undisturbed Soils**

The  $e$ - $\log \sigma_v'$  curves of undisturbed soils obtained from the EOP and proposed method are shown in Figure 7.20. The loading part is interpreted using the pore pressure estimate and the unloading by the swelling estimate. The comparison is reasonable. The deviation in the results may be attributed to the variability between specimens. The values of compression index and recompression index are summarized in Table 7.6. The preconsolidation pressure of the undisturbed specimens was determined by the  $\log(1+e)$  versus  $\log \sigma_v'$  plot (Sridharan *et al.* 1991). The values are comparable with the conventional one-dimensional consolidation test, with load duration up to EOP, as can be seen in Table 7.6. The slight variation of results in the preconsolidation pressure may be due to the variability between specimens and the error involved in its determination. The  $c_v$  values obtained from the proposed method tally well with the EOP test results as seen in Figure 7.21.

Table 7.6: Values of preconsolidation pressure,  $c_c$  and  $c_r$  from the EOP consolidation test and the proposed test (Inflection point method) for the undisturbed soils

Sl. No.	Soils	$\sigma_c'$ (kPa)		$c_c$		$c_r$	
		EOP	Proposed	EOP	Proposed	EOP	Proposed
1	CMC (21 m)	90	100	0.753	0.795	0.203	0.186
2	CMC (16 m)	100	90	1.125	1.076	0.194	0.209
3	MC (6 m)	90	90	0.135	0.136	0.033	0.037

Note: CMC-Cochin marine clay, MC-Madhavaram clay

### **Time Taken for Completion of Test**

The time required for completing the test for the selected soils is given in Table 7.7. For most of the soils, the time taken is less than 5 hours. Only for very low permeable soils, with  $c_v < 4 \times 10^{-9} \text{ m}^2/\text{s}$ , the total duration required is about 9 hours. When compared with the time required for EOP consolidation test, the proposed method is much faster by about 4 times. Clearly, the proposed procedure saves considerable time for one-dimensional consolidation testing and the test can be completed within the working hours of the day for most of the soils encountered in practice. If only loading part is required, the test could be completed within about 1.5 to 6 hours.

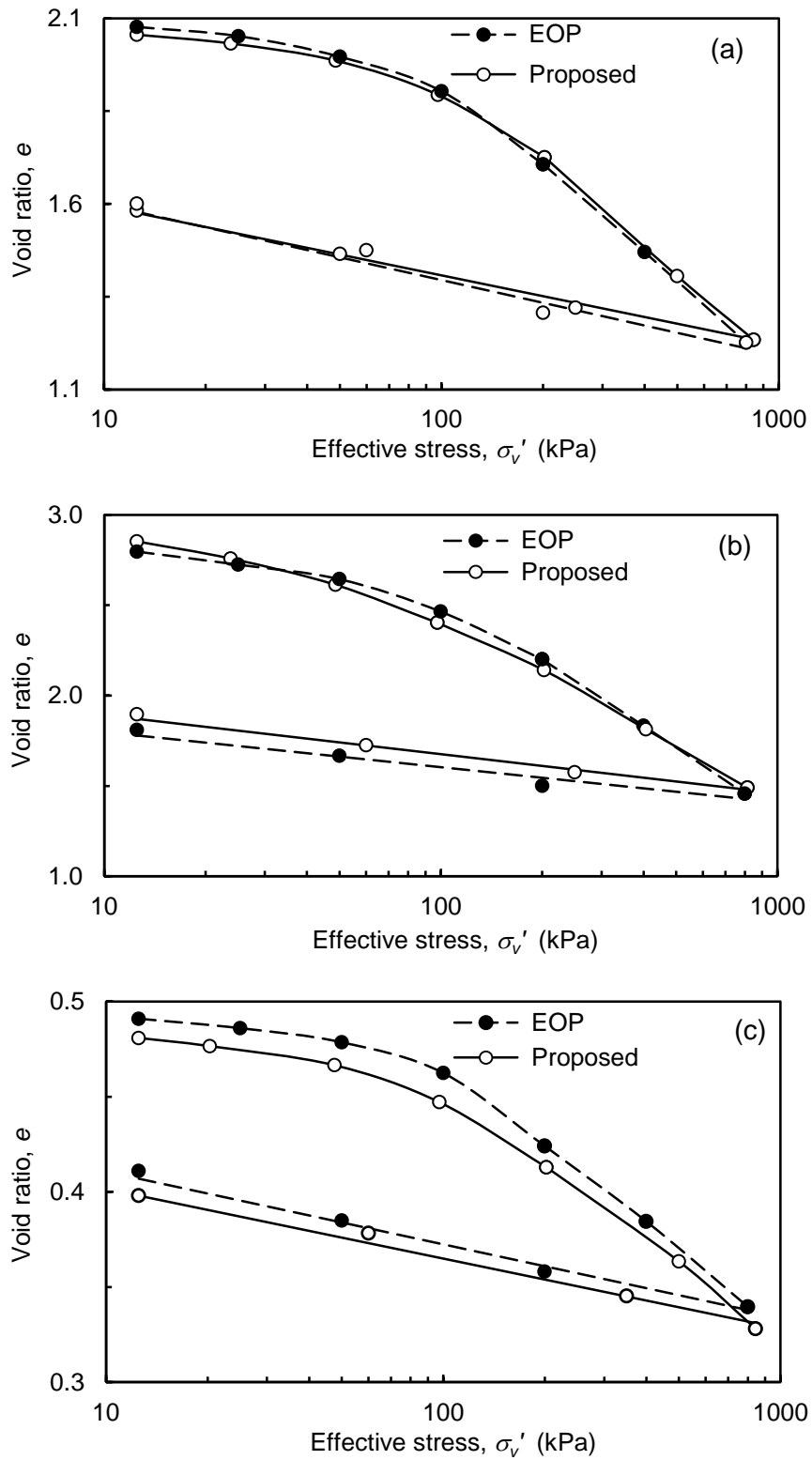


Figure 7.20: Comparison of  $e$ - $\log \sigma'_v$  curves of undisturbed soils obtained from the EOP and proposed method for (a) Cochin marine clay (21 m) (b) Cochin marine clay (16 m) and (c) Madhavaram clay (6 m)

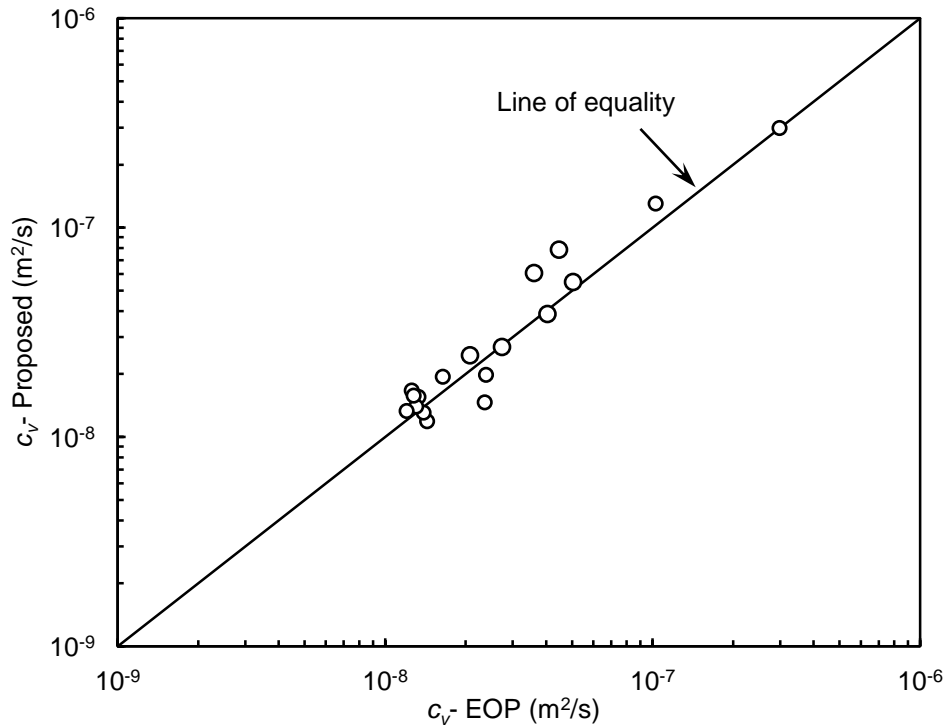


Figure 7.21: Coefficient of consolidation from the EOP and the proposed method (Inflection point method) for the undisturbed soils

### ***Coefficient of secondary compression***

Coefficient of secondary compression is often required to be determined. In the proposed methods (both  $\sqrt{t}$  and inflection point methods) the subsequent pressure increment is applied before the end-of-primary consolidation. Therefore, coefficient of secondary compression cannot be determined. However, if coefficient of secondary compression is required, one of the load increments can be kept for sufficient time for the secondary compression to occur in the secondary compression phase. This procedure is validated, typically for four soils such as Taramani clay, Bombay marine clay, Cochin marine clay (21 m) and Madhavaram clay (6 m). Typical time-settlement curve in the form of  $e$ - $\log t$  curve for Bombay marine clay in the pressure range of 200-400 kPa from conventional IL test is shown in Figure 7.22 along with that for the sample subjected to the proposed inflection method in the pressure range of 250–500 kPa. The values of coefficient of secondary compression obtained for the four soils are tabulated in Table 7.8. The values are practically the same suggesting that it is possible to determine the value of  $c_\alpha$  by allowing the sample to consolidate for longer time under any pressure range of interest.

Table 7.7: Time required for the conventional EOP consolidation test and the proposed inflection point method

Sl. No.	Soil Type	Number of increments		Range of $c_v$ , $m^2/s$	Time taken, hours					
		Loading	Unloading		EOP method			Proposed method		
					Loading	Loading	Loading	Loading	Unloading	Total
1	Red soil 1	6	3	$3 \times 10^{-8}$ - $6 \times 10^{-8}$	8.5	3.5	12	1.5	1.5	3.0
2	Red soil 2	6	3	$1 \times 10^{-8}$ - $3 \times 10^{-8}$	15	6	21	3.0	1.0	4.0
3	Gummudipoondi clay	6	3	$4 \times 10^{-9}$ - $6 \times 10^{-8}$	21.5	32.5	54	5.0	4.0	9.0
4	Taramani clay	6	3	$8 \times 10^{-9}$ - $1 \times 10^{-8}$	22	18	40	6.0	3.0	9.0
5	Bombay marine clay	6	3	$5 \times 10^{-8}$ - $6 \times 10^{-8}$	5	3.5	8.5	1.5	1.0	2.5
6	Cochin marine clay (21 m)	6	3	$4 \times 10^{-7}$ - $1 \times 10^{-8}$	21	6	27	4.0	1.0	5.0
7	Cochin marine clay (16 m)	6	3	$5 \times 10^{-8}$ - $2 \times 10^{-8}$	15	8	23	2.0	1.0	3.0
8	Madhavaram clay (6 m)	6	3	$3 \times 10^{-7}$ - $1 \times 10^{-8}$	7	8	15	3.0	1.5	4.5

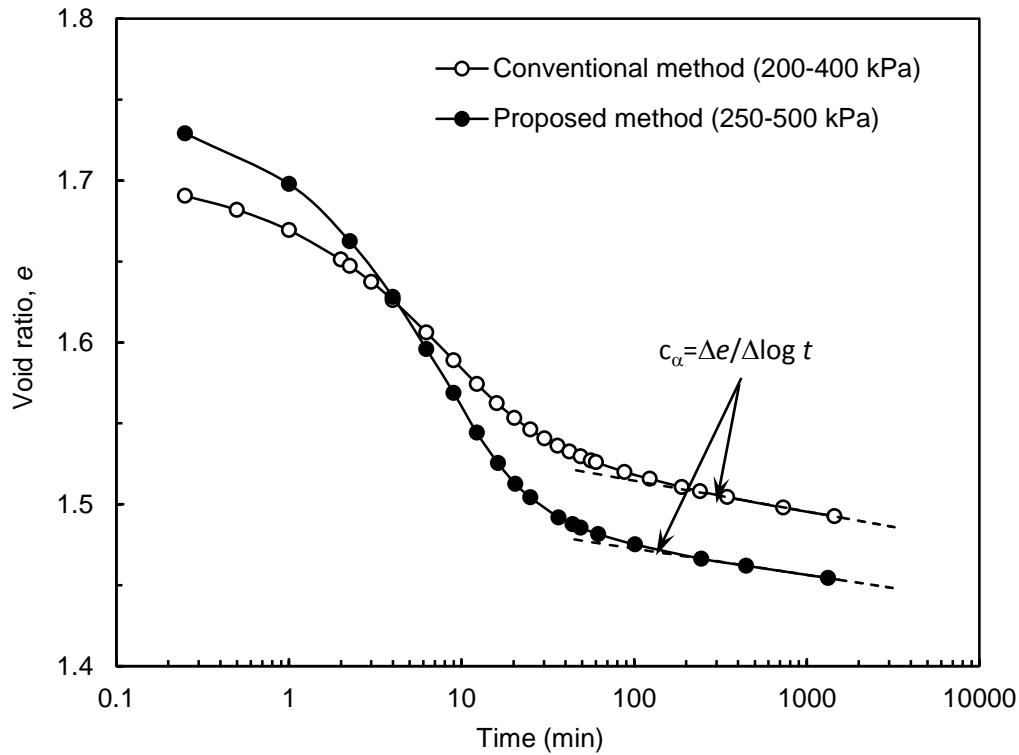


Figure 7.22: Coefficient of secondary compression from  $e$ - $\log t$  curve for Bombay marine clay

Table 7.8: Values of coefficient of secondary compression index

Sl. No	Soils	$c_\alpha$ by	
		EOP method	Proposed method
1	Taramani clay	0.018	0.018
2	Bombay marine clay	0.020	0.019
3	Cochin marine clay (21m)	0.030	0.041
4	Madhavaram clay (6m)	0.003	0.003

#### 7.4 SUMMARY

In this chapter, accelerated IL tests were proposed based on the curve fitting procedures such as  $\sqrt{t}$  method and inflection point method. The accelerated IL consolidation test yields consolidation parameters such as compression index, coefficient of consolidation and preconsolidation pressure, within a short duration, comparable to those of the conventional long duration tests and saving significant amount of time and effort.

In the accelerated IL consolidation test based on the  $\sqrt{t}$  curve-fitting procedure, the degree of consolidation corresponding to 90% is identified. The duration required for completion of the test, for soils with coefficient of consolidation greater than about  $3 \times 10^{-8} \text{ m}^2/\text{s}$  requires only about 2 to 5 hours. For low permeable soils, with  $c_v < 10^{-8} \text{ m}^2/\text{s}$ , the duration required is about 30 hours.

The applicability of the inflection point method for faster and complete end-of-primary consolidation testing and analysis is also brought out in this chapter. The samples were allowed to consolidate up to a degree of consolidation of 70.15%, where the inflection occurs in the  $\log t$  plot before the application subsequent pressure increment. The average effective stress was evaluated by estimating the mid-plane pore pressure using Terzaghi's one-dimensional consolidation theory. The method yields parameters comparable to those derived from the conventional consolidation test except the  $c_r$  values. However, it was noticed that the estimated negative pore pressure based on the pore pressures estimate during the unloading stages was found to be unreasonable. Similar observations were noted during  $\sqrt{t}$  method also. Hence, it is concluded that the negative pore pressure estimation based on Terzaghi's theory is not appropriate. Therefore, the interpretation of unloading phase was done based on ultimate swelling estimation and was found to predict the swelling curve very well. Comparison of consolidation parameters derived using the proposed procedure using inflection point method with the EOP test lends support to its validity. For soils with coefficient of consolidation more than  $1 \times 10^{-8} \text{ m}^2/\text{s}$ , the total duration required is less than 5 hours. For the soil with lowest  $c_v$  used in the study ( $4 \times 10^{-9} \text{ m}^2/\text{s}$ ), the time required is about 9 hours. The results clearly demonstrate that the end-of-primary consolidation tests can be performed faster than the conventional EOP consolidation test, within the working hours of the day using the inflection method.





## CHAPTER 8

### SUMMARY AND CONCLUSIONS

#### 8.1 SUMMARY

Knowledge of consolidation properties of soils is necessary for the design of geotechnical engineering structures. The consolidation properties are usually determined by performing one-dimensional consolidation test in the laboratory. Various laboratory one-dimensional consolidation tests are available in the literature (reviewed in the Chapter 2), out of which the conventional incremental loading (IL) test and constant rate of strain (CRS) consolidation test are the popular ones, because of the simplicity of testing procedures. If the strain rate is varied during strain controlled test, it is called as CSL test. Other one-dimensional consolidation tests are not popular, as they require continuous monitoring and automation.

The advantages of the IL consolidation test are that the testing procedure is well established and the interpretation of data is straight forward. The conventional IL consolidation test is a stress controlled test and the time–settlement data is continuously recorded for 24 hours under each loading stage. Many load increments are required to establish the void ratio ( $e$ )-consolidation pressure ( $\sigma_v'$ ) relationship, both during loading and unloading stages. Usually, the tests take about 10-14 days to complete, if the sustained loading is left for 24 hours. To overcome the limitations of conventional IL test, attempts were made in the literature to reduce the testing time. One such method developed is the constant rate of strain (CRS) consolidation test. The CRS test has gained popularity because of the reasons that the test is much faster than the incremental loading test and continuous data points are acquired. However, the major limitation is that the procedure for fixing proper rate of strain for CRS test is not yet fully established. Therefore, it is essential to develop a rational method to fix proper strain rate of CRS test.

Hence, one of the main objectives of the present work is the development of a rational method to fix the rate of strain in CRS test. The proposed method is developed based on the theory of Wissa *et al.* (1971). The initial strain rate is determined by measuring the

permeability of the specimen for a particular effective stress. A permeability set up was designed so as to measure the permeability faster. The proposed method for fixing the initial strain rate was validated by performing a series of CRS tests on several fine grained soils covering a wide range of plasticity characteristics with the liquid limit values ranging from 32%-165%. Conventional IL consolidation tests and End-Of-Primary (EOP) consolidation tests were conducted as the control tests. The results obtained from the proposed CRS tests were compared with the control test.

In the literature, various apparatus are suggested to perform CRS test. The apparatus suggested by Wissa *et al.* (1971) is widely used. The CRS apparatus, similar to Wissa *et al.* (1971) is incorporated in ASTM D4186-12 (2012). The commercially available CRS apparatus is generally expensive. Also, the design of CRS cell suggested as per ASTM is not simple. Hence, a simplified CRS apparatus with simple design which can be fabricated in any mechanical engineering workshop is proposed. The simplified CRS apparatus is very similar to the conventional oedometer cell except that a piston type loading cap with provision for applying back pressure and measuring pore pressure. The apparatus was validated by performing CRS consolidation tests on soils with varying plasticity characteristics. The results from the proposed apparatus were compared with those obtained from the consolidation tests using the conventional incremental loading (IL) oedometer apparatus and CRS test using standard CRS apparatus.

A modification to conventional fixed ring consolidometer without back pressure is also proposed to perform CRS consolidation test. An extra drainage line was provided at the base of the consolidation cell to connect a pore pressure transducer for measuring pore water pressure and a burette to de-air. The modified consolidometer was validated by performing CRS consolidation tests on soils with varying plasticity characteristics. The test results were compared with the incremental loading (IL) consolidation test results conducted on identical soil specimens.

The duration of completing CRS test was evaluated and it was observed that the time taken for low permeable soils is large, often as high as 10 days. Hence, a study of stress controlled consolidation test with pore pressure measurement was also attempted, where the duration of increment of load is controlled by the dissipation of excess pore pressure and was allowed only to pore pressure ratio ( $r_u$ ) of 15% of the total stress. Detailed

experimental programme was performed to validate the proposed method. The results obtained are compared with the IL test with 24 hours duration and the CSL consolidation test.

It was observed that the duration of the stress controlled test with pore pressure measurement is still large as the test is conducted under one-way drainage conditions. Hence, attempts were also made to accelerate the consolidation test by providing two-way drainage. The testing procedures were developed based on curve fitting procedures such as  $\sqrt{t}$  method and inflection point method. The results obtained are compared with EOP test.

## 8.2 CONCLUSIONS

The focus of the present study is to develop one-dimensional consolidation testing procedures so as to complete the test faster. Both stress controlled and strain controlled tests were study. Based on the study, the following conclusions are drawn:

- Accurate estimates of strain rates are possible to conduct constant rate of strain (CRS) consolidation tests by measuring the coefficient of permeability before the start of the CRS test. When 3 mm diameter stand pipes are used, permeability measurements can be completed within 1 hour even for soils with coefficient of permeability less than  $1 \times 10^{-10}$  m/s.
- When CRS tests are conducted at constant rate, the pore pressure ratio ( $r_u$ ) changes. The trend of change of  $r_u$  is not unique but depends on the trend of variation of coefficient of consolidation ( $c_v$ ) with consolidation pressure ( $\sigma_v'$ ). For soils whose  $c_v$  increases with consolidation pressure,  $r_u$  decreases as the test progresses and vice-versa.
- A procedure was developed to control the strain rate during the test, so as to keep the pore pressure ratio within the allowable limits in a controlled-strain loading (CSL) test. By knowing the current strain rate and current pore pressure ratio, the procedure was developed based on the theory of Wissa *et al.* (1971) so as to obtain the required strain rate for a target pore pressure ratio. By adopting this

procedure, it is possible to complete the test faster by controlling the strain rate close to the upper limit of  $r_u = 0.15$ .

- Though CSL test is believed to be faster than the conventional incremental load test, the test may take very long time for low permeable soils whose  $c_v$  decreases as the consolidation pressure increases. Typically, for a soil with  $c_v < 1 \times 10^{-8} \text{ m}^2/\text{s}$ , the test may take as many days as 10 days.
- A simplified CRS cell without a pressure chamber was developed, which can be fabricated in any mechanical engineering workshop. The performance of the apparatus was validated by comparing the results with those obtained from standard CRS apparatus as per ASTM D4186-12 (2012). The comparison is very good which lends support to the validity of the apparatus.
- In the absence of standard CRS cell with provisions for pore pressure measurements, it is possible to use the conventional oedometer cells. The slight modifications required are described in the thesis.
- Stress controlled test with pore pressure measurements is a viable option to reduce the testing time of CSL test. When the specimen is allowed to consolidate till the pore pressure ratio of 0.15, which corresponds to a degree of consolidation of about 83%. The test is about 1.5-2.5 times faster than the CSL test. The test is still slow because it is conducted under one-way drainage. Depending on  $c_v$ , the test may take as much as 120 hours.
- Standard curve fitting procedures such as  $\sqrt{t}$  method and inflection point method can be employed to perform accelerated consolidation test using conventional cells, as the tests are performed under two-way drainage conditions. The undissipated mid-plane pore pressure is estimated using Terzaghi's theory to obtain the effective stress.
- If  $\sqrt{t}$  method is adopted as an accelerated consolidation test, the time taken to complete the test is nearly 4 to 6 times faster than the SC test with pore pressure measurements. However, low permeable soils (with  $c_v < 1 \times 10^{-8} \text{ m}^2/\text{s}$ ) may take as much as 30 hours to complete the test.
- Using the inflection point method, it is possible to complete the consolidation test within the working hours of a day even for the soils with very low permeability. If recompression part is not required, the test can be completed within 1.5 to 6 hours.

- The  $c_c$  values obtained using  $\sqrt{t}$  method and inflection point method compare well with the conventional IL consolidation tests. However, the  $c_r$  values deviate significantly from the conventional IL tests. Careful monitoring of pore pressure during unloading phase using Rowe cell shows that interpretation of swelling data using Terzaghi's theory is not appropriate. The reason is attributed to the fact that the unloading results in separation of soil specimen from the walls of the cell (Mair, 1979). Therefore, the data was interpreted using swelling estimate, which gives comparable test results
- As the proposed methods are short-duration tests, secondary compression cannot be evaluated. However, it is possible to allow any increment for longer duration to obtain the coefficient of secondary compression.
- In summary, using the proposed procedures it is possible to obtain reliable estimates of consolidation parameters within a very short duration.

### **8.3 SCOPE FOR FUTURE STUDY**

Based on the experimental studies conducted on fine grained soils with varying plasticity characteristics, it was concluded that duration of one-dimensional consolidation tests can be reduced to working hours of a day. Manual intervention was required continuously. Hence, the proposed methods need to be automated using any interface and without any manual intervention during the test.

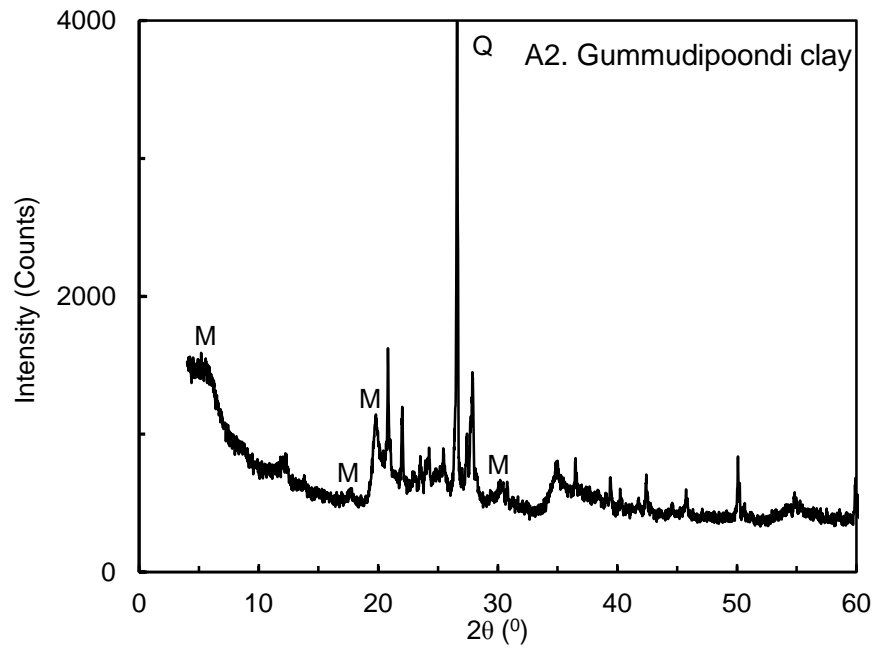
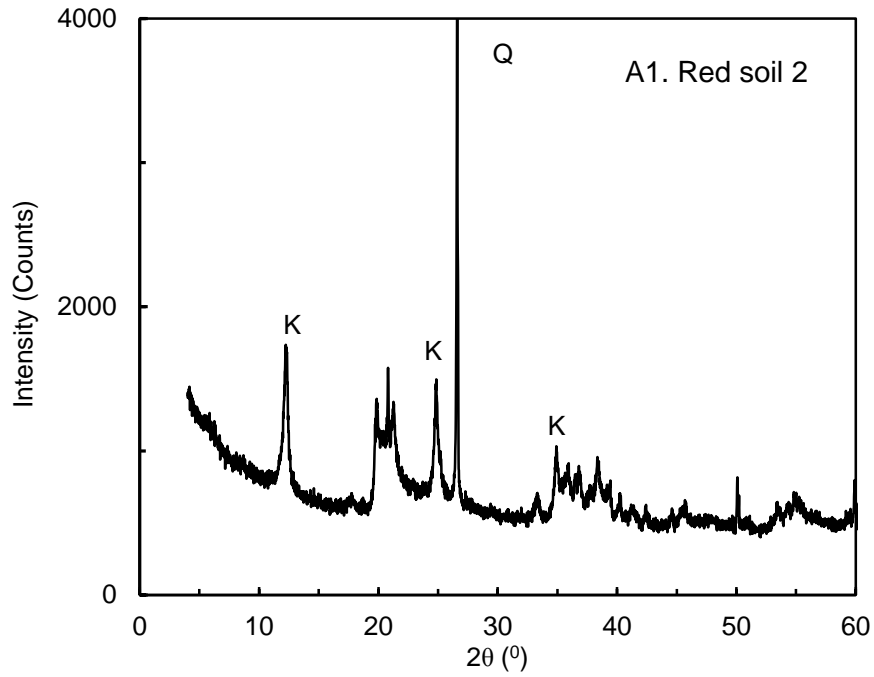
It was observed that there is a time-lag in the SC test with pore pressure measurement. A theory which captures this behaviour will be useful.

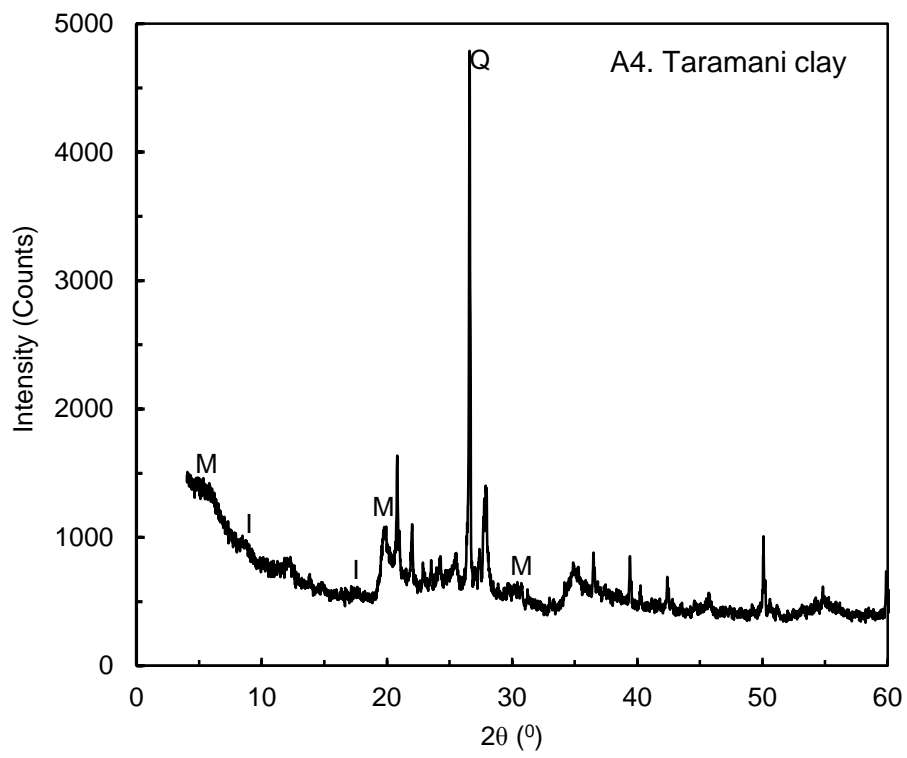
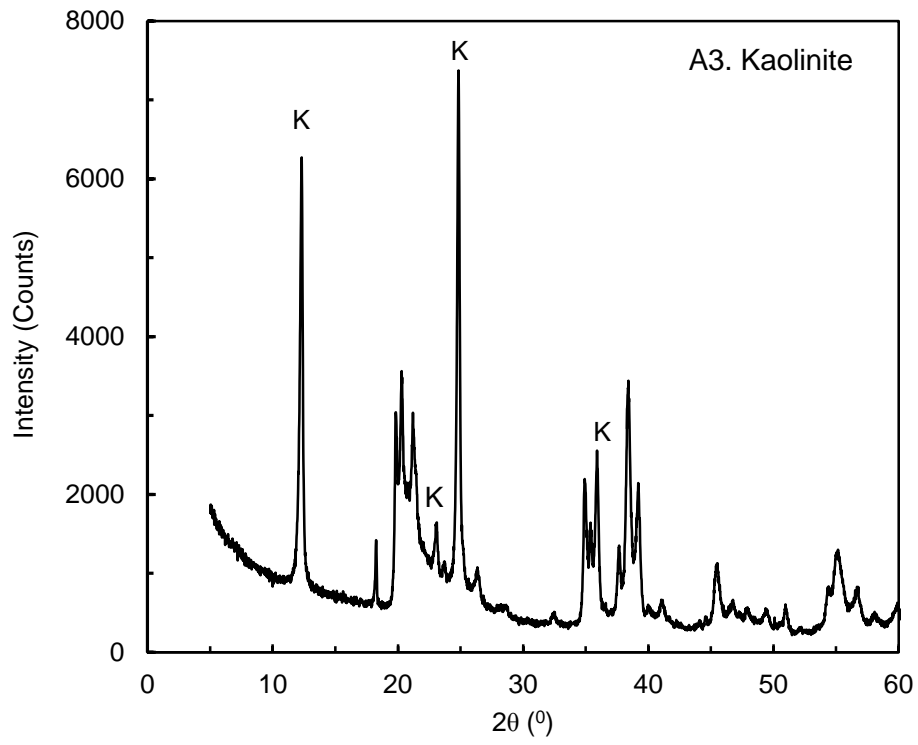
Terzaghi's theory is unable to capture the pore pressure during unloading. A theory that considered separation during unloading phase is essential.



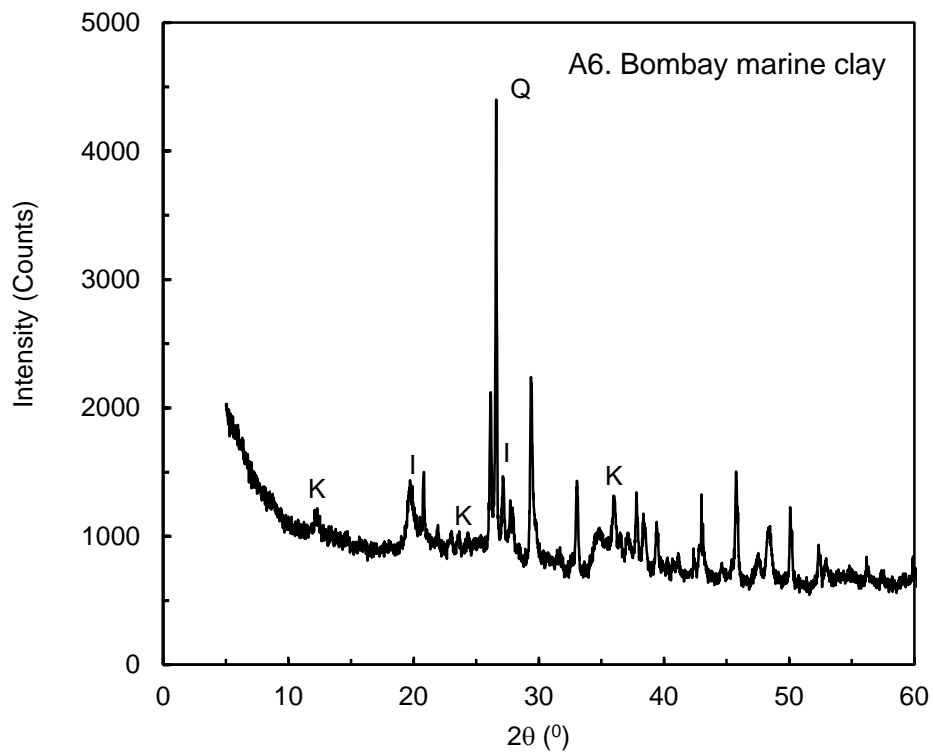
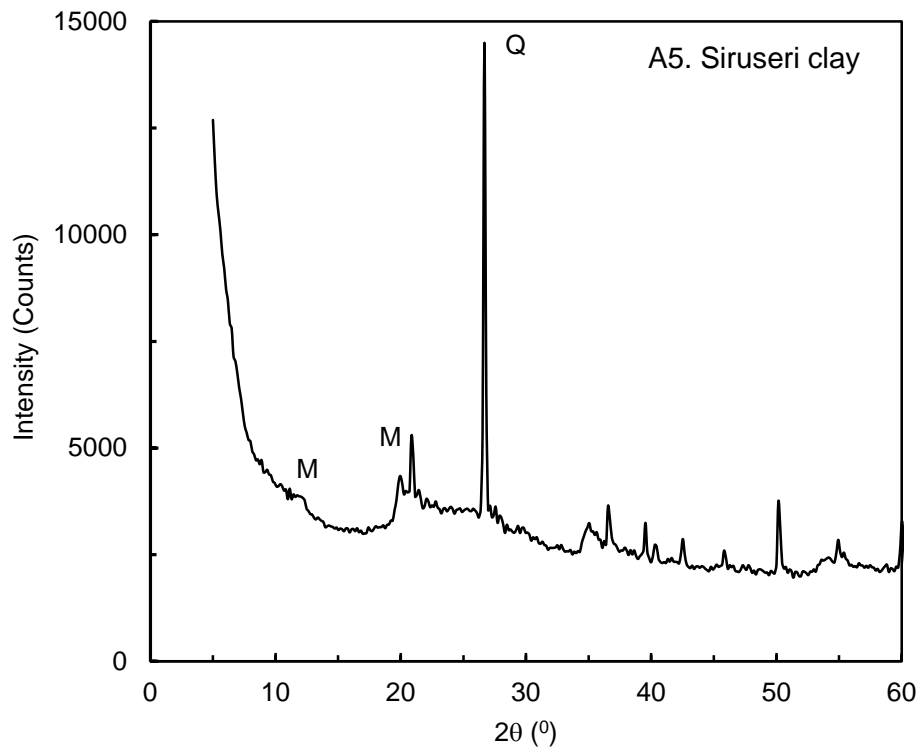
# APPENDIX A

## XRD PATTERN OF THE RECONSTITUTED SOILS





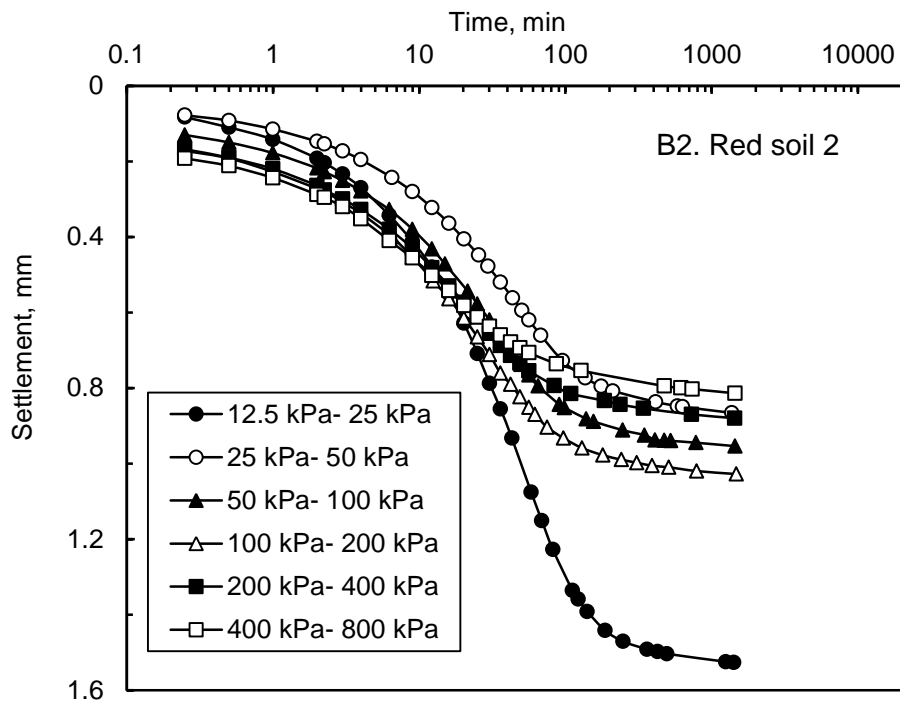
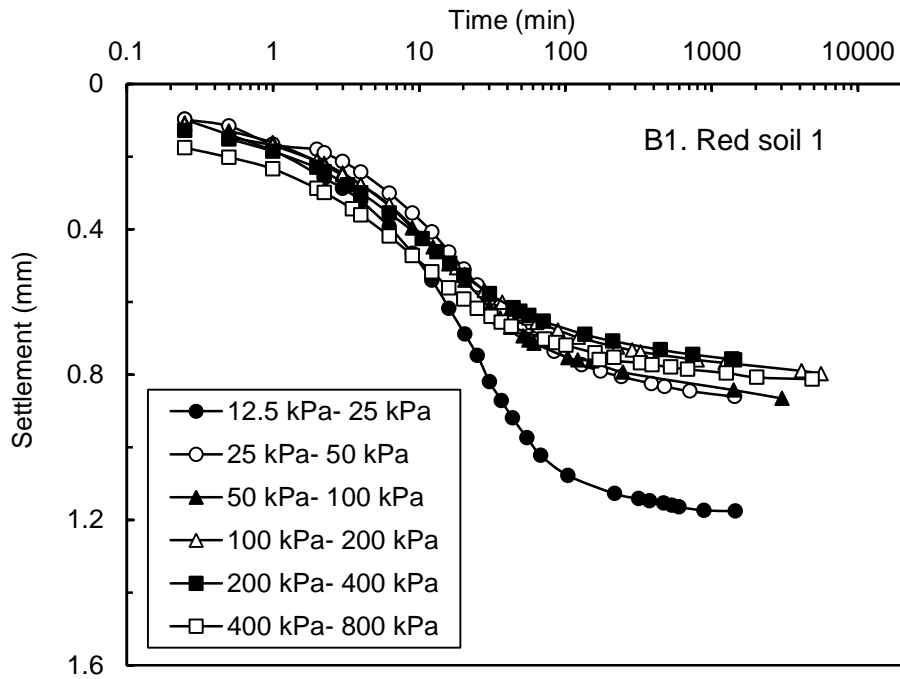


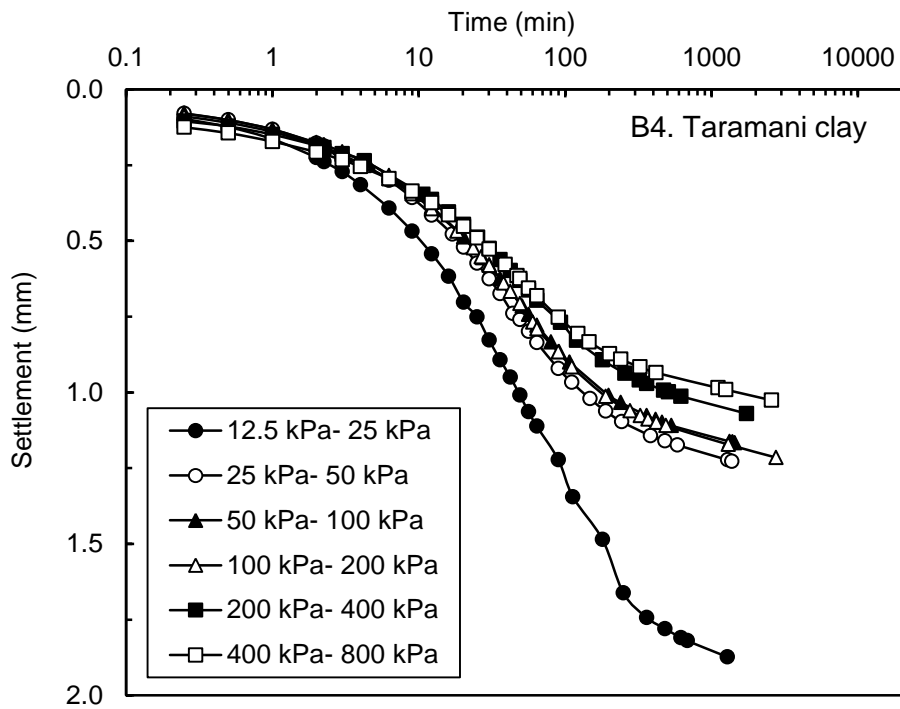
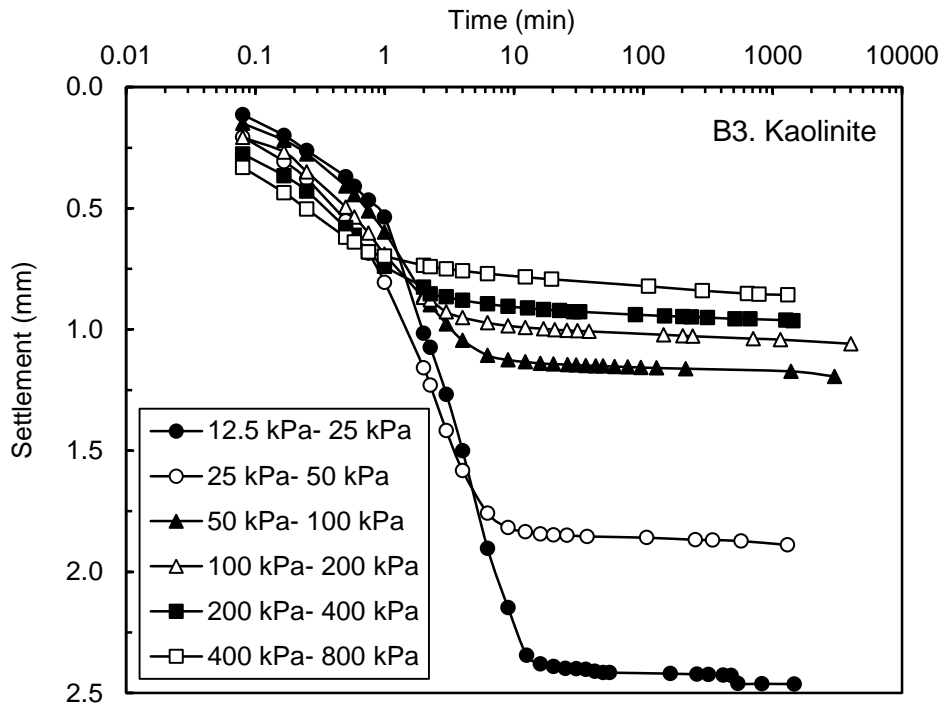


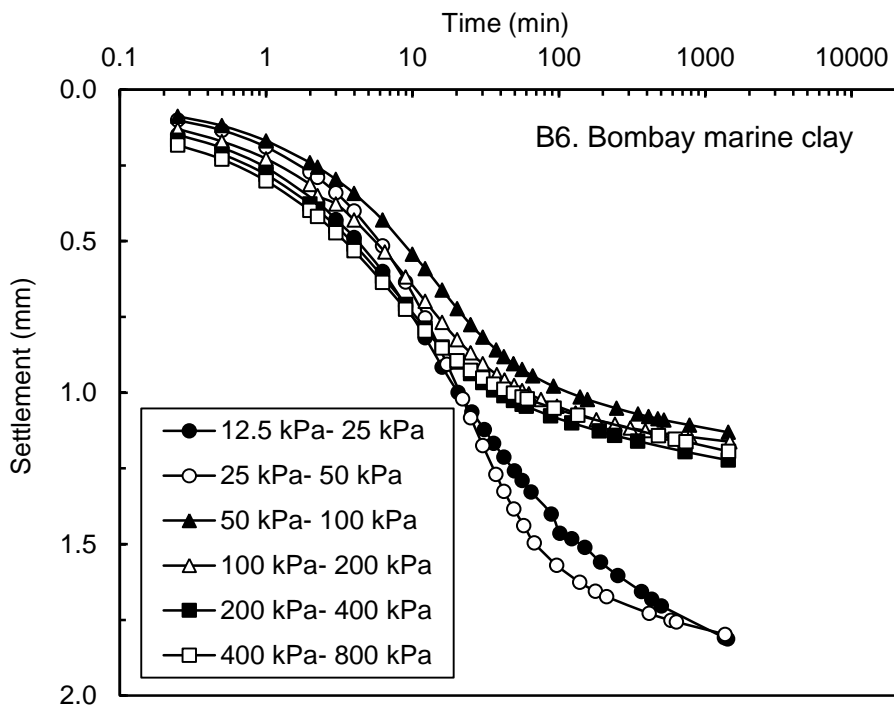
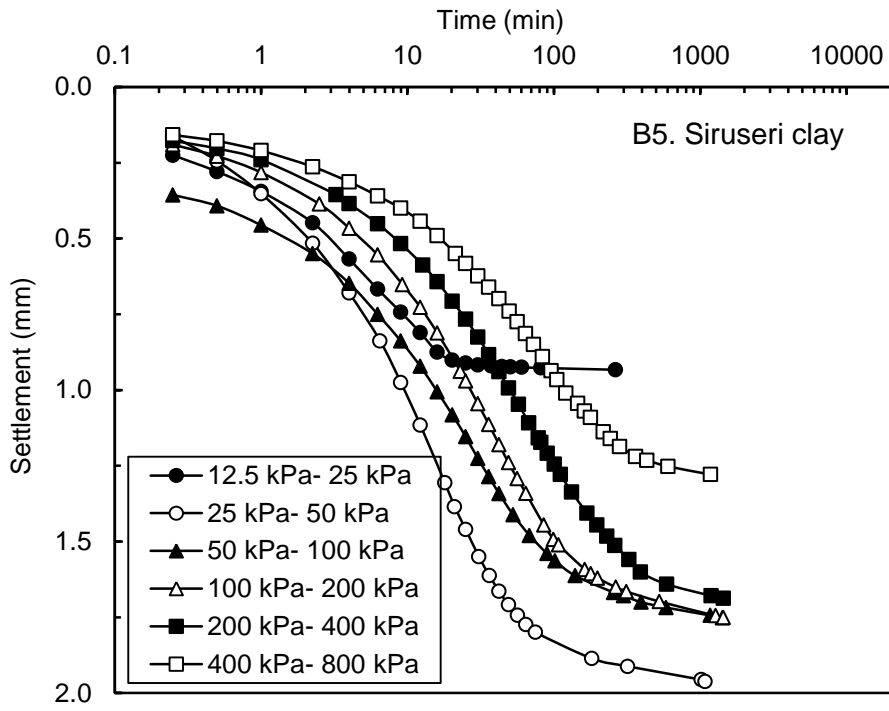


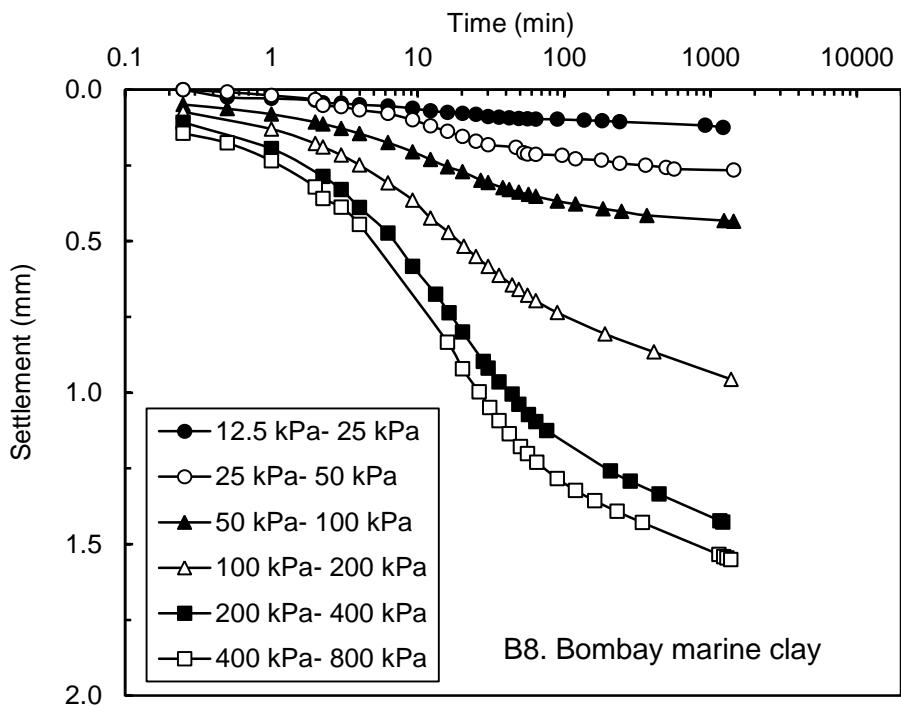
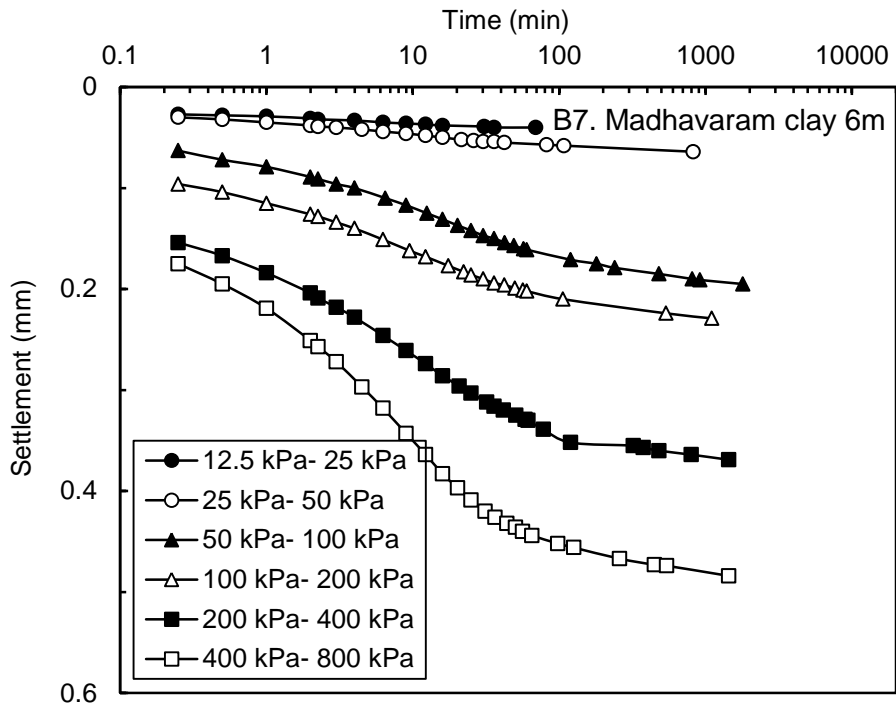
## APPENDIX B

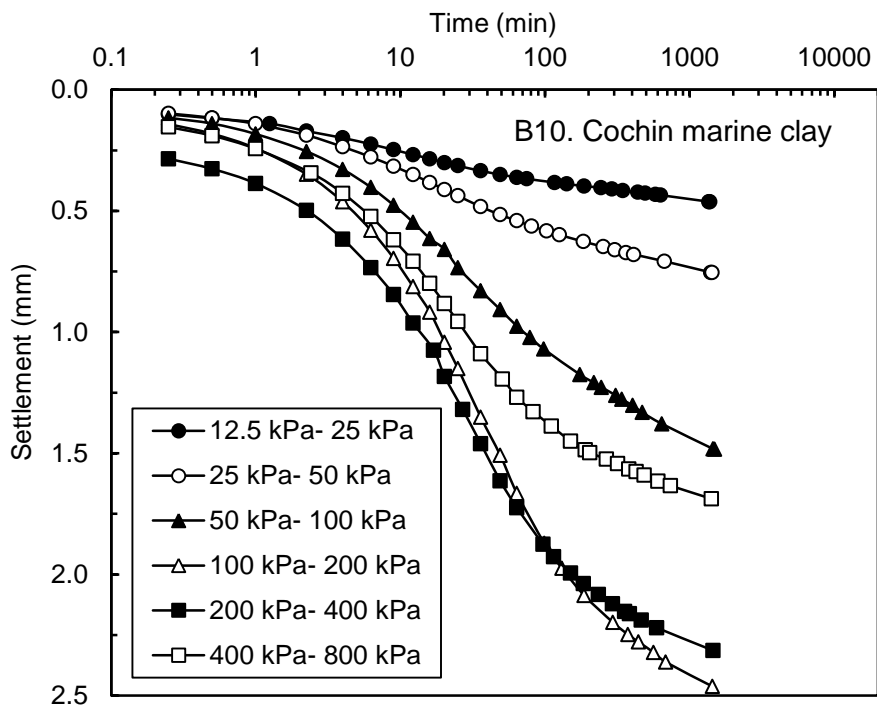
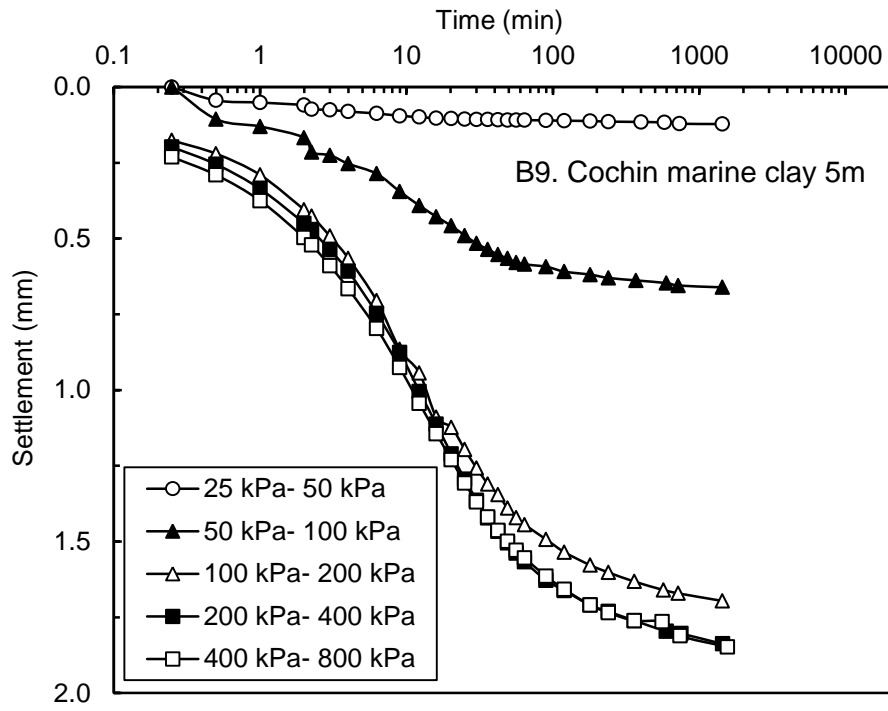
### TIME- SETTLEMENT CURVES FROM CONVENTIONAL IL TEST – 24 HOURS

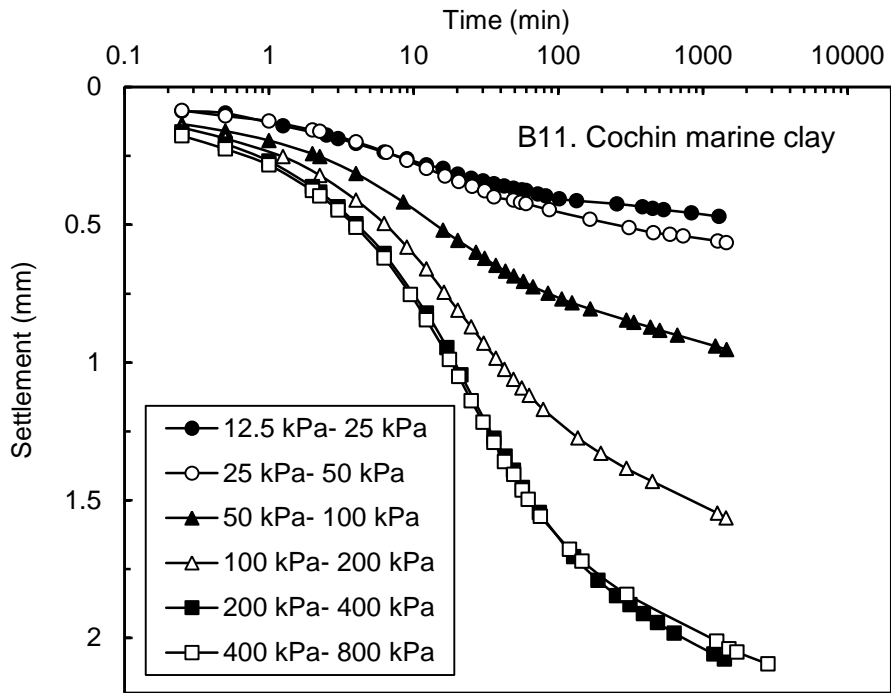








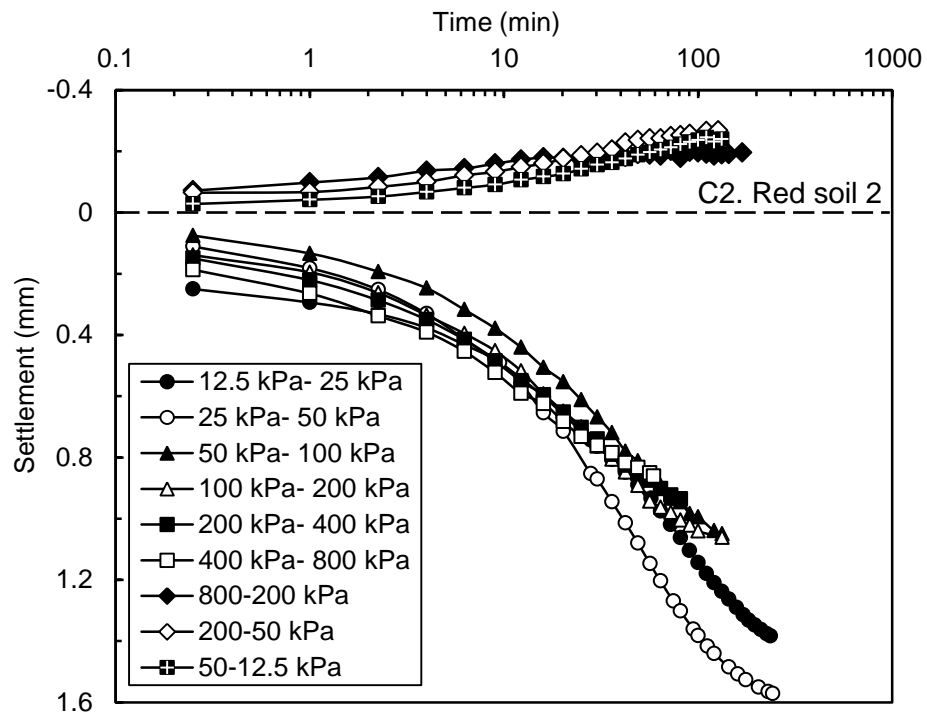
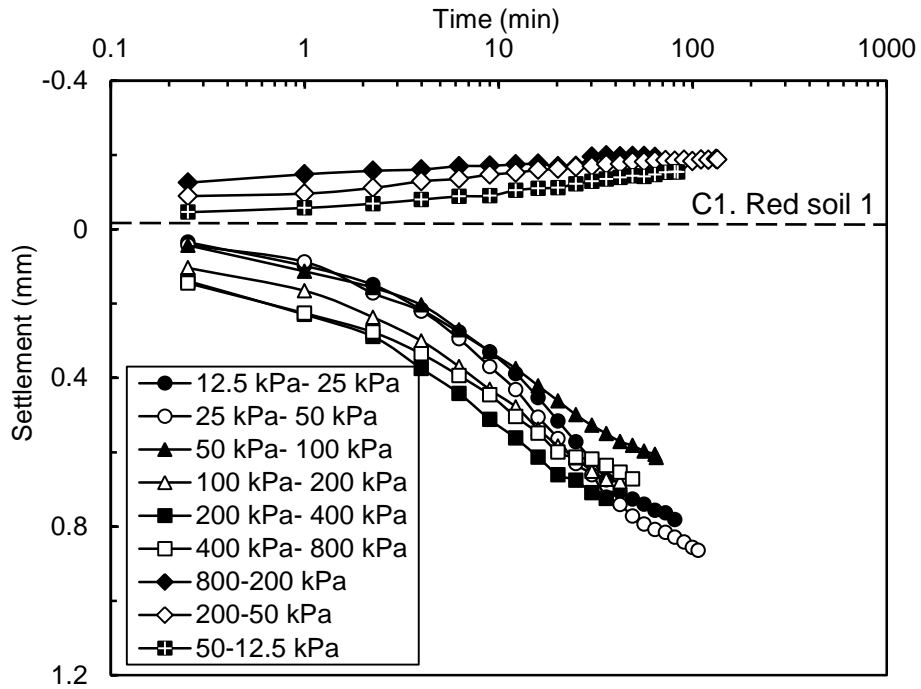


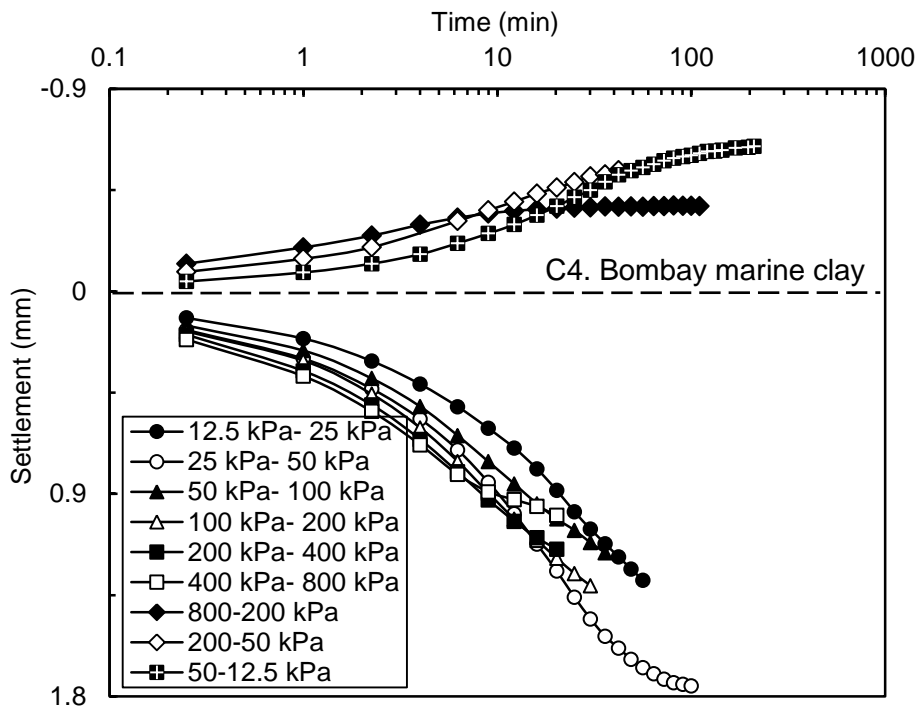
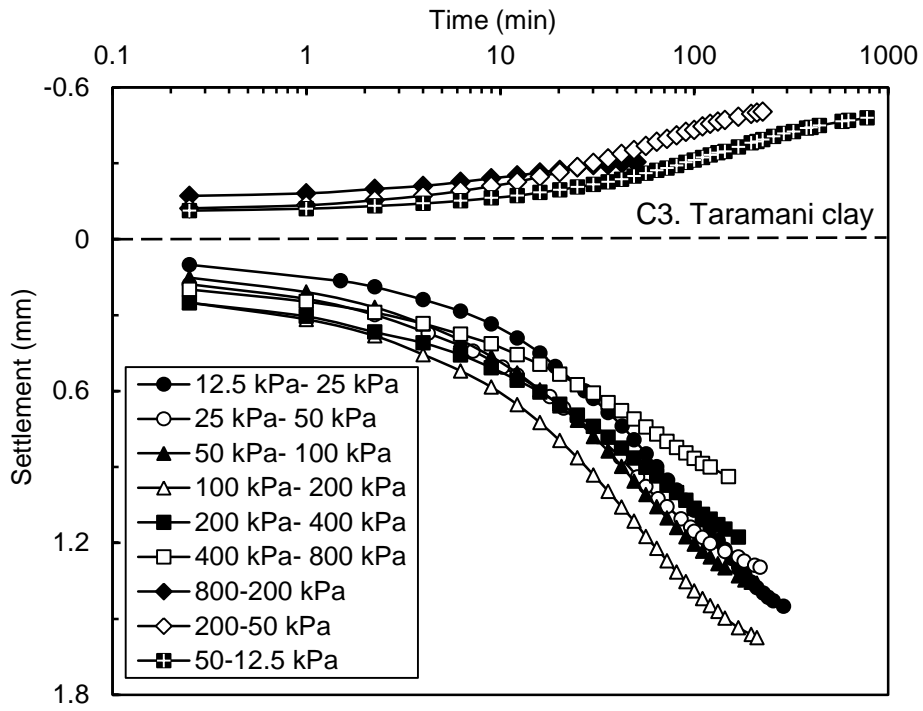




## APPENDIX C

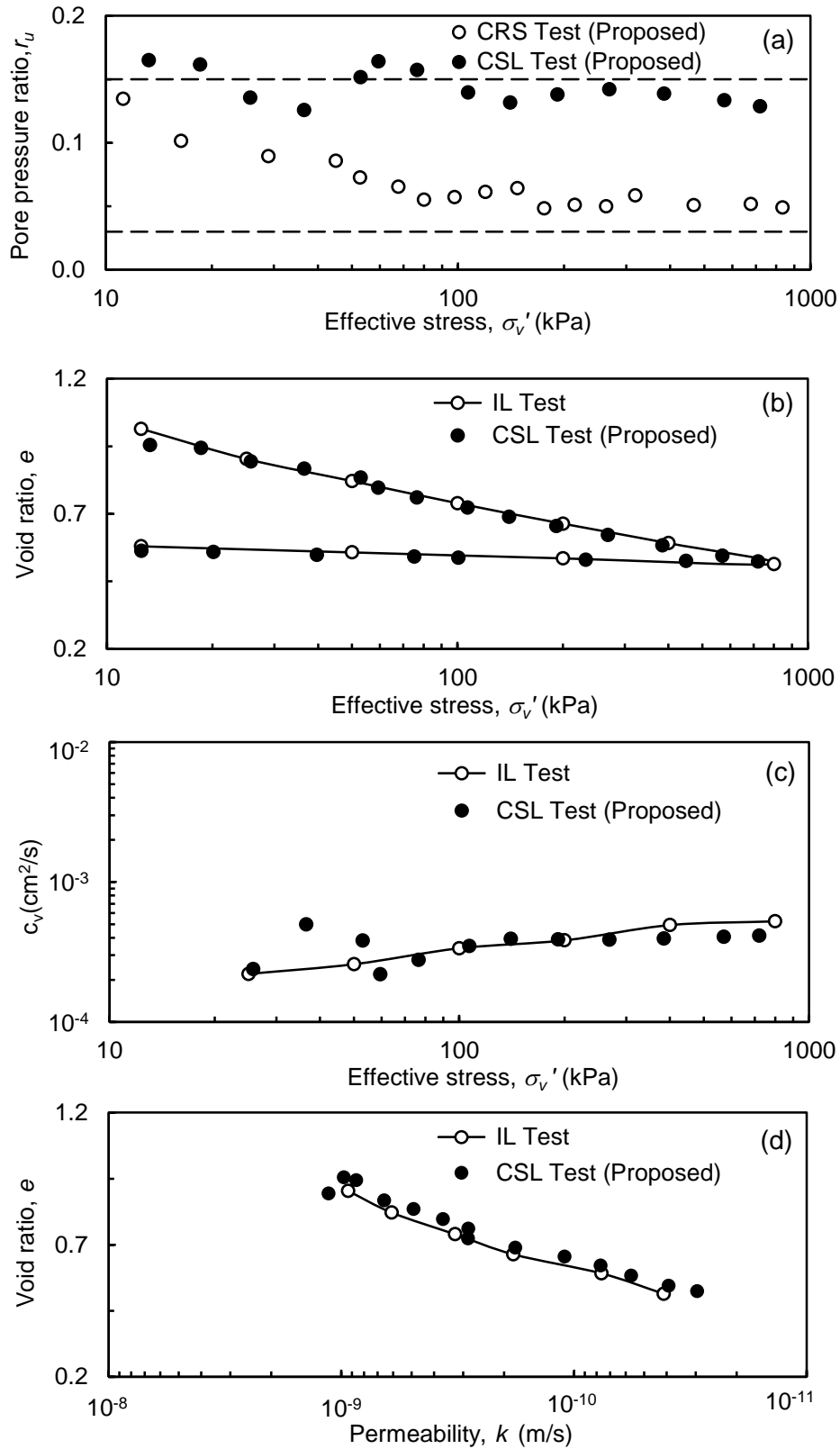
### TIME- SETTLEMENT CURVES FROM EOP TEST USING $\sqrt{t}$ METHOD



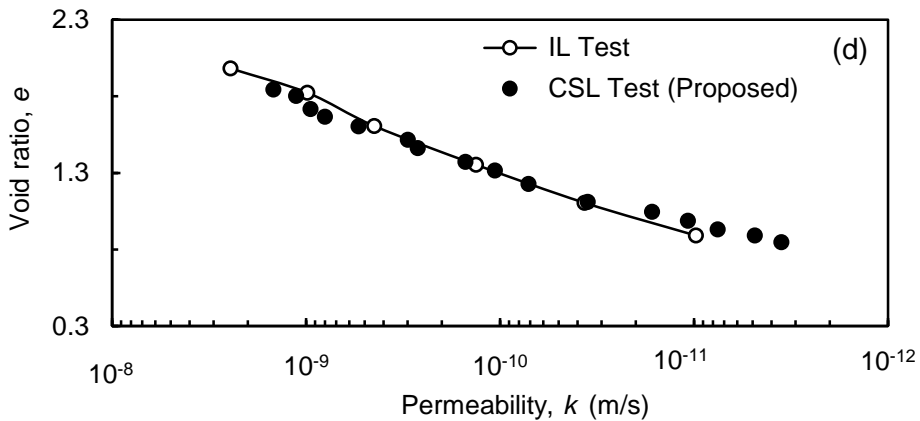
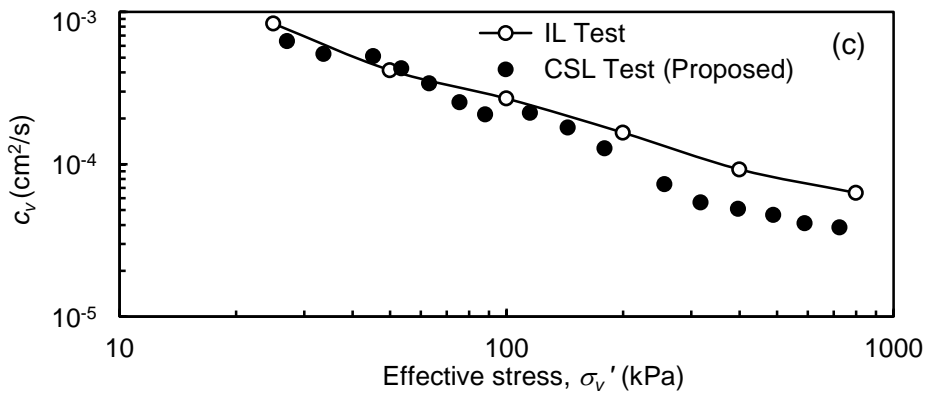
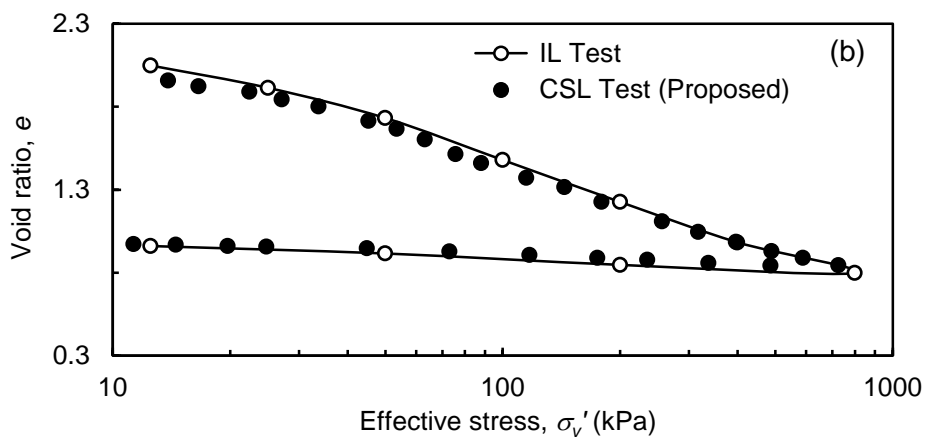
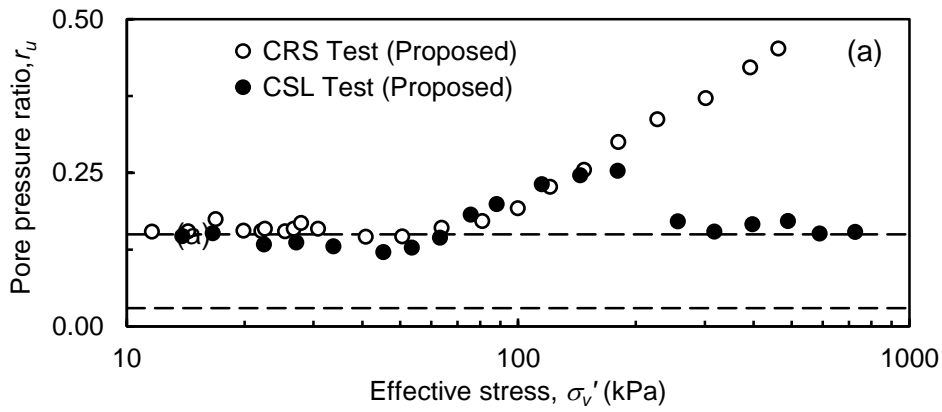


# APPENDIX D: COMPARISON OF CSL TEST WITH IL TEST RESULTS

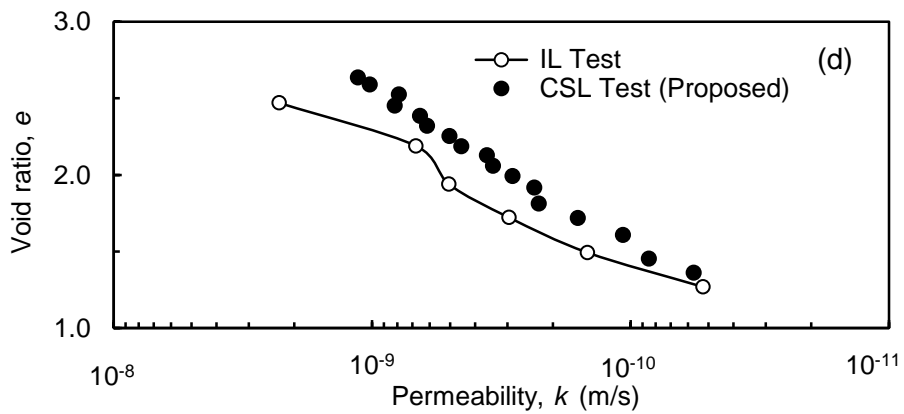
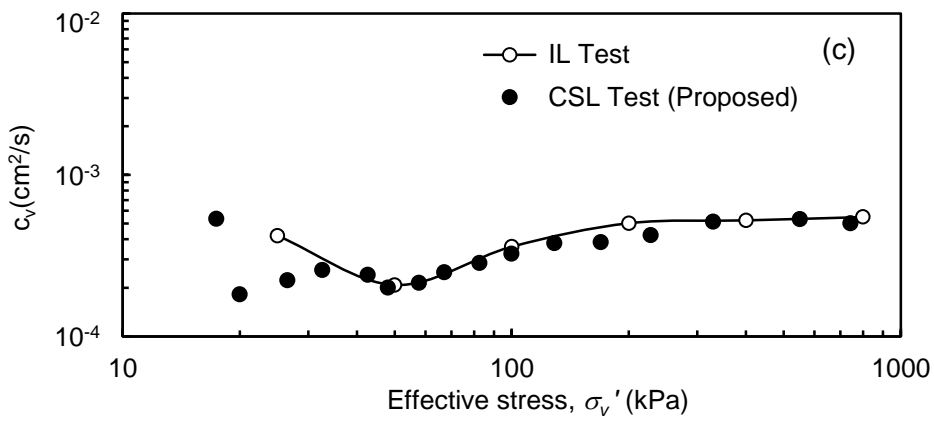
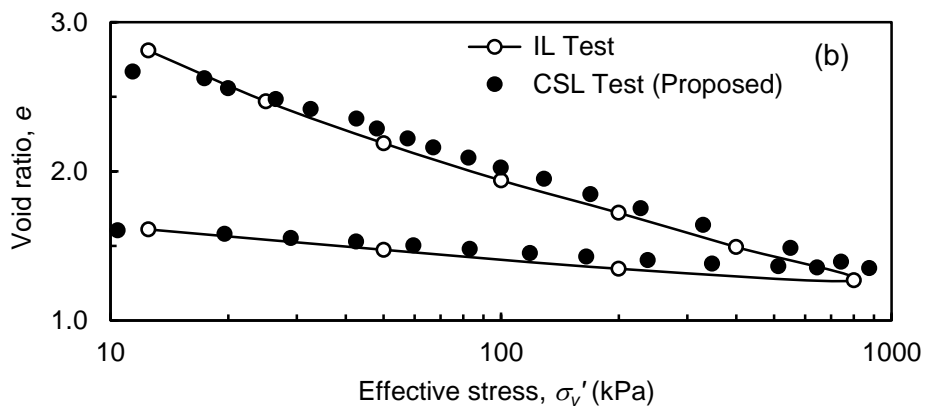
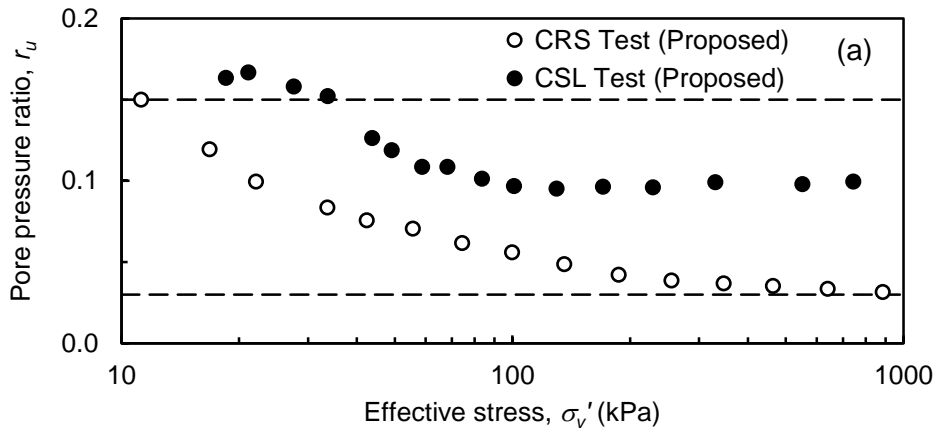
## D1. Red soil 1



## D2. Siruseri clay

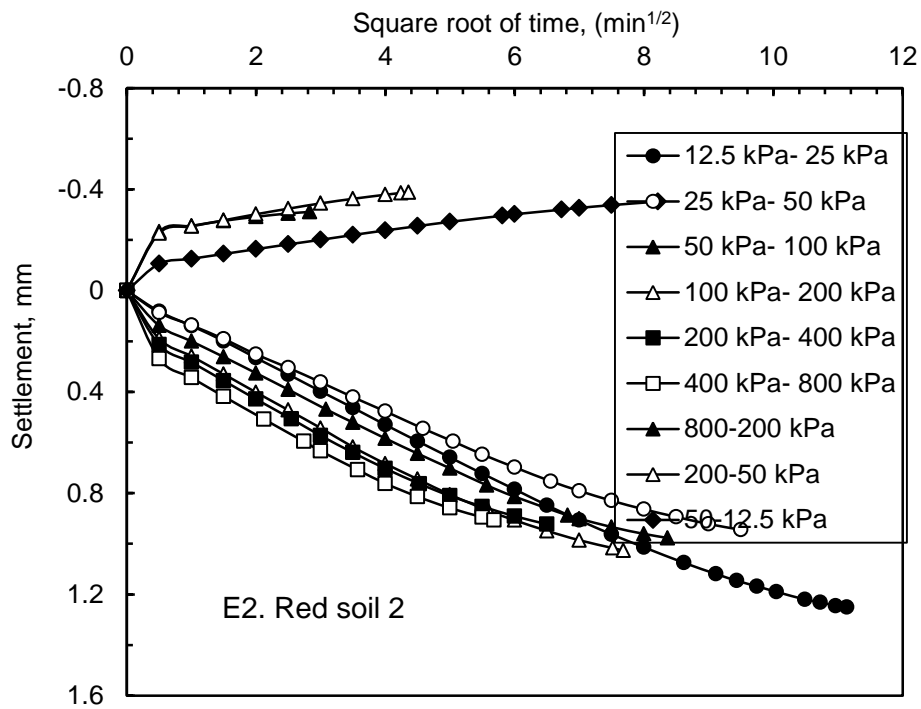
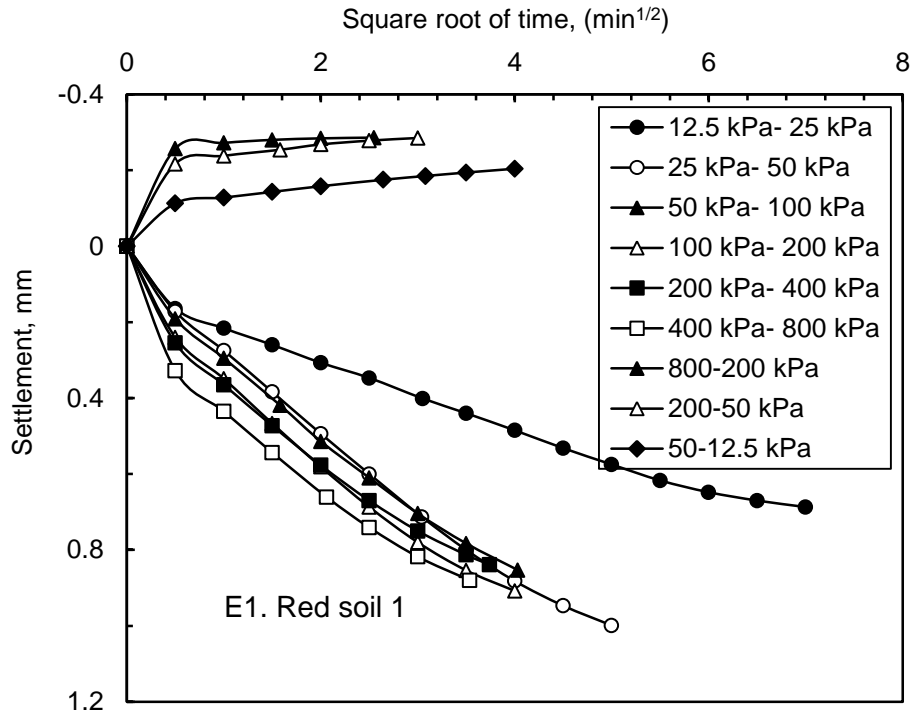


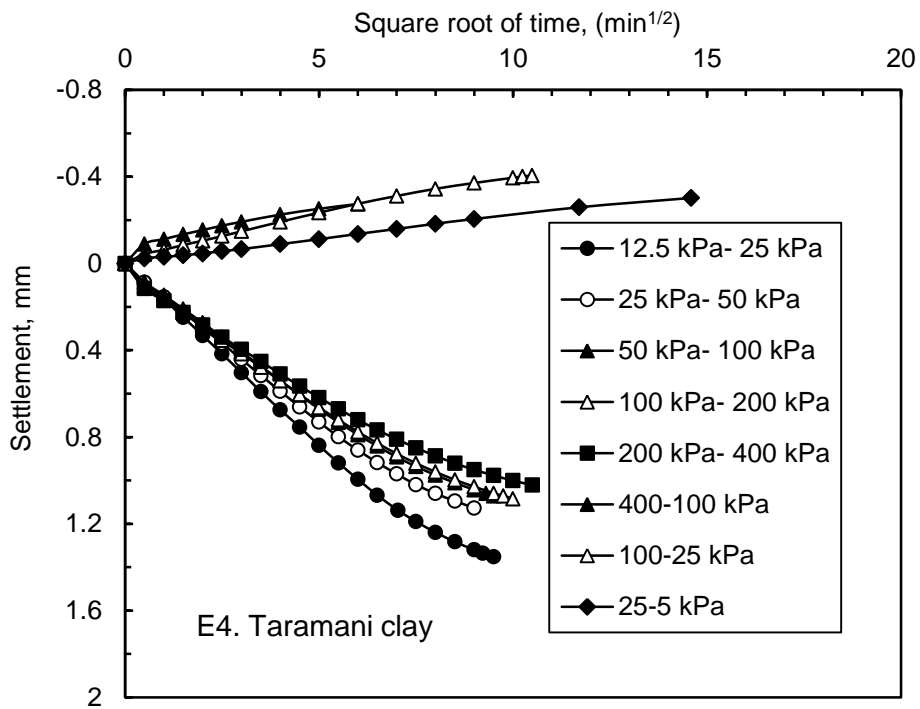
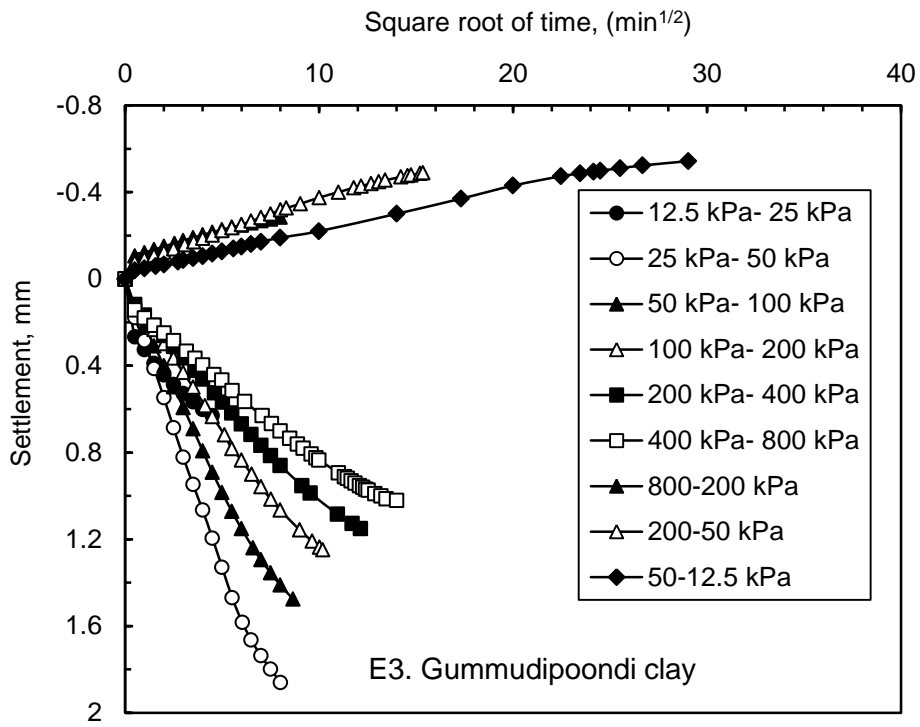
### D3. Bombay marine clay



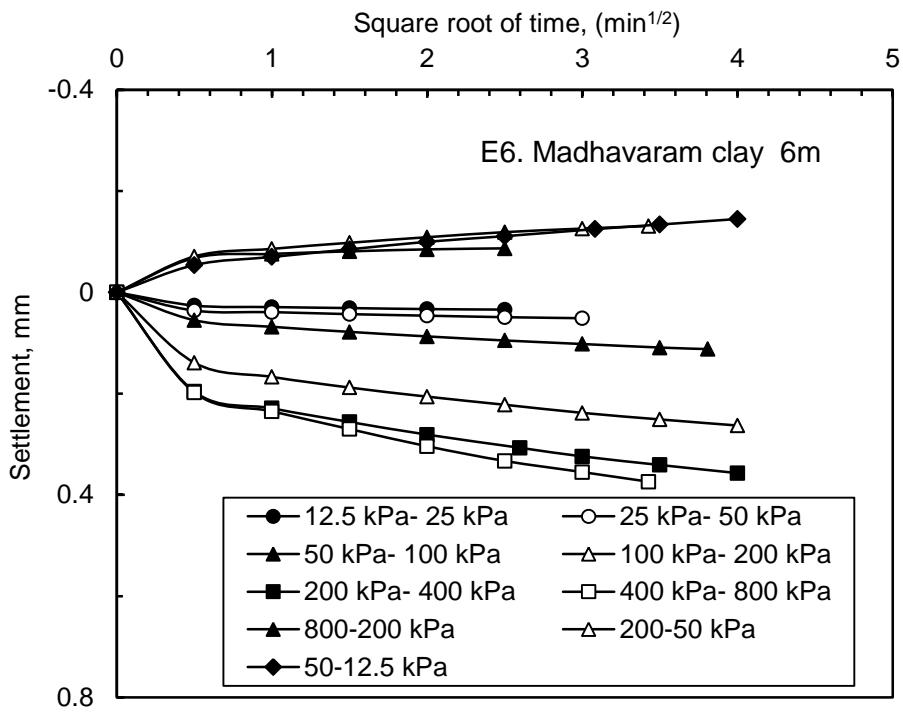
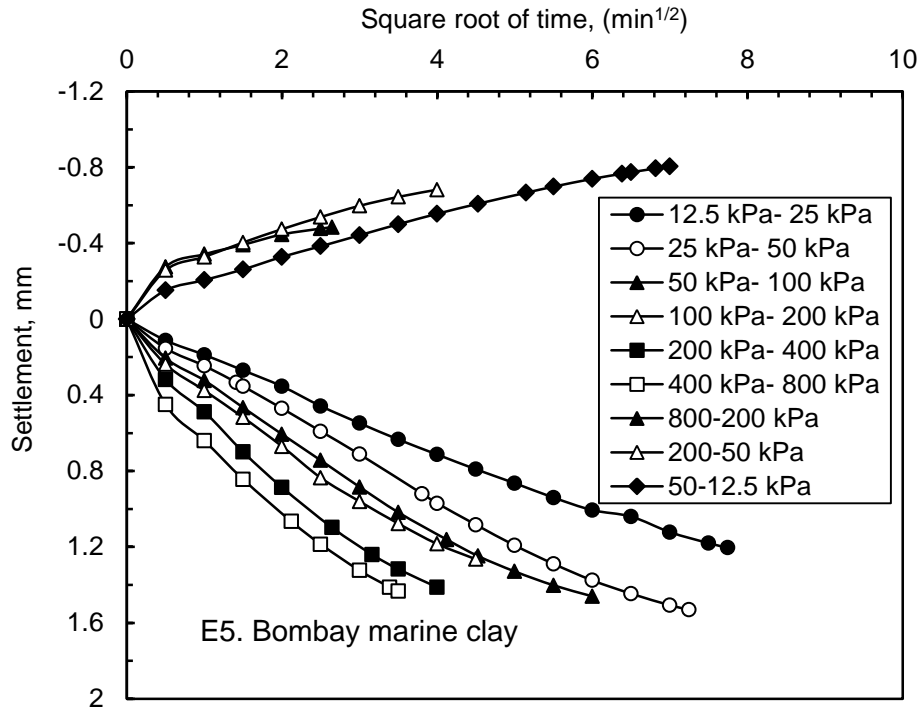


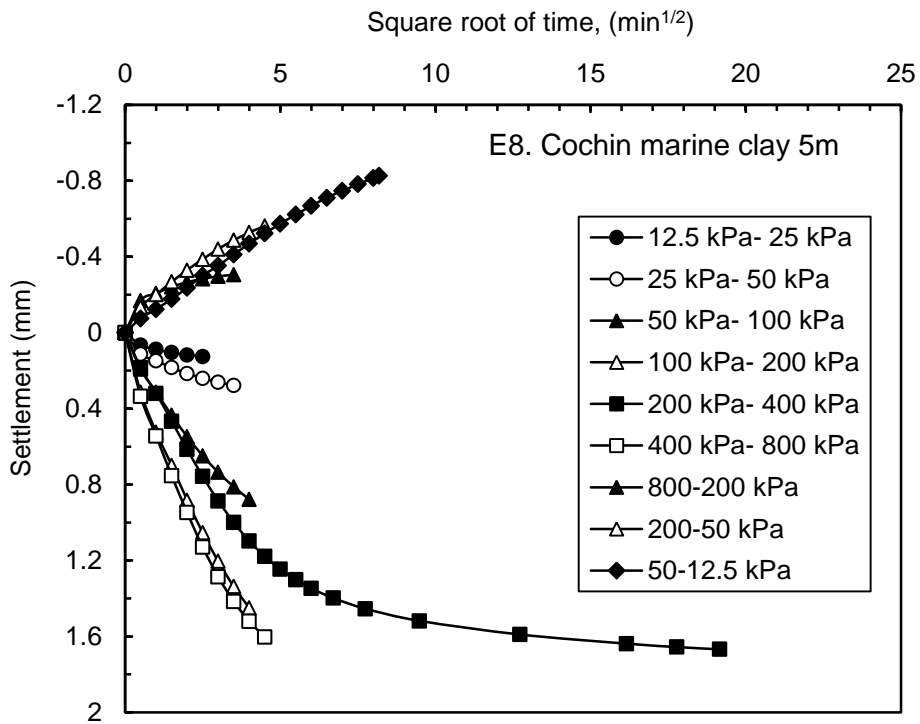
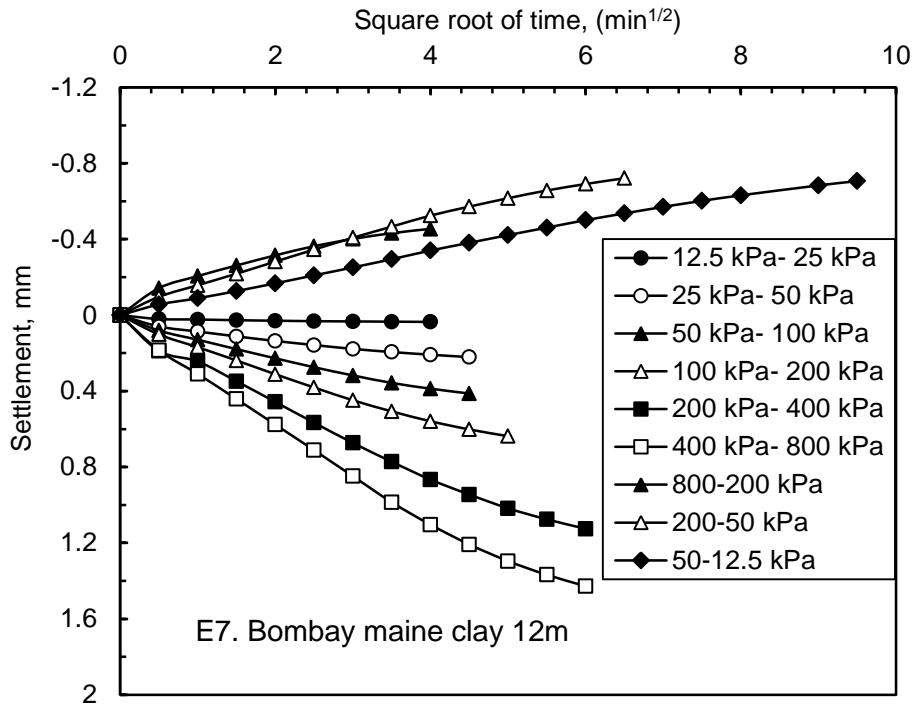
## APPENDIX E: $\sqrt{t}$ -SETTLEMENT PLOT OF ACCELERATED IL TEST USING $\sqrt{t}$ METHOD



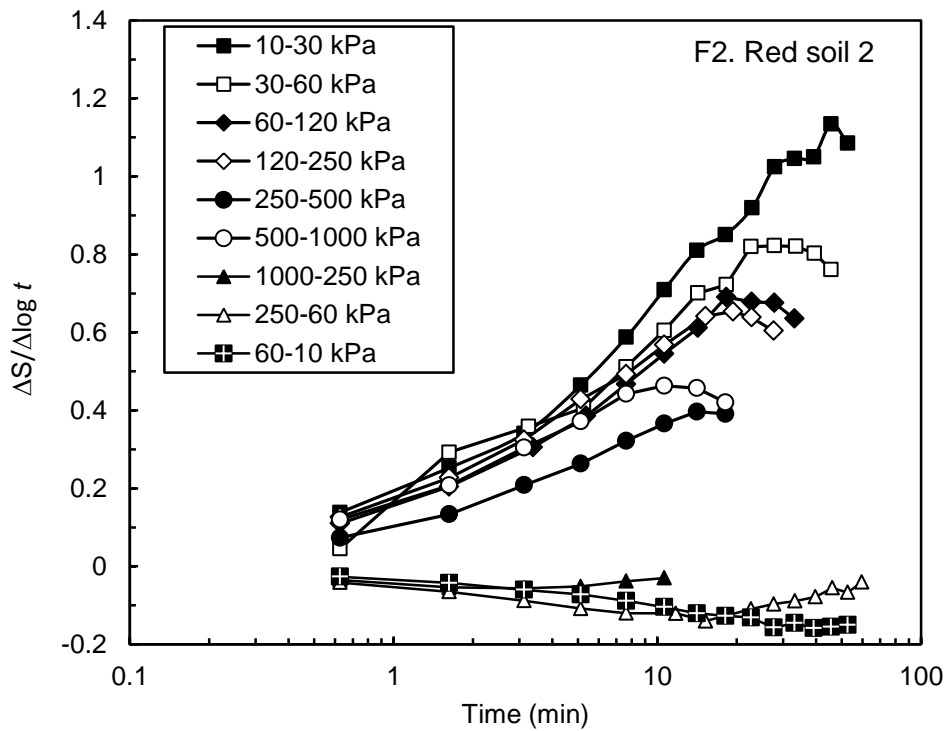
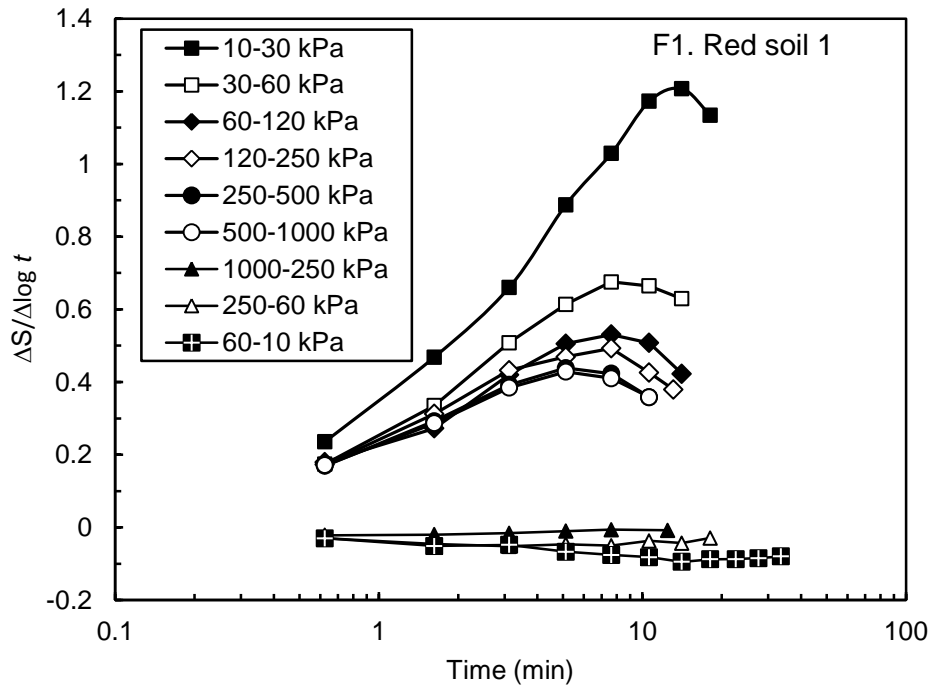


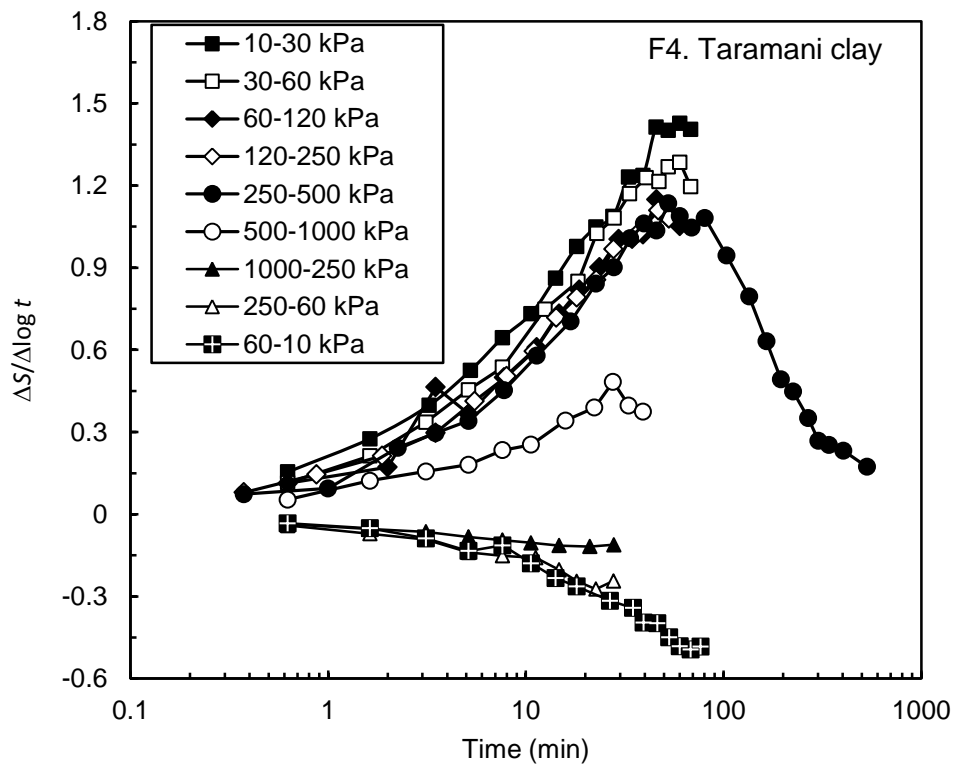
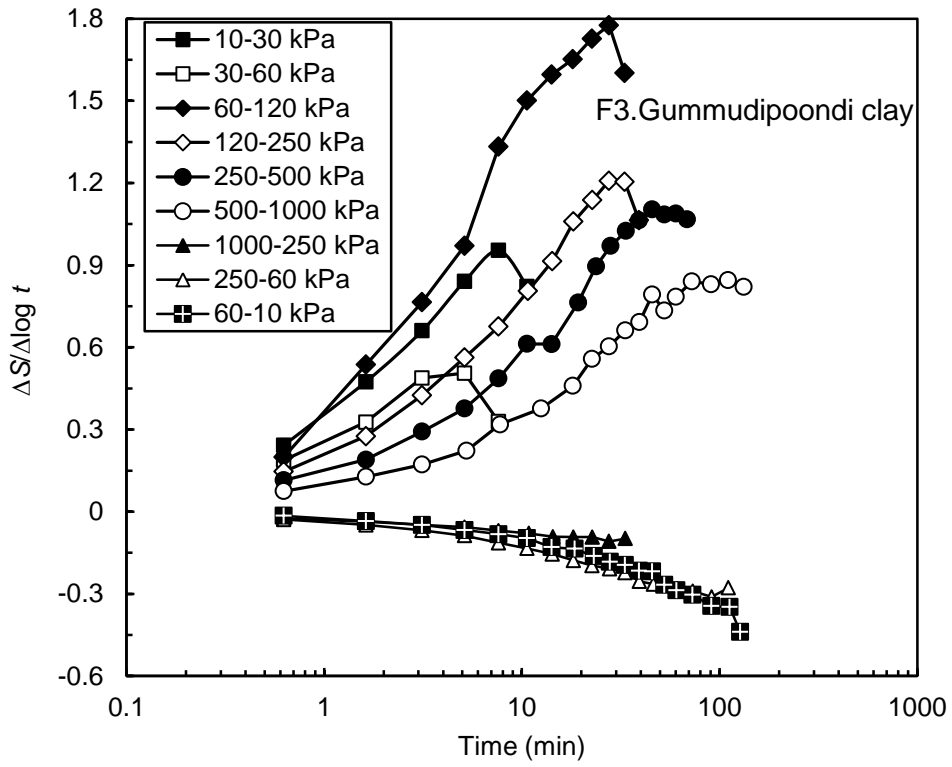


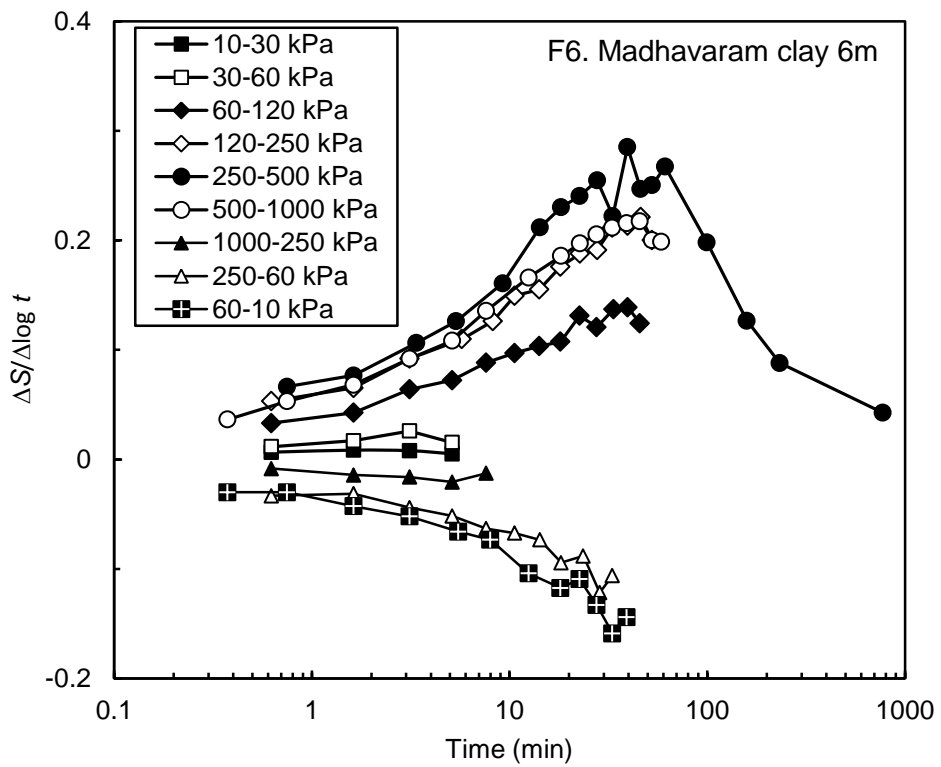
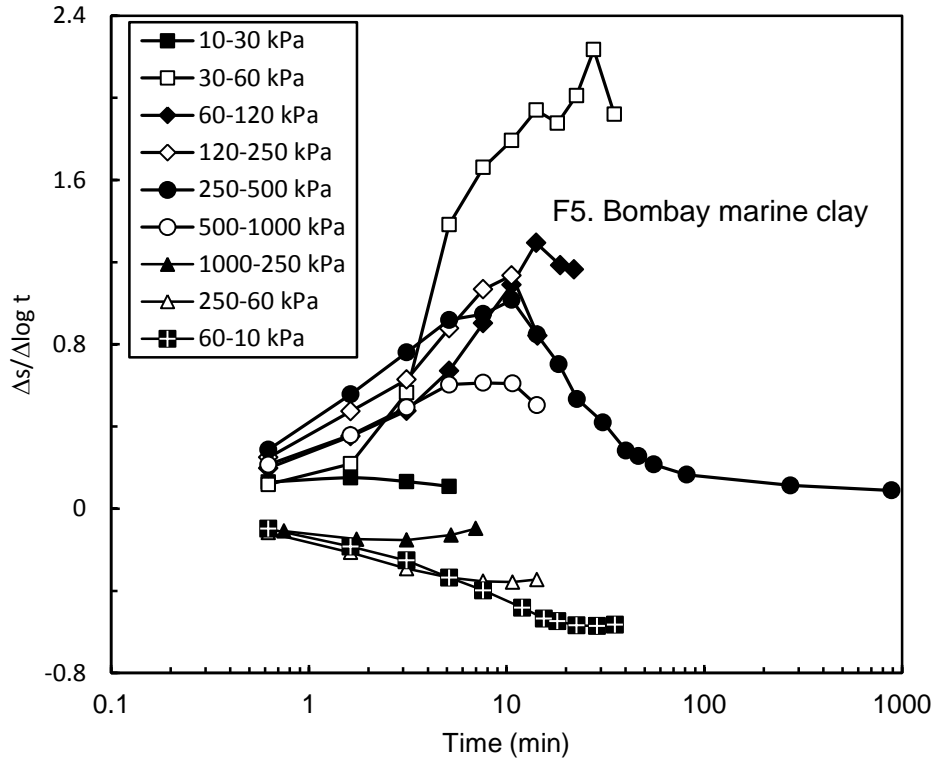


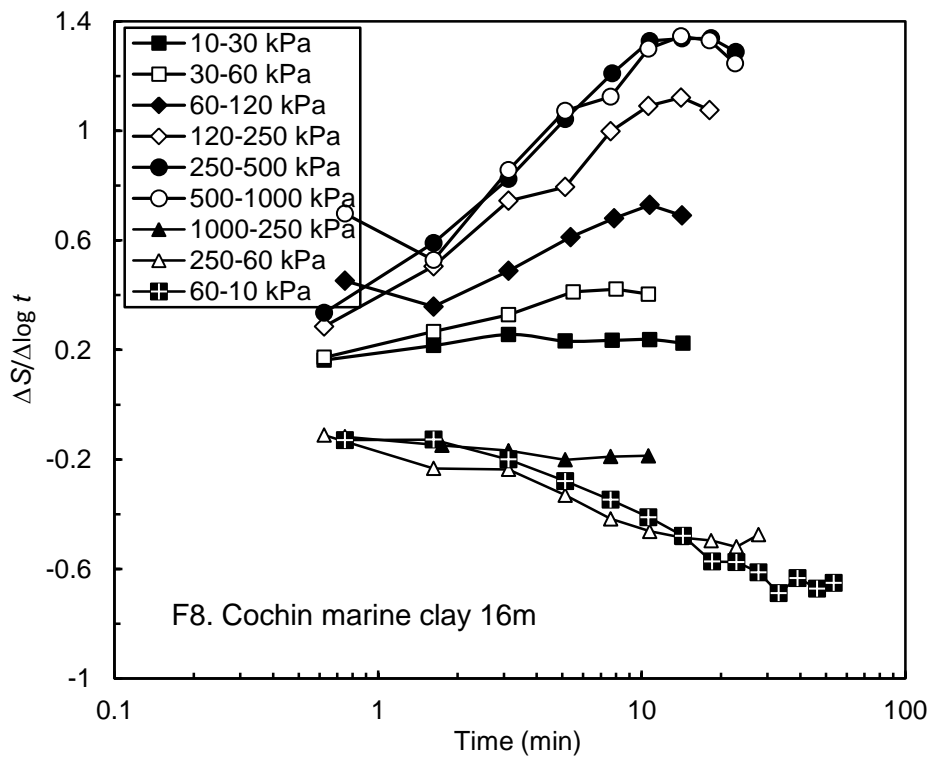
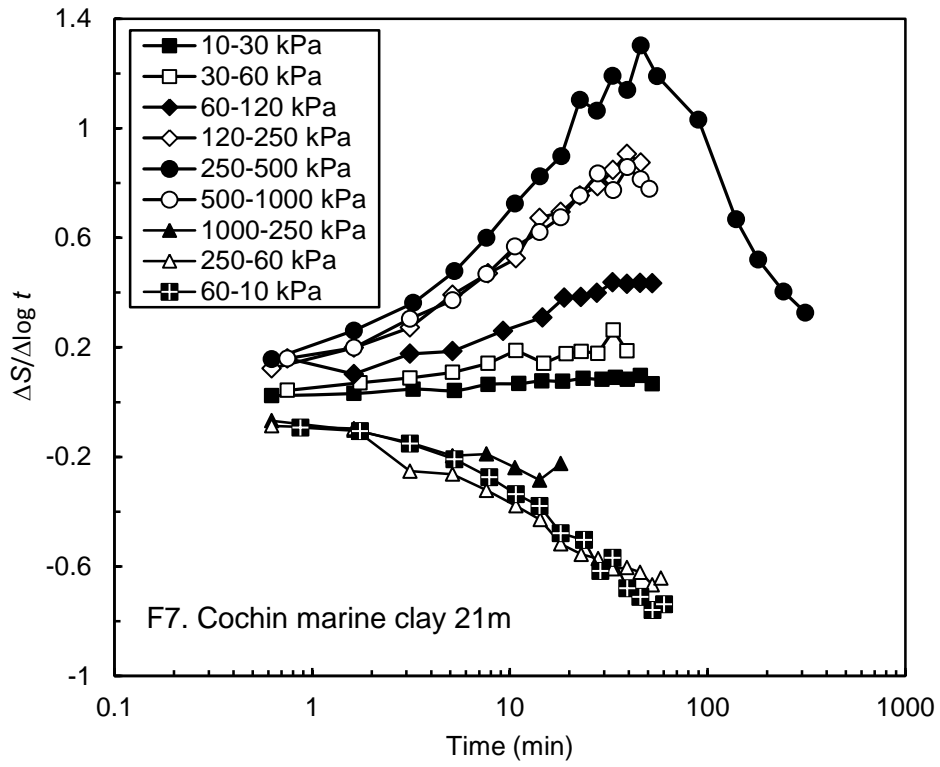


## APPENDIX F: $\Delta S/\Delta \log t - \log t$ PLOTS OF ACCELERATED IL TEST USING INFLECTION POINT METHOD









## REFERENCES

1. **Aboshi, H., H. Yoshikuni, and S. Maruyama** (1970) Constant loading rate consolidation test. *Soils and Foundations*, **10**(1), 43-56.
2. **Adams, A. L.** *Laboratory Evaluation of the Constant Rate of Strain and Constant Head Techniques for Measurement of the Hydraulic Conductivity of Fine Grained Soils*. M.S. thesis, Department of Civil and Environmental Engineering, Massachusetts Institute of Technology, Cambridge, Mass, 2011.
3. **Ahmadi, H., H. Rahimi, A. Soroush, and C. Alén** (2014) Experimental Research on Variation of Pore Water Pressure in Constant Rate of Strain Consolidation Test. *Acta Geotechnica Slovenica*, **11**(2), 46-57.
4. **Ahmadi, H., H. Rahimi, and A. Soroush** (2011) Investigation on the characteristics of pore water flow during CRS consolidation test. *Geotechnical and Geological Engineering*, **29**, 989–997.
5. **Armour, D. W. Jr. and V. P. Drnevich** (1986) Improved techniques for the constant -rate-of strain consolidation test. *Consolidation of Soils: Testing and Evaluation*, *ASTM Special Technical Publication No. 892*, Philadelphia, 170–183.
6. **ASTM D2435-11** (2011) Standard test method for one-dimensional consolidation properties of soils using Incremental loading. *ASTM International*, West Conshohocken, PA, USA.
7. **ASTM D4186-06** (2006) Standard test method for one-dimensional consolidation properties of saturated cohesive soils using controlled-strain loading. *ASTM International*, West Conshohocken, PA, USA.
8. **ASTM D4186-12** (2012) Standard test method for one-dimensional consolidation properties of saturated cohesive soils using controlled-strain loading. *ASTM International*, West Conshohocken, PA, USA.
9. **ASTM D4186-82** (1982) Standard test method for one-dimensional consolidation properties of saturated cohesive soils using controlled-strain loading. *ASTM International*, West Conshohocken, PA, USA.
10. **ASTM D5084-10** (2010) Standard Test Methods for Measurement of Hydraulic Conductivity of Saturated Porous Materials Using a Flexible Wall Permeameter. *ASTM International*, West Conshohocken, PA.
11. **Ayyar, T. S. R., N. Balasubramanian, V. Raman, and S. Esakku** (1990) Discussion: Influence of drying on the liquid limit behaviour of a marine clay. *Geotechnique*, **40**, 673–676.
12. **Babu, T. Jose., A. Sridharan, and Benny Mathews Abraham** (2008) A study of geotechnical properties of Cochin Marine Clays. *Marine Geotechnology*, **7**(3), 189-209.
13. **Basma, A. A., A. S. Al-Homoud, and E. Y. Al-Tabari** (1994) Effects of methods of drying on the engineering behavior of clays. *Applied Clay Science*, **9**,151–164.
14. **Bjerrum**, (1967) Engineering Geology of Norwegian Normally Consolidated Clays as Related to Settlements of Buildings. *Géotechnique*, **17**, 81-118.

15. **BS 1377-5 (1990)** Methods of test for soils for civil engineering purposes. Compressibility, permeability and durability tests. *British Standards Institution*, London.
16. **Casagrande, A. (1936)** Characteristics of cohesionless soils affecting the stability of slopes and earth fills. *Journal of Boston Society of Civil Engineering*, 13-32.
17. **Casagrande, A. and R. E. Fadum** *Notes on Soil Testing for Engineering Purposes*. Harvard Soil Mechanics, Series No. 8, Cambridge, Mass, 1940.
18. **Coduto, D. P.** *Geotechnical Engineering: Principles and Practices*, Allen apt, New Jersey, 1998.
19. **Cour, F. R.** (1971) Inflection point method for computing  $c_v$ . *Journal of the Soil Mechanics and Foundations Division, ASCE*, **97**(5), 827–831.
20. **Crawford, C. B.** (1988) On the Importance of Rate of Strain in the Consolidation Test. *Geotechnical Testing Journal, ASTM*, **11** (1), 60–62.
21. **Fox, P. J. and H. Pu** (2012) Enhanced CS2 model for large strain consolidation. *International Journal of Geomechanics, ASCE*, 574–583.
22. **Fox, P. J., H. Pu, and J. T. Christian** (2014) Evaluation of Data Analysis Methods for the CRS Consolidation Test. *Journal of Geotechnical Geoenvironmental Engineering, ASCE*, **140** (6).
23. **Gibson, R. E.** (1963) An analysis of system flexibility and its effect on time lag in pore-water pressure measurements. *Géotechnique*, **8**, 1-9.
24. **Gorman, C. T., T. C. Hopkins, R. C. Deen, and V. P. Drnevich** (1978) Constant-rate-of-strain and controlled-gradient consolidation testing. *Geotechnical Testing Journal, ASTM*, **1**(1), 3 – 15.
25. **Hamilton, J. J. and C. B. Crawford** (1959) Improved determination of preconsolidation pressure of a sensitive clay. *ASTM Special Technical Publication No. 254*, 254–270.
26. **Head, K. H.** (1983) Continuous consolidation testing. *Ground Engineering*, **16**(4), 24-25.
27. **Head, K. H.** *Manual of soil laboratory testing: Volume 3 Effective Stress Tests*, 3<sup>rd</sup> edition, Wiley, Chichester, 1986.
28. **Henniche, A. and S. Belkacemi** (2018) Numerical Simulation to Select Proper Strain Rates during CRS Consolidation Test. *Periodica Polytechnica Civil Engineering*, **62**(2), 404-412.
29. **Hoare, S. O.** *Consolidation with flow restrictor: an improved laboratory test*. University of Oxford Department of Engineering Science, Report No.2, SM014, 1980.
30. **IS 1498 (1970)** Classification and Identification of Soils for General Engineering Purposes. *Bureau of Indian Standards*, New Delhi.
31. **IS 2720-15 (1986)** Methods of Test for Soils: Determination of Consolidation Properties. *Bureau of Indian Standards*, New Delhi.
32. **IS 2720-3 (1980)** Methods of Test for Soils: Determination of Specific Gravity, Section 1: Fine Grained Soils. *Bureau of Indian Standards*, New Delhi.



33. **IS 2720-4 (1985)** Methods of Test for Soils: Grain Size Analysis. *Bureau of Indian Standards*, New Delhi.
34. **IS 2720-5 (1985)** Methods of Test for Soils: Determination of Liquid and Plastic Limit. *Bureau of Indian Standards*, New Delhi.
35. **Janbu, N., O. Tokheim, and K. Senneset** (1981) Consolidation tests with continuous loading. *XICSMFE Stockholm*, **1**, 645-65.
36. **Jia, R., J. C. Chai, T. Hino, and Z. S. Hong** (2010) Strain-rate effect on consolidation behavior of Ariake clay. *Proceedings of ICE-Geotechnical Engineering*, **163**(5), 267–277.
37. **Ladd, C. C. and D. J. DeGroot** (2003) Recommended practice for soft ground site characterization. *Proceedings of 12<sup>th</sup> Pan American Conference*, **1**, 3–57.
38. **Larsson, R. and G. Sallfors** (1986) Automatic Continuous Consolidation Testing in Sweden. *Consolidation of Soils: Testing and Evaluation*, *ASTM Special Technical Publication No. 892*, 299-328.
39. **Lee, K.** (1981) Consolidation with constant rate of deformation. *Géotechnique*, **31**(2), 215–229.
40. **Lee, K. and G. C. Sills** (1980) The Consolidation of a Soil Stratum including Self Weight Effects and Large Strains. *International Journal for Numerical and Analytical Methods in Geomechanics*, **5**, 405-428.
41. **Lee, K., V. Choa, S. H. Lee, and S. H. Quek** (1993) Constant Rate of Strain Consolidation of Singapore Marine Clay. *Géotechnique*, **43** (3), 471–488.
42. **Leonards, G. A. and B. K. Ramiah** (1959) Time effects in the consolidation of clays. *ASTM Special Technical Publication No.254*, 117-130.
43. **Leroueil, S., L. Samson, and M. Bozozuk** (1983) Laboratory and Field Determination of Preconsolidation Pressures at Gloucester. *Canadian Geotechnical Journal*, **20**(3) 477–490.
44. **Leroueil, S., M. Kabbaj, F. Tavenas, and R. Bouchard** (1985) Stress-Strain-Strain Rate Relation for the Compressibility of Sensitive Natural Clays. *Géotechnique*, **35** (2) 159–180.
45. **Lowe, J., E. Jonas, and V. Obrician** (1969) Controlled Gradient Consolidation Test. *Journal of the Soil Mechanics and Foundations Division, ASCE*, **95**(1), 77- 97.
46. **Mair, R. J.** *Centrifugal modelling of tunnel construction in soft clay*. PhD Thesis, Geotechnical and Geoenvironmental Division, University of Cambridge, UK, 1979.
47. **Mesri, G.** (1973) Coefficient of secondary compression. *Journal of Soil Mechanics and Foundation Division, ASCE*, **99** (1), 123-137.
48. **Mesri, G.** (2003) Primary Compression and Secondary Compression. Symposium on *Soil Behavior and Soft Ground Construction*, October 5-6, Cambridge.
49. **Mesri, G. and A. Castro** (1987)  $C_d/C_c$  concept and  $K_0$  during Secondary Compression. *Journal of Geotechnical Engineering, ASCE*, **113**(3), 230-247.
50. **Mesri, G. and P. M. Godlewski** (1977) Time and stress compressibility interrelationships. *Journal of Geotechnical Engineering, ASCE*, **103**(GT5), 417-430.
51. **Mesri, G., T. W. Feng, and M. Shahein** (1999) Coefficient of consolidation by inflection point method. *Journal of Geotechnical and Geoenvironmental Engineering*,

- ASCE, **125** (8), 716-718.
52. **Mikasa, M.** (1963) The consolidation of soft clay-a new consolidation theory and its application. *Kajima Shuppan-Kai* (in Japanese).
  53. **Moriwaki, T. and K. Umehara** (2003) Method for Determining the Coefficient of Permeability of Clays. *Geotechnical Testing Journal, ASTM*, **26** (1), 47–56.
  54. **Nakase, A., O. Kusakabe, and Sing-Fang Wong** (1984) Centrifuge model tests on bearing capacity of clays. *Journal of Geotechnical Engineering Division, ASCE*, **110**, 1749-1765.
  55. **Newland, P. L. and B. H. Allely** (1960) A Study of the Consolidation Characteristics of a clay. *Géotechnique*, **10**, 62-74.
  56. **Olson, R. E.** (1986) State of the art: Consolidation testing, consolidation of soils: Testing and evaluation, *ASTM Special Technical Publication No. 892*, 7-70.
  57. **Olson, R. E. and G. Mesri** (1970) Mechanisms controlling the compressibility of clays. *Journal of the Soil Mechanics and Foundations Division, ASCE*, **96**, 1853-1878.
  58. **Ozer, A. T., E. C. Lawton, and S. F. Bartlett** (2012) New method to determine proper strain rate for Constant rate of strain consolidation tests. *Canadian Geotechnical Journal*, **49**, 18-26.
  59. **Perloff, W. H., K. Nair, and J. G. Smith** (1965) Effects of measuring system on pore water pressures in the consolidation test. *6<sup>th</sup> International Conference of Soil Mechanics and Foundation Engineering*, **3**, 338-341.
  60. **Prashant, A. and G. Vikash** (2014) Consolidation Characteristics of Clay Using Constant Rate of Deformation Test,” *Golden Jubilee Conference of the IGS Bangalore chapter, Geo- Innovations*, 30–31.
  61. **Pratoom, W. and S. Tangwiboonpanich** (2004) Self-Adjusted Pneumatic Loading Oedometer for 1D Consolidation. *6<sup>th</sup> International Science, Social Sciences, Engineering and Energy Conference*, 17-19 December, 2014, Prajaktra Design Hotel, UdonThani, Thailand.
  62. **Pu, H. and P. J. Fox** (2016) Numerical Investigation of Strain Rate Effect for CRS Consolidation of Normally Consolidated Soil. *Geotechnical Testing Journal*, **39** (1), 80-90.
  63. **Pu, H., P. J. Fox, and Y. Liu** (2013) Model for Large Strain Consolidation Under Constant Rate of Strain. *International Journal for Numerical and Analytical in Geomechanics*, **37** (11), 1574–1590.
  64. **Rao, S. M., A. Sridharan, and S. Chandrakaran** (1989) Influence of drying on the liquid limit behaviour of a marine clay. *Géotechnique*, **39**, 715–719.
  65. **Robinson, R. G.** (1997) Consolidation analysis by inflection point method. *Géotechnique*, **47**(1), 199-200.
  66. **Robinson, R. G. and M. M. Allam** (1998) Effect of Clay Mineralogy on Coefficient of Consolidation. *Clays and Clay Minerals*, **46** (5) 596-600.
  67. **Rowe, P. W. and L. Barden** (1966) A new consolidation cell. *Géotechnique*, **16** (2), 162-170.
  68. **Rui, J., C. Jinchun, and H. Takenori** (2013) Interpretation of coefficient of

- consolidation from CRS test results. *Geomechanics and Engineering*, **5**(1), 57–70.
69. **Salfors, G.** *Preconsolidation pressure of soft, high-plastic clays*. Ph.D thesis, Department of Civil and Environmental Engineering, Chalmers University of Technology, Goteborg, Sweden, 1975.
  70. **Samarasinghe, A. M., Y. H. Huang, and V. P. Drnevich** (1982) Permeability and consolidation of normally consolidated soils. *Journal of the Geotechnical Engineering Division, ASCE*, **108**(6), 835-850.
  71. **Sample, K. M. and C. D. Shackelford** (2012) Apparatus for Constant Rate-Of-Strain Consolidation of Slurry Mixed Soils. *Geotechnical Testing Journal, ASTM*, **35** (3), 409–419.
  72. **Sandbaekken, G., T. Berre, and S. Lacasse** (1986) Oedometer testing at the Norwegian Geotechnical Institute. *Consolidation of soils: testing and evaluation, ASTM Special Publication No. 892*, 329–353.
  73. **Schiffman, R. L.** (1958) Consolidation of Soil under Time Dependent Loading and Varying Permeability. Proceedings of 37<sup>th</sup> Annual Meeting of the Highway Research Board, Washington DC, 6-10 January, 584-617.
  74. **Sheahan, T. C. and P. J. Watters** (1997) Experimental Verification of CRS Consolidation Theory. *Journal of Geotechnical Geoenvironmental Engineering*, **123** (5), 430-437.
  75. **Shukla, S., N. Sivakugan, and B. Das** (2009) Methods for determination of the coefficient of consolidation and field observations of time rate of settlement-an overview. *International Journal of Geotechnical Engineering*, **3**(1), 89-108.
  76. **Silvestri, V., R. N. Yong, M. Soulié, and F. Gabriel** (1986) Controlled-Strain, Controlled Gradient, and Standard Consolidation Testing of Sensitive Clays. *ASTM Special Technical Publication No. 892*, 170–183.
  77. **Smith, R. E. and H. E. Wahls** (1969) Consolidation under constant rate of strain. *Journal of the Soil Mechanics and Foundations Division, ASCE*, **95**(2), 519–539.
  78. **Sridharan, A. and G. V. Rao** (1976) Mechanisms Controlling Volume Change of Saturated Clays and the Role of Effective stress concept. *Géotechnique*, **29**, 249-260.
  79. **Sridharan, A. and H. Nagaraj** (2004) Coefficient of Consolidation and its Correlation with Index Properties of Remolded Soils. *Geotechnical Testing Journal, ASTM*, **27**(5), 469-474.
  80. **Sridharan, A. and K. Prakash** (1997) The  $\log \delta - \log t$  method for the determination of the coefficient of consolidation. Proceedings of *Institution of the Civil Engineers, Geotechnical Engineering*, **125**(1): 27–32.
  81. **Sridharan, A., B. M. Abraham, and B. T. Jose** (1991) Improved technique for estimation preconsolidation pressure. *Géotechnique*, **41**(2), 263-268.
  82. **Sridharan, A., H. B. Nagaraj, and N. Srinivas** (1999) Rapid method of consolidation testing. *Canadian Geotechnical Journal*, **36**, 392-400.
  83. **Sridharan, A., K. Prakash, and S. R. Asha** (1995) Consolidation behavior of soils. *Geotechnical Testing Journal, ASTM*, **18**(1), 58–68.
  84. **Sridharan, A., N. S. Murthy, and K. Prakash** (1987) Rectangular hyperbola method of consolidation analysis. *Géotechnique*, **37**(3):355–368.

85. **Sridharan, A., P. V. Sivapullaiah, and V. K. Stalin** (1994) Effect of short duration of load increment on the compressibility of soils. *Geotechnical Testing Journal, ASTM*, **17**(4), 488–496.
86. **Suganya, K. and P. Sivapullaiah** (2016) Effect of Changing Water Content on the Properties of Kuttanad Soil. *Geotechnical and Geological Engineering*, **33**, 913–921.
87. **Taylor, D. W.** *Research on Consolidation of Clays*. Department of Civil and Sanitary Engineering, Mass. Inst. Technology, 1942.
88. **Terzaghi, K. (1925)** Principles of Soil Mechanics: Settlement and consolidation of clay. *Engineering news records*, **95**(22), 874-878.
89. **Terzaghi, K., and R. B. Peck** *Soil Mechanics in Engineering Practice*, 2<sup>nd</sup> ed., Wiley, New York, 1967.
90. **Terzaghi, K., R. B. Peck, and G. Mesri** *Soil Mechanics in Engineering Practice*, 3<sup>rd</sup> edition Wiley, New York, 1996.
91. **Umehara, Y. and K. Zen** (1980) Constant rate of strain consolidation for very soft clayey soils. *Soils and Foundations*, **20**(2).
92. **Vaid, Y. P., P. K. Robertson, and R. G. Campanella** (1979) Strain Rate Behaviour of Saint-Jean-Vianney Clay. *Canadian Geotechnical Journal*, **16** (1), 34–42.
93. **Vikash, G.** *A New CRS Consolidation Theory and A Compressibility Model for Kaolin Clay with Micro-fabric Effects*. PhD Thesis, Department of Civil Engineering, Indian Institute of Technology Kanpur, India, 2013.
94. **Wissa, A. E. Z., J. T. Christian, E. H. Davis, and S. Heiberg** (1971) Consolidation testing at constant rate of strain. *Journal of the Soil Mechanics and Foundations Division, ASCE*, **97**(10), 1393–1413.
95. **Yoshikuni, H., T. Moriwaki, S. Ikegami, and T. Xo** (1995) Direct determination of permeability of clay from constant rate of strain consolidation tests. *Proceeding of International Symposium on Compression and Consolidation of Clayey Soils*, **1**, 609-614.

## LIST OF PUBLICATIONS

### REFEREED JOURNALS BASED ON THE THESIS

1. **Raheena, M. and R. G. Robinson (2017)** Accelerated consolidation test using  $\sqrt{t}$  method. *Indian Geotechnical Journal*, **48**(1), 84-91.
2. **Raheena, M., G. Sridhar, and R. G. Robinson (2018)** Simplified apparatus for CRS consolidation testing of soils. *Geotechnical Testing Journal, ASTM* (Accepted).
3. **Raheena, M., G. Sridhar, and R. G. Robinson (2018)**. Constant Rate of Strain Consolidation Test Using Conventional Fixed Ring Consolidation Cell. *Indian Geotechnical Journal*. DOI 10.1007/s40098-018-0299
4. **Raheena. M and Robinson. R.G. (2017)**. Inflection point method for faster and completer consolidation testing. *Geotechnical Testing Journal ASTM*. Communicated.